Polio is (still) not dead:
Vaccine vectors, antiviral drugs, pathogenesis, and unexpected mutants

by

Shane Crotty

DISSERTATION

Submitted in partial satisfaction of the requirements for the degree of

DOCTOR OF PHILOSOPHY

in

Biochemistry

in the

GRADUATE DIVISION

of the

UNIVERSITY OF CALIFORNIA SAN FRANCISCO

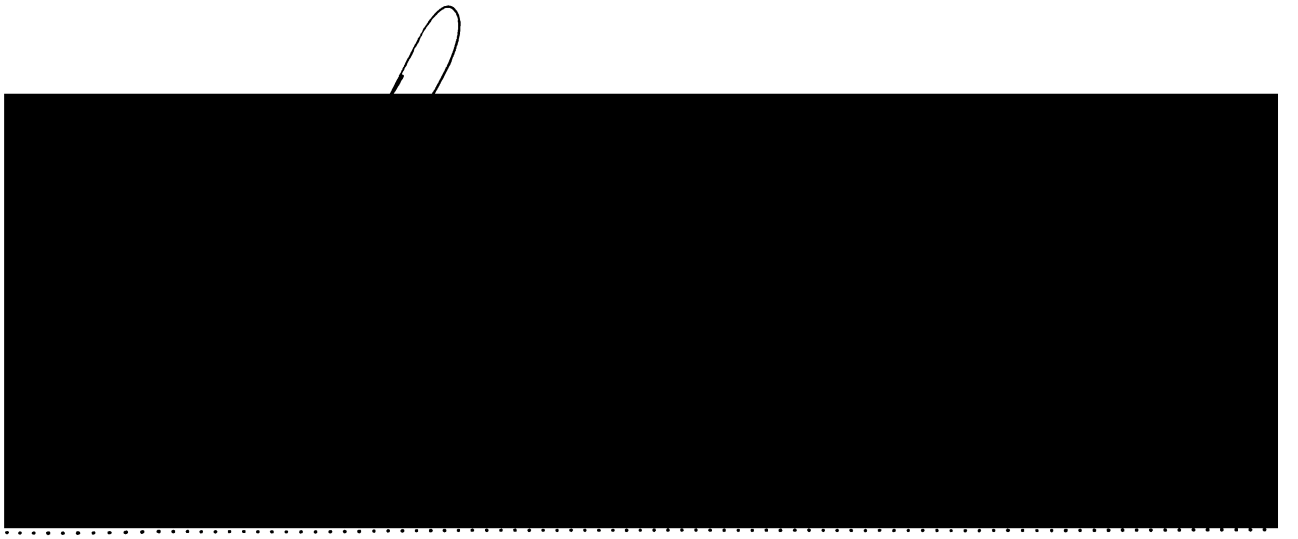

Date University Librarian

Degree Conferred: .....

For Aunt Gladys,
who told me not to be a dentist

Preface

A number of scientists have played critical roles in bringing to fruition the various projects presented in this dissertation, ranging from postdocs carrying out two years of experiments to fellow grad students betting me a beer that I couldn't discover a particularly elusive mutant virus. The contributions of those individuals, which were critical to success of the projects detailed herein, are acknowledged in the introductory chapter of each dissertation section. I would particularly like to thank co-authors Barbara Lohman and Lara Compton of Chris Miller's laboratory at UC Davis for their essential help holding together the AIDS vaccine project, and the members of Craig Cameron's laboratory at Penn St. University, especially David Gohara and Jamie Arnold, for being wonderful collaborators. Barbara Lohman is now in Kenya studying cellular immunology in HIV-infected infants, and I am happy that we have become long-term correspondents. Additionally, I am grateful to Luis Sigal for allowing me to participate in his groundbreaking study of the exogenous antigen presentation pathway in PVR mice.

Craig Cameron and I struck up a very productive collaboration that not only involved a large number of fascinating experiments but also are large number of intellectually fascinating conversations. He is a great enzymologist, and I learned a lot from him. The two of us have had a number of excruciating, exhausting, hour-long 120 decibel arguements, and may there be many more in the future, because we both end up scientifically the better from them. If there's no reason to be passionate about something there's no reason it's interesting. Regarding Chris Miller, his interest in the poliovirus

vector system and his frankness were both important factors in our successful monkey AIDS vaccine trial.

Then, of course, there is Raul. It would be a "cyclopean task" to recount the multitudinous and multifaceted ways in which Raul has been essential to the success of my graduate work. Raul is an excellent mentor, and he provided me with accurate guidance while also allowing me to wander freely through experiments and collaborations I found intriguing. I am immensely grateful for both of those aspects of his tutelage. He was very supportive, and also open and honest. His experimental insights regarding the poliovirus vector system led directly to our exciting successful monkey AIDS vaccine trial, and I hope those insights lead to successful human trials. He is an excellent scientist and I was lucky to be in his lab.

A couple of dozen people have been in the lab during my stay, and their presence has always made the lab and interesting and exciting place to be. Jens Herold was a godsend for the lab. He is an incredible experimentalist and an intellectually rigorous virologist and I was honored to have him as a labmate. May our paths cross again. The invaluable technical assistance of Laura Hix and Martha Neagu was central to the completion of two of the studies detailed herein, and they were always a pleasure to have around. I can only hope that I managed to pass along to them some useful skills and ways of thinking, and that their future careers may bring them happiness and success.

Steffi Mandl and Oren Beske have been the main graduate students in the Andino lab during my time here, and they have been wonderful colleagues. At a lab I was previously in, I regularly left lab meetings bored and nonchalant. In the Andino lab that has not been the case, and it has been in no small part due to arguements involving the

three of us. They are both kind and caring human beings, and I wish them the best in post-Andino lab life.

Rob Sadler, rest in peace. I will always cherish your boisterous and joyful presence.

Karla Kirkegaard, Jonathan Yewdell, Robert E. Johnston, Charlie Rice, John Holland, Art Weiss, J. Michael Bishop, and David Baltimore each were generous enough with their time to discuss with me one or several of the scientific problems explored during my graduate work, and I am thankful for their intellectual insights. And I am thankful for the professional advice provided by Phil Sharp and Keith Yamamoto over the years.

My thesis committee was always helpful, for which I am most appreciative. The excitement resulting from the ribavirin discovery led to several precarious political situations, and I am sincerely grateful to Alan Frankel for his sage advice helping me navigate the publication minefield. I also thank Alan Frankel for his mentorship during my first graduate school rotation. I thank Don Ganem for his prescient experimental insights over the years, and for directing me to Raul's lab for my thesis (inadvertent as it was).

My younger sister, who has always been incredibly supportive of what I do, actually has more expertise in mouse work than I do and taught me how to perform intranasal inoculations, which led to one of the interesting discoveries of my graduate work. More importantly, she's the best sibling I could ever hope for.

This dissertation is dedicated to the great Aunt Gladys, who not only scolded me into not becoming a dentist, but has been there my whole life encouraging my education

in all academic areas, from computers and mathematics to literature, art, and languages, for which I am eternally grateful.

My parents are the reason I am where I am today, in so many ways. May I someday be able to repay them for the loving care and multitudinous opportunities with which they have provided me.

And it is with immense gratitude that I thank my wife Anna for her boundless love and support during our years in San Francisco. We will always remember this as the beautiful place where we started our marriage.

Polio is (still) not dead: vaccine vectors, antiviral drugs, pathogenesis, and unexpected mutants

by Shane Crotty

Abstract

The results presented here are divided among four projects: I.) candidate AIDS vaccine, II.) Ribavirin is an RNA virus mutagen, III.) Poliovirus receptor (PVR) transgenic mice, and IV.) Novel poliovirus mutants. In project I, we provide the first report of protection against a vaginal challenge with a highly virulent SIV using a vaccine vector. We constructed new poliovirus vaccine vectors using Sabin 1 and 2 vaccine strain viruses, from which we generated a series of SabRV-SIV viruses containing SIV (simian immunodeficiency virus) gag, pol, env, nef, and tat in overlapping fragments. Two cocktails of poliovirus vectors (SabRV1-SIV and SabRV2-SIV) were then inoculated in a prime-boost regimen to vaccinate seven macaques. All seven vaccinated macaques, and twelve control macaques, were then challenged vaginally with highly pathogenic uncloned $SIV_{mac}251$. Strikingly, 4 of 7 vaccinated animals exhibited substantial protection against the vaginal SIV challenge. All twelve control monkeys became SIV^+. These results demonstrate the efficacy of SabRV as a potential human vaccine vector to prevent AIDS, and that a vaccine vector cocktail expressing an array of defined antigenic

sequences can be an effective vaccination strategy in an outbred population. In project II, we demonstrate that the important broad spectrum antiviral drug ribavirin (currently used to treat hepatitis C infections among others) is an RNA virus mutagen. We describe a molecular test of the error catastrophe theory and demonstrate that ribavirin's full antiviral activity is exerted through lethal mutagenesis of the viral genetic material. We conclude that mutagenic ribonucleosides may be an important new class of anti-RNA virus agents. In project III, we constructed a PVR transgenic mouse susceptible to a mucosal route of poliovirus infection. In project IV, we describe the discovery of two interesting independent sets of poliovirus mutants. One set of mutants contains novel manganese dependent RNA dependent RNA polymerases, and the other set of mutants is resistant to brefeldin A. Brefeldin A was the only anti-poliovirus compound for which no escape mutants were known. It has been presumed that the virus could not become resistant to brefeldin A because the drug targets a cellular host protein, not the virus directly.

Table of Contents

Section IV. Novel poliovirus mutants

List of Tables

Chapter 12

Chapter 15

Chapter 16

List of Figures

Chapter 3

Chapter 4

Chapter 5

Chapter 8

Chapter 9

Chapter 11

Chapter 12

Chapter 15

Chapter 16

Chapter 17

UNIVERSITY OF CALIFORNIA, SAN FRANCISCO

BERKELEY • DAVIS • IRVINE • LOS ANGELES • RIVERSIDE • SAN DIEGO • SAN FRANCISCO SANTA BARBARA • SANTA CRUZ

Shane Crotty
Dept. of Microbiology and Immunology
513 Parnassus Ave.
San Francisco, CA 94143
(415) 502-6357; FAX (415) 476-0939

February 14, 2001

Journal of Virology
Journals Department,
American Society for Microbiology
1752 N St., N.W.
Washington, DC 20036-2904.
FAX (202) 942-9355

To whom it may concern:

I would like to request permission to include in my thesis dissertation a copy of the following paper:

Shane Crotty, Barbara Lohman, Fabien Lu, ShenBei Tang, Chris Miller, and Raul Andino. "Mucosal immunization of cynomolgus macaques with two serotypes of live poliovirus vectors expressing simian immunodeficiency virus antigens: stimulation of humoral, mucosal, and cellular immunity." Vol. 73, pages 9485-95. *Journal of Virology* November 1999.

This dissertation will be microfilmed by University Microfilms Incorporated and they request permission to supply single copies upon demand.

I would greatly appreciate a response within 5 business days, by fax to (415) 476-0939.
Thank you very much.

Sincerely,

Shane Crotty

PERMISSION GRANTED FOR THE USE REQUESTED ABOVE
American Society for Microbiology
Journals Department
Date 2-15-01

UNIVERSITY OF CALIFORNIA, SAN FRANCISCO

BERKELEY • DAVIS • IRVINE • LOS ANGELES • RIVERSIDE • SAN DIEGO • SAN FRANCISCO SANTA BARBARA • SANTA CRUZ

Shane Crotty
Dept. of Microbiology and Immunology
513 Parnassus Ave.
San Francisco, CA 94143
(415) 502-6357; FAX (415) 476-0939.

February 14, 2001

Nature Medicine
Reprint Department
345 Park Avenue South
New York NY 10010-1707
tel: (212) 726-9278; FAX: (212) 679-0843

To whom it may concern:

I would like to request permission to include in my thesis dissertation a copy of the following paper:

Shane Crotty, David Maag, Jamie Arnold, Wei Zhong, Johnson Lau, Zhi Hong, Raul Andino, and Craig Cameron. "The broad-spectrum antiviral ribonucleoside ribavirin is an RNA virus mutagen." *Nature Medicine* (6:1375-1379) December 2000.

This dissertation will be microfilmed by University Microfilms Incorporated and they request permission to supply single copies upon demand.

I would greatly appreciate a response within 5 business days, by fax to (415) 476-0939.
Thank you very much.

Sincerely,

Shane Crotty

FEB 1

Nature America Inc.
345 Park Avenue South
New York NY 10010-1707

Tel: 212-726-9269
Fax: 212-696-9591

Email: permissions@natureny.com

Fax Cover

To: **Shane Crotty**

From: **Layonne Holmes**

Date: Feb. 16, 2001

Pages, including cover: 2

Comments:

Thank you for the permission request on the following page(s). Permission is hereby granted for one-time use, in print and microfilm, of your paper as specified, for your doctoral thesis, with the following specifications:

I. The paper is to be used for display/educational purposes only and will not be used to generate profit.

II. Usage is contingent upon the authors' permission.

III. The journal's name and the authors will be properly acknowledged.

IV. Any further usage will be requested in writing.

We are certain that all parties will benefit from this agreement and wish you the best in the use of this paper. Please mail or return fax to 212-696-9591.

Thank you,

Layonne Holmes
Reprints & Permissions
Nature Publishing Group
New York, NY

UNIVERSITY OF CALIFORNIA, SAN FRANCISCO

BERKELEY · DAVIS · IRVINE · LOS ANGELES · RIVERSIDE · SAN DIEGO · SAN FRANCISCO · SANTA BARBARA · SANTA CRUZ

Shane Crotty
Dept. of Microbiology and Immunology
513 Parnassus Ave.
San Francisco, CA 94143
(415) 502-6357; FAX (415) 476-0939

February 14, 2001

Journal of Biological Chemistry
American Society for Biochemistry and Molecular Biology
9650 Rockville Pike
Bethesda, Maryland 20814-3996
tel: (301) 530-7145; FAX: (301) 571-1824

To whom it may concern:

I would like to request permission to include in my thesis dissertation a copy of the following paper:

David Gohara, Shane Crotty, Jamie Arnold, Josh Yoder, Raul Andino, and Craig Cameron (2000). "Poliovirus RNA-dependent RNA Polymerase ($3D^{pol}$): Structural, biochemical, and biological analysis of conserved structural motifs A and B." *Journal of Biological Chemistry* (275:25523-25532)

This dissertation will be microfilmed by University Microfilms Incorporated and they request permission to supply single copies upon demand.

I would greatly appreciate a response within 5 business days, by fax to (415) 476-0939.
Thank you very much.

Sincerely,

Shane Crotty

PERMISSION GRANTED
contingent upon obtaining that of the author

FEB 14 2001

for the copyright owner
THE AMERICAN SOCIETY FOR BIOCHEMISTRY
& MOLECULAR BIOLOGY

UNIVERSITY OF CALIFORNIA, SAN FRANCISCO

BERKELEY • DAVIS • IRVINE • LOS ANGELES • RIVERSIDE • SAN DIEGO • SAN FRANCISCO SANTA BARBARA • SANTA CRUZ

Shane Crotty
Dept. of Microbiology and Immunology
513 Parnassus Ave.
San Francisco, CA 94143
(415) 502-6357; FAX (415) 476-0939

February 21, 2001

Nature America, Inc.
Reprints and Permissions
345 Park Ave. South
New York, NY 10010-1707
Tel: 212-726-9269, FAX: 212-696-9591

To whom it may concern:

I would like to request permission to include in my thesis dissertation a copy of the following paper:

Luis Sigal, Shane Crotty, Raul Andino, and Kenneth Rock (1999)
"Cytotoxic T-cell immunity to virus-infected non-haematopoietic cells requires presentation of exogenous antigen." *Nature* (398:77-80)

This dissertation will be microfilmed by University Microfilms Incorporated and they request permission to supply single copies upon demand.

I would greatly appreciate a response within 5 business days, by fax to (415) 476-0939.
Thank you very much.

Sincerely,

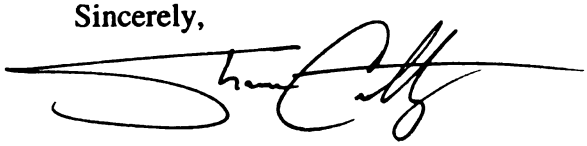

Shane Crotty

Subject: RE: Permisision request
Date: Thursday, March 1, 2001 8:27 AM
From: Williams, Marie <M.Williams@nature.com>
Reply-To: Permissions <Permissions@nature.com>
To: "'scrotty@itsa.ucsf.edu'" <scrotty@itsa.ucsf.edu>

1 March 2001

Dear Shane Crotty,

Nature, hereby grants permission for the reproduction of a figure from Nature 398:77-80 (1999)', providing that the authors agree and the following credit line is used:

Reprinted by permission from Nature (reference citation) copyright (year) Macmillan Magazines Ltd.

This is for print versions only.

Yours sincerely,

Marie Williams
Nature Permissions

Polio is (still) not dead: vaccine vectors, antiviral drugs, pathogenesis, and unexpected mutants

Introduction

Polio is still not dead. David Baltimore wrote an article in 1971 titled "Polio is not dead" (2) about the continued relevance of polio virology. I read that article while I was trying to decide what I would study during graduate school, and I thought, "Man, if polio virologists were having to defend the relevance of studying poliovirus in 1971, surely there is nothing important left to do 25 years later." But I talked to several virologists, and their consensus opinion was that polio virology would still be an excellent field to become educated in genetics, biochemistry, virology, and the scientific process. I accepted that opinion and began my graduate work on poliovirus with the mindset that it would be a great field to do science and accomplish some solid experiments, but nothing too exciting would probably happen. I was wrong. The past four years have been very exciting, both in the Andino Lab and the field in general. A crystal structure of the poliovirus polymerase was solved (10)—the first RNA-dependent RNA polymerase to be crystallized—which opened the door to fundamental biochemical and genetic analysis of this prototypic RNA virus polymerase (1, 3, 9, 12)(and see dissertation chapters 14-16), and some big surprises including a massive intermolecular polymerase interface (reviewed in (7)) and the ability of the poliovirus polymerase to incorporate the antiviral ribonucleoside ribavirin (5)(and see dissertation chapters 7-9). Luis Sigal used poliovirus receptor (PVR) transgenic mice to make a striking immunological discovery (17)(and see

dissertation chapters 10-12). Our laboratory demonstrated that poliovirus can be used as a successful viral vaccine vector, capable of protecting mice against a lethal melanoma tumor challenge (13), and capable of protecting monkeys against a lethal challenge with a highly virulent monkey AIDS virus ($SIV_{mac}251$) (Crotty et al., submitted; and see dissertation chapters 2-6). Additionally, beautiful cryo-EM structures of the poliovirus capsid-PVR interactions have been resolved (4, 11), new insights into poliovirus RNA synthesis initiation have been published (8, 14-16), poliovirus has been shown to inhibit MHC class I expression (6), and poliovirus has been shown to circularize its genome (Herold and Andino, *Molecular Cell*, in press). It has been a very exciting time to be involved in poliovirus research. It continues to amaze me that an entity consisting of only 7000 nts of genetic information can be so clever and complex.

Structure of the dissertation

This dissertation is divided into four complementary but independent sections that constituted the bulk of my work in Raul Andino's lab at UCSF. Those sections, as described in the abstract, are: I.) candidate AIDS vaccine, II.) Ribavirin is an RNA virus mutagen, III.) Poliovirus receptor (PVR) transgenic mice, and IV.) Novel poliovirus mutants. Each section contains its own scientific introduction chapter.

To clarify the relationship of this dissertation to the published literature: Chapter 3 was published in 1999 in the *Journal of Virology* (73:9485-95) as "Mucosal immunization of cynomolgus macaques with two serotypes of live poliovirus vectors expressing simian immunodeficiency virus antigens: stimulation of humoral, mucosal, and cellular immunity" with the authors Shane Crotty, Barbara Lohman, Fabien Lu,

ShenBei Tang, Chris Miller, and Raul Andino. Chapter 8 was published in 2000 in *Nature Medicine* (6:1375-1379) as "The broad-spectrum antiviral ribonucleoside ribavirin is an RNA virus mutagen" with the authors Shane Crotty, David Maag, Jamie Arnold, Wei Zhong, Johnson Lau, Zhi Hong, Raul Andino, and Craig Cameron. Chapter 11 was published in 1999 in *Nature* (398:77-80) as "Cytotoxic T-cell immunity to virus-infected non-haematopoietic cells requires presentation of exogenous antigen" with the authors Luis Sigal, Shane Crotty, Raul Andino, and Kenneth Rock. Chapter 15 was published in 2000 in the *Journal of Biological Chemistry* (275:25523-25532) as "Poliovirus RNA-dependent RNA Polymerase ($3D^{pol}$): Structural, biochemical, and biological analysis of conserved structural motifs A and B" with the authors David Gohara, Shane Crotty, Jamie Arnold, Josh Yoder, Raul Andino, and Craig Cameron.

To help quickly locate unpublished data, supplementary material to each published paper is provided at the end (after the published figures) of the chapter as a new section, "Supplementary Data," when appropriate.

Chapter 5 has been submitted for publication, Chapter 9 has been submitted for publication, and Chapter 12 has been submitted for publication. Chapters 16 and 17 will be submitted for publication in the near future.

References

1. **Arnold, J. J., and C. E. Cameron** 2000. Poliovirus RNA-dependent RNA polymerase (3D(pol)). Assembly of stable, elongation-competent complexes by using a symmetrical primer-template substrate (sym/sub) J Biol Chem. **275:**5329-36.
2. **Baltimore, D.** 1971. Polio is not dead, p. 1-14. *In* M. Pollard (ed.), Perspectives in Virology, vol. 7. Academic Press, New York.
3. **Beckman, M. T., and K. Kirkegaard** 1998. Site size of cooperative single-stranded RNA binding by poliovirus RNA- dependent RNA polymerase J Biol Chem. **273:**6724-30.
4. **Belnap, D. M., B. M. McDermott, D. J. Filman, N. Cheng, B. L. Trus, H. J. Zuccola, V. R. Racaniello, J. M. Hogle, and A. C. Steven** 2000. Three-dimensional structure of poliovirus receptor bound to poliovirus Proc Natl Acad Sci U S A. **97:**73-8.
5. **Crotty, S., D. Maag, J. J. Arnold, W. Zhong, J. Y. Lau, Z. Hong, R. Andino, and C. E. Cameron** 2000. The broad-spectrum antiviral ribonucleoside ribavirin is an RNA virus mutagen Nat Med. **6:**1375-1379.
6. **Deitz, S. B., D. A. Dodd, S. Cooper, P. Parham, and K. Kirkegaard** 2000. MHC I-dependent antigen presentation is inhibited by poliovirus protein 3A [In Process Citation] Proc Natl Acad Sci U S A. **97:**13790-5.
7. **Flint, S. J., L. W. Enquist, R. M. Krug, V. R. Racaniello, and A. M. Skalka** 1999. Principles of Virology, 1st ed. ASM Press, Washington, D.C.
8. **Gamarnik, A. V., and R. Andino** 1998. Switch from translation to RNA replication in a positive-stranded RNA virus Genes and Development. **12:**2293-304.
9. **Gohara, D. W., S. Crotty, J. J. Arnold, J. D. Yoder, R. Andino, and C. E. Cameron** 2000. Poliovirus RNA-dependent RNA Polymerase ($3D^{Pol}$): Structural, biochemical, and biological analysis of conserved structural motifs A and B Journal of Biological Chemistry. **275:**25523-25532.
10. **Hansen, J. L., A. M. Long, and S. C. Schultz** 1997. Structure of the RNA-dependent RNA polymerase of poliovirus Structure. **5:**1109-22.
11. **He, Y., V. D. Bowman, S. Mueller, C. M. Bator, J. Bella, X. Peng, T. S. Baker, E. Wimmer, R. J. Kuhn, and M. G. Rossmann** 2000. Interaction of the poliovirus receptor with poliovirus Proc Natl Acad Sci U S A. **97:**79-84.
12. **Hope, D. A., S. E. Diamond, and K. Kirkegaard** 1997. Genetic dissection of interaction between poliovirus 3D polymerase and viral protein 3AB J Virol. **71:**9490-8.
13. **Mandl, S., L. J. Sigal, K. L. Rock, and R. Andino** 1998. Poliovirus vaccine vectors elicit antigen-specific cytotoxic T cells and protect mice against lethal challenge with malignant melanoma cells expressing a model antigen Proceedings

of the National Academy of Sciences of the United States of America. **95:**8216-21.

14. **Paul, A. V., E. Rieder, D. W. Kim, J. H. van Boom, and E. Wimmer** 2000. Identification of an RNA hairpin in poliovirus RNA that serves as the primary template in the In vitro uridylylation of VPg J Virol. **74:**10359-70.
15. **Paul, A. V., J. H. van Boom, D. Filippov, and E. Wimmer** 1998. Protein-primed RNA synthesis by purified poliovirus RNA polymerase Nature. **393:**280-4.
16. **Rieder, E., A. V. Paul, D. W. Kim, J. H. van Boom, and E. Wimmer** 2000. Genetic and biochemical studies of poliovirus cis-acting replication element cre in relation to VPg uridylylation J Virol. **74:**10371-80.
17. **Sigal, L. J., S. Crotty, R. Andino, and K. L. Rock** 1999. Cytotoxic T-cell immunity to virus-infected non-haematopoietic cells requires presentation of exogenous antigen Nature. **398:**77-80.

Section I

Candidate AIDS Vaccine

Chapter 2

Introduction to Section I: Poliovirus vector candidate AIDS vaccine

The poliovirus vaccine vector concept was conceived of by Raul Andino and Mark Feinberg while they were in David Baltimore's lab (1), based on the ideas of related vaccine vectors being developed using vaccinia (reviewed in (2)). The initial focus was on developing an AIDS vaccine (1) and the primary focus remains directed at developing an AIDS vaccine, as described in the chapters in the section of the dissertation. After the initial success with the orginal construct (Mov1.4) (1), it was discovered that Mov1.4 had processing defects and a temperature sensitivity (7, 8), presumbly because an insert at the N-terminus of the poliovirus polyprotein disturbed myristylation of VP0. Development of new potential poliovirus vectors then ensued, with insertion sites between VP1 and 2A (Mov2.1), 2A and 2B (Mov2.5), and 3B and 3C (Mov3.5) being tested (R. Andino and D. Silvera unpublished data). Work proceeded using the Mov2.1 construct because of its wt replication kinetics. Unfortunately, inserts in this vector were rapidly deleted by RNA recombination after one to three passages (7). Therefore, Mov2.11 was developed, which had been modified to have nonhomologous flanking proteolytic cleavage site RNA sequences, which significantly reduced the levels

of insert deletion observed (7). That vector was successfully used in four mouse experiments (4-7), two of which were very successful: Steffi Mandl's demonstration that a poliovirus vaccine vector expressing a tumor antigen could elicit CTL responses and could successfully protect mice from a lethal challenge with a malignant melanoma tumor (5); and Luis Sigal's profound demonstration that CTL immunity to viruses infecting non-hematopoietic cells requires the exogenous antigen presentation pathway ((6), also see chapters 10-11 of this dissertation). The next step was to start using poliovirus vectors based on the Sabin oral poliovirus vaccine (OPV) strain viruses, which would be safe for use in humans. That is where the work in Chapter 3 begins. Additionally, it was essential to do more experiments in monkeys, and that is the focus of the work I present in the following chapters. Additional background information on the state of affairs in the worldwide AIDS vaccine effort is provided in the introduction and discussion section of each chapter.

The work presented in Chapter 3 was published in 1999 and was the first demonstration of poliovirus elicits CTLs in a primate (3). Additional unpublished data is provided as a "Supplementary Data" section appearing at the end of the chapter after the figures of the published manuscript.

The work presented in Chapter 4 has now been divided between a methods paper (manuscript in preparation) and the vaccine paper submitted to *Journal of Virology* mainly consisting of the data in Chapter 5.

Acknowledgements

Obviously an effort of this magnitude has been the work of many scientists, and several collaborators have played essential roles in bringing these projects to fruition. Professor Chris Miller was our UC Davis Primate Center collaborator, and Barbara Lohman and Lara Compton did the bulk of organizing and carrying out the experiments done at the UC Davis Primate Center. David Montefiori completed the neutralizing antibody analysis for Chapter 5, and Jeffrey Lifson analyzed the SIV viremia levels. The virus production and analysis in Chapters 4 and 5 was completed with the skilled assistance of Martha Neagu.

References

1. **Andino, R., D. Silvera, S. D. Suggett, P. L. Achacoso, C. J. Miller, D. Baltimore, and M. B. Feinberg** 1994. Engineering poliovirus as a vaccine vector for the expression of diverse antigens Science. **265:**1448-51.
2. **Carroll, M. W., and B. Moss** 1997. Poxviruses as expression vectors Curr Opin Biotechnol. **8:**573-7.
3. **Crotty, S., B. L. Lohman, F. X. Lu, S. Tang, C. J. Miller, and R. Andino** 1999. Mucosal immunization of cynomolgus macaques with two serotypes of live poliovirus vectors expressing simian immunodeficiency virus antigens: stimulation of humoral, mucosal, and cellular immunity J Virol. **73:**9485-95.
4. **Mandl, S., L. Hix, and R. Andino** 2001. Preexisting immunity to poliovirus does not impair the efficacy of recombinant poliovirus vaccine vectors [In Process Citation] J Virol. **75:**622-7.
5. **Mandl, S., L. J. Sigal, K. L. Rock, and R. Andino** 1998. Poliovirus vaccine vectors elicit antigen-specific cytotoxic T cells and protect mice against lethal challenge with malignant melanoma cells expressing a model antigen Proceedings of the National Academy of Sciences of the United States of America. **95:**8216-21.
6. **Sigal, L. J., S. Crotty, R. Andino, and K. L. Rock** 1999. Cytotoxic T-cell immunity to virus-infected non-haematopoietic cells requires presentation of exogenous antigen Nature. **398:**77-80.

7. **Tang, S., R. van Rij, D. Silvera, and R. Andino** 1997. Toward a poliovirus-based simian immunodeficiency virus vaccine: correlation between genetic stability and immunogenicity Journal of Virology. **71:**7841-50.
8. **Yim, T. J., S. Tang, and R. Andino** 1996. Poliovirus recombinants expressing hepatitis B virus antigens elicited a humoral immune response in susceptible mice Virology. **218:**61-70.

Chapter 3

Mucosal immunization of cynomolgus macaques with two serotypes of live poliovirus vectors expressing SIV antigens: stimulation of humoral, mucosal, and cellular immunity

Abstract

Poliovirus live viral vectors are a candidate recombinant vaccine system. Previous studies using this system showed that a live poliovirus vector expressing a foreign antigen from the P1/P2 junction generates both antibody and cytotoxic T lymphocyte responses in mice. Here we describe a novel *in vitro* method of cloning recombinant polioviruses involving a hybrid PCR approach. We report the construction of recombinant vectors of two different serotypes of poliovirus expressing SIV antigens, and the intranasal and intravenous inoculation of four adult cynomolgus macaques with these poliovirus vectors expressing SIV proteins $p17^{gag}$ and $gp41^{env}$. All macaques generated a mucosal anti-SIV IgA antibody response in rectal secretions. Two of the four macaques generated a mucosal antibody response detectable in vaginal lavages. Strong serum IgG antibody responses lasting for at least 1 year were detected in two of the four monkeys. SIV-specific T cell

lymphoproliferative responses were detected in three of the four monkeys. SIV-specific cytotoxic T lymphocytes were detected in two of the four monkeys. This study is the first report of poliovirus-elicited vaginal IgA antibodies or cytotoxic T lymphocytes in any naturally infectable primate, including humans. These findings support the concept that a live poliovirus vector is a potentially useful delivery system that elicits humoral, mucosal, and cellular immune responses against exogenous antigens.

Introduction

The current HIV pandemic has infected more than 30 million people, and the search for an AIDS vaccine continues. Live viral vectors are leading candidates in the hunt for a potential vaccine. Several viral vectors have showed promise in SIV protection experiments in monkeys, and numerous other live viral vector systems, including our live poliovirus vector, are in earlier testing phases of vaccine development (5, 7, 55).

Poliovirus is an attractive live viral vector for several reasons. The Sabin live poliovirus vaccine is one of the best vaccines in the world. It produces long lasting immunity (46) and herd immunity (60); it is very safe and easy to experimentally manipulate (32); it is cheap to produce and distribute in developing countries (19); and most importantly, it produces a potent mucosal immune response (42). The capacity of poliovirus to generate a strong mucosal immune response is particularly important given that greater than 90% of HIV-1 infections worldwide occurred via sexual transmission (62). Any strategy to truly control the AIDS pandemic must include a vaccine that prevents sexual transmission of HIV-1.

Natural HIV infections are persistent in virtually all infected individuals, indicating that the human immune system has grave difficulties combating the virus; however, there are several reasons to believe that a strong pre-existing mucosal anti-HIV immune response can be protective. Self-limited infections appear to occur, and a vaccine that further tips that balance at the mucosal barrier in the favor of the vaccinee may be able to fully prevent sexually transmitted HIV infections (54). Statistical data both from surveys

of individual multiple sexual partners and surveys tracking individuals exposed to HIV through needle stick injuries indicates that establishment of an HIV infection is a relatively uncommon event (30, 50). Epidemiological estimates indicate that HIV is only moderately infectious as a sexually transmitted disease, transmitted on average at a rate of 0.1% to 1% per at-risk sexual encounter (30). These statistics are supported by experiments in macaques where naive monkeys were inoculated intravaginally with a low dose of SIV and subsequent PCR analysis transiently detected SIV infected cells in circulation, without viral persistence or seroconversion (33). A strong anti-HIV mucosal immune response may prevent HIV from completing the pathogenic events necessary to establish a persistent and lethal infection.

The current gold standard for mucosal protection by a candidate AIDS vaccine is the published NYVAC-SIV work of J. Benson et al. showing almost 50% protection of macaques against a mucosal (rectal) challenge with the highly-virulent SIVmac251 (6). Interestingly, NYVAC-SIV was unable to provide protection against an intravenous challenge in this experiment. These challenge experiments suggest that generating local immunity may be as important as other characteristics of the anti-SIV immune response generated by candidate vaccines. This observation is further supported by the fact that though SIV subunit vaccinations have generally been unable to prevent disease following challenge with a virulent SIV strain, direct inoculation of a subunit vaccine into the iliac lymph nodes of macaques provided protection against a rectal mucosal challenge with a virulent SIV (23).

We have previously reported the development of a recombinant poliovirus live viral vector system where we inserted an immunogenic gene fragment of interest at the junction between the capsid proteins and the non-structural proteins (the P1/P2 junction) in the poliovirus polyprotein reading frame (61). The gene fragment is expressed with the rest of the poliovirus genome as part of the polyprotein, and is cleaved away from the polyprotein via the activity of poliovirus encoded proteases, which cleave at engineered proteolytic sites flanking the gene insert. (Fig. 1A). That recombinant poliovirus live viral vector was tested in mice susceptible to poliovirus infection (48) and demonstrated to elicit strong antibody (61) and cytotoxic T lymphocyte responses (29, 56).

Here we describe a novel *in vitro* method of generating recombinant polioviruses, the construction of recombinant polioviruses of two different serotypes, and the inoculation of cynomolgus macaques with these poliovirus live viral vectors expressing SIV antigens. Both the humoral and cellular immune responses directed against SIV antigens were characterized.

Materials and Methods

Recombinant poliovirus construction and DNA procedures. PCR reactions to construct the recombinant viruses used rTth polymerase (Perkin Elmer, Branchburg, NJ) with conditions as recommended by the manufacturer. Poliovirus type 1 cDNA (Mahoney strain) was used as template DNA to generate the type 1 poliovirus recombinants. Sabin 2 cDNA template was generated by infecting HeLa cells with an S0+3 stock (Sabin original virus isolate passaged three additional times), which was the kind gift of Konstantin Chumakov (FDA, Bethesda, MD). Total RNA from infected cells was prepared by phenol-chloroform extraction at 9 hrs post-infection and precipitated with ethanol. Reverse transcription was carried out using Superscript II (Life Technologies, Gaithersberg, MD) with either random hexamer or oligo dT primers. This Sabin 2 cDNA was used as template DNA to generate the Sabin 2 poliovirus recombinants. SIVmac239 plasmids p239SpSp5' and p239SpE3' (obtained from the AIDS Research and Reference Reagent Program, courtesy of Ronald Desrosiers (22)) were used as the PCR template to generate SIV inserts. Poliovirus type 1 5'Arm was amplified with primers 1 and 2, and the 3'Arm with 3 and 4. An XhoI restriction site was introduced at the P1/P2 junction of the 5'Arm, and an EcoRI site was introduced at the P1/P2 junction of the 3'Arm PCR product. Proteolytic cleavage sites flanking the restriction sites were designed to be non-homologous, and a five glycine linker was introduced upstream of the XhoI site on the 5' side of the P1/P2 junction, comparable to the design of pMov2.11 (61). Restriction enzyme cleavage of the PCR products was done prior to hybrid PCR to generate clean termini at the SIV gene fragment insertion site.

When necessary, PCR products were purified by agarose gel electrophoresis and recovered using a Qiagen Gel Extraction kit (Valencia, CA). Polio1 SIV inserts were generated with primers 5 and 6 (p17), 7 and 8 (gp41), 9 and 10 (p28). For Sabin 2, the 5'Arm was amplified with 11 and 12, and the 3'Arm with 13 and 14. Sabin 2 inserts were generated using primers 15 and 16 (gp41), 17 and 18 (p17), and 19 and 20 (p28).

Hybrid PCRs were carried out using approximately 200 ng 5'Arm template DNA and equimolar amounts of 3'Arm and the SIV DNA fragment. PCR conditions were as follows: 95°C for 3', then rTth polymerase was added and 11 cycles of PCR were carried out with 95°C for 1', 50°C for 1', and 72°C for 4'. Primers 1 and 4 were used to amplify the Polio1 recombinants, and primers 11 and 14 were used to amplify the Sabin2 recombinants.

Full length viral RNA was generated from hybrid PCR DNA using T7 RNA polymerase and 1 μg of template in a standard *in vitro* transcription reaction (10 x transcription buffer from Roche Molecular Biochemicals (Indianapolis, IN) and 20 U RNasin (Promega, Madison, WI)) at 37°C for 1 hr. The presence of full length RNA was confirmed by agarose gel electrophoresis.

Replication competent recombinant polioviruses were recovered by transfection of adherent HeLa S3 cells with 5 μg RNA using the DEAE-dextran method (61), overlaying the monolayer with 1% agar/ DMEM + 10% newborn calf serum (Life Technologies), incubating at 32°C, and picking individual viral plaques five days post-transfection. Individual plaques were then passaged twice on HeLa cells, with the first

passage at a multiplicity of infection (MOI) of 0.001 and the second at an MOI of 1, to generate the P2 stocks of 10-100 ml of virus used for immunizations.

Viral infections and stocks. In all experiments, 80% confluent 10 cm dishes of HeLa cells containing approximately 5 x 10^6 cells were used. Dishes were washed with phosphate-buffered saline (PBS), and virus was added at the desired MOI in a volume of 200 ul. Dishes were incubated at room temperature for 15 min to allow viral adsorption, then 3 ml of medium was added and dishes were incubated at 32°C (5% CO_2) until cytopathic effect (CPE) was visible. Virus was recovered by centrifugation of the cells and medium at 3000 g for 5 min followed by three quick freeze/thaw cycles. After re-centrifugation, the cleared supernatant containing recombinant poliovirus was transferred to a fresh tube and stored at -20°C.

Neutralization assays were carried out using the desired volume of monkey serum (25-90 ul) mixed with 1000 pfu of the appropriate virus (poliovirus type 1 (Mahoney strain) or 2 (Sabin 2)) in 100 ul total volume (brought to volume with PBS). Serum was incubated with virus for 30' at room temperature, then serial dilutions were made and added to HeLa cell dishes for 15 min to allow for viral adsorption. Plates were washed once with PBS before adding a 1x DMEM/F12 and 1% agar overlay. Plaque assays were then incubated at 37°C for 2 days (type 1 poliovirus assays) or 3 days (type 2 poliovirus assays). Agar overlays were then removed and plates were stained with a vital dye (0.1% crystal violet, 20% ethanol) to reveal the viral plaques, which were counted. 90% neutralization was established as a 10x reduction in the number of plaques as compared to

the number of plaques counted on a no monkey serum control plate, or by using preimmune monkey serum.

RT-PCR. Presence of the SIV gene fragments in the recombinant polioviruses was confirmed by RT-PCR. Total RNA was isolated from cells at 9.5 hrs post-infection using RNeasy (Qiagen) as per the manufacturer's protocol. cDNA was generated by reverse transcription using Superscript II (Life Technologies) and oligo dT primers, following the manufacturer's recommended protocol. PCR was carried out using PfuTurbo (Stratagene, La Jolla) with the manufacturer's recommended reagents and the following conditions: 95°C for 3 min, then 30 cycles of 95°C for 1 min, 50°C for 1 min, and 72°C for 1 min. PCR products were analyzed on a 1.2% agarose gel buffer. Primers used for Polio1 recombinants were designated 21 and 22. Primers for Sabin2 were designated 23 and 24.

Western blotting and immunofluorescence. Expression of the SIV antigens by the recombinant polioviruses was confirmed by western blotting and immunofluorescence assays. For western blotting, HeLa cells infected with wild-type - or SIV-recombinant polioviruses (MOI of 1 to 5) were incubated for 9 hr at 37°C. Cells were harvested, lysed on ice for 1' (lysis buffer: 10 mM Tris pH 7.5, 140 mM NaCl, 5 mM KCl, 1% Np-40), and nuclei were removed by centrifugation (3). 4 μg of total lysates was loaded on an SDS-12% polyacrylamide gel and analyzed by immunoblotting. The anti-SIV antiserum used was obtained as a pool of serum from SIV-infected rhesus macaques (*macaca mulatta*). Antiserum directed against poliovirus capsid proteins was obtained by inoculating rabbits with purified poliovirus. Horseradish peroxidase (HRP) conjugated

secondary antibodies (both anti-human and anti-rabbit), and ECL chemiluminescence detection kits were obtained from Amersham (Arlington Heights, IL).

Western blots were also used to test for monkey anti-poliovirus antibodies. In these experiments, HeLa cells were infected at an moi of 5 with type 1 (Mahoney strain), type 2 (Sabin 2 strain), or left uninfected. Cells were harvested at 5 hr (type 1) or 5.5 hr. (type 2) post-infection, lysed, and nuclei were removed by centrifugation. The protein concentrations were quantified by Bradford assay and 25 ug total lysate was run on a 12% SDS-PAGE gel before blotting. Blots were probed with 1:200 diluted monkey serum in TBST (10 mM Tris-HCl pH 7.5, 150 mM NaCl, 0.1% Tween-20), washed three times, probed with the HRP anti-human antibody (1:2000 dilution), and then detected using ECL. Images were digitally scanned and exported to Adobe Photoshop 3.0 and Illustrator 7.0 (San Jose, CA).

For immunofluorescence assays, adherent HeLa cells infected with wild-type- and SIV-recombinant polioviruses (MOI of 0.3) were incubated for 9 hr at 37°C. Cells were then fixed with 2% paraformaldehyde and stained with the appropriate primary antibody for 1 hr at 25°C in a PBS buffer supplemented with 3% BSA and 0.2% saponin buffer. After three PBS washes, cells were then stained with secondary antibody for 1 hr at 25°C in an identical buffer. Anti-SIV and anti-poliovirus antibodies were as described above. Anti-rabbit IgG conjugated to Texas Red and anti-monkey IgG conjugated to FITC secondary antibodies were obtained from Amersham. Stained cells were visualized for immunofluorescence using a Leica DMLB microscope, and images were captured via a CCD camera and exported to Adobe Photoshop 3.0.

Oligonucleotides. The oligonucleotides used were as follows: 1 (TAATACGACTCACTAT AGGTTAAAACAGCTCTGGGGTTGT [S1-T7]), 2 (GAGTTTCTCACGCCGAATTCACCTC CCCCACCTCCGCCATGACCAAAACCGTAAGTCGTTAAGTCCTTGGTGGAGAGGGGTG [RA5'3']), 3 (GAAATTACCTCGAGGATCTGACCACATATGGATTCGGACACCAAAACAA [RA3'5']), 4 (TTTTTTTTTTTTTTTTTTCTCCGAATTAAAGAAAAATTTACCCC [Mo3']), 5 (GGAGGTGGGGG AGGTGAATTCGGCGTGAGAAACTCCGTC [Sp175']), 6 (ATAGTGGGTCAGATCCTCGAGGT AATTTCCTCCTCTGCC [Sp173']), 7 (GGAGGTGGGGGAGGTGAATTCCCATGGCCAAATGCA [Gp41.b5']), 8 (ATAGTGGGTCAGATCCTCGAGGGAAGAGAACACTGG [Gp41.b3']), 9 (GGAGGTGGGGGAGGTGAA TTCCCAGTACAACAAATAGGT [Sp275']), 10 (ATAGTGGGTCAGATCCTCGAGCATTAATCTAG CCTTCTG [Sp283']), 11 (TAATACGACTCACTATAGGTTAAAACAGCTCTGGGGTTG [S2-T7]), 12 (TTTGGCCATGGCTCGAGACCTCCCCCACCTCCGCCATGACCAAAACCATAAGTCGTTAAT CCCTTTTC [S25'3']), 13 (CTCTTCCGAATTCGACTTAACGACTTACGGATTTGGACACCAAAACAA AGCTGTGTACACAGCTGGCTA [S23'5']), 14 (TTTTTTTTTTTTTTTTTTTCCCCGAATTAAAGAAA AATTTACCCC [S23']), 15 (GAAAAGGGATTAACGACTTATGGTTTTGGTCATGGCGGAGGTGG GGGAGGTCTCGAGCCATGGCCAAATGCAAGT [S2gp41.5'], 16 (GTACACAGCTTTGTTTTGGT GTCCAAATCCGTAAGTCGTTAAGTCG AATTCGGAAGAGAACACTGGCCT [S2gp41.3']), 17 (GAAAAGGGATTAACGACTTATGGTTTTGGTCATGGCGGAGGTGGGGGAGGTCTCGAGGG CGTGAGAAACTCCGTC [S2sp17.5']), 18 (GTACACAGCTTTGTTTTGGTGTCCAAATCCGTA AGTCGTTAAGTCGAATTCGTAATTTCCTCCTCTGCC [S2sp17.3']), 19 (GAAAAGGGATTAA CGACTTATGGTTTTGGTCATGGCGGAGGTGGGGGAGGTCTCGAGCCAGTACAACAAATAGG T [S2sp28.5']), 20 (GTACACAGCTTTGTTTTGGTGTCCAAATCCGTAAGTCGTTAAGTCGAA TTCCATTAATCTAGCCTTCTG [S2sp28.3']), 21 (CCTCCAAAATCAGAGTGTATC [P1-3240F]), 22 (GCCCTGGGCTCTTGATTCTGT [P1-3580R]), 23 (CACCTCCAAGATCAGAGTGTA [S2-3240F]), and 24 (ATCGAGTCGGTGCCAAGGGCC [S2-3540R]).

Animals. All animals used in this study were mature, cycling, female cynomolgus macaques *(Macaca fascicularis*, referred to as *Macaca iris* in old literature) from the California Regional Primate Research Center. The animals were housed in accordance with American Association for Accreditation of Laboratory Animal Care standards. When necessary, animals were immobilized with 10 mg of ketamine HCl (Parke-Davis, Morris Plains, N.J.) per kg of body weight injected intramuscularly. The investigators adhered to the Guide for the Care and Use of Laboratory Animals prepared by the Committee on Care and Use of Laboratory Animals of the Institute of Laboratory Resources, National Resource Council. Prior to use, animals were negative for antibodies to HIV-2, SIV, type D retrovirus, and simian T cell leukemia virus type 1.

Intranasal inoculations were done in a total volume of 1 ml. The animals were anesthetized and placed in dorsal recumbancy with the head tilted back. One half ml of virus was instilled dropwise into each nostril. The animals were kept in this position for 10 min and then placed in lateral recumbancy until recovery from the anesthesia (21). Intravenous inoculations were administered in the arm in a volume of 1 ml. Five cynomolgus macaques originally received the first series of intranasal inoculations with Polio1-p17 and Polio1-gp41. One monkey developed paralytic disease three weeks later and was euthanized; the CNS infection of this monkey was most likely via direct infection of the olfactory bulb, which is a specific alternative pathway poliovirus infection of macaques and irrelevant, not occurring in humans (10, 36).

Serum and vaginal and rectal lavage antibody responses. Anti-SIV IgG and IgA responses in vaginal and rectal washes and serum were measured at regular timepoints

during the study. Vaginal and rectal wash samples were collected and analyzed as previously described (27, 34). Briefly, vaginal washes were collected by infusing 6 ml of sterile PBS into the vaginal canal and aspirating the instilled volume. Rectal washes were collected in a comparable manner. Samples were immediately snap-frozen on dry ice and stored at -80°C until analysis. To account for the presence of IgG interfering with and reducing the detection of IgA, sera was first depleted of IgG using Protein G-sepharose beads (Pharmacia Biotech, Uppsala, Sweden) prior to use in the IgA ELISA. To deplete IgG, 25 ul of serum sample was incubated with 100 ul Protein G-sepharose beads for 1 hr at 37°C and then 4°C overnight, and then the Protein G-sepharose was pelleted and the supernatant was collected. Dilution of sample during this process was 1:3. All serum and secretion samples were initially screened for reactivity against whole SIV using a 1:100 final dilution of sera and a 1:4 dilution of vaginal or rectal washes. The ΔOD between test and control wells was defined as the difference between the mean OD of sample tested in two antigen-coated wells and the mean OD of the sample tested in two antigen-free control wells. The negative control OD value was determined from 12 uninfected monkey serum samples and defined stringently as the average OD plus 3 standard deviations. Endpoint titers were determined if the ΔOD of the test sample exceeded the negative control value by a factor of 2. To then quantify anti-SIV antibody titers, serial four-fold dilutions of duplicate samples of sera, vaginal wash, or rectal wash were tested by ELISA using whole pelleted SIVmac251 (Advanced Biologics Ind., Columbia, MD). Antibody binding was detected with peroxidase conjugated goat anti-monkey-IgG(Fc) or -IgA (Fc)

(Nordic Laboratories, San Juan Capistrano, CA) and developed with o-phenlyenediamine dihydrochloride (Sigma). The endpoint titer was defined as the reciprocal of the last dilution giving a ΔOD greater than 0.1.

Lymphocyte proliferative responses to SIV antigens. Antigen specific proliferative responses against SIV gag and Env proteins were measured in peripheral blood mononuclear cells (PBMCs) from fresh blood samples (31). PBMCs were purified from heperanized blood by Accu-Paque cell separation media (Accurate Chemical & Scientific Corp., Westbury, NY). The cells were suspended at 2×10^6 per ml in RPMI-1640 medium supplemented with 10% fetal calf serum (FCS) and plated in triplicate in volumes of 50 ml in a 96-well round-bottomed plate. SIV or control antigens at a concentration of 10, 1.0, and 0.01 mg/ml were added to the cells in 50 ml of complete medium. 100ml of fresh medium was added after 48 hrs and the plates were incubated 5 days at 37°C in a CO_2 incubator. The cell cultures were pulsed with [3H]thymidine overnight prior to harvest (1 mCi per well, NEN-DuPont, Wilmington, Del.). The SIV antigens were SIVmac239 $p55^{gag}$ and SIV$gp140^{env}$ (provided by F. Vogel (N.I.H.) via Biomolecular Technology, Frederick, MD). A lysate of the fall armyworm ovary cell line, Sf9 used for the production of baculovirus-expressed $p55^{gag}$, was used as a negative control for $p55^{gag}$, and the medium alone was the control for $gp140^{env}$. The stimulation index was defined as the mean radioactive counts per minute of replicate SIV antigen wells divided by the mean counts per minute of control wells and was considered significant if

≥ 2.0. In a series of preliminary experiments the proliferative responses to SIV antigens of 10 macaques that had not been exposed to SIV were tested. It was determined that a level of 200 cpm in the negative control wells was required to eliminate false positive SIs (31).

Detection of SIV-specific CTL activity. The details of culture and detection of bulk, secondary CTL responses have been previously reported (25, 26, 33). Briefly, PBMCs from immunized monkeys were stimulated with 10 ug/ml Con A (Sigma) and cultured for 14 days in complete medium supplemented with 5% human lymphocyte-conditioned medium (Hu IL-2, Hemagen Diagnostics, Waltham, MA). Autologous B cells were transformed by *Herpes papio* (595Sx1055 producer cell line, provided by M. Sharp, Southwest Foundation for Biomedical Research, San Antonio, TX), and infected overnight at an MOI of 30 with wild-type vaccinia virus (vvWR), or recombinant vaccinia expressing the $p55^{gag}$ (vv-gag) or $gp160^{env}$ (vv-env) of SIVmac239 (provided by L. Giavedoni and T. Yilma, University of California, Davis, CA). The level of vaccinia virus infection of target cells was estimated by indirect immunoflorescence using monkey anti-vaccinia virus antibody, followed by fluoresceinated goat anti-human IgG (Vector Laboratories, Burlingame, CA). The level of vaccinia virus infection of target cells in this series of experiments was estimated to fall between 5 and 15%.

Target cells were labeled with 50 mCi of ^{51}Cr (Na_2CrO_4, Amersham Holdings, Arlington Heights, IL) per 10^6 cells. Effector and target cells were added together at multiple E:T ratios in a 4 hr chromium release assay. Specific lysis was considered positive if it was greater than twofold above the lysis of vvWR targets and if it was at least

10%. For 2 animals at the time of necropsy (71 weeks post-inoculation), a limiting dilution assay for virus specific CTL precursors was preformed. The assay was based on a previously described methods (21, 26). Briefly, isolated PBMCs or mesenteric lymph node mononuclear cells (LNMCs) were diluted 11 times over the range of 10,000 cells per well to 100 cells per well and cultured in replicates of 24 wells. The cells were stimulated with Con A (5 ug/ml, Sigma) and supplemented with irradiated human PBMCs as feeder cells at a concentration of 4 x 10^5/well. The percentages of $CD3^+CD8^+$ T cells were identified by flow cytometry using double surface immunofluorescence staining with fluorescein isothiocyanate-conjugated anti-human CD3 (Gibco) and phycoerythrin-conjugated anti-human CD8 (Gibco). The cultures were maintained in AIM-V medium (Gibco), supplemented with 20% FCS and 5% human IL-2 (Hemagen Diagnostics). The level of cytolytic activity was measured on day 14, when wells were split three ways and incubated for 5 hr with an autologous target cell infected with vvWR, vv-gag, or vv-env, as described above. Positive wells were identified as wells that exceeded the negative control (the mean chromium release from wells without effector cells) by 3 standard deviations. Wells containing cells that lysed uninfected autologous targets were eliminated from the calculations. The precursor frequency was determined by chi-square analysis based on maximum likelihood by a computer program provided by Dr. R. Miller (University of Michigan, Ann Arbor, MI).

Results

***In vitro* construction of recombinant polioviruses.** We generated recombinant polioviruses containing SIV gene fragments by a novel *in vitro* PCR-based approach. Briefly, the 5' and 3' halves of the poliovirus genome (5'Arm and 3'Arm, respectively) were amplified as two separate PCR products from type 1 poliovirus cDNA (Fig. 1A,B). An SIV gene fragment coding for the Gag protein p17 was amplified from an SIVmac239 plasmid clone and flanked by poliovirus $2A^{pro}$ cleavage sites plus 45 bp of sequence identity with the 3' terminus of poliovirus PCR DNA fragment 5'Arm and 45 bp of overlap with the 5' terminus of poliovirus fragment 3'Arm. These three separate DNA fragments—poliovirus 5'Arm, SIV $p17^{gag}$, and poliovirus 3'Arm—were mixed together and amplified into a single full length recombinant virus DNA clone by hybrid PCR, where the termini of each overlapping DNA fragment serves as a primer for the synthesis of the complementary strands of its neighboring DNA fragment, resulting in the ligation of the three DNA fragments. Further amplification of the full length Polio1-p17 was provided by 10 cycles of standard polymerase chain reaction using 5' and 3' primers terminal to the full length product (see Materials and Methods). This amplified full length Polio1-p17 recombinant virus DNA contained the $p17^{gag}$ gene fragment (SIV Gag a.a. 2-135) at the P1/P2 junction, between the genes for the structural and nonstructural proteins of the virus. Infectious RNA was then generated by a standard *in vitro* T7 transcription reaction (Fig. 1C). The transcribed RNA was then transfected into HeLa

cells, and virus was recovered. The recovered Polio1-p17 virus exhibited growth characteristics comparable to other recombinant polioviruses we have previously generated (61). Two additional type 1 recombinant polioviruses containing fragments of SIV $p28^{gag}$ (SIV Gag a.a. 136-364) and $gp41^{env}$ (SIV Env a.a. 523-628) were generated using the same *in vitro* construction technique. Each of the viruses grew to titers of ~3 x 10^8 and generated plaques that were 50-80% as large as wild-type poliovirus type 1 (data not shown). Expression of SIV protein in HeLa cells infected with Polio1-p17, Polio1-gp41, and Polio1-p28 was confirmed by western blot (Fig. 1D). This SIV protein expression is equimolar to that of each of the endogenous poliovirus proteins, as the single poliovirus open reading frame is initially translated as a polyprotein (Fig. 1A).

This novel *in vitro* method for constructing recombinant polioviruses was then used to generate a poliovirus live viral vector utilizing the Sabin 2 vaccine strain, which is a type 2 serotype poliovirus and is not neutralized by antibodies directed against type 1 poliovirus (36). Sabin2-p17, Sabin2-gp41, and Sabin2-p28 viruses were produced this way, and expression of their respective SIV gene fragments in human HeLa cells was confirmed by western blot (data not shown) and fluorescent immunodetection (Fig. 2) (see Materials and Methods). Each of the Sabin 2 recombinant viruses grew to titers of ~5 x 10^8 and generated plaques that were 50-80% as large as Sabin 2 poliovirus (data not shown).

Genetic stability can be an issue with live poliovirus vectors (38, 61). Therefore we quantified the percentage of viruses still expressing SIV protein in immunodetection

assays done on the passage 1 (P1) viral stocks. The immunodetection was done at an MOI of 0.3, and greater than 90% of the HeLa cells positive for poliovirus proteins were also positive for SIV proteins (Fig. 2, and data not shown), indicating that the P1 viral stocks were greater than 90% pure. This percentage were confirmed by RT-PCR using primers flanking the P1/P2 junction. Viruses Polio1-p17, Polio1-gp41, Sabin2-p17, and Sabin2-gp41 were passaged one additional time (P2) at an MOI of 1 to generate the viral stocks used for immunization of monkeys. RT-PCR of the P2 virus stocks indicated that 60-80% of each viral population still contained the full SIV insert.

Monkey immunizations. Our primary goal was to determine whether these recombinant polioviruses expressing SIV gene fragments stimulated a mucosal anti-SIV immune response at multiple locations in macaques. Cynomolgus macaques *(Macaca fascicularis)* are known to be orally and intranasally susceptible to poliovirus, whereas most other Old World primate monkey species are not orally or intranasally susceptible to poliovirus infection and only present clinical symptoms after intracerebral or intraspinal inoculation (9, 10, 12, 51). Therefore, we first titered poliovirus in a group of cynomolgus monkeys and established that a dose of 10^6 PFU of type 1 poliovirus was the minimal dose necessary to reliably seroconvert 100% of cynomolgus macaques when inoculated intranasally (data not shown).

We then designed our recombinant poliovirus immunization as follows: four 2 x 10^7 pfu intranasal inoculations of a mixture of Polio1-p17 and Polio1-gp41 (one dose every three days), followed eleven weeks later by three 1 x 10^7 pfu intranasal inoculations of a mixture of Sabin2-p17 and Sabin2-gp41. By using poliovirus live viral vectors derived

from two different serotypes (1 and 2), we hoped to avoid vector neutralization problems and increase our ability to boost the immune response against the SIV fragments. The SIV fragments used in these experiments were previously shown to be immunogenic in mice when expressed by a recombinant poliovirus, therefore we had reason to believe that they may be immunogenic in macaques as well (61).

An intravenous booster inoculation was given to all four monkeys 38 weeks into the experiment, and will be discussed later.

Intranasal immunization induced serum anti-SIV IgG and IgA responses. The results of ELISA assays for serum IgG and IgA responses against SIV are shown in Figure 3. Three out of four monkeys (25136, 25137, 26394) developed strong anti-SIV IgG antibody responses after intranasal inoculation with Polio1-p17 and Polio1-gp41 (Fig. 3A). The second set of intranasal immunizations using Sabin2-p17 and Sabin2-gp41 induced an anamnestic response in two monkeys (25136 and 26394) as evidenced by enhanced serum anti-SIV IgG levels. Both of these monkeys then maintained a strong long-term anti-SIV IgG response with titers between 1:1,000 and 1:10,000 (Fig. 3A). In addition to this IgG response, monkey 25136 developed a strong and persistent serum anti-SIV IgA response after intranasal immunization (Fig. 3B).

In summary, intranasal immunization with these four recombinant polioviruses elicited anti-SIV serum IgG in three out of four monkeys and anti-SIV serum IgA in one monkey. Therefore the recombinant polioviruses replicated *in vivo* and effectively expressed immunogenic SIV antigens.

Intranasal immunization induced rectal and vaginal anti-SIV antibody responses. The common mucosal immune system theory proposes that immunization at one mucosal site will induce immunity detectable in other mucosal sites (40). Looking for evidence of such a broad mucosal response with poliovirus, we measured anti-SIV antibody titers in rectal washes and vaginal secretions after the intranasal inoculations with Polio1-p17, Polio1-gp41, Sabin2-p17, and Sabin2-gp41.

Following a single intranasal immunization, three of the four monkeys generated a rectal anti-SIV IgA response, and every monkey tested positive for rectal IgA after both sets of intranasal immunizations (Fig. 4A). One monkey (26394) had detectable anti-SIV IgA levels in vaginal lavage after the Sabin2-gp41 and Sabin2-p17 intranasal immunization (Fig. 4B). This monkey also made an IgG vaginal anti-SIV response (Fig. 4B). The vaginal and rectal lavages from the other three monkeys tested negative for anti-SIV IgG in the screening ELISA and were not analyzed further. Thus, intranasal immunization with recombinant polioviruses expressing SIV antigens generated a substantial IgA response in rectal secretions, even though only one monkey tested positive for serum IgA. In contrast, the IgA response to the SIV antigens was more limited in vaginal secretions.

Surprisingly, intranasal immunization induced a pure mucosal anti-SIV antibody response in one monkey. The anti-SIV response of monkey 22701 consisted only of IgA present in rectal secretions (Fig. 4A).

All monkeys seroconverted to poliovirus. Anti-poliovirus serum antibodies were detected in all four monkeys after the intranasal inoculations (Fig. 5A). These antibodies readily detected both type 1 and type 2 poliovirus (Fig. 5A). Three of the four monkeys

generated neutralizing antibodies against type 1 poliovirus that were detectable after the intranasal inoculations with Polio1-gp41 and Polio1-p17, and these neutralizing antibodies were maintained for at least three months (Fig. 5B). Two of the monkeys also developed neutralizing antibodies against Sabin2 (22701 and 26394). The strong vaginal IgA anti-SIV response seen in monkey 26394 was detected only after the Sabin2-gp41 and Sabin2-p17 inoculations. Therefore, neutralizing antibodies specific for type 1 poliovirus did not prohibit replication of the Sabin2 recombinant viruses in this monkey. Monkey 22701 appears to have generated uncommon cross-neutralizing antibodies after the Polio1-gp41 and Polio1-p17 infections.

Intranasal immunization induced anti-SIV T cell proliferative responses. Anti-poliovirus helper T cell immune responses have been reported in humans and mice immunized with the Sabin poliovirus vaccine (14, 28, 57). To determine if immunization of monkeys with our recombinant polioviruses elicited SIV-specific T helper lymphocytes, the proliferative response of primary blood mononuclear cells (PBMCs) was determined following *in vitro* stimulation with SIV antigens (see Materials and Methods). Data from all four monkeys are shown in Table 1. Two monkeys (25137 and 26394) generated an SIV Gag specific lymphoproliferative response after the intranasal immunizations.

Intravenous booster immunization induced an anamnestic anti-SIV antibody response in the intranasally primed monkeys. To augment the humoral and cellular responses generated after intranasal immunization, the monkeys were boosted intravenously with a mixture of all four recombinant polioviruses expressing SIV antigens

$p17^{gag}$ and $gp41^{env}$. The intravenous boost given 38 weeks after the initial intranasal immunization generated a rapid but transient increase in serum anti-SIV IgG titers in three of the four monkeys (25136, 25137, 26394), and a serum anti-SIV IgA increase in two of the four monkeys (25136, 26394), with levels soon returning to the pre-intravenous boost levels (Fig. 3).

Following the intravenous boost, monkeys 25136 and 26394 had low but detectable vaginal anti-SIV IgA titers (1:2 to 1:4) in the lavages collected between 2 and 12 weeks after the intravenous boost (Fig. 4B). Interestingly, 26394 was the same monkey that showed a vaginal IgA response after the intranasal inoculations. Monkeys 25136 and 26394 not only made a vaginal anti-SIV IgA response, but also vaginal anti-SIV IgG antibodies several weeks after the intravenous boost (Fig. 4B).

At the time of the intravenous boost, 9 months after the initial intranasal inoculation, anti-SIV IgA levels were undetectable in the rectal washes of all monkeys. The intravenous immunization resulted in an return of detectable anti-SIV rectal IgA in two of the four animals (25136 and 25137), present for at least 3 months after the immunization. As expected, the intravenous boost had no effect on specific IgG levels in rectal washes.

Animal 22701, which made a purely IgA anti-SIV response after the intranasal inoculations, did not produce detectable antibodies after the intravenous boost (Fig. 3, 4). However, this animal did make notable anti-SIV lymphoproliferative responses to both $p17^{gag}$ and $gp41^{env}$ antigens after the intravenous boost (Table 1).

Intravenous booster immunization induced anti-SIV cytotoxic T lymphocytes.

Cytotoxic T lymphocyte (CTL) responses have not been previously reported for live poliovirus vaccinations in humans or other primates (60). We have reported the ability of our poliovirus live viral vectors to generate a cytotoxic T lymphocyte response against a model antigen (chicken ovalbumin) in mice (29, 56). Additionally, anti-HIV CTLs may be an important part of an AIDS vaccine. Therefore, we were interested in whether or not our poliovirus vectors expressing SIV proteins would stimulate anti-SIV cytotoxic T lymphocytes in macaques.

Each monkey was tested at several timepoints for anti-SIV cytotoxic T cells using a bulk peripheral blood mononuclear cell (PBMCs) cytolytic assay. Anti-SIV CTLs specific for Env were consistently detected in monkey 25136 from week 19 through week 42, though it was difficult to obtain greater than 10% specific lysis (Fig. 6A). This was the only monkey with detectable Env specific CTLs by bulk culture assay. Anti-SIV CTLs specific for Gag were not detected in any monkeys after the two intranasal inoculations. But after the intravenous booster inoculation, Gag specific CTLs were detected in monkeys 25137 and 25136 (Fig. 6A and data not shown) using the bulk culture assay. These were the same two monkeys that made substantial rectal IgA and rapid serum IgG antibody responses following the intravenous inoculation (Fig. 3A, 4A).

At 71 weeks after the initial immunization, all four monkeys were euthanized. Our bulk culture CTL assays appeared to have limited sensitivity; therefore we tested for the presence of cytotoxic T cells by limiting dilution assay using cells isolated from mesenteric LN (26394) and peripheral blood (25137). PBMCs from monkey 25137

contained T cells with a substantial amount of anti-Env cytotoxic T lymphocyte activity (Fig. 6B), giving a calculated Env-specific CTL precursor frequency of 3539 per 10^6 $CD8^+$ cells. Gag-specific cytotoxic T cells were detectable at a lower frequency of 178 per 10^6 $CD8^+$ cells. This data, though striking, is partly inconsistent with the results obtained by bulk culture assay. We were able to detect Gag-specific CTLs in monkey 25137 by bulk culture assay at week 42, which is in agreement with the detection of Gag-specific CTLs by limiting dilution assay at week 71. However, we were unable to detect Env-specific CTLs in monkey 25137 by bulk culture at any time point, whereas the limiting dilution assay detected a high level of Env-specific CTLs in blood. The limiting dilution assay is a more sensitive assay, supporting the outgrowth of low frequency antigen specific precursors, while the bulk culture method is more dependent on initial strong stimulation of the T cells. Env-specific CTLs were not detectable in the mesenteric lymph nodes of monkey 26394, which had no detectable Gag- or Env-specific CTLs at any timepoint by bulk PBMC culture assay.

The results presented here indicate that inoculation of non-human primates with poliovirus recombinants results in both humoral and cellular immune responses. The vaccinated monkeys were not challenged with SIV because only two partial SIV proteins constituted our immunization cocktails, and it is likely that a more complex composition of antigens would be required to afford protection. We are currently developing a cocktail of recombinant polioviruses containing most of the SIV proteins, which will be much more suitable for a vaccination and challenge experiment.

Discussion

Here we have constructed a set of poliovirus live viral vectors *in vitro* that contain SIV antigens. The *in vitro* PCR-based technique that we describe in this paper should be generally applicable for working with RNA viruses that are very difficult or impossible to clone. We then used these polioviruses expressing SIV antigens to immunize macaques and have characterized the monkeys' immune responses.

Analyzing the mucosal immune response generated by the live poliovirus vector was a primary goal of this study. High levels of mucosal IgA poliovirus neutralizing antibodies are directly correlated with sterilizing immunity against poliovirus (24, 42, 53). These high levels of IgA are produced in humans vaccinees inoculated orally with the Sabin live attenuated poliovirus, and the vaccinees make a potent anti-polio IgA response throughout the nasopharyngeal, alimentary, and rectal mucosal surfaces, which persists for several years or more (41-43). Generally, humans secrete the highest anti-poliovirus neutralizing antibody titers in saliva, with moderately lower mucosal antibody production in both the rectum and the female vagina (43, 45). In the only human Sabin vaccinee who has been tested for anti-poliovirus vaginal antibodies, no IgA was detected (45). Our report here of anti-SIV IgA present in the vaginal secretions of two recombinant poliovirus inoculated monkeys is the first direct evidence of live poliovirus induced IgA in the vagina (Fig. 4B). Additionally, anti-poliovirus vaginal IgA was detected in other cynomolgus monkeys we have assayed (unpublished results).

We previously reported that a related recombinant poliovirus vector could infect a cynomolgus macaque via the rectal mucosa and generate a rectal IgA response (4). Here we have shown that the immunogenicity of poliovirus in stimulating a mucosal IgA response at multiple locations can be conferred on exogenous sequences expressed by a poliovirus live viral vector inoculated intranasally.

The one monkey exhibiting a purely mucosal anti-SIV antibody response is a fascinating case of local immunity. There have been some published reports in the past that live poliovirus infection can stimulate a purely mucosal immune response (52), but recent Sabin polio vaccine studies have all detected serum IgG in conjunction with mucosal IgA responses in immunized children (13, 59). In fact, we were able to detect some anti-poliovirus, but not anti-SIV, antibodies in the serum of this monkey. Using inactivated poliovirus, Ogra and Karzon could induce secretory IgA in the vagina, uterus, rectum, or nasopharynx of children following high dose local immunizations, and these children showed no evidence of anti-poliovirus IgG serum antibodies (42, 44, 45). However, since those experiments used inactivated poliovirus virions, and expression of the recombinant proteins in our live poliovirus vectors is dependent on replication, the relationship between the two experiments is unclear.

It is worth noting that, though we did not directly test this, the monkeys in our experiment most likely secrete similar or higher IgA levels in saliva than rectal and vaginal secretions, since the respiratory tract of cynomolgus monkeys is much more susceptible to poliovirus infection than the lower alimentary tract (10-12, 16, 51), and mucosal immunity is normally strongest at the site of inoculation (40). Salivary IgA is not a crucial

parameter in the development of a candidate SIV vaccine, but may be essential for the development of vaccines against pathogens that replicate in the respiratory tract. We plan to further characterize the breadth of the IgA response stimulated by this live poliovirus vector in future experiments.

Several of the monkeys made very high IgG responses, indicating that the recombinant polioviruses replicated quite well when administered intranasally. Additionally, the booster response seen in two of the monkeys when the second serotype of recombinant polioviruses was administered indicates that significant cross-neutralization between the serotypes does not occur, as was expected (36) (though one monkey did appear to generate cross-neuralizing anti-poliovirus antibodies this generally is not seen in human vaccinees). Therefore we may be able to utilize all three serotypes of poliovirus as serial vaccine vectors, giving multiple boosts to stimulate a strong and durable immune response, as we saw in monkeys 25136 and 26394 with the use of two serotypes in this study. These two monkeys maintained a high level of anti-SIV IgG serum antibodies for greater than a year. We note that natural poliovirus infections have been documented to result in persistent IgG neutralizing antibodies for greater than 40 years (46).

Human $CD4^+$ helper T cells specific for poliovirus were first identified several years ago by two seperate groups who isolated $CD4^+$ clones specific for capsid protein epitopes from people vaccinated with Sabin live attenuated poliovirus vaccine (14, 57). However, T cells specific for non-structural proteins were not identified. In addition, poliovirus-specific T cells have not previously been reported in monkey models. We

detected lymphoproliferative responses, indicative of $CD4^+$ helper T cells, specific for SIV antigens in three of the four monkeys (Table 1). Lymphoproliferative responses were detected to both viral SIV inserts, indicating that both the $p17^{gag}$ and $gp41^{env}$ recombinant polioviruses replicated within the monkeys and stimulated antigen specific helper T cell responses in this study. The level of the antigen specific proliferative responses was similar to levels reported in other studies using cynomolgus macaques (35, 39). $CD4^+$ helper T cells are essential for generating a strong antibody response and to promote heavy chain class switching to IgG and IgA (1). The monkey that we could not detect any lymphoproliferative response in (25136) was the monkey with the highest long-term anti-SIV IgG and IgA titers. We believe that it may be the case that monkey 25136 produced significant SIV-specific $CD4^+$ cells, but detection was difficult because the majority of SIV-specific $CD4^+$ cells were not circulating in the peripheral blood, and were instead locally present in the gut- and bronchus- associated lymphoid tissue (GALT and BALT) or the tonsillar tissue (40) (36). It is worth noting that IgA was detectable in the serum of only one monkey after the intranasal immunizations, but IgA was clearly present in the rectal mucosa of all four monkeys. This suggests that assays based on peripheral blood samples may be inappropriate and insensitive for measuring mucosal immune responses, humoral or cellular. Additionally, the difficulty in identifying a correlate of immunity in the few cases where protection from a virulent SIV challenge has been achieved may indicate that the correlate of SIV immunity is a specific mucosal

immune response that may be poorly measured by the standard peripheral blood assays used.

Cytotoxic T lymphocyte responses are important in several picornavirus infections, including Theiler's virus (49), hepatitis A virus (63), and coxsackievirus B3 (17). No previous study identified primate or human cytotoxic T cells ($CD8^+$ T cells) specific for poliovirus, and the role of cell mediated immunity in resolving poliovirus infections has remained unclear (47). Our laboratory has recently shown that strong cytotoxic T lymphocyte responses are elicited by recombinant polioviruses in polio-susceptible mice (mice transgenic for the human poliovirus receptor (48)) (29, 56). In this macaque study we attempted to identify anti-SIV cytotoxic T lymphocytes elicited by our recombinant polioviruses. Cytotoxic T lymphocyte activity was detectable in two of the four monkeys, by either bulk culture or limiting dilution analysis of PBMCs. Monkey 25136 was consistently positive for anti-SIV Env-specific CTLs beginning at 19 weeks after the first intranasal inoculation; however, it was difficult to detect much greater than 10% specific lysis in these bulk culture assays. The only other monkey to test positive for CTL activity by bulk culture assay was 25137, and this monkey only tested positive for CTLs specific for Gag at the final timepoint (42 wks). Monkey 25137 had a strong Env-specific CTL precursor frequency , and lower frequency of gag specific CTL precursors when analyzed by limiting dilution assay. However, due to the inconsistency of this data with the bulk assay data we must consider our CTL results indicative rather than conclusive. We plan to improve the consistency and sensitivity of our cytotoxic T cell assays for use in future primate experiments.

In summary, after inoculation of macaques with two serotypes of poliovirus live viral vectors expressing SIV antigens, all of the macaques made a mucosal IgA anti-SIV antibody response (Table 2). Three of four produced strong serum IgG antibody responses, and three of four made a detectable anti-SIV lymphoproliferative response (Table 2). These results are very encouraging for the future development of poliovirus-derived genetically engineered vaccines, as we have shown the poliovirus vector's ability to stimulate a broad immune response against the desired antigens in a primate model system.

When evaluating the data from these recombinant poliovirus immunizations in cynomolgus macaques, it is important to keep in mind that cynomolgus monkeys replicate the virus poorly in comparison with humans and chimpanzees. The ID_{50} of the Sabin vaccine in humans is 50 PFU (36), and the standard dose of the Sabin poliovirus vaccine in humans is ~2 x 10^7 (2). Cynomolgus macaques are several orders of magnitude less susceptible to poliovirus infection (ID_{100} = 10^6 PFU intranasally) and can be expected to generate a significantly lower immune response to poliovirus and recombinant polioviruses than humans.

With this cynomolgus data in hand, we believe that we can now plan to make a set of recombinant polioviruses containing the entirity of SIV, and carry out a mucosal challenge experiment in macaques to determine whether or not our poliovirus live viral vector system can confer protection against a pathogenic SIV challenge. As the recombinant poliovirus system is not limited to SIV vaccine work, we are currently

developing multiple additional candidate vaccines that may be well suited to a poliovirus live viral vector system.

The WHO wild poliovirus eradication effort has been wonderfully successful, and it is therefore necessary to address to future viability of a vaccine program based on poliovirus live viral vectors. We are very hopeful that wild poliovirus infections can be eliminated, and the WHO is well on its way of achieving that goal (18). However, we and others have expressed reservations about the ability to eliminate the Sabin live poliovirus vaccine viruses at any time in the near future (8). We believe that our work with these recombinant polioviruses demonstrates that the Sabin poliovirus vaccine strains should not be cast aside and have real potential as vectors for creating novel vaccines against major public health threats. The simple fact that the live poliovirus vaccine is so effective that wild polio eradication is conceivable is a strong argument that we should parlay this knowledge into the development of other vaccines, potentially using the live poliovirus itself as the delivery vector, as we propose.

The Sabin 1 poliovirus vaccine is one of the safest vaccines in existence, with significant side effects seen in less that 1 in 10 million individuals. It is notable that our recombinant polioviruses are even further attenuated that the vaccine strains in both mice (unpublished data, S. Crotty, S. Mandl, R. Andino) and macaques. The wealth of molecular knowledge about poliovirus should allow us to create even safer vaccine strains that, for example, contain modification in the 5' UTR that prevent neurovirulence and that do not revert to wild-type (15, 20). Our poliovirus vector system is also providing valuable groundwork that can inform the development of other positive strand RNA viral

vector systems. Live picornavirus systems based on rhinovirus (58) and mengovirus (64) are under development, and a poliovirus replicon system has also been tested in several model systems (37). Additionally, recombinant flaviviruses, such as one based on the yellow fever virus vaccine strain [A. McAllister, S. Mandl, A. Arbetman, R. Andino, manuscript in preparation], may also prove to be valuable vector systems.

References

1. **Abbas, A. K., A. H. Lichtman, and J. S. Pober** 1997. Cellular and Molecular Immunology, 3rd ed. Philadelphia, W. B. Saunders.
2. **AFHS** 1998. AFHS Drug Information. American Society of Hospital Pharmacists : SilverPlatter International, Bethesda, MD.
3. **Andino, R., G. E. Rieckhof, P. L. Achacoso, and D. Baltimore** 1993. Poliovirus RNA synthesis utilizes an RNP complex formed around the 5'-end of viral RNA Embo Journal. **12:**3587-98.
4. **Andino, R., D. Silvera, S. D. Suggett, P. L. Achacoso, C. J. Miller, D. Baltimore, and M. B. Feinberg** 1994. Engineering poliovirus as a vaccine vector for the expression of diverse antigens Science. **265:**1448-51.
5. **Barnett, S. W., J. M. Klinger, B. Doe, C. M. Walker, L. Hansen, A. M. Duliège, and F. M. Sinangil** 1998. Prime-boost immunization strategies against HIV Aids Research and Human Retroviruses. **14 Suppl 3:**S299-309.
6. **Benson, J., C. Chougnet, M. Robert-Guroff, D. Montefiori, P. Markham, G. Shearer, R. C. Gallo, M. Cranage, E. Paoletti, K. Limbach, D. Venzon, J. Tartaglia, and G. Franchini** 1998. Recombinant vaccine-induced protection against the highly pathogenic simian immunodeficiency virus SIV(mac251): dependence on route of challenge exposure Journal of Virology. **72:**4170-82.
7. **Buge, S. L., E. Richardson, S. Alipanah, P. Markham, S. Cheng, N. Kalyan, C. J. Miller, M. Lubeck, S. Udem, J. Eldridge, and M. Robert-Guroff** 1997. An adenovirus-simian immunodeficiency virus *env* vaccine elicits humoral, cellular and mucosal immune responses in rhesus macaques and decreased viral burden following vaginal challenge J. Virol. **71:**8531-8541.
8. **Dove, A. W., and V. R. Racaniello** 1997. The polio eradication effort: should vaccine eradication be next? Science. **277:**779-80.
9. **Faber, H., and R. Silverberg** 1941. Experimental airborne infection with poliomyelitis virus Science. **94:**566-568.
10. **Faber, H. K.** 1955. The pathogenesis of poliomyelitis, 1st ed. Charles C. Thomas, Springfield, Illinois.
11. **Faber, H. K., R. J. Silverberg, and L. Dong** 1948. Poliomyelitis in philippine cynomolgus monkeys after simple feeding American Journal of Hygiene. **48:**94-98.
12. **Faber, H. K., R. J. Silverberg, and L. Dong** 1944. Poliomyelitis in the cynomolgus monkey. III. Infection by inhalation of droplet nuclei and the nasopharyngeal portal of entry, with a note on this mode of infection in rhesus Journal of Experimental Medicine. **80:**39-57.
13. **Faden, H., J. Modlin, M. L. Thoms, A. M. McBean, M. B. Ferdon, and P. L. Ogra** 1990. Comparative evaluation of immunization with live attenuated and

enhanced-potency inactivated trivalent poliovirus vaccines in childhood: systemic and local immune responses The Journal of Infectious Diseases. **162:**1291-1297.

14. **Graham, S., E. C. Wang, O. Jenkins, and L. K. Borysiewicz** 1993. Analysis of the human T-cell response to picornaviruses: identification of T-cell epitopes close to B-cell epitopes in poliovirus Journal of Virology. **67:**1627-37.
15. **Gromeier, M., B. Bossert, M. Arita, A. Nomoto, and E. Wimmer** 1999. Dual stem loops within the poliovirus internal ribosomal entry site control neurovirulence Journal of Virology. **73:**958-64.
16. **Howe, H. A., and D. Bodian** 1948. Poliomyelitis in the cynomolgus monkey following oral inoculation American Journal of Hygiene. **48:**99-106.
17. **Huber, S. A., L. P. Job, and J. F. Woodruff** 1980. Lysis of infected myofibers by coxsackie B3-immune T lymphocytes American Journal of Pathology. **98:**681-694.
18. **Hull, H. F., and R. B. Aylward** 1997. Ending polio immunization Science. **277:**780.
19. **Hull, H. F., N. A. Ward, B. P. Hull, J. B. Milstien, and C. de Quadros** 1994. Paralytic poliomyelitis: seasoned strategies, disappearing disease Lancet. **343:**1331-7.
20. **Iizuka, N., M. Kohara, K. Hagino-Yamagishi, S. Abe, T. Komatsu, K. Tago, M. Arita, and A. Nomoto** 1989. Construction of less neurovirulent polioviruses by introducing deletions into the 5' noncoding sequence of the genome Journal of Virology. **63:**5354-63.
21. **Imaoka, K., C. J. Miller, M. Kubota, M. B. McChesney, B. Lohman, M. Yamamoto, K. Fugihashi, K. Someya, M. Honda, J. R. McGhee, and H. Kiyono** 1998. Nasal immunization of nonhuman primates with simian immunodeficiency virus p55gag and cholera toxin adjuvant induces Th1/Th2 help for virus specific immune responses in reproductive tissues J. Immunol. **161:**5952-5958.
22. **Kestler, H., T. Kodama, D. Ringler, M. Marthas, N. Pedersen, A. Lackner, D. Regier, P. Sehgal, M. Daniel, N. King, and R. Desrosiers** 1990. Induction of AIDS in rhesus monkeys by molecularly cloned simian immunodeficiency virus [see comments] Science. **248:**1109-12.
23. **Lehner, T., Y. Wang, M. Cranage, L. A. Bergmeier, E. Mitchell, L. Tao, G. Hall, M. Dennis, N. Cook, R. Brookes, L. Klavinskis, I. Jones, C. Doyle, and R. Ward** 1996. Protective mucosal immunity elicited by targeted iliac lymph node immunization with a subunit SIV envelope and core vaccine in macaques [see comments] Nature Medicine. **2:**767-75.
24. **Lepow, M. L., R. J. Warren, N. Gray, V. G. Ingram, and F. C. Robbins** 1961. Effect of Sabin type 1 poliomyelitis vaccine administered by mouth to newborn infants New England Journal of Medicine. **264:**1071-1078.
25. **Lohman, B. L., M. B. McChesney, C. J. Miller, E. McGowan, S. M. Joye, K. K. Van Rompay, E. Reay, L. Antipa, N. C. Pedersen, and M. L. Marthas** 1994. A partially attenuated simian immunodeficiency virus induces host immunity that

correlates with resistance to pathogenic virus challenge Journal of Virology. **68:**7021-9.

26. **Lohman, B. L., C. J. Miller, and M. B. McChesney** 1995. Antiviral cytotoxic T lymphocytes in vaginal mucosa of simian immunodeficiency virus-infected rhesus macaques J. Immunol. **155:**5855-5860.
27. **Lü, X., H. Kiyono, D. Lu, S. Kawabata, J. Torten, S. Srinivasan, P. J. Dailey, J. R. McGhee, T. Lehner, and C. J. Miller** 1997. Targeted lymph-node immunization with whole inactivated simian immunodeficiency virus (SIV) or envelope and core subunit antigen vaccines does not reliably protect rhesus macaques from vaginal challenge with SIVmac251 AIDS. **12:**1-10.
28. **Mahon, B. P., K. Katrak, A. Nomoto, A. J. Macadam, P. D. Minor, and K. H. Mills** 1995. Poliovirus-specific CD4+ Th1 clones with both cytotoxic and helper activity mediate protective humoral immunity against a lethal poliovirus infection in transgenic mice expressing the human poliovirus receptor Journal of Experimental Medicine. **181:**1285-92.
29. **Mandl, S., L. J. Sigal, K. L. Rock, and R. Andino** 1998. Poliovirus vaccine vectors elicit antigen-specific cytotoxic T cells and protect mice against lethal challenge with malignant melanoma cells expressing a model antigen Proceedings of the National Academy of Sciences of the United States of America. **95:**8216-21.
30. **Mastro, T. D., and D. Kitayaporn** 1998. HIV type 1 transmission probabilities: estimates from epidemiological studies Aids Research and Human Retroviruses. **14 Suppl 3:**S223-7.
31. **McChesney, M. B., J. R. Collins, D. Lu, X. Lü, J. Torten, R. L. Ashley, M. W. Cloyd, and C. J. Miller** 1998. Occult systemic infection and persistent simian immunodeficiency virus (SIV)-specific $CD4^+$-T-cell proliferative responses in rhesus macaques that were transiently viremic after intravaginal inoculation of SIV J. Virol. **72:**10029-10035.
32. **Melnick, J. L.** 1996. Enteroviruses: Polioviruses, coxsackieviruses, echoviruses, and newer enteroviruses, p. 655-712. *In* B. N. Fields, D. M. Knipe, and P. M. Howley (eds), Fields virology, 3rd ed, vol. 1. Lippincott-Raven Publishers, Philadelphia.
33. **Miller, C. J., M. Marthas, J. Torten, N. J. Alexander, J. P. Moore, G. F. Doncel, and A. G. Hendrickx** 1994. Intravaginal inoculation of rhesus macaques with cell-free simian immunodeficiency virus results in persistent or transient viremia Journal of Virology. **68:**6391-400.
34. **Miller, C. J., M. B. McChesney, X. Lü, P. J. Dailey, C. Chutkowski, D. Lu, P. Brosio, B. Roberts, and Y. Lu** 1997. Rhesus macaques previously infected with simian/human immunodeficiency virus are protected from vaginal challenge with pathogenic SIVmac239 J. Virol. **71:**1911-1921.
35. **Mills, K. H. G., P. A. Kitchin, B. P. Mahon, A. L. Barnard, S. E. Adams, S. M. Kingsman, and A. J. Kingsman** 1990. HIV p24-specific helper T cell clones from immunized primates recognize highly conserved regions of HIV-1 J. Immunol. **144:**1677-1683.

36. **Minor, P. D.** 1997. Poliovirus, p. 555-574. *In* N. Nathanson, and R. Ahmed (eds), Viral pathogenesis. Lippincott-Raven, Philadelphia.
37. **Morrow, C. D., D. C. Porter, D. C. Ansardi, Z. Moldoveanu, and P. N. Fultz** 1994. New approaches for mucosal vaccines for AIDS: encapsidation and serial passages of poliovirus replicons that express HIV-1 proteins on infection Aids Research and Human Retroviruses. **10 Suppl 2:**S61-6.
38. **Mueller, S., and E. Wimmer** 1998. Expression of foreign proteins by poliovirus polyprotein fusion: analysis of genetic stability reveals rapid deletions and formation of cardioviruslike open reading frames Journal of Virology. **72:**20-31.
39. **Nilsson, C., B. Mäkitalo, R. Thorstensson, S. Norley, D. Binninger-Schinzel, M. Cranage, E. Rud, G. Biberfeld, and P. Putkonen** 1998. Live attenuated simian immunodeficiency virus (SIV)mac in macaques can induce protection against mucosal infection with SIVsm AIDS. **12:**2261-2270.
40. **Ogra, P. L.** 1999. Mucosal immunology, 2nd ed. Academic Press, San Diego.
41. **Ogra, P. L., M. Fishaut, and M. R. Gallagher** 1980. Viral vaccination via the mucosal routes Reviews of Infectious Diseases. **2:**352-69.
42. **Ogra, P. L., and D. T. Karon** 1971. Formation and function of poliovirus antibody in different tissues Progess in Medical Virology. **13:**156-193.
43. **Ogra, P. L., and D. T. Karzon** 1969. Distribution of poliovirus antibody in serum, nasopharynx and alimentary tract following segmental immunization of lower alimentary tract with poliovaccine Journal of Immunology. **102:**1423-30.
44. **Ogra, P. L., and D. T. Karzon** 1969. Poliovirus antibody response in serum and nasal secretions following intranasal inoculation with inactivated poliovaccine Journal of Immunology. **102:**15-23.
45. **Ogra, P. L., and S. S. Ogra** 1973. Local antibody response to poliovaccine in the human female genital tract Journal of Immunology. **110:**1307-11.
46. **Paul, J. R., J. T. Riordan, and J. L. Melnick** 1951. Antibodies to three different antigenic types of poliomyelitis virus in sera from north Alaskan eskimos American Journal of Hygiene. **54:**275-285.
47. **Plotkin, S., and W. Orenstein** (eds.) 1999 Vaccines, 3rd ed. W. B. Saunders Company, Philadelphia.
48. **Ren, R. B., F. Costantini, E. J. Gorgacz, J. J. Lee, and V. R. Racaniello** 1990. Transgenic mice expressing a human poliovirus receptor: a new model for poliomyelitis Cell. **63:**353-62.
49. **Rossi, C. P., A. McAllister, M. Tanguy, D. Kägi, and M. Brahic** 1998. Theiler's virus infection of perforin-deficient mice Journal of Virology. **72:**4515-9.
50. **Royce, R. A., A. Seña, W. Cates, Jr., and M. S. Cohen** 1997. Sexual transmission of HIV New England Journal of Medicine. **336:**1072-8.
51. **Sabin, A. B.** 1956. Pathogenesis of poliomyelitis Science. **123:**1151-1157.
52. **Sabin, A. B.** 1959. Present position of immunization against poliomyelitis with live virus vaccines British Medical Journal. **1:**663-680.
53. **Savilahti, E., T. Klemola, B. Carlsson, L. Mellander, M. Stenvik, and T. Hovi** 1988. Inadequacy of mucosal IgM antibodies in selective IgA deficiency:

Excretion of attenuated poliovirus is prolonged Journal of Clinical Immunology. **8:**89-94.

54. **Schultz, A.** 1998. Encouraging vaccine results from primate models of HIV type 1 infection Aids Research and Human Retroviruses. **14 Suppl 3:**S261-3.
55. **Schultz, A.** 1998. Using recombinant vectors as HIV vaccines, p. 1-4, IAVI Report, vol. 3.
56. **Sigal, L. J., S. Crotty, R. Andino, and K. L. Rock** 1999. Cytotoxic T-cell immunity to virus-infected non-haematopoietic cells requires presentation of exogenous antigen Nature. **398:**77-80.
57. **Simons, J., M. Kutubuddin, and M. Chow** 1993. Characterization of poliovirus-specific T lymphocytes in the peripheral blood of Sabin-vaccinated humans Journal of Virology. **67:**1262-8.
58. **Smith, A. D., S. C. Geisler, A. A. Chen, D. A. Resnick, B. M. Roy, P. J. Lewi, E. Arnold, and G. F. Arnold** 1998. Human rhinovirus type 14:human immunodeficiency virus type 1 (HIV-1) V3 loop chimeras from a combinatorial library induce potent neutralizing antibody responses against HIV-1 Journal of Virology. **72:**651-9.
59. **Smith, J. W., J. A. Lee, W. B. Fletcher, C. A. Morris, D. A. Parker, R. Yetts, D. I. Magrathe, and F. T. Perkins** 1976. The response to oral poliovaccine in persons aged 16-18 years Journal of Hygiene. **76:**235-47.
60. **Sutter, R. W., S. L. Cochi, and J. L. Melnick** 1999. Live attenuated poliovirus vaccines, p. 1230. *In* S. Plotkin, and W. Orenstein (eds), Vaccines, 3rd ed. W. B. Saunders, Philadelphia.
61. **Tang, S., R. van Rij, D. Silvera, and R. Andino** 1997. Toward a poliovirus-based simian immunodeficiency virus vaccine: correlation between genetic stability and immunogenicity Journal of Virology. **71:**7841-50.
62. **UNAIDS, and WHO** 1998. Report on the Global HIV/AIDS Epidemic. World Health Organization.
63. **Vallbracht, A., Y. Maier, D. Stierhof, K. H. Wiedmann, B. Flehmig, and B. Fleischer** 1989. Liver-derived cytotoxic T cells in hepatitus A virus infection Journal of Infectious Diseases. **160:**209-217.
64. **Van der Ryst, E., T. Nakasone, A. Habel, A. Venet, E. Gomard, R. Altmeyer, M. Girard, and A. M. Borman** 1998. Study of the immunogenicity of different recombinant Mengo viruses expressing HIV1 and SIV epitopes Research in Virology. **149:**5-20.

TABLE 1. Lymphocyte responses to SIV proteins following immunization with poliovirus vectors expressing p17 and gp41.

Monkey	Weeks[a]		Lymphoproliferative responses[b] p55^{gag}	gp140^{env}
22701	11	(i.n.)	—	—
	19		—	—
	38	(i.v.)		
	40		—	2.4
	42		2.2	2.2
25136	11	(i.n.)	—	—
	19		—	—
	38	(i.v.)		
	40		—	—
	42		—	—
25137	11	(i.n.)	—	—
	19		2.4	—
	38	(i.v.)		
	40		—	—
	42		—	—
26394	11	(i.n.)	8.1	—
	19		—	2.0
	38	(i.v.)		
	40		nd	nd
	42		—	—

[a] Monkeys were inoculated intranasally with Polio1-gp41 and Polio1-sp17 on Day 0. Intranasal boost (i.n.) with Sabin2-gp41 and Sabin2-sp17 was on Week 11. Intravenous inoculation (i.v.) with all four viruses was done on Week 38.

[b] Proliferation assays were done using PBMCs and purified p55^{gag} or gp140^{env} (see Materials and Methods). Samples giving a proliferative response < 2.0 were considered negative and are indicated by (—).

Table 2. Immunization anti-SIV response summary

monkey	serum IgG	rectal IgA	vaginal Ig	helper T cell	CTLs
26394	√	√	√	√	
25136	√	√	√		√
25137	√	√		√	√
22701		√		√	

Figure Legends

Figure 1. *In vitro* construction of a recombinant poliovirus containing an SIV gene fragment.

(A) Strategy schematic. Three PCR fragments are synthesized independently (Polio 5'Arm, SIV insert, Polio 3'Arm), and then joined by a hybrid PCR reaction to generate a full length poliovirus genome that includes the SIV gene fragment inserted at the P1/P2 junction of the genome. Infectious poliovirus-SIV RNA is generated by *in vitro* transcription from a T7 promoter. The RNA is transfected into HeLa cells, where viral replication occurs. The viral polyprotein is translated, including the SIV insert, and the SIV insert is cleaved away from the polyprotein via two $2A^{pro}$ protease cleavage sites flanking the insert. The virus then continues its replication cycle and produces infectious virions containing the poliovirus genome with the SIV insert.

(B) The three independent PCR products: Polio 5'Arm, SIV insert, Polio 3'Arm.

(C) Poliovirus-SIV DNA hybrid PCR product (specifically Polio1-gp41), and full length Polio1-gp41 RNA from *in vitro* transcription.

(D) Western blot of whole cytoplasmic protein extract from HeLa cells infected with Polio1-p17 or Polio1-p28 or Polio1-gp41, and probed with SIV antiserum.

Figure 2. Expression of SIV proteins in infected human cells. 100% confluent HeLa cells were infected with Sabin2-gp41 or Sabin2-p28 at an MOI of 0.3. Cells were fixed and co-labeled with anti-poliovirus antibodies (Texas Red) and anti-SIV antibodies (FITC, green). 100% of Sabin2-SIVgp41 infected cells expressed the SIV protein, and 100% of Sabin2-SIVp28 infected cells expressed the SIV protein.

Figure 3. Serum antibodies.

(A) Anti-SIV serum IgG antibody titers in poliovirus-SIV immunized macaques. Four cynomolgus macaques were inoculated intranasally with Polio1-gp41 and Polio1-p17 at week 0. Intranasal inoculations of Sabin2-p17 and Sabin2-gp41 were done on week 11. Intravenous boosts of all four recombinant viruses were done on week 38. Monkeys are labeled as follows: 22701 (O), 25136 (◆), 25137 (▲), 26394 (❐).

(B) Anti-SIV serum IgA antibody titers in the poliovirus-SIV immunized macaques. Symbols are as above.

Figure 4. Mucosal antibodies.

(A) Anti-SIV rectal IgA antibody titers in the poliovirus-SIV immunized macaques. Four cynomolgus macaques were inoculated intranasally with Polio1-gp41 and Polio1-p17 at week 0. Intranasal inoculations of Sabin2-p17 and Sabin2-gp41 were done on week 11. Intravenous boosts of all four recombinant viruses were done on week 38. Monkeys are labeled as follows: 22701 (O), 25136 (◆), 25137 (▲), 26394 (❐).

(B) Anti-SIV vaginal antibody titers in monkeys 26394 and 25136. IgG antibody titers are indicated by white bars, IgA by filled bars.

Figure 5. Anti-poliovirus antibodies.

(A) Anti-poliovirus western blot. Serum from each monkey was taken at 20 weeks post-infection and used to detected poliovirus antigens (primarily Vp1) by western blot. Lanes: **U** = uninfected cell extract, **1** = type 1 poliovirus infected cell extract, **2** = type 2 poliovirus infected cell extract.

(B) Poliovirus neutralizing antibodies. Serum from each monkey was tested for poliovirus neutralizing antibodies by incubation with 1000 pfu of type 1 poliovirus (polio1) or type 2 poliovirus (polio2) (see Materials and Methods). +++ = 95% neutralization (using 25 ul serum), ++ = 90% neutralization (using 25 ul serum), + = 50% neutralization (using 25 ul serum), +/- = 50% neutralization (using 90 ul serum), — = no neuralizing antibodies detected (using 90 ul serum).

Figure 6. CTL responses.

(A) SIV-specific cytotoxic T lymphocytes detected using bulk PBMCs. Monkeys 25136 (left) and 25137 (right) tested positive for SIV-specific CTLs at some timepoints. Timepoints: 19 wks (◆), 38 wks (●), 40 wks (▲), and 42 wks (■). Empty symbols represent negative control target cells, filled symbols indicate Gag expressing target cells (see Materials and Methods).

(B) SIV-specific cytotoxic T lymphocytes detected using limiting dilution assay. Mesenteric lymph nodes from monkey 25137 were tested for Env-specific (○) and Gag-

specific (□) CTLs. Calculated precursor frequencies for monkey 25137 were 3,539 Env-specific precursor CTLs per 10^6 $CD8^+$ T cells (95% confidence interval (CI) of 2,600-4,460), and 178 Gag-specific precursor CTLs per 10^6 $CD8^+$ T cells (95% confidence interval of 100-250). Background lysis was subtracted out (see Materials and Methods). The dotted line indicates the predicted frequency of lysed cells at single hit kinetics (37%).

Figure 1

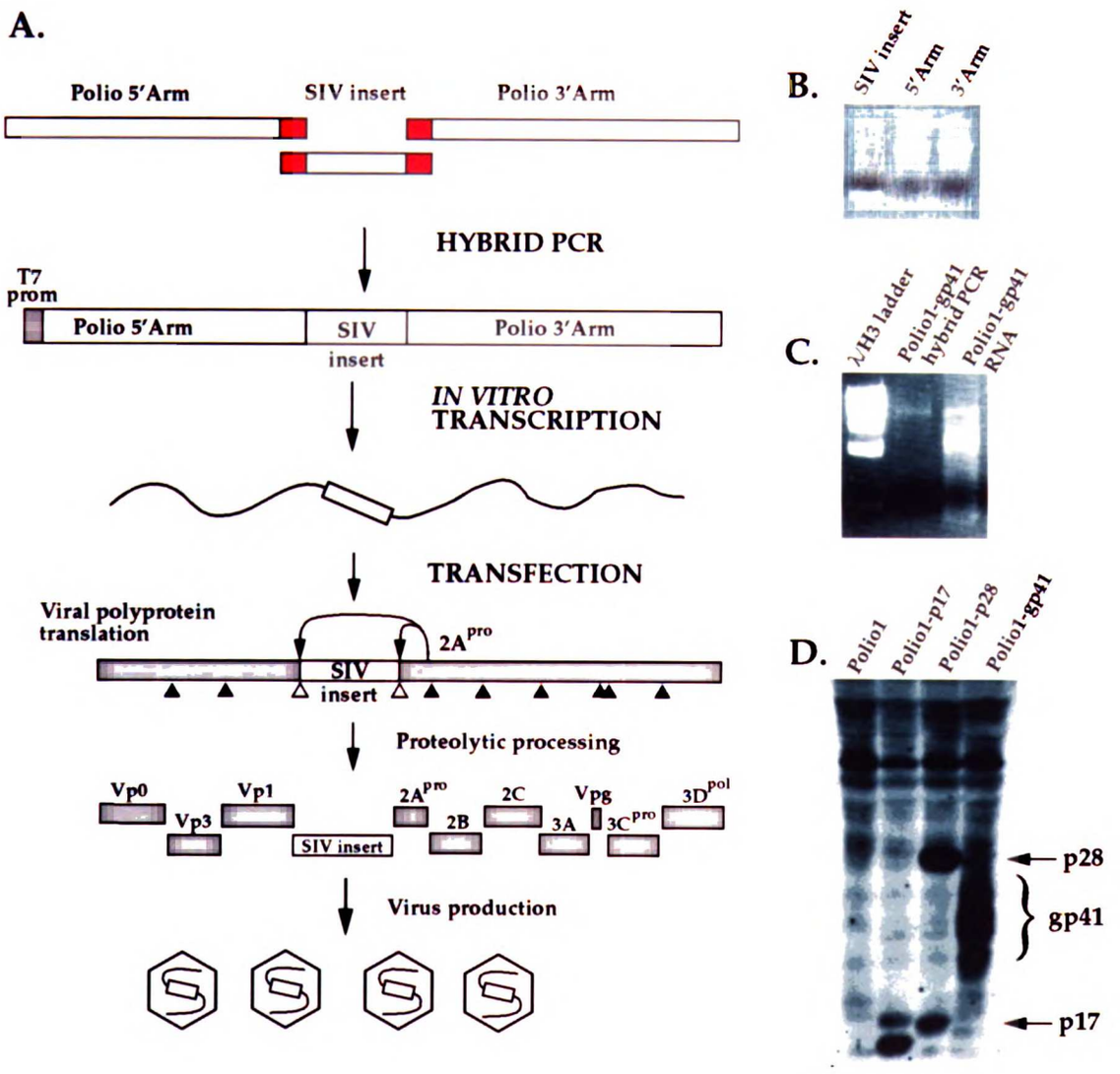
A.
Polio 5'Arm
SIV insert
Polio 3'Arm
HYBRID PCR
T7 prom
Polio 5'Arm
SIV insert
Polio 3'Arm
IN VITRO TRANSCRIPTION
TRANSFECTION
Viral polyprotein translation
2A pro
SIV insert
Proteolytic processing
Vp0
Vp1
2A pro
2C
Vpg
3D pol
Vp3
2B
3A
3C pro
SIV insert
Virus production
B.
SIV insert
5'Arm
3'Arm
C.
λ/H3 ladder
Polio1-gp41 hybrid PCR
Polio1-gp41 RNA
D.
Polio1
Polio1-p17
Polio1-p28
Polio1-gp41
p28
gp41
p17

Figure 2

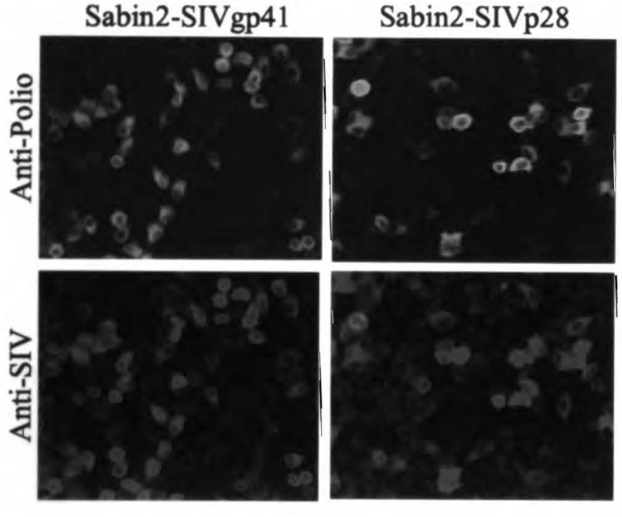

Figure 3

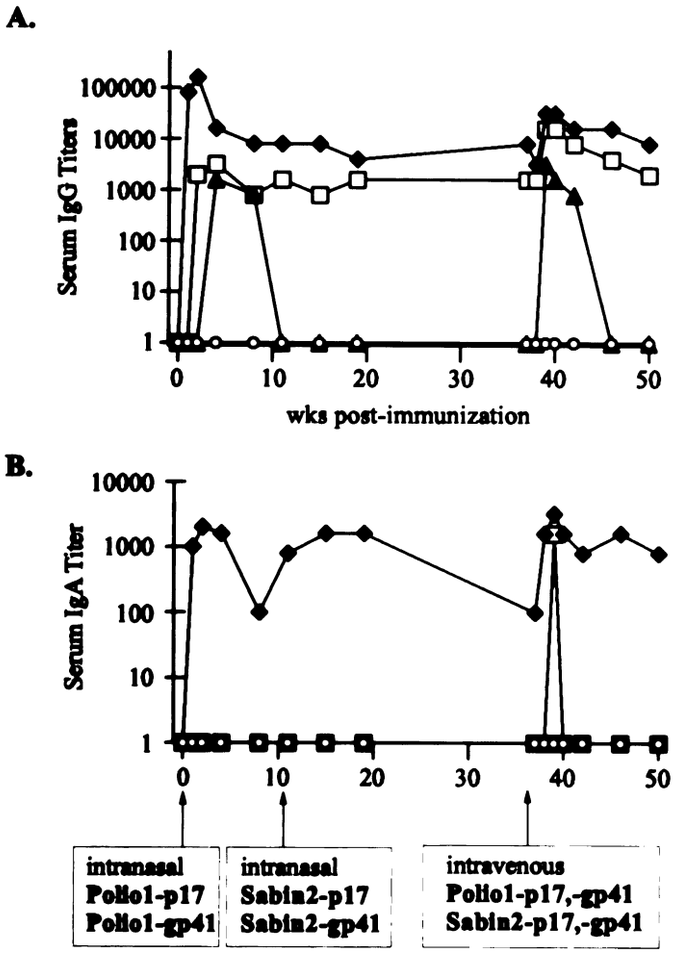
A.
Serum IgG Titers
100000
10000
1000
100
10
1
0
10
20
30
40
50
wks post-immunization
B.
Serum IgA Titer
10000
1000
100
10
1
0
10
20
30
40
50
intranasal
Polio1-p17
Polio1-gp41
intranasal
Sabin2-p17
Sabin2-gp41
intravenous
Polio1-p17,-gp41
Sabin2-p17,-gp41

Figure 4

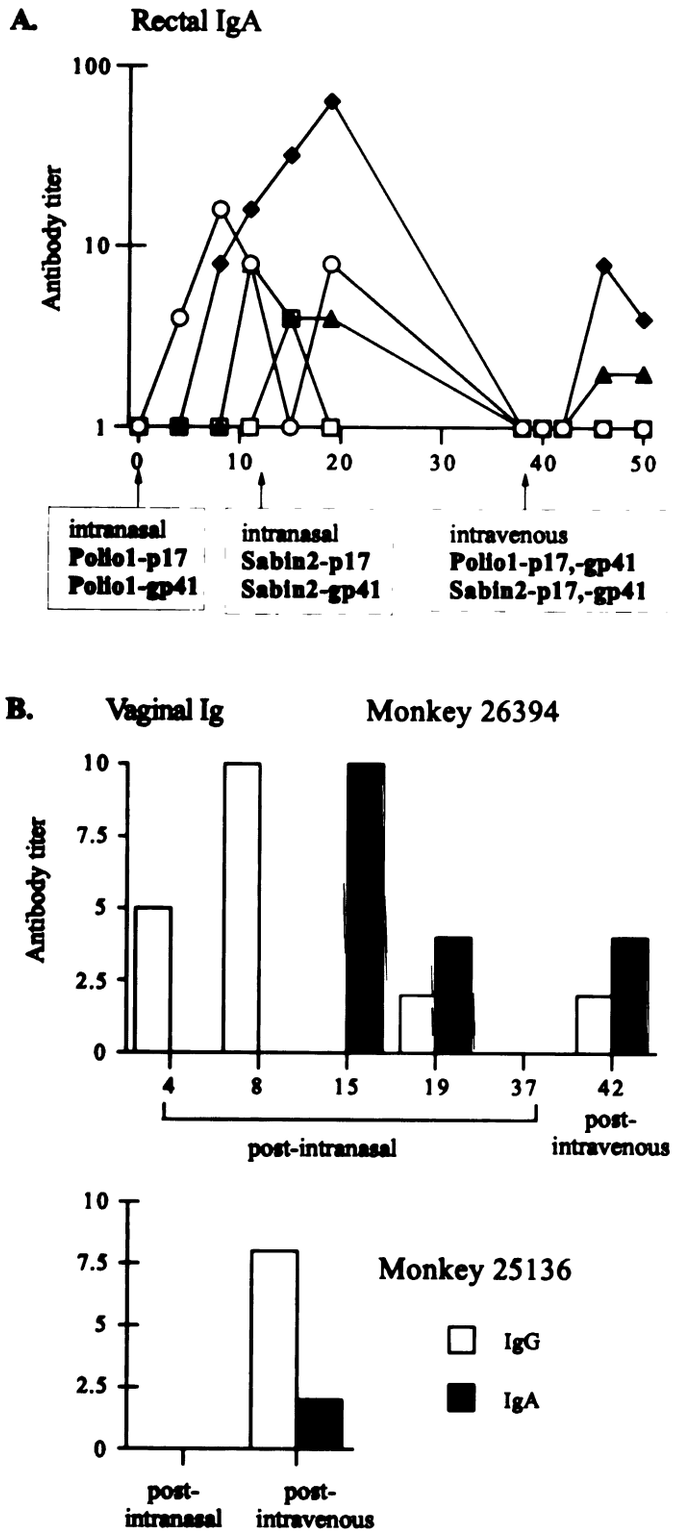
A.
Rectal IgA
100
10
1
Antibody titer
0
10
20
30
40
50
intranasal
Polio1-p17
Polio1-gp41
intranasal
Sabin2-p17
Sabin2-gp41
intravenous
Polio1-p17,-gp41
Sabin2-p17,-gp41
B.
Vaginal Ig
Monkey 26394
10
7.5
5
2.5
0
Antibody titer
4
8
15
19
37
42
post-intranasal
post-intravenous
Monkey 25136
IgG
IgA
post-intranasal
post-intravenous

Figure 5

A.

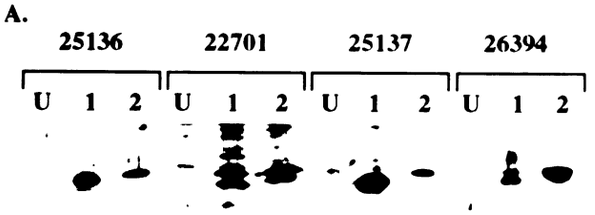

B.

	week 0		week 10		week 20	
	polio1	polio2	polio1	polio2	polio1	polio2
25136						
22701			+++	+++	+++	+++
25137			+/-		+	
26394			++		+	+

Figure 6

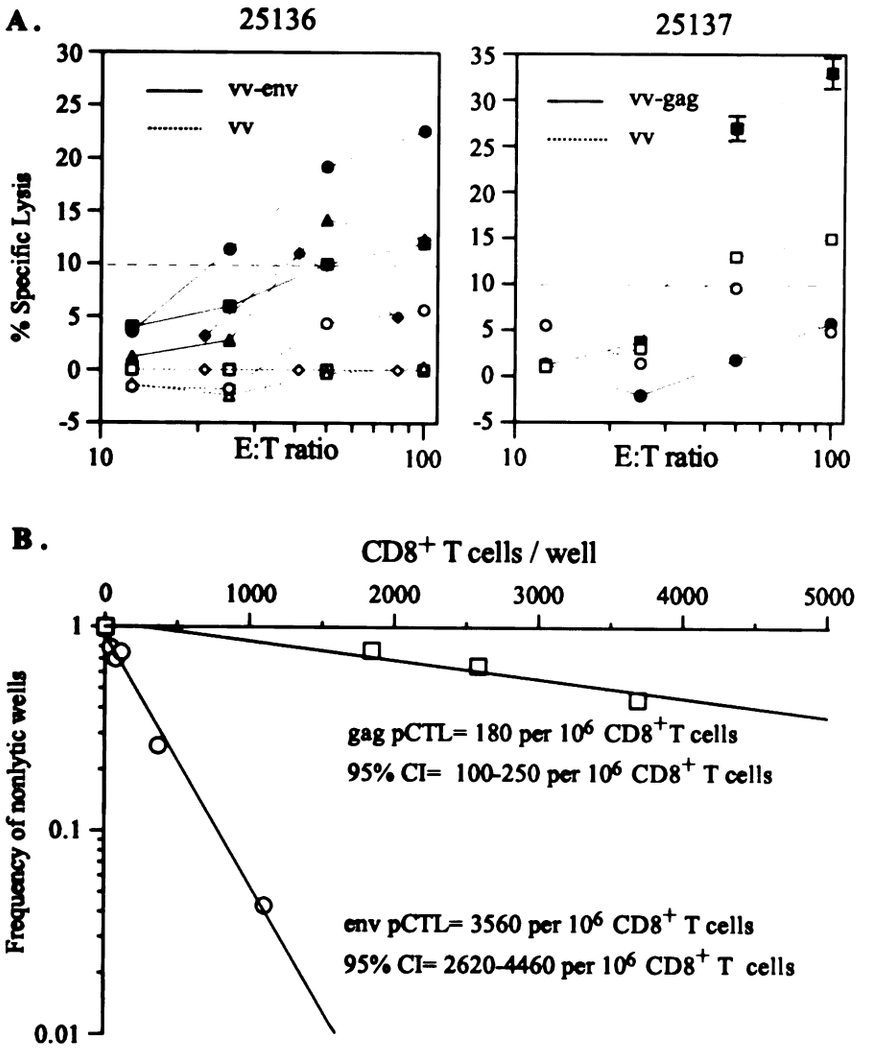
A.
25136
25137
vv-env
vv
vv-gag
vv
% Specific Lysis
E:T ratio
E:T ratio
B.
CD8+ T cells / well
Frequency of nonlytic wells
gag pCTL= 180 per 10^6 CD8+T cells
95% CI= 100-250 per 10^6 CD8+ T cells
env pCTL= 3560 per 10^6 CD8+ T cells
95% CI= 2620-4460 per 10^6 CD8+ T cells

Supplementary Data

Virus Constructs

One of the goals of this paper was to immunize cynos with Sabin-based poliovirus vector constructs. Unfortunately, ShenBei's cloning was incorrect and the type 1 poliovirus vectors were wildtype (Mahoney) and not vaccine strain (Sabin 1) based. Specifically, after extensive sequencing I determined that the Polio1-p17 construct had mixed genotypes, with the 5' half (from the 5' UTR to the start of 2A) being wt sequence, and the 3' half (from 2A through to the end of the 3' UTR) being Sabin1 sequence. Since the primary determinants of neurovirulence and wt characteristics are contained in the 5' UTR and the capsid genes, these hybrid genomes could be considered wildtype in characteristic. Additionally, the other type 1 constuct inoculated into the monkeys (Polio1-gp41), was complete based on wt Mahoney sequence. These observationa were made after the monkeys were immunized, but prior to publication. Therefore both of the type 1 poliovirus vector recombinants were published as being on a wildtype genetic background. The fact that these recombinants contained primarily wildtype sequence explained the paralysis of one of the five immunized monkeys (see Materials and Methods). I also sequenced the Sabin 2 based clones and confirmed that those clones were indeed correctly based on the Sabin 2 vaccine strain. To avoid these sorts of difficulties in future experiments, we shifted to using vectors that we constructed based on molecular clones of Sabin 1 and Sabin 2 to make sure that we were working with fully attenuated vectors (see Chapters 4 and 5). This updated vector strategy,

described in Chapters 4 and 5, based on plasmid clones of Sabin 1 and Sabin 2 has worked very nicely.

Neutralizing antibodies

Two comments on the Fig. 5 poliovirus neutralizing antibodies: 1.) the neutralizing antibody levels seen in the monkeys are much lower than that observed in human serum. That may be due to technical issues, or real biological differences. 2.) Monkey 22701 appears to have cross-neutralizing antibodies after the Sabin 1 immunization. This is probably due to a mislabelled serum sample that was actually obtained after the Sabin2 immunization.

Erratum

It was mistakenly stated in Figure 6B that mesenteric lymph nodes from monkey 25137 tested positive for Env-specific CTLs. That was incorrect. Monkey 25137 PBMCs tested positive for Env-specific CTLs. Mesenteric lymph nodes from 25136 tested negative at the time of necropsy.

Chapter 4

Live attenuated poliovirus vectors (SabRV) expressing a series of defined SIV fragments: growth characteristics and genetic stability

Abstract

In previous studies we demonstrated that live recombinant poliovirus vectors are immunogenic, eliciting humoral, mucosal, and cellular immune responses against expressed antigens in a primate model system (Crotty et al., Journal of Virology 73:9485-9495, 1999). As part of our continuing attempt to develop a candidate AIDS vaccine based on recombinant RNA virus vectors, we have constructed two new vectors, one derived from a poliovirus Sabin 1 vaccine strain molecular clone and the other derived from a poliovirus Sabin 2 vaccine strain molecular clone. These vectors were viable and grew comparably to their parental viruses. Because the length of insert that live poliovirus vectors can tolerate well is around 200 amino acids, we generated 31 different Sabin1-based recombinant viruses expressing defined fragments of simian immundeficiency virus (SIV, the cause of simian AIDS) and 26 different Sabin2-based recombinant viruses expressing defined fragments of SIV. These numerous viruses were designed to constitute a library of polioviruses expressing the entirity of SIV Gag, Pol,

Env, and Nef proteins as a series of overlapping 100-250 amino acid fragments. We were able to generate pure stocks of 90% of the recombinant viruses that retained the full insert (undetectable levels of insertless or partially-deleted insert virus). These recombinant viruses generally made plaques half the size of the parental viruses and grew to titers of 1 x 10^7 to 2 x 10^8 PFU/ml (SabRV1) or 3 x 10^5 to 7 x 10^6 PFU/ml (SabRV2). A mixture of nine different SabRV2-SIV viruses was then passaged to determine the insert stability of these viruses. All nine of the recombinant viruses retained the full inserted sequence for the 10-12 rounds of replication tested. These libraries of Sabin1-SIV and Sabin2-SIV massively expand the repertoire of live recombinant picornaviruses available, and were used in a large monkey SIV challenge experiment as a novel vaccine strategy.

Introduction

We and others have developed live picornavirus vectors capable of expressing a variety of exogenous sequences (1-3, 6, 27, 38, 40, 54, 60)(for review see (42)). These viral vectors have been useful for studying the basic biology of viral translation and replication (14, 40, 41), viral immunology (59), viral pathogenesis (27)(S. Crotty, L. Hix, R. Andino, manuscript in preparation), virus recombination (13, 43, 64), and virus attenuation (27)(S. Crotty, L. Hix, R. Andino, unpublished data). Picornavirus vectors have also been extensively studied as potential vaccine vectors for viral diseases (SIV (5, 18, 64), hepatitis B (66), HIV (7, 34), and adenovirus (27)) bacterial diseases (45, 55), and malignant tumors (36). Here we report the construction and characterization of two new vectors, one derived from a poliovirus Sabin 1 vaccine strain molecular clone and the other derived from a poliovirus Sabin 2 vaccine strain molecular clone.

Poliovirus is an attractive live viral vector for several reasons. The Sabin live poliovirus vaccine is one of the best human vaccines in the world. It produces long lasting immunity (52) and herd immunity (63); it is very safe and easy to experimentally manipulate (39); it has a proven safety and efficacy record in over 1 billion vaccinees (63); it is cheap to produce and distribute in developing countries (28); and most importantly, it produces a potent mucosal immune response (42, 46, 47, 65).

A variety of viral vectors have been explored as potential vaccine vectors (23, 58). Indeed, live viral vectors are leading candidates in the hunt for a potential AIDS vaccine. Several viral vectors have showed promise protecting monkeys against highly

virulent strains of SIV (a primate AIDS vaccine model system)(11, 19, 50)(Crotty et al., accompanying paper), and a number of other live viral vector systems are in earlier testing phases of vaccine development (for review see (58) and (62)). Viral vectors are also being explored as potential tumor vaccines, and poliovirus vectors (36), flavivirus vectors (37), and vaccinia vectors (51) have proven efficacious in difficult mouse tumor vaccine model systems.

In our live poliovirus vector system, we insert an immunogenic gene fragment of interest at the junction between the capsid proteins and the nonstructural proteins (the P1/P2 junction) in the poliovirus polyprotein reading frame (64). The gene fragment is expressed with the rest of the poliovirus genome as part of the polyprotein and is cleaved away from the polyprotein via the activity of the poliovirus-encoded protease $2A^{pro}$, which cleaves at engineered proteolytic sites flanking the insert (Fig. 2A).

Two of the more significant restrictions of the live picornavirus vectors are the insert size limit (which is approximately 300-400 amino acids), and problems in the ability of recombinant polioviruses to retain the insert after several rounds of replication, which leads to viruses containing insert deletions accumulating after multiple passages (18, 43, 64). Here we describe strategies used to alleviate these two problems, and we describe the construction and analysis of 57 new Sabin vector recombinant viruses expressing SIV protein fragments. Implications of these results for the manufacturing and use of picornavirus vectors are discussed.

Materials and Methods

Plasmids. Construct pMoV2.11 was previously described (64). The Sabin 1 plasmid (which we call pS1 for simplicity), was kindly provided by A. Nomoto (construct pVS(1)IC-0(25) (32, 49)). The entire Sabin 1 cDNA in pS1 was sequenced in our laboratory by the fluorescent dye terminator method using an ABI 310 machine (Perkin Elmer, CA). The accuracy of the genome sequence as published (44) was confirmed. To construct pSabRV1, first the EcoRI and XhoI sites upstream of the T7 promoter of pS1 were eliminated by inserting a SalI linker (oligos C and D) at that position to create plasmid pS1XT. Then the 747 bp BstEII fragment of pMoV2.11—containing the duplicated $2A^{pro}$ cleavage site, the 5 glycine spacer, and the EcoRI, NotI, and XhoI cloning sites—was swapped into pS1XT. Accuracy of the pSabRV1 construct was confirmed by restriction digest and DNA sequencing. This DNA swap between pMoV2.11 and Sabin 1 results in Sabin 1 gaining three wt coding changes in 2A and one in 2B. None of the changes are associated with neurovirulence or other wt phenotypes (10, 17, 25, 33, 35, 48). All pMoV2.11 and pSabRV1 plasmids contain an Amp^R selectable marker. Plasmid pS1, pS1XT, and pSabRV1 were grown by electroporation into SURE cells (Stratagene, CA) and plated on LB + ampicillin agar plates for 20-24 hrs at 37° C. Single colonies were then inoculated into 50 ml cultures of LB + ampicillin (50 mg/ml) and grown at 30° C for 16-18 hrs. Note: growth conditions for the Sabin 1 derivative plasmids (pS1, pS1XT, and pSabRV1) are important, as rearrangements of the plasmids and very low plasmid yields are otherwise seen. Growth conditions for

pMoV2.11 are less stringent, and pMoV2.11 transformed DH5α or SURE cells were cultured under normal conditions at 37° C. Plasmid DNA was isolated from cells by the QiaFilter Midiprep technique (Qiagen, CA).

Construct pMoV2.11-EGFP (from which virus polio-GFP is derived) was made by amplifying full length EGFP (enhanced green fluorescent protein) from pEGFP (Clontech, CA) with oligos A and E, and then cloning that PCR fragment into the EcoRI and XhoI sites of pMoV2.11 by standard techniques. Note: pSabRV1-EGFP has also been constructed and SabRV1-GFP virus has been produced (data not shown).

For pSabRV1-SIV clones, SIVmac239 plasmids p239SpSp5', p239SpE3', and pSIV239opennef (obtained from the AIDS Research and Reference Reagent Program, courtesy of Ronald Desrosiers (30)) were used as the PCR template to generate SIV inserts. Inserts were amplified using Pfu Turbo high-fidelity DNA polymerase, using conditions recommended by the manufacturer (Stratagene, CA). A complete table of the 62 oligos used for these reactions is avaliable upon request. PCR fragments were purifed on Qiaquick spin columns, digested with DpnI restriction enzyme (to eliminate any input SIV plasmid carried over), EcoRI, and XhoI, and then Qiaquick spin column purified a second time. Vector pSabRV1 plasmid was cut with EcoRI and XhoI, Qiaquick spin column purified, and then quantified by agarose gel electrophoresis. Gel purification of vector was generally avoided. SIV inserts were ligated into pSabRV1 using NEB T4 DNA ligase (New England BioLabs, MA) in a overnight reaction at 16° C containing 25 ng pSabRV1 and 20 ng SIV insert DNA. Ligations were dialyzed on 13mm 0.025mm VSWP membranes (Millipore, MA) against 50 mls deionized H_2O for 10 mins. Then 1 ml of ligation was electroporated into 25 ml SURE cells in a 0.1 cm cuvette (BTX

ElectroCell 600 electroporator conditions: 129 Ω, 1,400 V, 5 msec pulse). One ml of LB was immediately added to the cuvette, and 20-200 ml of electroporated SURE cells were plated onto LB + ampicillin plates and incubated at 37° C overnight. Further culturing and DNA isolation was as described above. All plasmid clones were analyzed by restriction digest and all inserts were DNA sequenced in their entirity to confirm that the appropriate clone had been obtained and was not mutated.

Sabin 2 early passage virus (SO + 3) was kindly provided by K. Chumakov. HeLa cells were infected with Sabin 2 at an MOI of > 1 and incubated at 37°C. Cells were harvested at 9 hrs post-infection, RNA was extracted using RNeasy (Qiagen, Santa Clarita, CA), and cDNA was synthesized using random primed Superscript II (Life Technologies, Gaithersburg, MD). Full length Sabin 2 was PCR amplified with primers SAB21 and SAB24, using XL polymerase (Perkin Elmer, CA), 2 mM Mg(OAc), and 500 μM dNTPs, with conditions: 30" at 94°, 8' at 65°, for 30 cycles. The full length Sabin 2 genome was then Qiaquick spin column purified, digested with SalI and HindIII, and ligated into SalI/HindIII digested pUC18. Ligations were introduced into DH5α chemically competent cells as recommended by the manufacturer (Life Technologies, MD). Plasmid minipreps of clones were analyzed by restriction digest and tested for the ability to produce infectious virus. The three plasmid clones that produced virus (pS2-2, pS2-3, and pS2-10) were sequenced and the genome sequence was compared to the Sabin 2 consensus sequence generated by Pollard et al. (53). Two coding mutations in pS2-10 were identified, one in Vp2 and one in 3C. The latter was corrected by swapping the 374 bp BsiWI-NcoI DNA fragment from a clone (pS2-3) with no 3C mutation into pS2-10 to create pS2-10F. We have since fixed the other coding mutation in pSabRV2 (nucleotide

1492, a.a. 249, F to L in Vp2) by site-directed mutagenesis and checked the resulting pSabRV2.2 by DNA sequencing.

To generate pSabRV2, the 60 bp cloning site—which contains a 5 glycine spacer and AvrII and NotI restriction sites flanked by $2A^{pro}$ cleavage sites (only the 5' (or N terminal) cleavage site is counted in the 60 bp, since it contains modifed codon usage (64) and the 3' (or C terminal) cleavage site is endogenous and essential)—was cloned into pS2-10F. A BstEII-SnaBI fragment containing the unique SabRV2 cloning sites was generated by overlapping PCR of DNA fragments B and S, and digestion with BstEII and SnaBI. DNA fragment B was made by PCR (Pfu Turbo, Stratagene, CA) using oligos B1 and oligo B2. Similarly, DNA fragment S was generated by PCR using oligos S1(63 nt long, 45 nt of which overlap with oligo B2, which together contain the full pSabRV2 cloning site) and S2. Both PCR fragments were gel purified using Qiagen and used together as template with oligos B1 and S2 in an overlapping PCR reaction to generate a 1635 bp fragment containing the 60 bp SabRV2 cloning site flanked by the BstEII and SnaBI restriction sites. The digested BstEII-SnaBI fragment was ligated into BstEII/SnaBI digested pS2-10F to create pSabRV2.

For pSabRV2-SIV cloning, SIV PCR fragments were generated as described above (using similar oligos; a complete list of all 50 oligos is available upon request) and cloning was done comparably to that of pSabRV1-SIV's, except AvrII/NotI digestions were used and Xl1-Blue cells (Stratagene, CA) were used for transformations. Stocks of pSabRV2-SIV plasmids were made by inoculating single colonies of transformed XL1-Blue cells (grown overnight on LB+amp plates) into 5 ml cultures of LB + ampicillin (50 μg/ml) and grown at 37°C for 8-14 hrs. Plasmid DNA was isolated from cells by the

Qiafilter Miniprep technique (Qiagen, CA). All clones were analyzed by restriction digest and all inserts were DNA sequenced in their entirety to confirm that the appropriate clone had been obtained and was not mutated.

All vectors and plasmids are readily available to any interested investigator.

Cells and Medium. HeLa S3 cells obtained from ATCC (ATCC stock + 5-30 passages) were grown in DMEM/F12 medium (Gibco/Life Technologies) supplemented with 10% fetal calf serum (FCS) (Gibco/Life Technologies), penicillin/streptomycin, and L-glutamine. Adherent cell cultures were maintained at 10-80% confluence at 37° C + 6% CO_2. 293 cells were grown under the same conditions, but were sometimes left to 100% confluence.

Transcriptions and electroporations. Transcriptions were generally done using T7 RNA Polymerase (150 U) from New England Biolabs, using the supplied transcription buffer supplemented with 40 U RNAsin (Promega, WI), and 1.25 mM NTPs. Plasmid templates (1-3 mg) were first linearized with ClaI (pMoV2.11, pS1, or pSabRV1 vector) or HinDIII (pS2-10F or pSabRV2) for 1 hr at 37° C in a 20 ml volume. On some occasions the restriction enzyme was then inactivated for 10 min at 60° C. Once linearized, plasmid template was added to the full transcription mixture (total volume 200 ml), and transcription was allowed to proceed for 60-90 mins at 37° C before terminating the reaction by freezing at -80° C. RNA quality and quantity was assessed by agarose gel electrophoresis before use in subsequent experiments. RNA from transcription reactions was used directly, without purification, in electroporations.

Electroporations were done using HeLa S3 cells at 40-75% confluence, plated the previous day, which were then trypsinized, centrifuged, and resuspended at a

concentration of 3 x 10^6 cells/ml in Ca^{++}/Mg^{++}-free phosphate buffered saline (on some occasions, 293 cells were used in an identical manner). 800 ml of cells was added to a cold 0.4 cm electroporation cuvette (BioRad, CA; or BTX, CA), 10-40 mg RNA was added to cells, cuvette was flicked multiple times to resuspend cells that had settled, and cuvette was immediately electroporated in a BTX electroporator with settings: 950 mF, 24 Ω, and 300 V. The entire contents of the cuvettes was then added to a 6 cm dish (10 cm dishes were used for SabRV2 viruses) with 3 ml of warm DMEM/F12 + 10% FCS (see (26) for related details). Sabin1 and SabRV1 recombinants were grown at 32° C, as Sabin 1 has a tendency to acquire wildtype characteristics when passaged multiple times at greater than 34° C (56). MoV2.11 derivatives, Sabin 2 (S2-10F), and SabRV2 recombinants were grown at 37° C. Plates were left until complete cytopathic effect (CPE) was observed; normally less than 24 hrs for MoV2.11 recombinants, and frequently 24-36 hrs for SabRV1 and SabRV2 recombinants.

Viral stocks, passages, and plaque assays. P_0 viral stock were harvested from electroporated cells exhibiting full CPE by taking the cells and supernatant, and freeze/thawing 3 times with a dry ice/ethanol bath and a 37° C water bath. Cellular debris was then pelleted by a 5 min, 300g centrifugation, and P_0 viral stock supernatant was transferred to a fresh tube. Note: some of the MoV2.11, SabRV1, and SabRV2 recombinant viral stocks appeared to lose some titer upon multiple freeze/thaw cycles. This was not observed with normal wildtype poliovirus. Therefore viral stocks were stored in constant temperature -30° C or -80° C freezers.

Concentration of certain viruses (see Results) was done using Centriprep concentration filters units with either a molecular weight limit of 30kD or 50kD

(Milipore, MA). 12-15 ml of low-titer SabRV1-SIV or SabRV2-SIV viral stocks were spun in Centriprep filter units for 30 minutes at 3,000g. This resulted in a 5-15 fold concentration of virus. Concentrated stocks were then titered by plaque assay.

Nine P_0 SabRV2-SIV viruses were mixed in equal amounts and passaged five times at an MOI of 0.1, at both 32° C and 37° C. Passaging of SabRV2-SIV viruses was done by infecting $3x10^6$ HeLa cells in 10 cm plates at an MOI of 0.1 with the P_0 viral cocktail stock. Cells were incubated in 3 ml DMEM/F12 medium supplemented with 10% fetal calf serum at 37° C or 32° C; and P_1 viral stock was harvested when complete CPE was observed (24-36 hrs post-infection). The same process was followed when carrying out passages P_2 through P_5. Each passage at MOI of 0.1 represents approximately 2 generations of viral replication. In total, P_5 viruses had gone through 10-12 generations of viral replication. The cocktail passages were tested for the presence of the SIV inserts by RT-PCR using primers in the poliovirus sequence flanking all of the SIV inserts.

All plaque assays were done as previously described (18). Plaque assays involving SabRV1 recombinants were incubated at 32° C for 5 days post-infection, plaque assays involving SabRV2 recombinants were incubated at 37° C for 4 days post-infection, and plaque assays involving MoV2.11 recombinants (polio-GFP) were incubated at 37° C for 2 days post-infection.

Immunofluorescence and microscopy. Poliovirus protein was detected using a rabbit anti-2C peptide (seq: CNIGNCMEALFQ; O.Beske and R. Andino, manuscript in prep.) antibody (purified by HiTrap Protein A chromatography (Pharmacia, NJ) using a 0.1M Na-citric acid (pH 2.8) elution buffer) that had been conjugated to Alexa 594 (a bright,

Texas Red-like fluorophore)(Molecular Probes, OR; Alexa 594 Protein Labelling Kit). 1 x 10^6 HeLa cells infected with polio-GFP for 7-9 hrs (or transfected with polio-GFP RNA for 6-8 hrs) were trypsinized (cells in the supernatant were collected as well), fixed, and permeablized (CalTag Fix and Perm cell permeabilization kit, CalTag, CA) in the presence of 0.5 ml Alexa 594 fluorescently labelled anti-2C antibody in a 50 ml total volume. Stained cells were visualized for immunofluorescence using a Leica DMLB microscope, and images were captured via a CCD camera and exported to Adobe Photoshop 5.5. Polio-GFP plaques (Fig. 2C) were directly visualized on the microscope without fixation, by simply inverting the polio-GFP infected 10cm plate and observing the bright fluorescence through the bottom of the tissue culture dish. To determine the percentage of GFP^+ virus in a viral stock, polio-GFP was plaque assayed with propiduim iodide (Sigma) added to the agar at 1 mg/ml. GFP^+ plaques were then visualized, using a long-pass FITC filter, as a green ring of cells surrounding a circle of red cells (dead, propidium iodide stained cells). GFP^- plaques were seen simply as red circles of dead propidium iodide stained cells.

RT-PCR. 2-5 x 10^5 HeLa cells in 6-well dishes were infected with an MOI of 0.5-10 of the appropriate virus (an MOI of 10 was used if available). Cells were incubated at 37° C in 1 ml of DMEM/F12 + 10% FCS for 8 hrs (SabRV1 recombinants) or 6.5 hrs (MoV2.11 and SabRV2 recombinants), and then harvested by scraping or trypinization. RNA was collected using RNeasy (Qiagen) and cDNA was synthesized using random primed Superscript II (Life Technologies) reactions. PCR was done using rTth (Perkin Elmer XL polymerase) and primers S1-3240F and S1-3580R (MoV2.11, S1, and SabRV1 recombinants) or primers S2-3151F and S2-3518R (S2-10F and SabRV2

recombinants). Conditions were: 0.5 ml cDNA, 2.2 mM $Mg(OAc)_2$, 0.5 ml XL polymerase, and manufacturer recommended buffer and primer concentrations in a 50 ml reaction, with 94° C for 1', 50° C for 1', and 72° C for 1' with 30 cycles. Generally 1-5 ml of the final product was loaded on a 1.5% agarose gel for analysis.

Oligonucleotides.

A = GGTGGGGGAGGTGAATTCATGGTGAGCAAGGGCGAGGAG

E = GTGGTCAGATCCTCGAGCTTGTACAGCTCGTCCATGCCG

C = AATTGGTTCCTGGTCGACCGATGATCCGCG

D = TCGACGCGGATCATCGGTCGACCAGGAACC

B1 = ACATATTCGAGATTTGAC

B2 =

TGCGGCCGCTGCCCTAGGCCCTCCGCCACCTCCATGACCGAAACCGTATGTGGTCAGACCCTT TTCTGG

S1 =

GGTTTCGGTCATGGAGGTGGCGGAGGGCCTAGGGCAGCGGCCGCAGGATTAACGACTTATGG A

S2 = GCTCAATACGGTGCTTGC

SAB21 =

AAAAGGTCGACTAATACGACTCACTATAGGTTAAAACAGCTCTGGGGTTG

SAB24 =

GGGGGAAGCTTAGGCCTTTTTTTTTTTTTTTTTTTCCTCCGAATTAAAGAAAA AT

S1-3240F = CCTCCAAAATCAGAGTGTATC

S1-3580R = GCCCTGGGCTCTTGATTCTGT

S2-3151F = GAAGGCGATTCGTTGTAC

S2-3518R = CTTGATTCAGCCACTAAG

Western blot analysis. 2 x 10^6 HeLa cells infected (MOI of 10) with SabRV1 or SabRV2 (or SabRV1-SIV or SabRV2-SIV recombinants (SabRV2-SIV recombinants at an MOI= 1-5) were incubated for 7 hours at 37°C. Cells were harvested and lysed on ice for 1 min (lysis buffer consisted of 10 mM Tris [pH 7.5], 140 mM NaCl, 5 mM KCl, and 1% IGEPAL), and nuclei were removed by centrifugation. 20 µl of whole-cell lysate was electrophoresed through a 12% SDS-polyacrylamide gel and analyzed by immunoblotting. The anti-SIV serum used was obtained as a pool serum from SIV-infected rhesus macaques (*Macaca mulatta*) and was kindly provided by Chris Miller. Secondary antibody (Horseradish peroxidase-conjugated rabbit anti-human IgG) was obtained from DAKO (Carpinteria, CA). Blots were probed with 1:100-diluted monkey serum in TBST (10 mM Tris-HCl [pH 7.5], 150 mM NaCl, 0.15% Tween-20) with 5% Carnation fat-free dry milk, washed twice in TBST containing 0.15% Tween-20 and once in TBST containing 0.5% Tween 20, probed with the horseradish peroxidase anti-human antibody (1: 2,000 dilution), and then detected by enhanced chemiluminescence (Amersham, Arlington Heights, IL) as specified by the manufacturer. Films were digitally scanned and exported to Photoshop 5.5 (Adobe, San Jose, CA).

Results

Construction and characterization of Sabin vectors

Using our wildtype type 1 poliovirus vector, pMoV2.11, we previously constructed several recombinant polioviruses expressing simian immunodeficiency virus (SIV) fragments, and we demonstrated that the recombinant viruses elicited anti-SIV antibody responses in poliovirus-susceptible mice (64). Other recombinant polioviruses generated by our laboratory were capable of eliciting cytotoxic T lymphocyte responses against the exogenous antigen in poliovirus-susceptible mice (36, 59). More recently, we reported the construction of several recombinant polioviruses using a PCR-based technique (18). These newer viruses expressed two SIV antigens—$p17^{gag}$ and part of $gp41^{env}$—in both a wildtype type 1 poliovirus and the Sabin 2 poliovirus type 2 vaccine strain background. Importantly, these recombinant polioviruses (Polio1-sp17, Polio1-gp41, Sabin2-sp17, and Sabin2-gp41) elicited strong anti-SIV humoral, mucosal, and cellular immune responses in cynomolgus monkeys (18). Having demonstrated the immunogenicity of recombinant polioviruses in a primate model system, our next goal was to generate vectors well-defined and safe for use in humans. Given the excellent safety record of Sabin vaccine strain polioviruses in humans (63), we wished to do all future experiments, in primates and humans, using only Sabin based viruses produced from molecularly defined constructs. Hence, we engineered plasmid clones of Sabin 1 and Sabin 2 derived vectors.

The Sabin 1 recombinant viral vector (pSabRV1) was constructed in a modified pS1 (a molecular clone of Sabin 1 (32)). A pS1 BstEII fragment encoding the junction

between the P1 and P2 regions was replaced by the corresponding fragment of our standard poliovirus vector, pMoV2.11 (64), to add the cloning sites and proteolytic cleavage site before 2A (Fig. 1A, also see Materials and Methods). This pSabRV1 plasmid was sequenced across the modified region and then used to produce SabRV1 virus. SabRV1 grew comparably to the S1 molecular clone, and moderately smaller than an uncloned population of Sabin 1 vaccine (Fig. 1B, and data not shown).

To construct the Sabin 2 recombinant viral vector (pSabRV2) we first generated a plasmid clone of Sabin 2, pS2-10F (see Materials and Methods).The EcoRI and XhoI cloning sites used in pMoV 2.11 and pSabRV1 could not be used in pSabRV2 due to the presence of the restriction sites within the Sabin 2 genome. Therefore, we constructed pSabRV2 by overlapping PCR adding AvrII and NotI as cloning sites (see Fig. 1A and Materials and Methods). The resulting pSabRV2 plasmid was used to produce a SabRV2 viral stock, and SabRV2 grew comparably to Sabin2 and uncloned Sabin 2 by plaque assay (Fig. 1C, and data not shown).

Polio-GFP

In some cases, one difficulty with the use of recombinant polioviruses is producing genetically pure stocks, since viruses with deletions in their insert sequences begin to accumulate as recombinant polioviruses replicate through a number of generations (18, 43, 64). Therefore, to generate uniformly pure viral stocks, we developed a new strategy for producing stocks of 1st generation virus (called P_0 stocks here). To optimize the protocol we used green fluorescent protein (GFP) as a model insert. Polio-GFP was constructed using the pMoV2.11 vector (see Materials and

Methods). Upon transfection of polio-GFP viral RNA into HeLa cells, GFP was expressed to high levels in all cells positive for 2C, one of the nonstructural viral proteins (Fig. 2A-B). Having demonstrated that polio-GFP was replication competent and easy to assay, we then proceeded to electroporate HeLa cells with increasing concentrations of polio-GFP RNA under various electroporation conditions. In this manner we identified conditions that consistently give a 50-80% maximal electroporation efficiency (Fig. 2D).

P_0 stocks of polio-GFP generated in this manner were 100% genetically pure, as determined by RT-PCR (presence of full GFP gene, data not shown) and plaque assay, where 100% of plaques were GFP^+ (see example plaque in Fig. 2C). This procedure is a great improvement over our previous approach, because polio-GFP stocks generated by our original technique (pasaging an individual plaque pick) were only 0% – 10% GFP^+ (data not shown).

Library of SabRV1 viruses expressing SIV fragments

Our major goal is to make a poliovirus-vector based vaccine that generates protective immunity against SIV induced AIDS. Available data indicates that an AIDS vaccine is possible(9, 19), but the exact nature of the antigens necessary to elicit a protective response have remained unclear. Live poliovirus vectors cannot accomodate full length SIV Gag, Pol, or Env coding sequences, due to the RNA length packaging limitations of the poliovirus virion. Given the size limitation of live poliovirus vectors, and given the fact that the SIV antigens necessary to elicit a protective immune response are unknown, we have adopted the strategy of expressing the entirity of SIV Gag, Pol, Env, and Nef proteins as a series of overlapping 100-250 amino acid fragments (Fig. 3A),

to be administered all together, in a cocktail, as an SIV vaccine. This approach has been previously tested on a smaller scale in our lab by immunizing mice with a cocktail of five polioviruses expressing SIV fragments (64).

Using the pSabRV1 vector, we cloned a series of 31 viral vector plasmids each containing a single SIV gene fragment (Table 1 and Fig. 3A). We then used our high efficiency electroporation technique to generate P_0 stocks of each of these 31 SabRV1-SIV viruses. Each virus was analyzed for plaque size, viral titer, and genetic purity. As might have been expected, plaque sizes ranged from 1-3 mm, somewhat smaller than the parental SabRV1 virus (4-6 mm) (Fig. 3B). Most viral titers ranged from 1×10^7 to 1.5×10^8 pfu/ml (Table 1), 5-100x lower than the parental SabRV1 virus, similar to that seen with our previous recombinant polioviruses (18, 64). To standardize the viral stock concentrations, several of the low titer stocks were concentrated 5-10x (see Table 1) using a Centriprep spin column (see Materials and Methods).

Viral RNA from P_0 stocks was checked by RT-PCR for the presence of the inserted sequences. Control PCR experiments were done which showed that insert deletions could be detected at frequencies as low as 1%. Briefly, titrated cDNA from a stock of SabRV1 virus with a large insert (virus L, with a ~600 nt insert) was mixed with cDNA from a stock of SabRV1 virus with a small insert (virus S, with a ~300 nt insert) in varying L:S ratios (1000:1 ; 100:1 ; 10:1 ; 1:1) and then PCR amplified. Small virus S insert served as a mock deletion of the virus L insert, and could be detected after PCR (as a clear second band of the appropriate size) when present as 1% of the initial cDNA template (data not shown). This high sensitivity is due to the preferential amplification of shorter fragments during PCR reactions.

By RT-PCR analysis of the P_0 stocks, 24 out of 31 of the SabRV1-SIV viruses fully retained the original inserted sequence (Fig. 3C, and data not shown). The two viruses with the largest inserts, SabRV1-Env19 (786 nts) and SabRV1-Nef25 (789 nts), did not grow well. SabRV1-Env19 was recovered with 30% of plaques larger than the original virus, suggesting that the insert had been deleted in 30% of the population. And SabRV1-Nef25 was recovered with 400-450 nts of the insert deleted (Fig. 3C). The poor growth of these two recombinant viruses appears to be due to the size of the insert involved, because when these regions of SIV were split between two recombinant polioviruses (SabRV1-Env17/SabRV1-Env18 and SabRV1-Nef23/SabRV1-Nef24) the viruses grew well and we were able to recover genetically pure stocks without deletions (Table 1 and Fig. 3). Viruses carrying the next three largest inserts, SabRV1-Pol13 (672 nt), SabRV1-Env21XL (588 nt), and SabRV1-Gag3 (585 nt) grew to low titers (Table 1) but retained their inserts in P_0 stocks. Viruses SabRV1-Pol6, SabRV1-Pol12, and SabRV1-Env22 had minor deletion products detectable by RT-PCR; by plaque assay, revertants represented approximately 1% of each stock. SabRV1-Env16 was only recovered as a wildtype revertant, making SabRV1 sized plaques and containing no insert by PCR (data not shown). Therefore, new overlapping fragments of Env were cloned as pSabRV1-Env16M and pSabRV1-Env16C to see if there was a particular sequence in this region of Env that was toxic for expression in poliovirus. Both SabRV1-Env16M and SabRV1-Env16C grew to substantial titers, and pure P_0 viral stocks were obtained (Table 1), indicating that there was no specific toxic sequence. By nucleotide and amino acid sequence gazing, there was no obvious explanation for why SabRV1-

Pol6/Pol12/Env16/Env22 would be predisposed to deleting the insert at an early timepoint.

In the case of SabRV1-Env21S, SabRV1-Env21L, and SabRV1-Env21XL, the transmembrane domain of gp41 did not appear to be toxic to SabRV1, as the titers of SabRV1-Env21XL were similar to those of viruses with a comparable insert size. Additionally, the fusion domain of gp41, also highly hydrophobic, had no negative effect on viral titer. Notably, virus Mo-gp41.b (64) contains the full gp41 transmembrane domain flanked by part of the cytoplasmic and extracellular domains, and that virus replicates well and is even glycosylated upon expression in Mo-gp41.b infected cells. These results are in contrast with certain other picornavirus constructs containing transmembrane domains (4, 16, 34). Therefore it appears that the context of long hydrophobic stretches of amino acids is important in determining the effect of the insert on viral replication.

Library of SabRV2 viruses expressing SIV fragments

We then used the pSabRV2 vector to clone a series of 26 viral vector plasmids each containing a single SIV gene fragment (Table 2 and Fig. 4A). Having a library of SIV fragments in polioviruses of two different serotypes (type 1 and type 2) allows us to give booster immunizations (18). We generated P_0 stocks of each of these 26 SabRV2-SIV viruses, using the technique described above. Each virus was analyzed for plaque size, viral titer, and genetic purity. Plaque sizes generally ranged from 3-5 mm (Fig.4B)—moderately smaller than the parental virus (6-7mm)—although three recombinant viruses (Gag2, Gag4, Nef23) exhibited plaques (1 mm) that were

substantially smaller than the parental virus. Most viral titers ranged from 1.1 x 10^6 to 6.8 x 10^6 PFU/ml (Table 2); 30-200x lower than parental SabRV2 virus. Several low-titer viruses with titers ranging from 3 x 10^5 to 9 x 10^5 PFU/ml were concentrated 5-20 fold, as described above (Table 2).

Since SabRV1-Gag3 grew to low titers, overlapping fragments of Gag3 were cloned into pSabRV2-Gag3N and pSabRV2-Gag3C. Pure P_0 stocks were obtained, and both viruses exhibited a small plaque phenotype.

Recently Cafaro et al. published the intriguing result that a Tat vaccine may protect against SIV (12). Therefore, we constructed SabRV2-Tat25, which expresses the full-length Tat protein (390 bp), as part of our vector library. The Tat is presumably biologically active (with RNA binding and transcription factor activities (24, 61)), but had no obvious effect on poliovirus replication. SabRV2-Tat25 grew to a good titer ($4.2x10^6$ pfu/ml) and made standard sized plaques for a SabRV2 recombinant virus (Fig.4B).

As with SabRV1 recombinants, viral RNA from P_0 stocks was checked by RT-PCR for the presence of the desired insert. Both SabRV2-13M and SabRV2-13C had partially deleted inserts by RT-PCR, and by plaque assay approximately 5% of the population exhibited wildtype plaque phenotype (Fig. 4C and data not shown). SabRV2-Pol6P (containing the SIV protease) was only recovered as wildtype revertant, making SabRV2-sized plaques and containing no insert by RT-PCR (data not shown). This indicates that the full-length protease might be toxic for expression in poliovirus, presumably due to proteolytic activity. Notably, SabRV1 and SabRV2 viruses with a larger insert (Pol6), which completely contains the SIV protease as well as flanking

sequence, are viable and P_0 stocks of SabRV1-Pol6 and SabRV2-Pol6 mostly contain the full length insert (Fig. 3C and data not shown). We interpret this to mean that expression of the longer SIV protease precursor contained in the Pol6 insert may inhibit the self-processing of SIV protease to an active form, though firmly establishing this would require further study.

To verify the expression of SIV proteins by the Sabin based vectors, we made cytosolic extracts from HeLa cells infected with SabRV1 viruses (Env15C, Env20, Pol9, Gag1) and SabRV2 viruses (Env15C, Gag1, Gag4). Western blotting of the cytosolic extracts showed that the SIV proteins are expressed in SabRV1-SIV and SabRV2-SIV infected cells (Fig. 5A-B).

Insert Stability

To analyze the ability of SabRV viruses to retain the inserted sequences, we passaged nine SabRV2-SIV viruses that replicated well, as a cocktail. Nine P_0 SabRV2-SIV viruses were mixed in equal amounts and passaged five times at an MOI of 0.1, at both 32° C and 37° C. Each passage at MOI of 0.1 represents approximately 2 generations of viral replication. In total, P_5 viruses had gone through 10-12 generations of viral replication. The cocktail passages were tested for the presence of the SIV inserts by RT-PCR using primers in the poliovirus sequence flanking all of the SIV inserts. Inserts were fully retained through the 10-12 generations assayed, without indication of any insertless virus (Fig. 6A).

We then checked the composition of this SabRV2 cocktail throughout the passages by RT-PCR using primers specific for each SIV insert. All nine SIV full-length

inserts were maintained through all the passages at both 32° C and 37° C (Fig.6 and data not shown), though SabRV2-Gag4, -Env15C, -Pol14, and -Env17 showed evidence of the presence of viral subpopulations containing partial deletions in the 37° C P_5 (Fig.6B).

Discussion

The utility of live picornavirus vectors has been somewhat controversial (43). Our data demonstrates that, though live poliovirus vectors have limitations, they can be powerful expression systems. Live poliovirus vectors have shown utility as experimental tools (18, 59) and as efficacious vaccine vectors (36)(Crotty et al., accompanying paper) in several highly informative studies.

The two most significant limitations of live picornavirus vectors are the packaging limit (34) and insert maintenance (2, 3, 15, 18, 34, 43, 64).

The packaging limit of picornavirus vectors (~1000-1500 nts) is a solid barrier. We describe one useful strategy for alleviating this problem in vaccine development. A library of defined overlapping fragments (150-250 a.a.) of large genes can be cloned into poliovirus vectors to make a more complete representation of the antigenic content of the target pathogen. We demonstrate here that the construction of such a library of viruses is feasible (the SabRV1-SIVs and SabRV2-SIV), and in the accompanying paper (Crotty et al.) these viruses were then used as a successful cocktail vaccine in a difficult SIV challenge experiment. Therefore, the defined library approach is a feasible and productive strategy for the use of live picornavirus vaccine vectors.

In recombinant picornaviruses, large inserts (> 600 nts) tend to get deleted more rapidly than smaller inserts, and obtaining rec$^-$ polioviruses (see below) would be a long term solution to the expression of larger inserts than we currently use in the defined library strategy. Notably, the packaging size limit is not a problem when the correlate of protection is a known CTL epitope (such as in certain tumor (37) or viral (3) vaccine model systems), as CTL epitopes are very small (9-10 a.a.) and are stably maintained by

recombinant picornaviruses (M. Slifka and L. Whitton, personal comm.; W. Melchers, personal comm.).

The second significant limitation of picornavirus vectors is insert maintenance. As poliovirus vectors containing insert are passaged for multiple rounds they accumulate insert deletions (18, 43, 64). We have previously described a progression of techniques and vectors to produce more stable viruses (7, 64, 66) and more genetically pure stocks (18, 64). In this report we have described a P_0 stock production technique that alleviates the problem of insert retention. Importantly, we also demonstrate that we can passage a cocktail of nine of these SabRV2-SIV viruses for 10-12 rounds of replication and maintain full-length insert in all nine recombinant viruses. This experiment indicates that the viral stocks produced should replicate well in vivo and express their SIV inserts for a number of rounds of replication. In the accompanying paper, we demonstrate that these SabRV-SIV stocks express SIV antigens in vivo at levels sufficent to be highly immunogenic and can even be protective against a very difficult virulent SIV challenge. Additionally, we have previously demonstrated that a recombinant poliovirus expressing a 200 a.a. fragment of Ova (polio-Ova) can stably express the Ova protein for numerous rounds of replication, and polio-Ova is potently immunogenic in vivo in mice, capable of providing 100% protection against a difficult malignant melanoma tumor challenge (B16-Ova) (36). It has been previously reported that wildtype poliovirus Mahoney strain-based expression vectors are severely impaired in viral replication and are highly genetically unstable, and that upon replication, inserted sequences are rapidly deleted (43). Results presented here and in previous publications (18, 64), using newer poliovirus vector constructs and virus production techniques, are in disagreement with those observations,

as most of our constructs grow to substantial titers, plaque well, and are genetically stable enough for substantial replication in vitro and impressive immunogenicity in vivo. Interestingly, it is also possible that the Sabin strain vectors are capable of better retaining the insert than the original Mahoney-based vectors.

However, though we feel that we have now demonstrated that Sabin vector technology is advanced enough to produce sufficient viral stocks for any pre-clinical vaccine experiment, we have not eliminated the root problem of insert retention and do not currently have a vector or a vector production strategy feasible for manufacturing Sabin vectors for human use. We propose two plausible strategies for the production of Sabin vectors for use in humans.

The first approach is to use a manufacturing strategy being considered for the production of replicons: high-throughput electroporation. Such a technique would effectively make P_0 stocks in a high-throughput manner. After vaccination, the viruses would eventually lose their inserts after multiple rounds of replication in the vaccinated individuals. However, that amount of replication in vivo before insert loss has proven to be sufficient to induce protective immunity in two different difficult challenge systems ((36) and Crotty et al., accompanying paper). Thus, after having served their purpose of stimulating a potent immune response against the desired target pathogen, insertless poliovirus could continue inducing anti-polio protective immunity until infection is resolved.

The second approach to producing Sabin vectors for use in humans is to identify recombination-deficient (rec^-) polioviruses. It is believed that the inserted sequences in poliovirus are deleted by RNA recombination via a copy-choice mechanism (31)

involving the RNA-dependent RNA polymerase (8, 21). It is not known whether mutations can effectively alter the capacity of poliovirus to recombine, but such mutations have been identified in the polymerase of another positive-strand RNA virus (22). Our hypothesis is that RNA recombination is a sophisticated process that the virus actively uses to improve its genetic fitness. As such, it is reasonable to propose that one can identify mutants defective for this complex biochemical process (rec$^-$ mutants). These mutants, due to their deficiency at RNA recombination, will be genetically stable. Supporting this hypothesis is the observation that the recombination frequency of RNA virus species greatly varies. For example, for poliovirus, which has a high recombination frequency, up to 20% of progeny are products of recombination (20, 29). In the other side of the spectrum, it is very rare or impossible to find recombinants of flaviviruses like yellow fever virus and Kunjin virus (less than 0.01% recombination) (57). Therefore, though our current vectors and techniques are sufficient for most experimental purposes, we are now actively searching for rec$^-$ poliovirus mutants as a long term solution to picornavirus insert retention.

References

1. **Alexander, L., H. H. Lu, M. Gromeier, and E. Wimmer** 1994. Dicistronic polioviruses as expression vectors for foreign genes AIDS Res Hum Retroviruses. **10**:S57-60.
2. **Altmeyer, R., N. Escriou, M. Girard, A. Palmenberg, and S. van der Werf** 1994. Attenuated Mengo virus as a vector for immunogenic human immunodeficiency virus type 1 glycoprotein 120 Proceedings of the National Academy of Sciences of the United States of America. **91**:9775-9.
3. **Altmeyer, R., M. Girard, S. van der Werf, V. Mimic, L. Seigneur, and M. F. Saron** 1995. Attenuated Mengo virus: a new vector for live recombinant vaccines Journal of Virology. **69**:3193-6.
4. **Anderson, M. J., D. C. Porter, P. N. Fultz, and C. D. Morrow** 1996. Poliovirus replicons that express the gag or the envelope surface protein of simian immunodeficiency virus SIV(smm) PBj14 Virology. **219**:140-9.
5. **Anderson, M. J., D. C. Porter, Z. Moldoveanu, T. M. Fletcher, 3rd, S. McPherson, and C. D. Morrow** 1997. Characterization of the expression and immunogenicity of poliovirus replicons that encode simian immunodeficiency virus SIVmac239 Gag or envelope SU proteins Aids Research and Human Retroviruses. **13**:53-62.
6. **Andino, R., G. E. Rieckhof, P. L. Achacoso, and D. Baltimore** 1993. Poliovirus RNA synthesis utilizes an RNP complex formed around the 5'-end of viral RNA Embo Journal. **12**:3587-98.
7. **Andino, R., D. Silvera, S. D. Suggett, P. L. Achacoso, C. J. Miller, D. Baltimore, and M. B. Feinberg** 1994. Engineering poliovirus as a vaccine vector for the expression of diverse antigens Science. **265**:1448-51.
8. **Arnold, J. J., and C. E. Cameron** 1999. Poliovirus RNA-dependent RNA polymerase (3Dpol) is sufficient for template switching in vitro J Biol Chem. **274**:2706-16.
9. **Benson, J., C. Chougnet, M. Robert-Guroff, D. Montefiori, P. Markham, G. Shearer, R. C. Gallo, M. Cranage, E. Paoletti, K. Limbach, D. Venzon, J. Tartaglia, and G. Franchini** 1998. Recombinant vaccine-induced protection against the highly pathogenic simian immunodeficiency virus SIV(mac251): dependence on route of challenge exposure Journal of Virology. **72**:4170-82.
10. **Bouchard, M. J., D. H. Lam, and V. R. Racaniello** 1995. Determinants of attenuation and temperature sensitivity in the type 1 poliovirus Sabin vaccine J Virol. **69**:4972-8.
11. **Buge, S. L., E. Richardson, S. Alipanah, P. Markham, S. Cheng, N. Kalyan, C. J. Miller, M. Lubeck, S. Udem, J. Eldridge, and M. Robert-Guroff** 1997. An adenovirus-simian immunodeficiency virus *env* vaccine elicits humoral, cellular and mucosal immune responses in rhesus macaques and decreased viral burden following vaginal challenge J. Virol. **71**:8531-8541.
12. **Cafaro, A., A. Caputo, C. Fracasso, M. T. Maggiorella, D. Goletti, S. Baroncelli, M. Pace, L. Sernicola, M. L. Koanga-Mogtomo, M. Betti, A.**

Borsetti, R. Belli, L. Akerblom, F. Corrias, S. Butto, J. Heeney, P. Verani, F. Titti, and B. Ensoli 1999. Control of SHIV-89.6P-infection of cynomolgus monkeys by HIV-1 Tat protein vaccine [see comments] Nat Med. **5**:643-50.

13. **Cao, X., and E. Wimmer** 1996. Genetic variation of the poliovirus genome with two VPg coding units Embo J. **15**:23-33.
14. **Cao, X., and E. Wimmer** 1995. Intragenomic complementation of a 3AB mutant in dicistronic polioviruses Virology. **209**:315-26.
15. **Cho, S. P., B. Lee, and M. K. Min** 2000. Recombinant polioviruses expressing hepatitis B virus-specific cytotoxic T-lymphocyte epitopes Vaccine. **18**:2878-85.
16. **Choi, W. S., R. Pal-Ghosh, and C. D. Morrow** 1991. Expression of human immunodeficiency virus type 1 (HIV-1) gag, pol, and env proteins from chimeric HIV-1-poliovirus minireplicons J Virol. **65**:2875-83.
17. **Christodoulou, C., F. Colbere-Garapin, A. Macadam, L. F. Taffs, S. Marsden, P. Minor, and F. Horaud** 1990. Mapping of mutations associated with neurovirulence in monkeys infected with Sabin 1 poliovirus revertants selected at high temperature J Virol. **64**:4922-9.
18. **Crotty, S., B. L. Lohman, F. X. Lu, S. Tang, C. J. Miller, and R. Andino** 1999. Mucosal immunization of cynomolgus macaques with two serotypes of live poliovirus vectors expressing simian immunodeficiency virus antigens: stimulation of humoral, mucosal, and cellular immunity J Virol. **73**:9485-95.
19. **Davis, N. L., I. J. Caley, K. W. Brown, M. R. Betts, D. M. Irlbeck, K. M. McGrath, M. J. Connell, D. C. Montefiori, J. A. Frelinger, R. Swanstrom, P. R. Johnson, and R. E. Johnston** 2000. Vaccination of macaques against pathogenic simian immunodeficiency virus with Venezuelan equine encephalitis virus replicon particles [published erratum appears in J Virol 2000 Apr;74(7):3430] J Virol. **74**:371-8.
20. **Domingo, E., J. J. Holland, and P. Ahlquist** 1988. RNA genetics. CRC Press, Boca Raton, Fla.
21. **Figlerowicz, M., P. D. Nagy, and J. J. Bujarski** 1997. A mutation in the putative RNA polymerase gene inhibits nonhomologous, but not homologous, genetic recombination in an RNA virus Proc Natl Acad Sci U S A. **94**:2073-8.
22. **Figlerowicz, M., P. D. Nagy, N. Tang, C. C. Kao, and J. J. Bujarski** 1998. Mutations in the N terminus of the brome mosaic virus polymerase affect genetic RNA-RNA recombination J Virol. **72**:9192-200.
23. **Flint, S. J., L. W. Enquist, R. M. Krug, V. R. Racaniello, and A. M. Skalka** 1999. Principles of Virology, 1st ed. ASM Press, Washington, D.C.
24. **Frankel, A. D., and J. A. Young** 1998. HIV-1: fifteen proteins and an RNA Annu Rev Biochem. **67**:1-25.
25. **Georgescu, M. M., J. Balanant, A. Macadam, D. Otelea, M. Combiescu, A. A. Combiescu, R. Crainic, and F. Delpeyroux** 1997. Evolution of the Sabin type 1 poliovirus in humans: characterization of strains isolated from patients with vaccine-associated paralytic poliomyelitis J Virol. **71**:7758-68.
26. **Gohara, D. W., S. Crotty, J. J. Arnold, J. D. Yoder, R. Andino, and C. E. Cameron** 2000. Poliovirus RNA-dependent RNA Polymerase ($3D^{Pol}$): Structural, biochemical, and biological analysis of conserved structural motifs A and B Journal of Biological Chemistry. **275**:25523-25532.

27. **Hofling, K., S. Tracy, N. Chapman, K. S. Kim, and J. Smith Leser** 2000. Expression of an antigenic adenovirus epitope in a group B coxsackievirus [In Process Citation] J Virol. **74**:4570-8.
28. **Hull, H. F., N. A. Ward, B. P. Hull, J. B. Milstien, and C. de Quadros** 1994. Paralytic poliomyelitis: seasoned strategies, disappearing disease Lancet. **343**:1331-7.
29. **Jarvis, T. C., and K. Kirkegaard** 1991. The polymerase in its labyrinth: mechanisms and implications of RNA recombination Trends Genet. **7**:186-91.
30. **Kestler, H., T. Kodama, D. Ringler, M. Marthas, N. Pedersen, A. Lackner, D. Regier, P. Sehgal, M. Daniel, N. King, and R. Desrosiers** 1990. Induction of AIDS in rhesus monkeys by molecularly cloned simian immunodeficiency virus [see comments] Science. **248**:1109-12.
31. **Kirkegaard, K., and D. Baltimore** 1986. The mechanism of RNA recombination in poliovirus Cell. **47**:433-43.
32. **Kohara, M., S. Abe, S. Kuge, B. L. Semler, T. Komatsu, M. Arita, H. Itoh, and A. Nomoto** 1986. An infectious cDNA clone of the poliovirus Sabin strain could be used as a stable repository and inoculum for the oral polio live vaccine Virology. **151**:21-30.
33. **Kohara, M., T. Omata, A. Kameda, B. L. Semler, H. Itoh, E. Wimmer, and A. Nomoto** 1985. In vitro phenotypic markers of a poliovirus recombinant constructed from infectious cDNA clones of the neurovirulent Mahoney strain and the attenuated Sabin 1 strain J Virol. **53**:786-92.
34. **Lu, H. H., L. Alexander, and E. Wimmer** 1995. Construction and genetic analysis of dicistronic polioviruses containing open reading frames for epitopes of human immunodeficiency virus type 1 gp120 J Virol. **69**:4797-806.
35. **Lu, Z., G. V. Rezapkin, M. P. Douthitt, Y. Ran, D. M. Asher, I. S. Levenbook, and K. M. Chumakov** 1996. Limited genetic changes in the Sabin 1 strain of poliovirus occurring in the central nervous system of monkeys J Gen Virol. **77**:273-80.
36. **Mandl, S., L. J. Sigal, K. L. Rock, and R. Andino** 1998. Poliovirus vaccine vectors elicit antigen-specific cytotoxic T cells and protect mice against lethal challenge with malignant melanoma cells expressing a model antigen Proceedings of the National Academy of Sciences of the United States of America. **95**:8216-21.
37. **McAllister, A., A. E. Arbetman, S. Mandl, C. Pena-Rossi, and R. Andino** 2000. Recombinant Yellow Fever Viruses Are Effective Therapeutic Vaccines for Treatment of Murine Experimental Solid Tumors and Pulmonary Metastases J Virol. **74**:9197-9205.
38. **McKnight, K. L., and S. M. Lemon** 1996. Capsid coding sequence is required for efficient replication of human rhinovirus 14 RNA J Virol. **70**:1941-52.
39. **Melnick, J. L.** 1996. Enteroviruses: Polioviruses, coxsackieviruses, echoviruses, and newer enteroviruses, p. 655-712. *In* B. N. Fields, D. M. Knipe, and P. M. Howley (eds), Fields virology, 3rd ed, vol. 1. Lippincott-Raven Publishers, Philadelphia.

40. **Molla, A., S. K. Jang, A. V. Paul, Q. Reuer, and E. Wimmer** 1992. Cardioviral internal ribosomal entry site is functional in a genetically engineered dicistronic poliovirus Nature. **356:**255-7.
41. **Molla, A., A. V. Paul, M. Schmid, S. K. Jang, and E. Wimmer** 1993. Studies on dicistronic polioviruses implicate viral proteinase 2Apro in RNA replication Virology. **196:**739-47.
42. **Morrow, C. D., M. J. Novak, D. C. Ansardi, D. C. Porter, and Z. Moldoveanu** 1999. Recombinant viruses as vectors for mucosal immunity Current Topics in Microbiology and Immunology. **236:**255-73.
43. **Mueller, S., and E. Wimmer** 1998. Expression of foreign proteins by poliovirus polyprotein fusion: analysis of genetic stability reveals rapid deletions and formation of cardioviruslike open reading frames Journal of Virology. **72:**20-31.
44. **Nomoto, A., T. Omata, H. Toyoda, S. Kuge, H. Horie, Y. Kataoka, Y. Genba, Y. Nakano, and N. Imura** 1982. Complete nucleotide sequence of the attenuated poliovirus Sabin 1 strain genome Proc Natl Acad Sci U S A. **79:**5793-7.
45. **Novak, M. J., L. E. Smythies, S. A. McPherson, P. D. Smith, and C. D. Morrow** 1999. Poliovirus replicons encoding the B subunit of Helicobacter pylori urease elicit a Th1 associated immune response Vaccine. **17:**2384-91.
46. **Ogra, P. L., M. Fishaut, and M. R. Gallagher** 1980. Viral vaccination via the mucosal routes Reviews of Infectious Diseases. **2:**352-69.
47. **Ogra, P. L., and D. T. Karon** 1971. Formation and function of poliovirus antibody in different tissues Progess in Medical Virology. **13:**156-193.
48. **Omata, T., M. Kohara, S. Kuge, T. Komatsu, S. Abe, B. L. Semler, A. Kameda, H. Itoh, M. Arita, E. Wimmer, and et al.** 1986. Genetic analysis of the attenuation phenotype of poliovirus type 1 J Virol. **58:**348-58.
49. **Omata, T., M. Kohara, Y. Sakai, A. Kameda, N. Imura, and A. Nomoto** 1984. Cloned infectious complementary DNA of the poliovirus Sabin 1 genome: biochemical and biological properties of the recovered virus Gene. **32:**1-10.
50. **Ourmanov, I., C. R. Brown, B. Moss, M. Carroll, L. Wyatt, L. Pletneva, S. Goldstein, D. Venzon, and V. M. Hirsch** 2000. Comparative efficacy of recombinant modified vaccinia virus Ankara expressing simian immunodeficiency virus (SIV) Gag-Pol and/or Env in macaques challenged with pathogenic SIV J Virol. **74:**2740-51.
51. **Overwijk, W. W., D. S. Lee, D. R. Surman, K. R. Irvine, C. E. Touloukian, C. C. Chan, M. W. Carroll, B. Moss, S. A. Rosenberg, and N. P. Restifo** 1999. Vaccination with a recombinant vaccinia virus encoding a "self" antigen induces autoimmune vitiligo and tumor cell destruction in mice: requirement for CD4(+) T lymphocytes Proc Natl Acad Sci U S A. **96:**2982-7.
52. **Paul, J. R., J. T. Riordan, and J. L. Melnick** 1951. Antibodies to three different antigenic types of poliomyelitis virus in sera from north Alaskan eskimos American Journal of Hygiene. **54:**275-285.
53. **Pollard, S. R., G. Dunn, N. Cammack, P. D. Minor, and J. W. Almond** 1989. Nucleotide sequence of a neurovirulent variant of the type 2 oral poliovirus vaccine J Virol. **63:**4949-51.
54. **Porter, D. C., D. C. Ansardi, W. S. Choi, and C. D. Morrow** 1993. Encapsidation of genetically engineered poliovirus minireplicons which express

human immunodeficiency virus type 1 Gag and Pol proteins upon infection Journal of Virology. **67:**3712-9.

55. **Porter, D. C., J. Wang, Z. Moldoveanu, S. McPherson, and C. D. Morrow** 1997. Immunization of mice with poliovirus replicons expressing the C-fragment of tetanus toxin protects against lethal challenge with tetanus toxin Vaccine. **15:**257-64.
56. **Rezapkin, G. V., W. Alexander, E. Dragunsky, M. Parker, K. Pomeroy, D. M. Asher, and K. M. Chumakov** 1998. Genetic stability of Sabin 1 strain of poliovirus: implications for quality control of oral poliovirus vaccine Virology. **245:**183-7.
57. **Rice, C. M.** 1996. Flaviviridae: The Viruses and their Replication, p. 2 v. (xxi, 2950). *In* B. N. Fields, D. M. Knipe, and P. M. Howley (eds), Fields virology, 3rd ed. Lippincott - Raven Press, New York.
58. **Schultz, A.** 1998. Using recombinant vectors as HIV vaccines, p. 1-4, IAVI Report, vol. 3.
59. **Sigal, L. J., S. Crotty, R. Andino, and K. L. Rock** 1999. Cytotoxic T-cell immunity to virus-infected non-haematopoietic cells requires presentation of exogenous antigen Nature. **398:**77-80.
60. **Smith, A. D., S. C. Geisler, A. A. Chen, D. A. Resnick, B. M. Roy, P. J. Lewi, E. Arnold, and G. F. Arnold** 1998. Human rhinovirus type 14:human immunodeficiency virus type 1 (HIV-1) V3 loop chimeras from a combinatorial library induce potent neutralizing antibody responses against HIV-1 Journal of Virology. **72:**651-9.
61. **Smith, C. A., S. Crotty, Y. Harada, and A. D. Frankel** 1998. Altering the context of an RNA bulge switches the binding specificities of two viral Tat proteins Biochemistry. **37:**10808-14.
62. **Stott, J., S. L. Hu, and N. Almond** 1998. Candidate vaccines protect macaques against primate immunodeficiency viruses Aids Research and Human Retroviruses. **14 Suppl 3:**S265-70.
63. **Sutter, R. W., S. L. Cochi, and J. L. Melnick** 1999. Live attenuated poliovirus vaccines, p. 1230. *In* S. Plotkin, and W. Orenstein (eds), Vaccines, 3rd ed. W. B. Saunders, Philadelphia.
64. **Tang, S., R. van Rij, D. Silvera, and R. Andino** 1997. Toward a poliovirus-based simian immunodeficiency virus vaccine: correlation between genetic stability and immunogenicity Journal of Virology. **71:**7841-50.
65. **Weeks-Levy, C., and P. L. Ogra** 1996. Polioviruses and mucosal vaccines. *In* H. Kiyono, P. Ogra, and J. McGhee (eds), Mucosal Vaccines, 1st ed. Academic Press, New York.
66. **Yim, T. J., S. Tang, and R. Andino** 1996. Poliovirus recombinants expressing

hepatitis B virus antigens elicited a humoral immune response in susceptible mice

Virology. **218:**61-70.

Table 1. Sabin 1 vector viruses expressing SIV proteins.

Virus name	Amino acid coverage	bp length	Stock titer (pfu/ml)
SabRV1-Gag1	Gag 2-134 (p17)	399	1.4×10^8
SabRV1-Gag2	Gag 92-263 (p17/p24)	516	4×10^{7}*
SabRV1-Gag3	Gag 214-408 (p24)	585	1×10^5
SabRV1-Gag4	Gag 362-509 (p24/p9)	444	9×10^7
SabRV1-Gag5	Gag 454-509 (p9)	168	6×10^7
SabRV1-Pol6	Pol (-)29-146 (protease)[f]	501	8×10^7
SabRV1-Pol7	Pol 97-266	510	4×10^{7}*
SabRV1-Pol8	Pol 218-330	339	4×10^7
SabRV1-Pol9	Pol 290-472	549	3×10^{7}*
SabRV1-Pol10	Pol 397-530	402	5×10^7
SabRV1-Pol11	Pol 490-631	426	5×10^7
SabRV1-Pol12	Pol 597-767	510	3×10^{7}*
SabRV1-Pol13	Pol 728-951	672	3×10^5
SabRV1-Pol14	Pol 828-981	372	5×10^7
SabRV1-Env15	Env 18-164 (no signal sequence)	441	8×10^7
SabRV1-Env16	Env 110-278 (gp120)	507	—[b]
SabRV1-Env16C	Env 181-326 (gp120)	438	9×10^7
SabRV1-Env16M	Env 148-249 (gp120)	306	1.8×10^8
SabRV1-Env17	Env 237-380 (gp120)	432	6×10^7
SabRV1-Env18	Env 335-498 (gp120)	492	3×10^{7}*
SabRV1-Env18N	Env 279-395 (gp120)	351	8×10^7
SabRV1-Env18C	Env 361-510 (gp120)	450	6×10^7
SabRV1-Env19	Env 237-498 (gp120)	786	2×10^{7}a
SabRV1-Env20	Env 486-632 (gp120/gp41)	441	4×10^{7}*
SabRV1-Env21S	Env 540-698 (gp41 short)	477	1×10^7
SabRV1-Env21L	Env 526-698 (gp41 w/fusion)	519	3×10^{7}*
SabRV1-Env21XL	Env 526-721 (gp41 w/fusion + TM)[c]	588	6×10^5
SabRV1-Env22	Env 712-879 (gp41, cyto domain)[d]	504	4×10^{7}*
SabRV1-Nef23	Nef 1-145	438	5×10^7
SabRV1-Nef24	Nef 126-262	411	5×10^7
SabRV1-Nef25	Nef 1-262 (full length)	789	1.5×10^{8}e

* Indicates viruses that were later concentrated to a titer between 1.4×10^8 and 2.2×10^8pfu/ml (see text for details).

a 30% of SabRV1-Env19 stock had deleted the insert, reverting to SabRV1.

b 100% of SabRV1-Env16 stock had deleted the insert, reverting to SabRV1.

c SabRV1-Env21XL includes the gp41 fusion domain as well as the transmembrane domain (TM).

d SabRV1-Env22 has the gp41 cytoplasmic (cyto) domain.

e SabRV1-Nef25 viral stock had no full length insert. The entire stock contained a 2/3 deletion (see Fig. 4B).

f Amino acid 1 of the protease is position +1 of Pol in our nomenclature.

Table 2. Sabin2 vector viruses expressing SIV proteins

Virus Name	Amino Acid coverage	bp length	Stock titer (pfu/ml)
SabRV2-Gag1	Gag 2-134 (p17)	399	$4.7x10^6$
SabRV2-Gag2	Gag 92-263 (p17/p24)	516	$1.6x10^6$
SabRV2-Gag3N	Gag 133-299	500	$8x10^5$*
SabRV2-Gag3C	Gag 266-432	500	$1.3x10^6$
SabRV2-Gag4	Gag 362-509 (p24/p9)	444	$3.6x10^6$
SabRV2-Pol6	Pol (-)29-146[c]	501	$9x10^5$
SabRV2-Pol6P	Pol 1-99 (full length protease)	297	—[a,c]
SabRV2-Pol7	Pol 97-266	510	$1.2x10^6$
SabRV2-Pol8	Pol 218-330	339	$6.8x10^6$
SabRV2-Pol9	Pol 290-472	549	$1.2x10^6$
SabRV2-Pol10	Pol 397-530	402	$5.8x10^6$
SabRV2-Pol11	Pol 490-631	426	$1.3x10^6$
SabRV2-Pol12	Pol 597-766	510	—[d]
SabRV2-Pol12C	Pol 681-810	387	$1x10^6$
SabRV2-Pol13C	Pol 751-840	270	$3x10^5$[b]
SabRV2-Pol13M	Pol 732-859	387	—[a]
SabRV2-Pol14	Pol 828-981	372	$5.6x10^6$
SabRV2-Env15C	Env 71-211	420	$1.5x10^6$
SabRV2-Env16M	Env 148-249 (gp120)	306	$1.2x10^6$*
SabRV2-Env17	Env 237-380 (gp120)	432	$2.2x10^6$
SabRV2-Env18	Env 335-498 (gp120)	492	$1.7x10^5$
SabRV2-Env20	Env 486-632 (gp120/gp41)	441	$1.5x10^6$
SabRV2-Env21L	Env 526-698 (gp41 w/fusion domain)	519	$7x10^5$*
SabRV2-Nef23	Nef 1-145	438	$7.6x10^5$*
SabRV2-Nef24	Nef 126-262	411	$1.1x10^6$*
SabRV2-Tat25	Tat 1-130	390	$4.2x10^6$

* Indicates viruses were later concentrated to a titer between $9x10^5$ and $3.0x10^6$ (see text for deails).

a 100% of SabRV2-Pol6P and SabRV2-Pol13M had deleted the insert, reverting to SabRV2

b SabRV2-Pol13C had partially deleted the insert resulting in a mixed population

c Amino Acid 1 of the protease is position +1 of Pol in our nomenclature

d No virus was recovered

Figure Legends

Figure 1

(A) Recombinant Sabin poliovirus vectors. Grey boxes indicate 2A proteolytic cleavage sites (GLTTY/GFGH). In all three vectors the first proteolytic cleavage site coding sequence is followed by a 5 glycine spacer (not marked) and the in frame cloning sites (white boxes) immediately prior to the second proteolytic cleavage site. In total, 60-70 extra nts are added to the viral genome.

(B) Plaque assay of cloned Sabin 1 virus (pS1) and the Sabin 1 recombinant virus vector (SabRV1) at 32° C.

(C) Plaque assay of cloned Sabin 2 (pS2-10F) and the Sabin 2 recombinant virus vector (SabRV2) at 37° C.

Figure 2

(A) Virus production schematic. The plasmid vector contains a full length poliovirus genome (in this case wildtype Mahoney type 1 poliovirus) that includes the GFP gene fragment inserted at the junction between the structural and nonstructural genes of the genome. Infectious poliovirus-GFP RNA is generated by *in vitro* transcription from a T7 promoter. The RNA is transfected into HeLa cells via high efficiency electroporation, and infection begins. The viral polyprotein is translated, including the GFP insert, and the GFP insert is cleaved away from the polyprotein via two $2A^{pro}$ protease cleavage sites

flanking the insert. The virus then continues its replication cycle and produces infectious virions containing the poliovirus genome with the GFP gene insert.

(B) GFP expression. Cells transfected with polio-GFP RNA express high levels of GFP. 100% of cells that stain positive for poliovirus nonstructural protein 2C (bottom panel, fluorescently conjugated a-2C antibody staining) are also brightly positive for GFP expression (middle panel). An uninfected cell is indicated by a hollow white arrow, and an infected cell is indicated by a filled white arrow.

(C) Polio-GFP plaque assay. Polio-GFP virus can replicate and spread through a monolayer of cells. A polio-GFP plaque started by a single polio-GFP virion in a HeLa cell monolayer. Photo taken at 48 hrs. post-infection. The thick ring of GFP-positive cells were currently infected with polio-GFP, and the dark center of the ring are the cells already killed by the virus (confirmed by propidium iodide staining, data not shown). Plaque is approximately 50% the size of a wildtype poliovirus plaque at the same timepoint. Polio-GFP plaques can be grown for over 5 days post-infection without loss of GFP expression in the polio infected cells at the periphery of the plaque.

(D) Demonstration of high-efficiency electroporation technique. Use of ≥ 5 μg polio-GFP RNA in this experiment resulted in greater than 80% GFP^+ cells by 6 hrs. post-electroporation (cell condition changes causes some variability in these electroporations. Therefore, in later experiments we generally used 10-20 μg to ensure at least a 50% electroporation efficiency). Note that the GFP expression is sufficiently strong enough to be seen in the presence of the standard 480 nm light plus normal white light (right column). The ratio of GFP^+ cells/(GFP^+ cells + uninfected cells), is the measure of

efficiency of transfection of the live poliovirus vector (uninfected cells can be seen in the righthand column).

Figure 3

(A) SabRV1-SIV library schematic. Major SIV open reading frames (Gag, Pol, Env, and Nef) are shown to scale. Bars indicate each of the individual SIV coding regions inserted into the SabRV1 vector.

(B) SabRV1-SIV plaque assays. All SabRV1-SIV viruses made were titered by plaque assay. Growth of several representative viruses at 32° C is shown here. SabRV1 without an insert is shown as a control. SabRV1-Env22 was the smallest plaque size virus recovered.

(C) SabRV1-SIV insert analysis. SabRV1-SIV viral stocks were tested for the presence of the SIV insert by RT-PCR (see Material and Methods). SRV1 RT-PCR is indicated by (V) and is shown in both the uper and lower panel. The size of the SRV1 band (360 bps) is the size of a virus containing no insert, but does contain the dupliated $2A^{pro}$ cleavage site, the glycine linker, and the multiple conling sites. Other viruses are indicated by their number. Sixteen out of twenty viruses, some of them with large (> 500 nt) inserts, showed no sign of deletions. Four viruses presented some form of deletion. SabRV1-Pol6 contained a deletion of half of the insert in a small percentage of the population. SabRV1-Pol12 and SabRV1-Env22 contained complete deletions (apparently including the multiple cloning site and the second $2A^{pro}$ cleavage site in the case of SabRV1-Pol12) in approximately 1% of the population.

Figure 4

(A) SabRV2-SIV library schematic. Major SIV open reading frames (Gag, Pol, Env, and Nef) are shown to scale. Bars indicate each of the individual SIV coding regions inserted into the SabRV2 vector. Note that Tat is shown simply as full length Tat, as the genomic Tat gene is divided into two exons.

(B) SabRV2-SIV plaque assays. All SabRV2-SIV viruses made were titered by plaque assay. Growth of several representative viruses at 37°C is shown here at day 4. SabRV2 without insert is shown as a control.

(C) SabRV2-SIV insert analysis. SabRV2-SIV viral stocks were tested for the presence of the SIV insert by RT-PCR (see Materials and Methods). SabRV2 empty vector RT-PCR is indicated by (V) and is shown in both the upper and lower panel. The size of the SabRV2 band (427 bp) is the size of the virus containing no insert, but that does contain the duplicated $2A^{pro}$ cleavage site, the glycine linker, and the multiple cloning sites. Other viruses are indicated by their number.

Figure 5

(A) Expression of the SIV proteins in cells infected with SabRV1-SIV. Cytoplasmic extracts were prepared from HeLa cells 7 hours after infection either with SabRV1 or with SabRV1 recombinant viruses (indicated by number). Expression of SIV proteins was analyzed by Western blotting with pooled polyclonal serum from SIV-positive rhesus monkeys. Sizes are indicated in kilodaltons.

(B) Expression of the SIV proteins in cells infected with SabRV2-SIV.

Cytoplasmic extracts were prepared as described above, either with SabRV2 or with SabRV2 recombinant viruses (indicated by number). Western blotting was performed as described above.

Figure 6

(A) Stability of SabRV2 recombinant viruses passaged as a cocktail. Nine SabRV2-SIV viruses were mixed in equal amounts and passaged five times at an MOI of 0.1, for a total of 10-12 generations of viral replication) either at 32° C or at 37° C. P_0 indicates the original cocktail in which the nine P_0 viral stocks obtained directly from high-efficiency transfection were mixed in equal proportion. P_1 through P_5 indicate stocks from subsequent passages of the P_0 cocktail. Cocktail stocks were tested for the presence of the SIV inserts by RT-PCR using primers within the poliovirus sequence flanking the SIV inserts. SabRV2 empty vector RT-PCR is indicated by (V) and is shown in both the left and right panel and the P_0 RT-PCR is shown in the left panel. The size of the SabRV2 band (427 bp) is the size of the virus containing no insert. Throughout all five passages, at both 32° C and 37° C, inserts are fully retained.

(B) Composition of Sab-RV2 cocktail over a series of passages. The passaged cocktail stocks were checked for the presence of the individual viruses by RT-PCR with primers specific for each SIV insert. In the left panel, the P_0 stock contains all nine viruses by RT-PCR. The middle and right panel show the presence of all nine SabRV2-SIV viruses both after P_3 and after P_5 at an MOI of 0.1 at 37° C (identical data was obtained for passages at 32° C and is not shown).

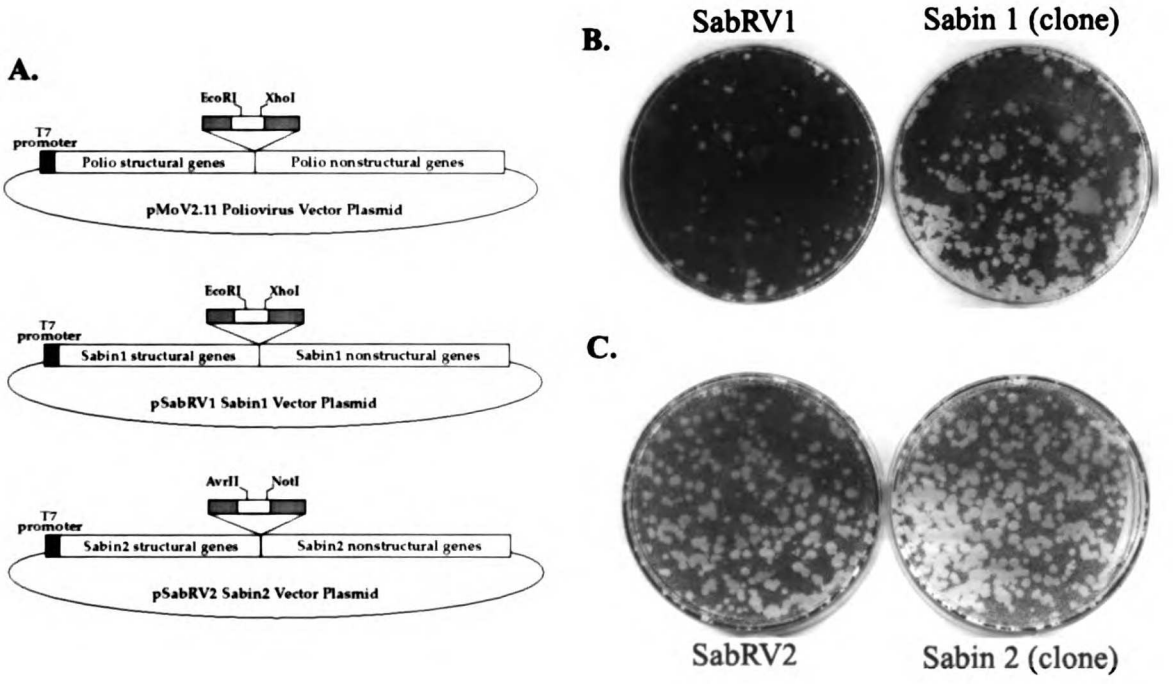
A.
EcoRI
XhoI
T7 promoter
Polio structural genes
Polio nonstructural genes
pMoV2.11 Poliovirus Vector Plasmid
EcoRI
XhoI
T7 promoter
Sabin1 structural genes
Sabin1 nonstructural genes
pSabRV1 Sabin1 Vector Plasmid
AvrII
NotI
T7 promoter
Sabin2 structural genes
Sabin2 nonstructural genes
pSabRV2 Sabin2 Vector Plasmid
B.
SabRV1
Sabin 1 (clone)
C.
SabRV2
Sabin 2 (clone)

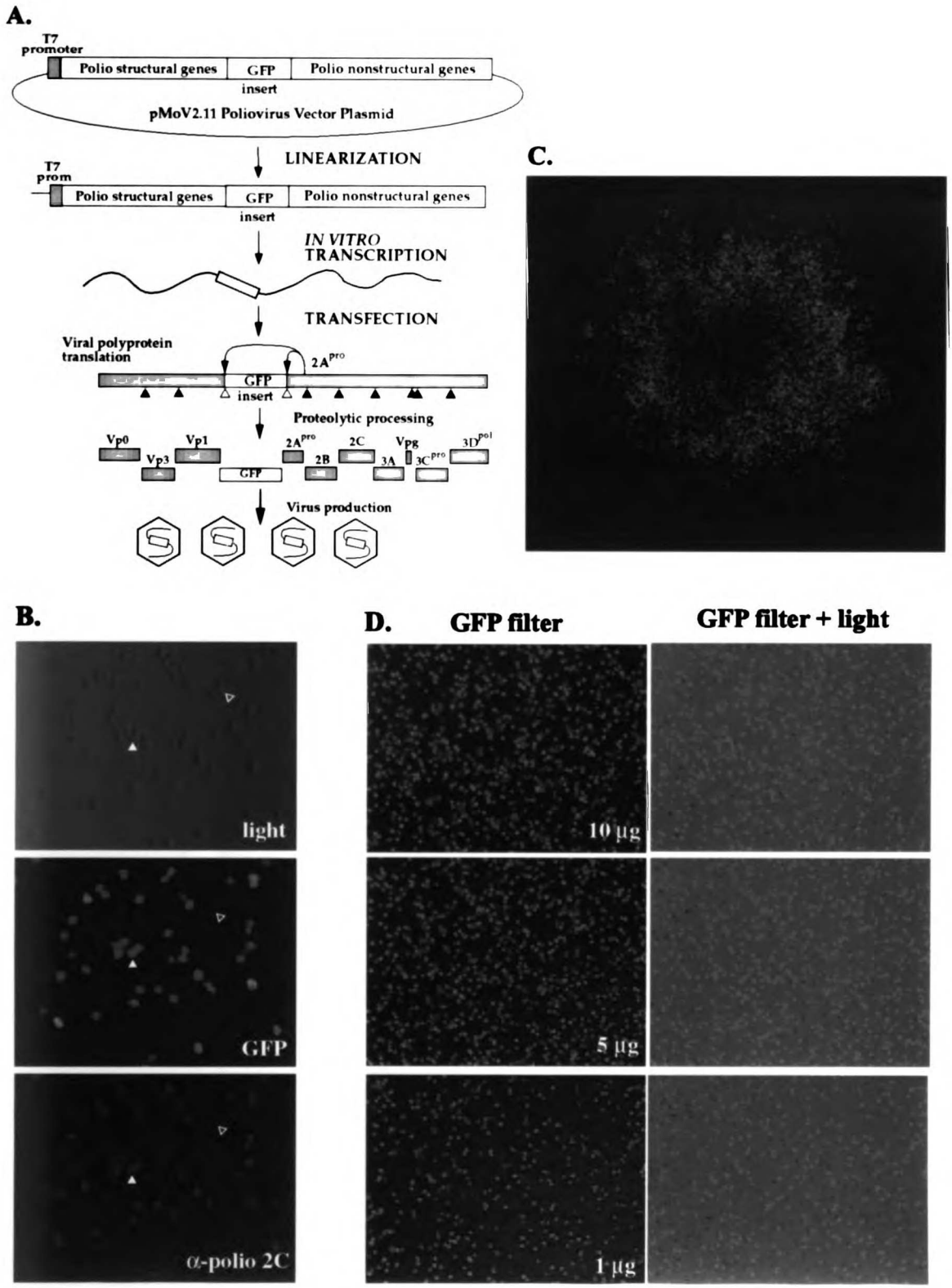
A.
T7 promoter
Polio structural genes
GFP
Polio nonstructural genes
insert
pMoV2.11 Poliovirus Vector Plasmid
LINEARIZATION
T7 prom
Polio structural genes
GFP
Polio nonstructural genes
insert
IN VITRO TRANSCRIPTION
TRANSFECTION
Viral polyprotein translation
2A^pro
GFP
insert
Proteolytic processing
Vp0
Vp1
2A^pro
2C
Vpg
3D^pol
Vp3
2B
3A
3C^pro
GFP
Virus production
C.
B.
light
GFP
α-polio 2C
D.
GFP filter
GFP filter + light
10 µg
5 µg
1 µg

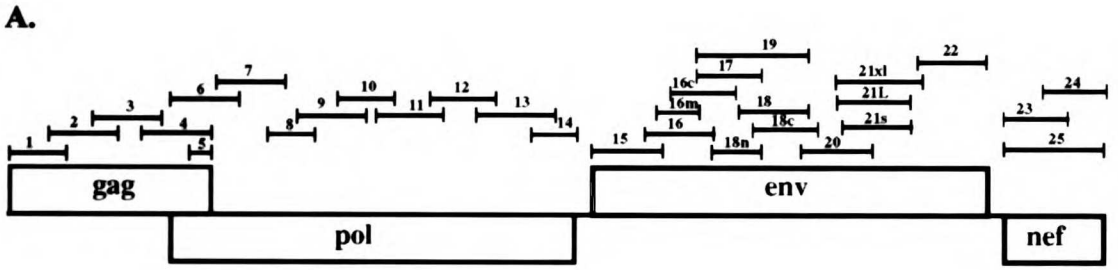
A.
1
2
3
4
5
6
7
8
9
10
11
12
13
14
15
16
16c
16m
17
18
18c
18n
19
20
21L
21s
21xl
22
23
24
25
gag
pol
env
nef

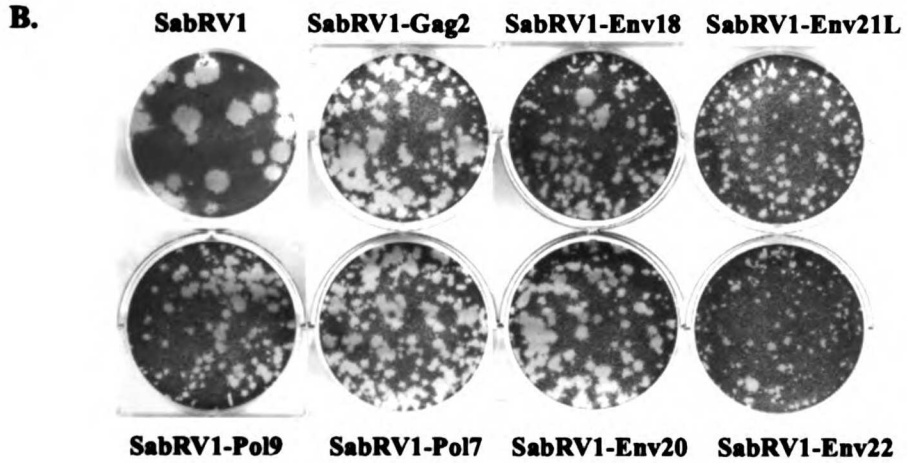
B.
SabRV1
SabRV1-Gag2
SabRV1-Env18
SabRV1-Env21L
SabRV1-Pol9
SabRV1-Pol7
SabRV1-Env20
SabRV1-Env22

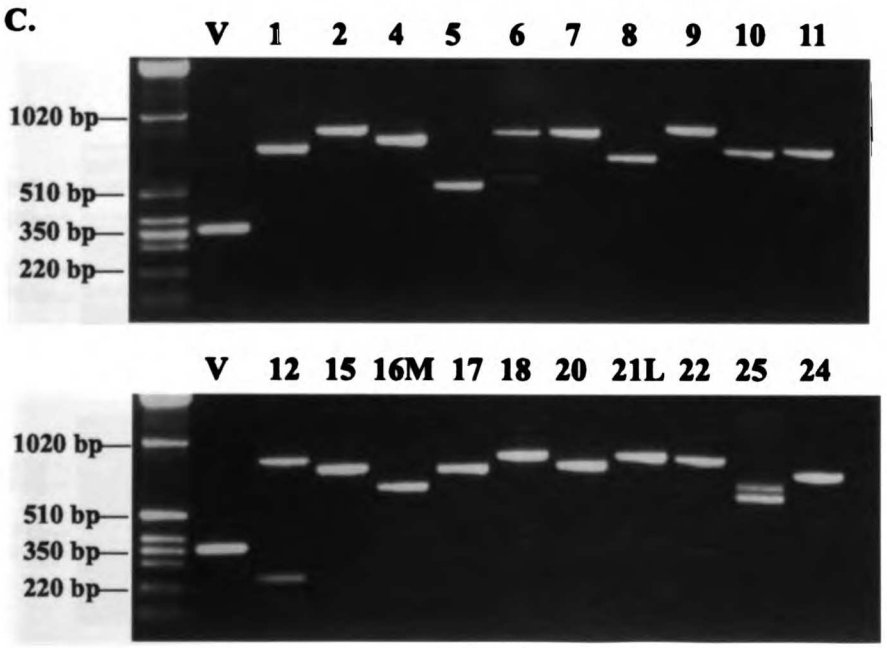
C.
V 1 2 4 5 6 7 8 9 10 11
1020 bp
510 bp
350 bp
220 bp
V 12 15 16M 17 18 20 21L 22 25 24
1020 bp
510 bp
350 bp
220 bp

Figure 4

A.

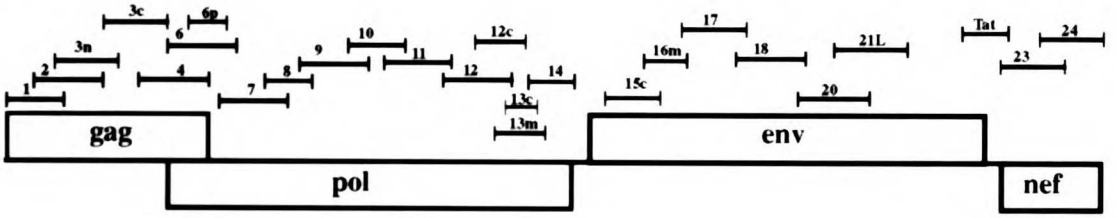
3c
6p
6
3n
2
4
1
7
8
9
10
11
12c
12
14
13c
13m
17
16m
18
21L
15c
20
Tat
24
23
gag
pol
env
nef

B.

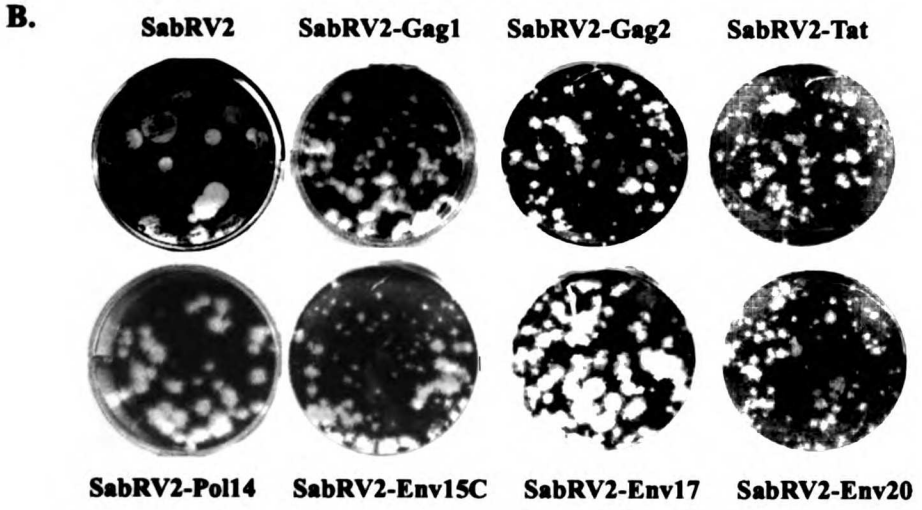
SabRV2
SabRV2-Gag1
SabRV2-Gag2
SabRV2-Tat
SabRV2-Pol14
SabRV2-Env15C
SabRV2-Env17
SabRV2-Env20

C.

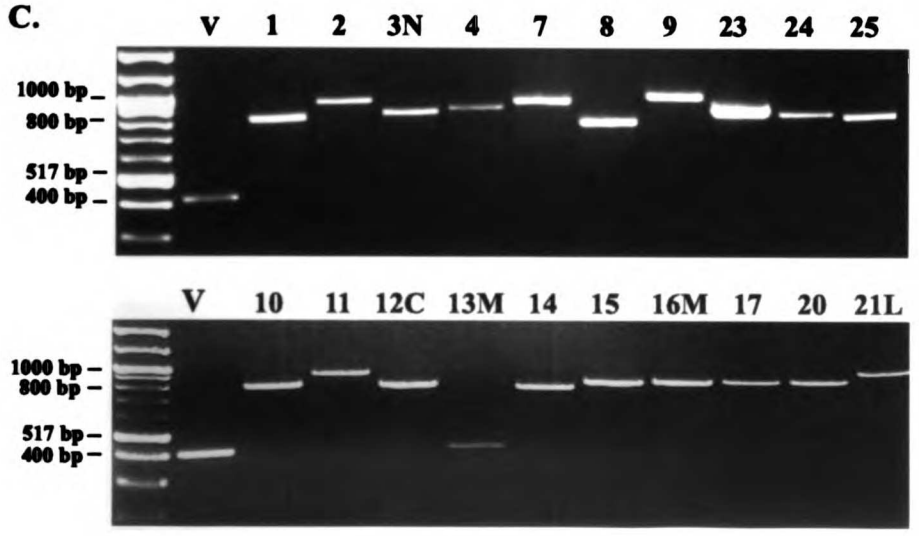
V 1 2 3N 4 7 8 9 23 24 25
1000 bp
800 bp
517 bp
400 bp
V 10 11 12C 13M 14 15 16M 17 20 21L
1000 bp
800 bp
517 bp
400 bp

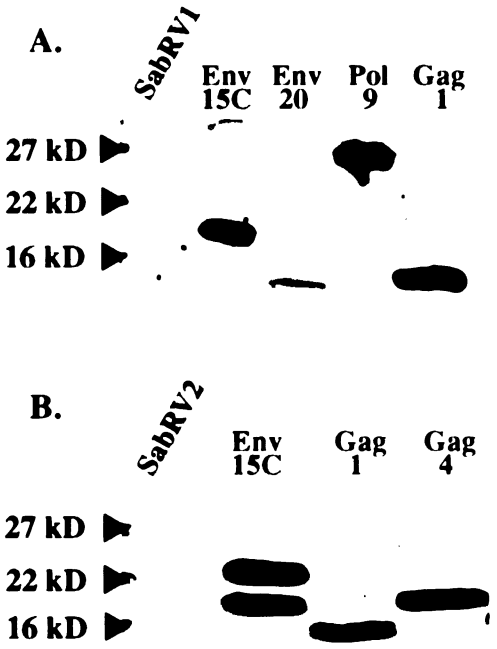
A.
SabRV1
Env 15C
Env 20
Pol 9
Gag 1
27 kD
22 kD
16 kD
B.
SabRV2
Env 15C
Gag 1
Gag 4
27 kD
22 kD
16 kD

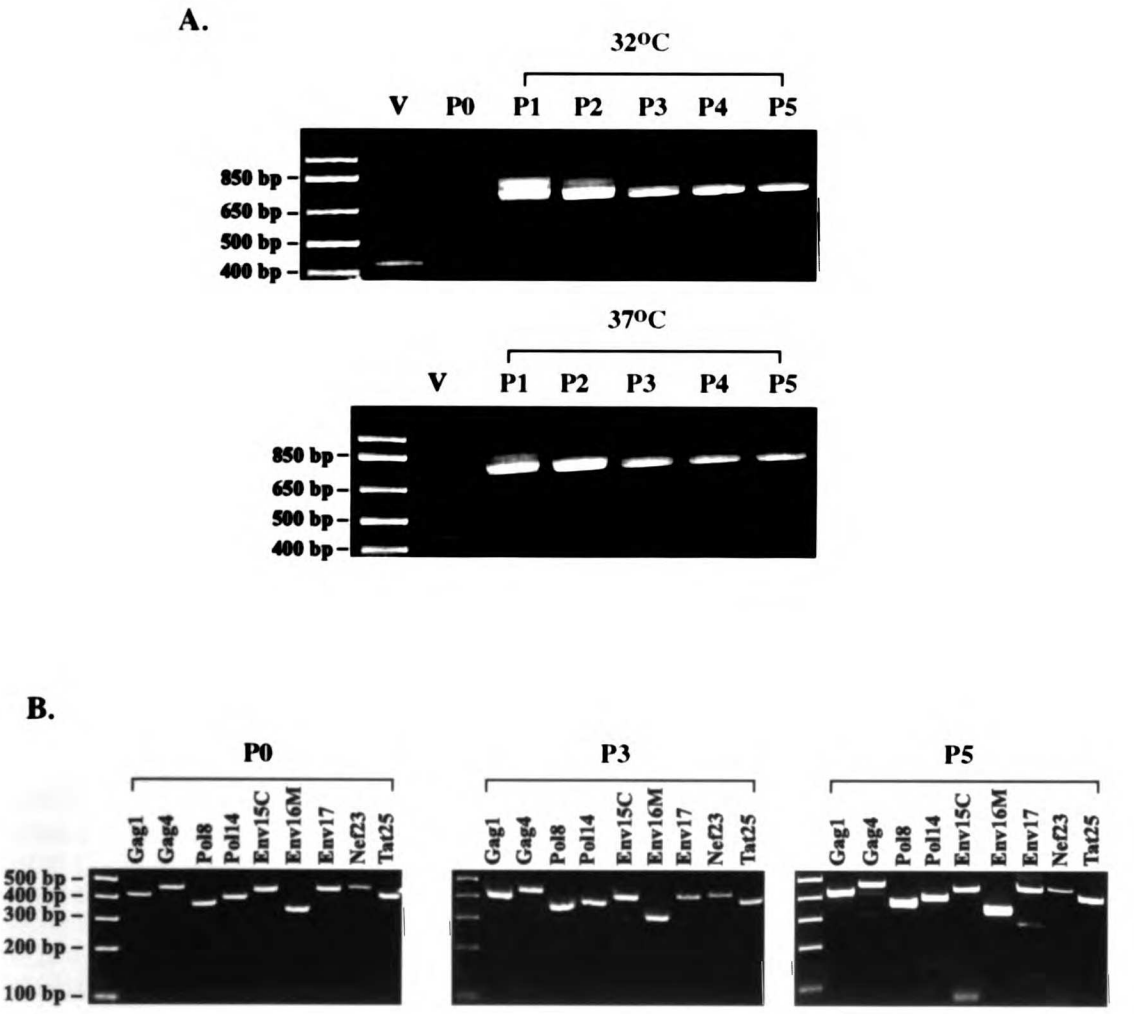
A.
32°C
V
P0
P1
P2
P3
P4
P5
850 bp
650 bp
500 bp
400 bp
37°C
V
P1
P2
P3
P4
P5
850 bp
650 bp
500 bp
400 bp
B.
P0
P3
P5
Gag1
Gag4
Pol8
Pol14
Env15C
Env16M
Env17
Nef23
Tat25
500 bp
400 bp
300 bp
200 bp
100 bp

Supplementary Data

Table of SabRV1-SIV oligos used

Primer	Sequence (5' – 3')	AA
SIV1312F-1	GGAGGTGAATTCGGCGTGAGAAACTCCGTC	Gag 2
SIV1710R-1	CAGATCCTCGAGATTTCCTCCTCTGCCGCT	Gag134
SIV1585F-1	GGAGGTGAATTCAAAGTGAAACACACTGAG	Gag 92
SIV2100R-1	CAGATCCTCGAGCCTGTAAATGTTGCCTAC	Gag 263
SIV1951F-1	GGAGGTGAATTCGACTTGCAGCACCCACAA	Gag 214
SIV2535R-1	CAGATCCTCGAGTGGGGCTCTGCATTGCCT	Gag 408
SIV2395F-1	GGAGGTGAATTCTTAATGGCAGAAGCCCTG	Gag 362
SIV2671F-1	GGAGGTGAATTCGGGCTGATGCCAACTGCT	Gag 454
SIV2838R-1	CAGATCCTCGAGCTGGTCTCCTCCAAAGAG	Gag 509
SIV2748F-1	GGAGGTGAATTCGAGAGAAAAGCAGAGAGA	Pol 89
SIV3248R-1	CAGATCCTCGAGCAACTGACCATCCTTTTC	Pol 255
SIV3099F-1	GGAGGTGAATTCCTAAATTTTCCCATAGCT	Pol 206
SIV3608R-1	CAGATCCTCGAGCACATGTCTCATAGTGTA	Pol 375
SIV3462F-1	GGAGGTGAATTCCCTCTAGATGAAGAATTT	Pol 327
SIV3800R-1	CAGATCCTCGAGCCCCATCCATTGAAATGG	Pol 375
SIV3678F-1	GGAGGTGAATTCAGTGACAGGACAGACCTG	Pol 399
SIV4226R-1	CAGATCCTCGAGTTTCTGTATTACATGTGC	Pol 581
SIV3999F-1	GGAGGTGAATTCATGGCAGAAGCAGAATAT	Pol 506
SIV4400R-1	CAGATCCTCGAGGTCCTTCACTAGATTGAA	Pol 659
SIV4278F-1	GGAGGTGAATTCCCAGTTGAGAAGGATGTATGG	Pol 599
SIV4703R-1	CAGATCCTCGAGTACATAAATTTCTGACTT	Pol 740
SIV4599F-1	GGAGGTGAATTCTCACAATATGTTATGGGA	Pol 706
SIV5108R-1	CAGATCCTCGAGCCATCTGCCTGCCAATTT	Pol 876
SIV4992F-1	GGAGGTGAATTCGGAAAAATAATCATAGTT	Pol 837
SIV5292F-1	GGAGGTGAATTCAATTCAGTAGAAACCATA	Pol 937
SIV5663R-1	CAGATCCTCGAGTGCCACCTCTCTAGCCTC	Pol 1090
SIV6911F-1	GGAGGTGAATTCTATGGGATCTATTGTACT	Env 18
SIV7351R-1	CAGATCCTCGAGTTGCTCTTGTTCCAAGCC	Env 163
SIV7190F-1	GGAGGTGAATTCAGATGCAATAAAAGTGAG	Env 110
SIV7696R-1	CAGATCCTCGAGTCCATTAAAGCCAAACCA	Env 278
SIV7568F-1	GGAGGTGAATTCGGTTATGCTTTGCTTAGA	Env 236
SIV7999R-1	CAGATCCTCGAGCGTCAAATTGATTTTATC	Env 379
SIV7862F-1	GGAGGTGAATTCCTTTGGCCTATCATTGAT	Env 334
SIV8353R-1	CAGATCCTCGAGTTTATAATCTCCCAATTCCAGTCGATA	Env 497
SIV8315F-1	GGAGGTGAATTCGTGGCAGAACTGTATCGACTGGAATT G	Env 485
SIV8755R-1	CAGATCCTCGAGCCACTTTGGTGTTAGACT	Env 631
SIV8435F-1	GGAGGTGAATTCGGGGTCTTTGTGCTAGGG	Env 525
SIV8477F-1	GGAGGTGAATTCGGTTCTGCAATGGGCGCG	Env 539
SIV8953R-1	CAGATCCTCGAGAACTATATAAACTCCATA	Env 697
SIV9022R-1	CAGATCCTCGAGATACCCCTGCCTTAACTT	Env 720
SIV8993F-1	GGAGGTGAATTCCAAATGCTAGCTAAGTTA	Env 711
SIV9496R-1	CAGATCCTCGAGCAAGAGAGTGAGCTCAAG	Env 878
SIV9333F-1	GGAGGTGAATTCATGGGTGGAGCTATTTCC	Nef 1

SIV10121R-1	CAGATCCTCGAGGCGAGTTTCCTTCTTGTC	Nef 262
SIV9711F-1	GGAGGTGAATTCGGGGGACTGGAAGGGATT	Nef 126
SIV9770R-1	CAGATCCTCGAGTAAGTATATGTCTAAGAT	Nef 145
SIV7301F-1	GGAGGTGAATTCACTAGTTCTTGTATAGCC	Env 148
SIV7606R-1	CAGATCCTCGAGTGAATAATTTGTGTCATT	Env 249
SIV7400F-1	GGAGGTGAATTCAAAGAGTACAATGAAACT	
SIV7837R-1	CAGATCCTCGAGAGACATAATGGTGACTGG	
SIV7940F-1	GGAGGTGAATTCATTGTCAAACATCCCAGG	
SIV7694F-1	GGAGGTGAATTCGGAACTAGAGCAGAAAAT	
SIV8044R-1	CAGATCCTCGAGGCAATTTGTCCACATGAA	
SIV8389R-1	CAGATCCTCGAGTGTGGGGGCCAAGCCAAT	

Chapter 5

Protection from SIV vaginal challenge using Sabin poliovirus vectors

Abstract

Here we provide the first report of protection against a vaginal challenge with a highly virulent SIV using a vaccine vector. We have developed a live poliovirus based vaccine vector system. With this system it is possible to insert gene fragments derived from various pathogens into the full poliovirus genome. We previously reported that these gene fragments are expressed during poliovirus infection and are able to stimulate potent immune responses directed against desired viral pathogens both in mice and primates. Here we report the construction of new poliovirus vectors using Sabin 1 and 2 vaccine strain viruses, from which we generated a series of new SabRV-SIV viruses containing SIV gag, pol, env, nef, and tat in overlapping fragments. Two cocktails of 20 transgenic polioviruses (SabRV1-SIV and SabRV2-SIV) were then inoculated into seven macaques as a candidate SIV vaccine. All monkeys made substantial anti-SIV serum and mucosal antibody responses. SIV-specific CTL responses were detected in 3 of 7 monkeys after vaccination. All seven vaccinated macaques, and twelve control macaques, were challenged vaginally with pathogenic $SIV_{mac}251$. Strikingly, 4 of 7 vaccinated

animals exhibited substantial protection against the vaginal SIV challenge. All twelve control monkeys became SIV^+. In two of the seven SabRV-SIV vaccinated monkeys we found no virological evidence of infection following challenge, indicating that these two monkeys were completely protected. Two additional SabRV-SIV vaccinated monkeys exhibited a pronounced reduction in post-acute viremia to $< 10^3$ copies/ml, suggesting that the vaccine elicited an effective cellular immune response. Three of 6 control animals developed clinical AIDS by 48 weeks post-challenge. In contrast, all 7 vaccinated monkeys remain healthy as judged by all clinical parameters. These results demonstrate the efficacy of SabRV as a potential human vaccine vector, and that a vaccine vector cocktail expressing an array of defined antigenic sequences can be an effective vaccination strategy in an outbred population.

Introduction

The current HIV pandemic has infected a cumulative total approaching 40 million people, and the search for an AIDS vaccine continues. Live viral vectors are leading candidates in the hunt for a potential vaccine. Several viral vectors have showed promise in SIV protection experiments in monkeys (11, 18, 53, 58), and numerous other viral vector systems are in earlier testing phases of vaccine development (8, 12, 14, 71, 73).

Poliovirus is an attractive live viral vector for several reasons. The Sabin live poliovirus vaccine is one of the best human vaccines in the world. It produces long lasting immunity (59, 75) and herd immunity (75); it is very safe and easy to experimentally manipulate (47); it has a proven safety and efficacy record in over 1 billion vaccinees (75); it is cheap to produce and distribute in developing countries (29); and most importantly, it produces a potent mucosal immune response (51, 56, 79). The capacity of poliovirus to generate a strong mucosal immune response is particularly important given that greater than 90% of HIV-1 infections worldwide have occurred via sexual transmission (77). Any strategy to control the AIDS pandemic must include a vaccine that prevents sexual transmission of HIV-1.

Excluding live-attenuated viruses (which are generally considered too pathogenic for use in humans (7, 68)), no candidate AIDS vaccine has been demonstrated to consistently provide protection against mucosal challenge with a highly virulent SIV. Direct inoculation of a subunit vaccine into the iliac lymph nodes of macaques did provide protection against a rectal mucosal challenge with a virulent SIV (34), though that subunit vaccine was unable to consistently protect against infection after a vaginal

challenge with the highly virulent $SIV_{mac}251$ (40). Those experiments suggest that generating local mucosal immunity may be as important as other characteristics of the anti-SIV immune response generated by candidate vaccines.

More vaginal challenge experiments need to be done, as an AIDS vaccine needs to protect against vaginal-penile sexual transmission of HIV. At this point in time, there have been relatively few SIV vaginal challenge experiments, and no vaccine vector has been demonstrated to provide any protection against a vaginal challenge.

We have previously reported the development of a recombinant poliovirus live viral vector system in which we inserted an immunogenic gene fragment of interest at the junction between the capsid proteins and the non-structural proteins (the P1/P2 junction) in the poliovirus polyprotein reading frame (76). The gene fragment is expressed with the rest of the poliovirus genome as part of the polyprotein, and is cleaved away from the polyprotein via the activity of poliovirus-encoded protease $2A^{pro}$, which cleaves at engineered proteolytic sites flanking the insert (76). That recombinant poliovirus live viral vector was tested in mice susceptible to poliovirus infection and demonstrated to elicit strong antibody (76) and cytotoxic T lymphocyte responses (42, 72).

We further demonstrated that poliovirus vectors are immunogenic in primates, in a study where we immunized four cynomolgus macaques with two recombinant polioviruses expressing SIV antigens. Significant humoral, mucosal, and cellular anti-SIV immune responses were elicited (15). Notably, all macaques generated a mucosal anti-SIV IgA antibody response in rectal secretions, and strong anti-SIV serum IgG antibody responses lasting for at least 1 year were detected in two of the four monkeys (15).

Here we report the development of Sabin vaccine based vectors, which we used to produce a defined series of SabRV1/2-SIV viruses containing SIV gag, pol, env, nef, and tat in overlapping fragments. We then evaluated the safety, immunogenicity, and protective efficacy of the SabRV1/2-SIV candidate SIV vaccine. Strikingly, 4 of 7 vaccinated monkeys showed substantial protection against SIV viremia after a vaginal challenge with highly virulent $SIV_{mac}251$. Two of those vaccinated animals appear to have been completely protected by the SabRV1/2-SIV vaccine. And all seven of the vaccinated monkeys have remained healthy for over 48 weeks post-challenge, while 3 of 6 control monkeys developed clinical AIDS. These results suggest that a Sabin-based viral vector may be a promising approach for developing a vaccine for the prevention of mucosal transmission of HIV.

Materials and Methods

Plasmids. The Sabin 1 plasmid (which we call pS1 for simplicity), was kindly provided by A. Nomoto (construct pVS(1)IC-0(25) (33, 57)). The entire Sabin 1 cDNA in pS1 was sequenced in our laboratory by the fluorescent dye terminator method using an ABI 310 machine (Perkin Elmer, CA). The accuracy of the genome sequence as published (54) was confirmed. To construct pSabRV1, first the EcoRI and XhoI sites upstream of the T7 promoter of pS1 were eliminated by inserting a SalI linker (oligos C and D) at that position to create plasmid pS1XT. Then the 747 bp BstEII fragment of pMoV2.11—containing the duplicated $2A^{pro}$ cleavage site, the 5 glycine spacer, and the EcoRI, NotI, and XhoI cloning sites—was swapped into pS1XT to create pSabRV1. Accuracy of the pSabRV1 construct was confirmed by restriction digest and DNA sequencing. This DNA swap between pMoV2.11 and Sabin 1 results in Sabin 1 gaining three wt coding changes in 2A and one in 2B. None of the changes are associated with neurovirulence or other wt phenotypes. All pSabRV1 plasmids contain an Amp^R selectable marker. Plasmid pS1, pS1XT, and pSabRV1 were grown by electroporation into SURE cells (Stratagene, CA) and plated on LB + ampicillin agar plates for 20-24 hrs at 37° C. Single colonies were then inoculated into 50 ml cultures of LB + ampicillin (50 μg/ml) and grown at 30° C for 16-18 hrs. Note: growth conditions for the Sabin 1 derivative plasmids (pS1, pS1XT, and pSabRV1) are important, as rearrangements of the plasmids and very low plasmid yields are frequently seen otherwise. Plasmid DNA was isolated from cells by the QiaFilter Midiprep technique (Qiagen, CA).

For pSabRV1-SIV clones, SIVmac239 plasmids p239SpSp5', p239SpE3', and pSIV239opennef (obtained from the AIDS Research and Reference Reagent Program, courtesy of Ronald Desrosiers (32)) were used as the PCR template to generate SIV inserts. Inserts were amplified using Pfu Turbo high-fidelity DNA polymerase, using conditions recommended by the manufacturer (Stratagene, CA). A complete table of the 40 oligos used for these reactions is available upon request. PCR fragments were purified on Qiaquick spin columns, digested with DpnI restriction enzyme (to eliminate any input SIV plasmid carried over), EcoRI, and XhoI, and then Qiaquick spin column purified a second time. Vector pSabRV1 plasmid was cut with EcoRI and XhoI, Qiaquick spin column purified, and then quantified by agarose gel electrophoresis. Gel purification of vector was generally avoided. SIV inserts were ligated into pSabRV1 using NEB T4 DNA ligase (New England BioLabs, MA) in a overnight reaction at 16° C containing 25 ng pSabRV1 and 20 ng SIV insert DNA. Ligations were dialyzed on 13mm 0.025μm VSWP membranes (Millipore, MA) against 50 ml of deionized H_2O for 10 min. Then 1 μl of ligation was electroporated into 25 μl SURE cells in a 0.1 cm cuvette (BTX ElectroCell 600 electroporator conditions: 129 Ω, 1,400 V, 5 msec pulse). One ml of LB was immediately added to the cuvette, and 20-200 μl of electroporated SURE cells were plated onto LB + ampicillin plates and incubated at 37° C overnight. Further culturing and DNA isolation was as described above. All plasmid clones were analyzed by restriction digest and all inserts were DNA sequenced in their entirety to confirm that the appropriate clone had been obtained and was not mutated.

Sabin 2 early passage virus (SO + 3) was kindly provided by K. Chumakov. HeLa cells were infected with Sabin 2 at an MOI of > 1 and incubated at 37°C. Cells were

harvested at 9 hrs post-infection, RNA was extracted using RNeasy (Qiagen, Santa Clarita, CA), and cDNA was synthesized using random primed Superscript II (Life Technologies, Gaithersburg, MD). Full length Sabin 2 was PCR amplified with primers SAB21 and SAB24, using XL polymerase (Perkin Elmer, CA), 2 mM Mg(OAc), and 500 μM dNTPs, with conditions: 3) min at 94°, 8 min at 65°, for 30 cycles. The full length Sabin 2 genome was then Qiaquick spin column purified, digested with SalI and HindIII, and ligated into SalI/HindIII digested pUC18. Ligations were introduced into DH5α chemically competent cells as recommended by the manufacturer (Life Technologies, MD). Plasmid minipreps of clones were analyzed by restriction digest and tested for the ability to produce infectious virus. The three plasmid clones that produced virus (pS2-2, pS2-3, and pS2-10) were sequenced and the genome sequence was compared to the Sabin 2 consensus sequence generated by Pollard et al. (63). Two coding mutations in pS2-10 were identified, one in Vp2 and one in 3C. The latter was corrected by swapping the 374 bp BsiWI-NcoI DNA fragment from a clone (pS2-3) with no 3C mutation into pS2-10 to create pS2-10F. We have since fixed the other coding mutation in pSabRV2 (nucleotide 1492, a.a. 249, F to L in Vp2) by site-directed mutagenesis and checked the resulting pSabRV2.2 by DNA sequencing. Viruses derived from pS2-10, pS2-10F, pSabRV2, and pSabRV2.2 all grow identically to Sabin 2 by plaque assay.

To generate pSabRV2, the 60 bp cloning site—which contains a 5 glycine spacer and AvrII and NotI restriction sites flanked by $2A^{pro}$ cleavage sites (only the 5' (or N terminal) cleavage site is counted in the 60 bp, since it contains modified codon usage (76) and the 3' (or C terminal) cleavage site is endogenous and essential)—was cloned into pS2-10F. A BstEII-SnaBI fragment containing the unique SabRV2 cloning sites was

generated by overlapping PCR of DNA fragments B and S, and digestion with BstEII and SnaBI. DNA fragment B was made by PCR (Pfu Turbo, Stratagene, CA) using oligos B1 and oligo B2. Similarly, DNA fragment S was generated by PCR using oligos S1(63 nt long, 45 nt of which overlap with oligo B2, which together contain the full pSabRV2 cloning site) and S2. Both PCR fragments were gel purified using Qiagen and used together as template with oligos B1 and S2 in an overlapping PCR reaction to generate a 1635 bp fragment containing the 60 bp SabRV2 cloning site flanked by the BstEII and SnaBI restriction sites. The digested BstEII-SnaBI fragment was ligated into BstEII/SnaBI digested pS2-10F to create pSabRV2. Viruses derived from pS2-10, pS2-10F, pSabRV2, and pSabRV2.2 all grow identically to Sabin 2 by plaque assay (Fig. 1C and data not shown).

For pSabRV2-SIV cloning, SIV PCR fragments were generated as described above (using similar oligos; a complete list of all 42 oligos is available upon request) and cloning was done comparably to that of pSabRV1-SIV's, except AvrII/NotI digestions were used and Xl1-Blue cells (Stratagene, CA) were used for transformations. Stocks of pSabRV2-SIV plasmids were made by inoculating single colonies of transformed XL1-Blue cells (grown overnight on LB+amp plates) into 5 ml cultures of LB + ampicillin (50 μg/ml) and grown at 37oC for 8-14 hrs. Plasmid DNA was isolated from cells by the Qiafilter Miniprep technique (Qiagen, CA). All clones were analyzed by restriction digest and all inserts were DNA sequenced in their entirety to confirm that the appropriate clone had been obtained and was not mutated.

All vectors and plasmids are readily available to any interested investigator.

Oligonucleotides.

A = GGTGGGGGAGGTGAATTCATGGTGAGCAAGGGCGAGGAG

E = GTGGTCAGATCCTCGAGCTTGTACAGCTCGTCCATGCCG

C = AATTGGTTCCTGGTCGACCGATGATCCGCG

D = TCGACGCGGATCATCGGTCGACCAGGAACC

B1 = ACATATTCGAGATTTGAC

B2 =

TGCGGCCGCTGCCCTAGGCCCTCCGCCACCTCCATGACCGAAACCGTATGTGGTCAGACCCTT

TTCTGG

S1 =

GGTTTCGGTCATGGAGGTGGCGGAGGGCCTAGGGCAGCGGCCGCAGGATTAACGACTTATGG

A

S2 = GCTCAATACGGTGCTTGC

SAB21 =

AAAAGGTCGACTAATACGACTCACTATAGGTTAAAACAGCTCTGGGGTTG

SAB24 =

GGGGGAAGCTTAGGCCTTTTTTTTTTTTTTTTTTTCCTCCGAATTAAAGAAAA

AT

S1-3240F = CCTCCAAAATCAGAGTGTATC

S1-3580R = GCCCTGGGCTCTTGATTCTGT

S2-3151F = GAAGGCGATTCGTTGTAC

S2-3518R = CTTGATTCAGCCACTAAG

Transcriptions and electroporations. Transcriptions were generally done using T7 RNA Polymerase (150 U) from New England Biolabs, using the supplied transcription buffer supplemented with 40 U RNAsin (Promega, WI), and 1.25 mM NTPs. Plasmid

templates (1-3 μg) were first linearized with ClaI (pS1, or pSabRV1 vector) or HinDIII (pS2-10F or pSabRV2) for 1 hr at 37° C in a 20 μl volume. The restriction enzyme was then inactivated for 10 min at 65° C. Once linearized, plasmid template was added to the full transcription mixture (total volume 200 μl), and transcription was allowed to proceed for 60-90 min at 37° C before terminating the reaction by freezing at -80° C. RNA quality and quantity was assessed by agarose gel electrophoresis before use in subsequent experiments. RNA from transcription reactions was used directly, without purification, in electroporations.

Electroporations were done using HeLa S3 cells at 40-75% confluence, plated the previous day, which were then trypsinized, centrifuged, and resuspended at a concentration of 3 x 10^6 cells/ml in Ca^{++}/Mg^{++}-free phosphate buffered saline (on some occasions, 293 cells were used in an identical manner). 800 μl of cells was added to a cold 0.4 cm electroporation cuvette (BioRad, CA; or BTX, CA), 10-40 μg RNA was added to cells, cuvette was flicked multiple times to resuspended cells that had settled, and cuvette was immediately electroporated in a BTX electroporator with settings: 950 μF, 24 Ω, and 300 V. The entire contents of the cuvette was then added to a 6 cm dish (10 cm dishes were used for SabRV2 viruses) with 3 ml of warm DMEM/F12 + 10% FCS (see (23) for related details). These electroporation conditions consistently give a 50-80% electroporation efficiency (data not shown), resulting in first generation (P_0) virus stocks. Sabin1 and SabRV1 recombinants were grown at 32° C, as Sabin 1 has a tendency to acquire wild type characteristics when passaged multiple times at greater than 34° C (65). Sabin 2 (S2-10F), and SabRV2 recombinants were grown at 37° C.

Plates were left until complete cenotaphic effect (CPE) was observed; frequently 24-36 hrs for SabRV1 and SabRV2 recombinants.

HeLa S3 cells obtained from ATCC (ATCC stock + 5-30 passages) were grown in DMEM/F12 medium (Gibco/Life Technologies) supplemented with 10% fetal calf serum (FCS) (Gibco/Life Technologies), penicillin/streptomycin, and L-glutamine. Adherent cell cultures were maintained at 10-80% confluence at 37° C + 6% CO_2. 293 cells were grown under the same conditions, but were sometimes left to 100% confluence.

Viral stocks, passages, and plaque assays. P_0 viral stock were harvested from electroporated cells exhibiting full CPE by taking the cells and supernatant, and freeze/thawing 3 times with a dry ice/ethanol bath and a 37° C water bath. Cellular debris was then pelleted by a 5 min, 300g centrifugation, and P_0 viral stock supernatant was transferred to a fresh tube. Note: some of the MoV2.11, SabRV1, and SabRV2 recombinant viral stocks appeared to lose some titer upon multiple freeze/thaw cycles. This was not observed with normal wild type poliovirus. Therefore viral stocks were stored in constant temperature -30° C or -80° C freezers.

Concentration of several viruses was done using Centriprep concentration filters units with a molecular weight limit of 50kD (Milipore, MA). 12-15 ml of low-titer SabRV1-SIV or SabRV2-SIV viral stocks were spun in Centriprep filter units for 30 minutes at 3,000g. This resulted in a 5-15 fold concentration of virus. Concentrated stocks were then titered by plaque assay.

Nine P_0 SabRV2-SIV viruses were mixed in equal amounts and passaged five times at an MOI of 0.1, at both 32° C and 37° C (only the data from 37° C is shown in

Fig. 2; identical data was obtained for passages at 32° C and is not shown). Passaging of SabRV2-SIV viruses was done by infecting $3x10^6$ HeLa cells in 10 cm plates at an MOI of 0.1 with the P_0 viral cocktail stock. Cells were incubated in 3 ml DMEM/F12 medium supplemented with 10% fetal calf serum at 32° C or 37° C; and P_1 viral stock was harvested when complete CPE was observed (24-36 hrs post-infection). The same process was followed when carrying out passages P_2 through P_5. Each passage at MOI of 0.1 represents approximately 2 generations of viral replication. In total, P_5 viruses had gone through 10-12 generations of viral replication, represented as "generation 10" in Figure 2. P_1 virus is conservatively represented as generation 2 in Figure 2 for simplicity. The cocktail passages were tested for the presence of the SIV inserts by RT-PCR using primers in the poliovirus sequence flanking all of the SIV inserts.

All plaque assays were done as previously described (15, 16). Plaque assays involving SabRV1 recombinants were incubated at 32° C for 5 days post-infection, plaque assays involving SabRV2 recombinants were incubated at 37° C for 4 days post-infection.

Viruses used in the SabRV1-SIV and SabRV2-SIV vaccines are listed in Table 1. Viruses were mixed together such that, in the SabRV1-SIV cocktail, each virus (of the 20) was present at 2.5×10^6 PFU/ml, giving a final concentration of 5×10^7 PFU/ml. The SabRV2-SIV cocktail was mixed such that each virus (of the 20) was present at 5×10^4 Pfu/ml, giving a final concentration of 1×10^6 PFU/ml. The cocktails were made using pure P_0 viral stocks.

$SIV_{mac}251$ stock used for challenge was from May 1998, and has not been previously published. The $SIV_{mac}251$ (5/98) stock has a titer of $> 10^5$ $TCID_{50}$ per 1 ml.

RT-PCR of recombinant polioviruses. 2-5 x 10^5 HeLa cells in 6-well dishes were infected with an MOI of 0.5-10 of the appropriate virus (an MOI of 10 was used if available). Cells were incubated at 37° C in 1 ml of DMEM/F12 + 10% FCS for 6-8 hrs, and then harvested by scraping or trypinization. RNA was collected using RNeasy (Qiagen) and cDNA was synthesized using random primed Superscript II (Life Technologies) reactions. PCR was done using rTth (Perkin Elmer XL polymerase) and primers S1-3240F and S1-3580R (MoV2.11, S1, and SabRV1 recombinants) or primers S2-3151F and S2-3518R (S2-10F and SabRV2 recombinants). Conditions were: 0.5 µl cDNA, 2.2 mM $Mg(OAc)_2$, 0.5 µl XL polymerase, and manufacturer recommended buffer and primer concentrations in a 50 µl reaction, with 94° C for 1 min, 50° C for 1 min, and 72° C for 1 min with 30 cycles. Generally 1-5 µl of the final product was loaded on a 1.5% agarose gel for analysis.

Animals. All animals used in this study were mature, cycling, female cynomolgus macaques from the California Regional Primate Research Center. The animals were housed in accordance with American Association for Accreditation of Laboratory Animal Care standards. When necessary, animals were immobilized with 10 mg of ketamine HCl (Parke-Davis, Morris Plains, N.J.) per kg of body weight injected intramuscularly. The investigators adhered to the Guide for the Care and Use of Laboratory Animals prepared by the Committee on Care and Use of Laboratory Animals of the Institute of Laboratory Resources, National Resource Council. Prior to use, animals were negative for antibodies to HIV-2, SIV, type D retrovirus, and simian T cell leukemia virus type 1.

Intranasal inoculations of SabRV1-SIV and SabRV2-SIV were done in a total volume of 1 ml. The animals were anesthetized and placed in dorsal recumbancy with the

head tilted back. One half ml of virus was instilled dropwise into each nostril. The animals were kept in this position for 10 min and then placed in lateral recumbancy until recovery from the anesthesia (30). Seven animals were inoculated intranasally with 1 ml (5×10^7 PFU) of SabRV1-SIV on days 1, 3, 14, and 16, for a total of four immunizations. Nineteen weeks after the first series of inoculations, these same seven animals were boosted with two intranasal inoculations of 1 ml (1×10^6 PFU/ml) SabRV2-SIV, one on week 19, and a second at week 21. Intranasal inoculations were done because cynomolgus macaques can be consistently infected with poliovirus by this route (15), and also, macaque experiments with the model antigen cholera toxin indicate that intranasal immunization is better at eliciting vaginal immune responses than oral immunization (30).

The animals were challenged with 10^5 $TCID_{50}$ of $SIV_{mac}251$ intravaginally using the $SIV_{mac}251$ (5/98) stock (see above). A total of 2 intravaginal SIV inoculations were given to each monkey in a single day, with a four hour rest period between the inoculation procedures. Procedure and technique used were the same as previously described (48).

Serum and vaginal and rectal lavage antibody responses. Anti-SIV IgG and IgA responses in vaginal and rectal washes and serum were measured at weekly timepoints during the study. Vaginal and rectal wash samples were collected and analyzed as previously described (38, 40, 48). Briefly, vaginal washes were collected by infusing 2 ml of sterile PBS into the vaginal canal and aspirating the instilled volume. Rectal washes were collected in a comparable manner. Samples were immediately snap-frozen on dry ice and stored at -80°C until analysis. To account for the presence of IgG interfering with

and reducing the detection of IgA, sera was first depleted of IgG using Protein G-sepharose beads (Pharmacia Biotech, Uppsala, Sweden) prior to use in the IgA ELISA. To deplete IgG, 25 μl of serum sample was incubated with 100 μl Protein G-sepharose beads for 1 hr at 37°C and then 4°C overnight, and then the Protein G-sepharose was pelleted and the supernatant was collected. Dilution of sample during this process was 1:3. The ΔOD between test and control wells was defined as the difference between the mean OD of sample tested in two antigen-coated wells and the mean OD of the sample tested in two antigen-free control wells. The negative control OD value was determined from 12 uninfected monkey serum samples and defined stringently as the average OD plus 3 standard deviations. Endpoint titers were determined if the ΔOD of the test sample exceeded the negative control value by a factor of 2. To then quantify anti-SIV antibody titers, serial four-fold dilutions of duplicate samples of sera, vaginal wash, or rectal wash were tested by ELISA using whole pelleted $SIV_{mac}251$ (Advanced Biologics Inc., Columbia, MD). Antibody binding was detected with peroxidase conjugated goat anti-monkey-IgG(Fc) or -IgA (Fc) (Nordic Laboratories, San Juan Capistrano, CA) and developed with o-phenlyenediamine dihydrochloride (Sigma). The endpoint titer was defined as the reciprocal of the last dilution giving an ΔOD greater than 0.1 (15).

Neutralizing antibody responses. Assays were done as previously described (11, 50); neutralizing antibody titers are the dilution at which cell killing by lab adapted $SIV_{mac}251$ was inhibited 50%.

SIV virus isolation and serum viral RNA load determination. Virus was isolated from heparinized whole blood obtained from the SIV-inoculated cynomolgus macaques. PBMC were isolated by Ficoll gradient separation (Lymphocyte Separation Medium,

Organon Teknika, West Chester, PA) and co-cultured with CEMx174 cells (28), (provided by James A. Hoxie, University of Pennsylvania, Philadelphia) as previously described (37). Five million PBMC were co-cultivated with 2-3 million CEMx174 cells. Aliquots of the culture media were assayed regularly for the presence of SIV major core protein (p27) by antigen capture ELISA (37). Cultures were considered positive if they were antigen positive at 2 consecutive time points. A detailed description of the technique and criteria to determine if culture media was antigen positive has been published (43). All cultures were maintained for 8 weeks and tested for SIV p27 by ELISA before being scored as virus negative. Blood samples for virus isolation were collected at the times indicated in Table 2. SIV RNA loads (Figure 9) were determined using a modification (Lifson et al., in preparation) of a real time RT-PCR assay on monkey plasma samples, essentially as previously described (74). The assay has a threshold sensitivity of 100 copy Eq/mL of plasma, and an interassay coefficient of variation of < 25%.

SIV provirus PCR analysis. Nested PCR was carried out on genomic PBMC DNA in a DNA Thermal Cycler (Perkin-Elmer Cetus, Emeryville, CA) as previously described (48). Briefly, cryopreserved PBMCs isolated from whole blood of each monkey in the experiment were washed 3 times in Tris buffer at 4°C and resuspended at 10^7 cells/ml. Ten microliters of the cell suspension were added to 10 microliters of PCR lysis buffer (50mM Tris-HCl (pH 8.3), 0.45% NP-40, 0.45% Tween-20) with 200 ug/ml Proteinase K. The cells were incubated for 3 hours at 55 °C, followed by 10 minutes at 96 °C. Two rounds of 30 cycles of amplification were performed on aliquots of plasmid DNA containing the complete genome of SIVmac1A11 (positive control) or aliquots of cell lysates using conditions described elsewhere (48). The primers used specifically amplify

SIV Gag. DNA from uninfected CEMx174 cells was amplified as a negative control in all assays to monitor potential reagent contamination. β-actin DNA sequences were amplified with 2 rounds of PCR (30 cycles/round) from all PBMC lysates to detect potential inhibitors of Taq polymerase. Following the second round of amplification, a 10 μl aliquot of the reaction product was removed and run on a 1.5% agarose gel. Amplified products in the gel were visualized by ethidium bromide staining. Blood samples for PCR analysis were collected at the times indicated in Table 3.

Western blot analysis of serum antibody responses. 2 x 10^6 HeLa cells infected with wild type poliovirus were incubated for 7 hours at 37°C. Cells were harvested and lysed on ice for 1 min (lysis buffer consisted of 10 mM Tris [pH 7.5], 140 mM NaCl, 5 mM KCl, and 1% IGEPAL), and nuclei were removed by centrifugation. 20 μl of polio-infected whole-cell lysate and 22 μg of sucrose-gradient purified $SIV_{mac}251$ (ABI, Columbia, MD) were electrophoresed in parallel lanes through a 10% or 12% SDS-polyacrylamide gel and analyzed by immunoblotting. The anti-SIV serum used as a positive control for SIV proteins was pooled serum from SIV-infected rhesus macaques. The anti-polio serum used as a positive control for poliovirus proteins was obtained from a polio-immune human. Antisera from all vaccinated cynomolgus macaques were used as primary antibody (serum from day of challenge was used for monkeys 27270, 27244, 28508, 27273, 27253 and serum from one month pre-challenge was used for monkeys 25231 and 27250). Also, pre-immune serum from monkey 27250 was used. Secondary antibody (horseradish peroxidase-conjugated rabbit anti-human IgG) was obtained from DAKO (Carpinteria, CA) and used for monkeys 27270, 27244, 28508, 27273, 27253, and 27250-pre-immune). A horseradish peroxidase-conjugated rabbit anti-rhesus monkey

IgG (Sigma, Saint Louis, MO) was used for monkeys 25231 and 27250, using one month pre-challenge serum. Blots were probed with 1:100-diluted monkey serum in TBST (10 mM Tris-HCl [pH 7.5], 150 mM NaCl, 0.15% Tween-20) with 10 % fat-free dry milk (Biorad, Hercules, CA), washed twice in TBST containing 0.15% Tween-20 and once in TBST containing 0.5% Tween 20, probed with the secondary antibody (1: 2,000 dilution), and then detected by enhanced chemiluminescence (ECL; Amersham, Arlington Heights, IL) as specified by the manufacturer. Rhesus monkey serum was used at a dilution of 1:200 and polio-immune human serum was used at a dilution of 1:25. Films were digitally scanned and exported to Photoshop 5.5 (Adobe, San Jose, CA).

Statistical Methods. SIV viremia levels were analyzed by Student's T-test comparison of the 24-32 week average log viral load of each animal in the two groups (vaccinated:control) with two-tailed distribution. Weight gain (or loss) was analyzed by Mann-Whitney rank test of the 33-44 week average weight change (from day of challenge) of each animal in the two groups (vaccinated:control) with two-tailed distribution. Mortality differences between the two groups at week 48 were analyzed by Fisher's exact test.

Lymphocyte proliferative responses to SIV antigens. Antigen specific proliferation was tested using PBMC from fresh blood samples as described (46). The cells were suspended at 2 x 10^6 per ml in RPMI 1640 medium supplemented with 10% FCS and plated in triplicate at 50 µl per well in 96-well round bottom microtiter plates. Antigen dilutions or control reagents were plated at 50 µl per well. 100 µl fresh medium was added after 48 hrs and the plates were incubated for 7 days in a CO_2 incubator. The wells were pulsed with ^{3}H-thymidine (1 µCi per well, NEN-DuPont Co., Wilmington, DE)

overnight prior to harvest. The plates were aspirated onto fiberglass filters and washed with a cell harvestor (Inotech Biosystems International, Lansing, MI). The filters were saturated with scintillation cocktail and sealed, and counts in the ^{3}H window were measured using a 96-well scintillation counter (Microbeta 1450, Wallac Biosystems, Gaithersburg, MD). The SIV antigen was whole-inactivated $SIV_{mac}239$ (kindly provided by Dr. Larry Arthur). ConA was tested as a positive control antigen. Medium alone was the control for spontaneous proliferation. The antigens were tested at 0.1, 1.0 and 10 μg/ml in every assay. This assay was used in our previous study (15). Lymphocyte proliferation assays were performed before immunization and at regular intervals after immunization (data not shown) using PBMCs. Due to an unusually high level of spontaneous proliferation (~10,000 - 100,000 cpm/well) in negative control wells (PBMCs plus medium alone) at all time points tested over a 28 week period, it was difficult to assess SIV-specific $CD4^{+}$ T cell responses in the immunized animals, as minimal additional stimulation was seen in the presence of antigen or Con A.

SIV-specific CTL responses. The presence of SIV specific CTLs in cynomolgus PBMCs was assessed as previously reported (15). Briefly, PBMCs from immunized monkeys were stimulated with 10 μg/ml Con A (Sigma) and cultured for 14 days in complete medium supplemented with 5% human lymphocyte-conditioned medium (Hu IL-2, Hemagen Diagnostics, Waltham, MA). Autologous B cells were transformed by *Herpes papio* (595Sx1055 producer cell line, provided by M. Sharp, Southwest Foundation for Biomedical Research, San Antonio, TX), and infected overnight at an MOI of 30 with wild-type vaccinia virus (vvWR), or recombinant vaccinia expressing the $p55^{gag}$ (vv-gag) or $gp160^{env}$ (vv-env) of SIVmac239 (provided by L. Giavedoni and T.

Yilma, University of California, Davis, CA). The level of vaccinia virus infection of target cells was estimated by indirect immunofluorescence using monkey anti-vaccinia virus antibody, followed by fluoresceinated goat anti-human IgG (Vector Laboratories, Burlingame, CA). The level of vaccinia virus infection of target cells in this series of experiments was estimated to fall between 5 and 15%. Target cells were labeled with 50 μCi of ^{51}Cr (Na_2CrO_4, Amersham Holdings, Arlington Heights, IL) per 10^6 cells. Effector and target cells were added together at multiple E:T ratios in a 4 hr chromium release assay. Assays were considered reliable if specific lysis was > 10% and at least twice the level of spontaneous lysis of vvWR infected cells. At many time points the data from the CTL assays could not be meaningfully interpreted due to high spontaneous lysis of the cynomolgus macaque transformed-B cell targets. Lysis was not due to NK cell activity, as no lysis was seen when the NK target cell line K562 was substituted as a negative control (data not shown). Numerous variations of the CTL assay were attempted to generate consistently reliable chromium release assay data in immunized or infected cynomolgus macaques. Cold-target inhibition, a variety of stimulation procedures, and enrichment of $CD8^+$ cells using anti-CD8 bead purification failed to consistently resolve this problem.

Results

Sabin-based vaccine vector construction and production

Given the excellent safety record of Sabin vaccine strain polioviruses in humans (75), we wished to do all future experiments, in primates and humans, using only Sabin based viruses produced from molecularly defined constructs. Hence, we engineered new plasmid clones of Sabin 1 and Sabin 2 derived vectors (pSabRV1 and pSabRV2) (Fig. 1A-C). We then constructed a collection of 20 SabRV1 viruses expressing SIV gag, pol, env, and nef that represent nearly the entire SIV genome (Fig. 1F and Table 1). These viruses grew well, as assessed by plaque assay (Fig. 1D). Twenty SabRV2-SIV viruses were produced in a comparable manner, selected to represent a similar coverage of the major SIV genes, plus Tat (Fig. 1F and Table 1). These viruses also grew well, as assessed by plaque assay (Fig. 1E). In some cases, one difficulty with the use of recombinant polioviruses is producing genetically pure stocks, since viruses with deletions in their insert sequences can accumulate as recombinant polioviruses replicate through a number of generations (15, 52, 76). Therefore we took great care to check the viral stocks for deletions. We did so by using a sensitive RT-PCR assay capable of detecting deleted virus comprising as little as 0.1% of the stock (data not shown). The SabRV1-SIV vaccine stocks were greater that 99.9% pure in total (data not shown), as were the SabRV2-SIV stocks (Fig. 2B). To further test the viability and stability of the recombinant viruses, a cocktail of nine of the SabRV2-SIV viruses was then passaged repeatedly and assessed by RT-PCR (Fig. 2). The vaccine cocktail as a whole maintained

the SIV sequences for at least ten generations (Fig. 2A), and all of the individual component viruses maintained their inserts and viability (Fig. 2B).

The twenty SabRV1-SIV virus stocks were then mixed to create a defined vaccine cocktail of 5 x 10^7 PFU/ml for use in the primate vaccinations described below. The twenty SabRV2-SIV virus stocks were mixed to make a defined vaccine cocktail of 1 x 10^6 PFU/ml.

Monkey immunizations

Producing a candidate SIV vaccine in two different serotypes of poliovirus (type 1 and type 2 strains) was a strategy employed in our last macaque study to create a better opportunity for an effective booster immunization using the second vector serotype, as there is no significant cross-neutralization or cross-protection between these two serotypes. That approach resulted in anemnestic booster responses in the immunized animals (15), and led us to utilize the same strategy in the study reported here.

Cynomolgus macaques are used in our studies because they are orally and intranasally susceptible to poliovirus. As the goal of our studies is to test poliovirus vectors as potential mucosal AIDS vaccines, we used a route of inoculation that would elicit a vaginal immune response. An intranasal route of inoculation was chosen for these experiments because previous experiments using SIV subunits plus cholera toxin have demonstrated that the intranasal route of inoculation elicits a better vaginal mucosal immune response than oral or rectal immunization (30).

In this study, seven cynomolgus macaques were immunized intranasally with SabRV1-SIV (5 x 10^7 PFU) at week 0 and 2 (Fig. 3). Then at week 19 and 21, these

animals were booster immunized intranasally with SabRV2-SIV (1 x 10^6 PFU). These doses are comparable to normal Sabin oral poliovirus vaccine (OPV) doses used in children (2).

Immunization induces strong serum anti-SIV IgG and IgA responses.

The results of ELISAs for serum IgG and IgA responses against SIV are shown in Figure 5. All seven monkeys made a rapid and strong anti-SIV IgG response after immunization with SabRV1-SIV (Fig. 4A). Three of the seven monkeys made serum anti-SIV IgA responses and in two of those animals the SabRV1-SIV elicited IgA responses persisted for at least 19 weeks (Fig. 4B).

The SabRV2-SIV booster immunization at 19 weeks resulted in a 20-80x increase in anti-SIV IgG antibody titers in all monkeys within 7 days, a classic anamnestic antibody response (Fig. 4A). Additionally, all 7 monkeys were positive for anti-SIV serum IgA at one week post-boost, with a greater than 10x titer increase in all monkeys, confirming the presence of an anamnestic IgA response in all vaccinated monkeys (Fig. 4B).

All seven monkeys made comparable serum IgG anti-SIV antibody titers; and, generally, the monkeys made comparable serum IgA anti-SIV antibody titers after the SabRV2-SIV booster immunization. Individual variability in the immune response to the vaccine was seen; monkey 27270 made the strongest anti-SIV serum IgG and IgA response after both the SabRV1-SIV and SabRV2-SIV immunizations (Fig. 4).

Immunization induces vaginal and rectal anti-SIV antibody responses

We found in our previous study (15) that recombinant polioviruses expressing SIV antigens could induce anti-SIV vaginal and rectal antibody responses after intranasal inoculation. In this study, we again analyzed antibody samples taken from the vaginal and rectal mucosal surfaces. It was recently shown that macaque vaginal antibody secretions are affected by the menstrual cycle (38), and therefore in this study we took mucosal antibody samples on a weekly basis, to assess the antibody levels more accurately.

In our previous study we observed that four of four monkeys made rectal anti-SIV IgA antibody responses. In this study, we again observed that 100% of the immunized monkeys made rectal mucosal anti-SIV antibody responses. After the SabRV1-SIV immunization, all seven monkeys made at least transient anti-SIV rectal IgA responses, even though only three had made detectable serum anti-SIV IgA (Fig. 4B, Fig. 5B). These results were consistent with our previous study, where one monkey made a mucosal IgA anti-SIV response even though it showed no detectable serum anti-SIV IgG or IgA titers at any time point (15). Conversely, neither of the two monkeys that made long-lasting serum IgA responses (27270 and 28508, Fig. 4B) after SabRV1-SIV immunization in the current study, made detectable rectal IgA antibodies for longer than 2 weeks.

We detected anti-SIV IgG in rectal secretions from all seven monkeys after the SabRV2-SIV immunization (Fig. 5A). It is uncommon to observe IgG in rectal secretions (38, 55, 78). Monkeys 27253 and 27270 made particularly strong, 50-100x anamnestic rectal IgG responses after the SabRV2-SIV immunization. Additionally, we were

intrigued that the SabRV2-SIV immunization appeared to reduce rather than boost the rectal IgA anti-SIV response in the monkeys (Fig. 5B). Four monkeys that made a transient rectal IgA response after the SabRV1-SIV immunization (25231, 28508, 27244, and 27270), had no detectable anti-SIV rectal IgA after the SabRV2-SIV immunization (Fig. 5B), even though all four monkeys had a substantial increase in serum anti-SIV IgA titers (Fig. 4B).

All of the monkeys made vaginal IgG anti-SIV responses after SabRV1/2-SIV immunization, and six out of seven monkeys made vaginal IgA anti-SIV responses (Fig. 6). Interestingly, the monkey with the most substantial vaginal IgA antibody response (27250) after SabRV1-SIV immunization (Fig. 6B) did not make a concurrent serum IgA response (Fig. 4B). This animal also had a robust rectal IgA response (Fig. 5B), providing more evidence for compartmentalization of the immune responses to the vaccine in some animals.

As with rectal antibodies, the strongest vaginal IgG antibody responses occurred after the SabRV2-SIV booster immunization. A 200-1000x increase in vaginal anti-SIV IgG was seen in monkeys 27270 and 25231 after the booster immunization. A 100x increase in vaginal IgA anti-SIV antibodies was seen in these same two monkeys. For each individual monkey, the pattern of vaginal IgA and IgG anti-SIV responses were general similar in profile (Fig. 6).

Taken together, though all monkeys made similar serum IgG anti-SIV antibody responses, and similar serum IgA responses after the booster immunization, there were substantial differences in the mucosal antibody responses of different monkeys. In animals with a strong initial rectal IgA response (monkeys 27253 and 27273, Fig. 5B),

vaginal IgA responses were weak or absent. SabRV2 appeared to elicit rectal IgG antibody responses but not rectal IgA responses, as noted above. The three monkeys that made anti-SIV serum IgA responses after SabRV1-SIV immunization made the strongest rectal IgG responses after the SabRV2-SIV booster immunization, but the significance of this is unclear. The results of these experiments clearly demonstrate that serum antibody titers are not a good indicator of mucosal antibody responses, consistent with compartmentalization of the immune response.

Diversity of antigens recognized in SabRV1/2-SIV immunized monkeys

We are unaware of any precedent for immunization of primates with a viral vector (or any vector) expressing a defined library of antigens. Therefore, it was important to determine whether the measured antibody responses were against a single antigen (expressed by a single SabRV-SIV virus) or multiple antigens (expressed by different SabRV-SIV viruses). To explore this issue, we examined the anti-SIV and anti-polio specificities of the serum antibodies in immunized animals by western blotting. All seven monkeys seroconverted to poliovirus antigens, generally with a strong response against capsid protein VP1 and weaker responses against two to four other poliovirus proteins (Fig. 7). All seven monkeys also seroconverted to SIV antigens by western blot, confirming the SIV ELISA results in Figure 4. Importantly, a majority of monkeys made substantial antibody responses to multiple SIV proteins (Fig. 7). Antibody responses against RT (p51/65) (all seven monkeys), Gag (p55 (six monkeys: 27244, 28508, 27270, 27273, 27253, and 27250); p17 (monkeys 27270, 27253); and p27 (monkeys 27244, 27250)), Env gp41 (monkeys 27270, 27253), and Env gp120 (monkeys 27244, 28508,

27270, 25231, 27253) were all apparent (Fig.7). Antibodies against Nef and Tat (also represented in the SabRV1-SIV and/or SabRV2-SIV cocktail) are not assayed in this experiment, as they are not packaged in SIV virions, which is the target material for the immunoblots. At least five different SabRV1/2-SIV viruses, and possibly many more, were immunogenic and elicited antibody responses, as the responses against SIV p27, RT, p17, gp41, and gp120 must have been elicited from different SabRV-SIV's. In summary, a majority of monkeys responded to multiple poliovirus and SIV proteins, indicating that the library vaccine approach is successful at eliciting responses to multiple expressed proteins, even in a complex cocktail of twenty different viruses.

Cellular immune responses

Poliovirus vectors can elicit potent cytotoxic T lymphocyte (CTL) responses in both mice (42, 72) and primates (15). Here we were able to detect SIV Env specific CTLs in 3 of 7 monkeys after SabRV1-SIV vaccination (25231, 27244, 27250) by a standard bulk PBMC cytolytic assay (Fig. 8A). After the SabRV2-SIV vaccinations we detected SIV Gag and Env specific CTLs in monkey 25231 (Fig. 8C). Cellular immune responses are technically difficult to assess in cynomolgus macaques (see Materials and Methods), and we frequently experienced difficulties with high background lysis. This technical complication prevented accurate assessment of CTL activity at additional time points.

The three monkeys that tested positive for SIV-specific CTLs after SabRV-SIV vaccination (25231, 27244, 27250) also tested positive for SIV-specific lymphoproliferative responses (S.I. of 3.3, 4.1, and 2.7 respectively).

Virologic outcome of vaginal challenge with SIVmac251

All seven vaccinated monkeys and a total of 12 control monkeys were challenged with a vaginal inoculum of $SIV_{mac}251$. $SIV_{mac}251$ is an uncloned and highly virulent virus that has proven to be extremely difficult to protect against (i.e. prevent infection) or control with vaccine induced immune responses (14, 17, 22, 25, 39, 40, 69). The vaginal challenge route was chosen because our primary interest in the SabRV vector is as a vaccine capable of protecting against sexually transmitted HIV.

Six control cynomolgus macaques were first challenged intravaginally with 1 x 10^5 $TCID_{50}$ $SIV_{mac}251$ twice in one day (this dose had previously infected 15 of 15 rhesus macaques intravaginally (Miller, unpublished)). All 6 of those control cynomolgus macaques became infected, as judged by positive SIV virus isolation, positive SIV provirus PCR, and seroconversion to SIV antigens (data not shown).

At week 30, nine weeks after the last immunization, we challenged all seven of the SabRV-SIV vaccinated animals, and six additional concurrent control cynomolgus macaques, with two vaginal inoculations of 1 x 10^5 $TCID_{50}$ $SIV_{mac}251$ in one day (Fig. 3). All six concurrent control monkeys became SIV^+ by virus isolation (Table 2), SIV provirus PCR (Table 3), and seroconversion to SIV (neutralizing antibodies, Table 4; ELISA, Fig. 9), bringing the total to 12 of 12 control cynomolgus macaques infected after vaginal inoculation with the challenge dose. In the group of SabRV-SIV immunized monkeys, two of the monkeys appeared to be fully protected. SIV was never isolated from the PBMC of one animal (27244), while the other animal (27270) was SIV virus isolation positive at a single time point, 4 weeks post-challenge (Table 2). We were unable to detect SIV gag in PBMC samples from either animal by PCR (Table 3). Neither

animal made an anamnestic serum antibody response to SIV antigens after the challenge exposure (Fig. 9), again indicating that they were fully protected from SIV infection.

All seven vaccinated monkeys and the six new control monkeys were assayed for SIV neutralizing antibody titers. No serum neutralizing antibody titers were detected before the vaginal SIV challenge in any animal (Table 4). No neutralizing antibody titers were seen post-challenge in vaccinated monkeys 27270 and 27244, again consistent with the SIV viral load data indicating that these two monkeys were fully protected from infection. Among the remaining monkeys, 4-fold higher neutralizing antibody titers were seen in the vaccinated monkeys versus the control monkeys post-challenge.

In order to quantify the SIV viremia in the challenged animals, a sensitive quantitative RT-PCR assay was used, which has been used in several macaque SIV studies (36, 53, 67). All six concurrent control monkeys had significant SIV viral loads, peaking between week 2-4 and reaching post-acute geometric mean viral loads of 9.3 x 10^5 copies/ml by week 24-32 (Fig. 10).

SabRV-SIV vaccinated animals 27244 and 27270 had no detectable SIV RNA in plasma at any time point and confirming that these two animals were solidly protected (Fig. 10). Compared with the control monkeys, the seven SabRV1/2-SIV vaccinated monkeys had a 3.0 $\log_{10}$ reduction in post-acute geometric mean viral load ($P < 0.01$). Control of post-acute viremia was particularly obvious in two vaccinated monkeys: vaccinated monkey 28508 exhibited stable long term control of viremia to ~1 x 10^3 copies/ml, and vaccinated monkey 25231 reduced its $SIV_{mac}251$ viremia by more than 10^6 fold during the post-acute phase, implicating a strong vaccine-elicited cellular immune response (Fig. 10).

Clinical outcome of vaginal challenge with $SIV_{mac}251$

The clinical outcome of SIV infection was much worse in the control animals compared to the SabRV-SIV immunized animals. Five of 6 control animals had marked decreases in $CD4^+$ T lymphocyte counts (Fig. 11A) and body weight (Fig. 11B) over the 48 week post-challenge observation period. Three of the 6 control animals were euthanized at 34, 35, and 44 weeks post challenge due to severe clinical AIDS (Fig. 11C). At necropsy, 2 of the animals (23414, 26560) had lymphoma and the other animal (28118) has severe non-responsive enteritis and wasting.

In sharp contrast, all 7 of the vaccinated monkeys are alive ($P < 0.07$) and healthy (significantly better body weight, $P < 0.003$, Fig. 11B) at 48 weeks post-challenge. Although $CD4^+$ T cell counts declined initially after challenge, the counts stabilized at about 16 weeks post-challenge for 5 of the 7 vaccinated animals (Fig. 11A). Over the course of the study, the SabRV-SIV vaccinated animals had higher average $CD4^+$ counts than the control animals. At 36 weeks post-challenge, the average $CD4^+$ cell count of vaccinated animals was 840 cells/μl, while 5 of 6 control monkeys had $CD4^+$ counts below 150 cells/μl. Two vaccinated animals (27250,27273) had depressed $CD4^+$ T cell counts after challenge, consistent with their higher SIV viremia levels, but their body weights have remained stable (Fig. 11B) and they appear clinically normal. The other 5 animals have gained weight steadily since the vaccine challenge (Fig. 11B). These results demonstrate that the SabRV-SIV vaccine protects monkeys from SIV-related disease progression.

Discussion

The primary goals of this study were to construct SabRV-SIV candidate SIV vaccine viruses, and assess their immunogenicity and efficacy in preventing vaginal transmission of SIV. A vaginal challenge was chosen because our primary interest in the SabRV vector is as a vaccine vector capable of protecting against sexually transmitted HIV. Given that greater than 90% of HIV-1 infections worldwide occurred via sexual transmission, any strategy to truly control the AIDS pandemic must include a vaccine that prevents sexual transmission of HIV-1. $SIV_{mac}251$ is an uncloned and highly virulent virus that has proven to be extremely difficult to protect against in rhesus and cynomolgus macaque challenge experiments (14, 17, 22, 25, 39, 69). We decided to use $SIV_{mac}251$ as the challenge virus because the use of a pathogenic, uncloned, difficult to neutralize virus models "real world" HIV transmission.

The SabRV1/2-SIV vaccine provided protection from SIV infection in 2 of 7 vaccinated monkeys, and protection from disease progression in all vaccinated monkeys. SIV replication was controlled (650 copies/ml and <100 copies/ml at wk 32) in two monkeys. Thus, there was a clear difference between the clinical course of the post-challenge SIV infection in the control and vaccinated animals. Half of the control animals developed endstage clinical AIDS, while all of the vaccinated monkeys were protected from AIDS through the 48 weeks post-challenge observation period ($P < 0.07$). Although not all vaccinated monkeys were protected from infection, the SabRV-SIV vaccine clearly protected all the immunized monkeys from SIV-related disease progression, both in terms of viral load ($P < 0.01$) and general health (body weight, $P < 0.003$). This is the

first report of protection against a vaginal challenge with a highly virulent SIV using a vaccine vector. Indeed, though experiments with cynomolgus macaques and rhesus macaques are not necessarily directly comparable, the results reported here appear equivalent to or better than the highest levels of mucosal protection afforded by any published subunit (40), DNA vaccine (25), or viral vector system (3, 11, 14, 24) in macaques challenged with a highly virulent uncloned SIV. Given the significant levels of protection observed in this study, SabRV has considerable potential as a human vaccine vector.

Immunogenicity

We previously showed that live poliovirus-based vaccine vectors elicit humoral, mucosal, and cellular immune responses in primates (15). In the current study we observed better serum and mucosal antibody responses than we observed with the previous polio vector system, in terms of the proportion of monkeys responding, maximum antibody titers, and the consistency of the immune responses. We believe that these enhanced responses are due to higher quality virus stocks, the use of vectors based on Sabin 1 and Sabin 2 molecular clones, and the use of a cocktail vaccine approach that allowed the expression of a 10-fold greater number of SIV antigens. This was our first use of pSabRV2 or pSabRV1 derived viruses, and the results demonstrate that Sabin 1 and Sabin 2-based constructs are immunogenic as viral vectors. Also, this data shows the effectiveness of a prime and boost strategy using two serotypes of the same viral vector.

A consistent feature in both of our live poliovirus vector primate experiments to date is the compartmentalization of the IgA immune responses in some monkeys. We found that after SabRV1-SIV immunization all seven monkeys made at least transient

anti-SIV rectal IgA responses, even though only three had detectable serum anti-SIV IgA (Fig. 4B, Fig. 5B).Neither of the two monkeys that made long-lasting serum IgA responses after SabRV1-SIV immunization (27270 and 28508, Fig. 4B), made detectable rectal IgA antibodies for longer than 2 weeks. The results of these experiments are consistent with the conclusion that the serum IgA and rectal IgA are from different sources (local vs. systemic) and demonstrate that serum antibody levels (IgG or IgA) cannot be used as an indicator of mucosal antibody levels.

Poliovirus vectors can elicit potent CTL responses in both mice (41, 42, 72) and primates (15). In this study we were able to detect SabRV-SIV elicited SIV-specific CTL responses in 3 of 7 monkeys. Monkey 25231 had the strongest cellular immune responses, generating an SIV antigen specific lymphoproliferative response, and having CTLs specific for both SIV Gag and Env antigens. SIV-specific $CD4^+$ cells were likely present in all seven monkeys after the SabRV-SIV immunizations reported here, because Ig class switching to IgA and IgG is T help dependent (1).

Correlates of protection

Correlates of protective immunity have not been clearly determined in any HIV or SIV vaccine study. In vaccinia vector studies, vaccine-elicited anti-SIV envelope antibodies strongly correlated with protection against intravenous or rectal infection with a moderately virulent uncloned SIV isolate (61, 62). Recent experiments have shown that passive immunization with large quantities of HIV neutralizing antibodies can protect macaques from an intravaginal challenge with a highly virulent lentivirus (SHIV 89.6PD) (6, 44, 66). Those results are encouraging, because antibodies are the correlate of protection for all currently licensed human vaccines for which a correlate of protection is

known (60). However, even the most robust antibody responses in HIV-infected patients do not appear to protect from disease progression, and thus the role of vaccine-induced antibodies in eliciting protection from SIV infection and disease remains unclear.

Likewise the role of vaccine-induced cellular immune responses in protecting against an SIV infection is unclear. It is generally accepted that cellular immune responses play a major role in controlling (i.e. reducing the viral load of) primate lentiviral infections (9, 35, 70). Although fully protective anti-SIV cellular immunity has not been directly demonstrated in any vaccine challenge experiment (9, 21, 25, 80), experiments utilizing a live attenuated SIV vaccine implicate cellular immune responses in protection (31).

Successful viral vector vaccine challenges with uncloned, highly virulent SIVs such as $SIV_{mac}251$ (11) and $SIV_{sm}E660$ (18), have not identified clear vaccine-induced correlates of protection, and no arm of the adaptive immune system can be ruled out as a critical component of an AIDS vaccine. The idea that multiple antigens and a range of immune responses are needed for protective immunity against a retrovirus is supported by studies in the Friend mouse retrovirus system. In that system, a combination of antigen-specific B-cell, $CD4^+$ cell, and $CD8^+$ cell responses are necessary for full protection (19); no single arm of the adaptive immune system is sufficient.

No clear and consistent correlate of immunity was observed in the SabRV-SIV vaccination and vaginal challenge experiment reported here, but several vaccine-elicited immune responses appear to be associated with protection. Of the five monkeys with anti-Env gp120 antibody responses, 4 animals exhibiting substantial protection against the SIV challenge. The monkey with the strongest anti-gp120 antibody response (27270),

as measured in serum and vaginal secretions, was one of the two fully protected monkeys. The other fully protected monkey (27244) had the strongest anti-Env response by western blot (Fig. 7). It is therefore reasonable to propose that the SabRV-SIV vaccine induced anti-SIV envelope antibody responses in the four protected monkeys may have played a role in the observed protection. It is intriguing to consider that protective anti-HIV or SIV mucosal antibodies may not need to be classical neutralizing antibodies (as determined by in vitro neutralization assays). Direct neutralization is not the only effector function of antibodies. Binding of antibody to envelope protein on whole SIV virions may efficiently trap virus in the thick mucus layer, preventing the virus from reaching its target cell type. Alternatively, mucosal antibodies may activate complement-mediated destruction of virions, or may prevent transcytosis of virions (55, 66). These additional mechanisms of antibody action warrant further investigation in vaccine experiments designed to prevent mucosal transmission.

Regarding possible cellular correlates of immunity, monkey 25231 had the strongest vaccine elicited CTL responses, and the CTL response may explain the striking $> 10^6$ reduction in post-acute viremia in that monkey. One of the fully protected monkeys (27244) also had SIV-specific CTLs and lymphoproliferative responses after SabRV-SIV vaccination, and those cellular responses may have played an important role in the observed protection. In summary, a variety of mechanisms may play a role in the observed protection.

RNA virus vectors

This is the first report of a successful primate protection experiment using a live RNA virus vector. In addition, recent data by Davis et al. showed successful protection of

some vaccinated animals against a highly virulent SIV by using Venezuelan Equine Encephalitis RNA Virus (VEE) propagation defective replicon vectors (18). Together these results prove the principle that RNA viruses can be effective vaccine vectors. It would be prudent to pursue the development of multiple RNA virus vaccine vector systems in the interest of developing novel human and animal vaccines (4, 5, 10, 13, 18, 27, 45).

This was the first SIV challenge experiment using live poliovirus SIV vaccine vectors. It is likely that the efficacy of the SabRV-SIV vaccine can be improved. It is possible to elicit neutralizing antibodies against SIV with a vaccine (14, 26, 58), and we plan to examine the ability of various new SabRV-Env viruses to elicit SIV neutralizing antibodies in a mouse model system. We also plan to explore which SabRV-SIV viruses in the cocktail are required for protection, by using smaller cocktails in future challenge experiments (for example, inoculating one group of monkeys with SabRV-Gag/Pol/Tat and a second group with SabRV-Env). Additionally, combining SabRV with other vaccine strategies may improve the efficacy of the vaccine. Priming macaques first with a DNA vaccine, or boosting SabRV1/2-SIV vaccinated macaques with gp41/gp120 protein or a second viral vaccine vector may drive the anti-SIV immune response and provide more consistent protection from challenge.

The SabRV doses used in our SIV challenge experiment are comparable to normal Sabin oral poliovirus vaccine (OPV) doses used in infants, children, and adults (2). We believe that SabRV would be substantially more efficacious in humans than it was in monkeys because Sabin viruses are several orders of magnitude more infectious in people (ID_{50} = 50 PFU) (49) than in cynomolgus macaques (ID_{100}= 10^6 PFU) (15). Thus

Sabin virus based vectors are also likely to replicate more efficiently in people than they did in monkeys. The enhanced replication of the vectors would be expected to generate a significantly stronger immune response to SabRV expressed antigens in people than in monkeys.

There has been some belief that the WHO polio eradication effort makes a vaccine vector based on poliovirus a moot line of study. We strongly disagree with that notion. There are several reasons to pursue SabRV as a human vaccine vector. The WHO wild poliovirus eradication effort has been wonderfully successful, and we are very hopeful that wild poliovirus infections can be eliminated. However, we and others have expressed reservations about the ability to eliminate the Sabin live poliovirus vaccine viruses at any time in the near future (15, 20, 64). We believe that the experiments reported here and previously (5, 15, 42, 72, 81) with recombinant poliovirus vectors demonstrate that the Sabin strains have real potential as human vaccine vectors. Finally, to our knowledge, this is the first report of a successful primate protection experiment using a defined library cocktail vaccination approach. This indicates that vaccination with an array of defined antigenic sequences can be an effective strategy, and could be pursued in other vectors. Furthermore, due to the great antigenic variability of HIV, a similar strategy using a cocktail of multiple HIV antigens could possibly be used to protect against diverse HIV strains.

References

1. **Abbas, A. K., A. H. Lichtman, and J. S. Pober** 2000. Cellular and molecular immunology, 4th ed. W.B. Saunders, Philadelphia.
2. **AFHS** 1998. AFHS Drug Information. American Society of Hospital Pharmacists : SilverPlatter International, Bethesda, MD.
3. **Ahmad, S., B. Lohman, M. Marthas, L. Giavedoni, Z. el-Amad, N. L. Haigwood, C. J. Scandella, M. B. Gardner, P. A. Luciw, and T. Yilma** 1994. Reduced virus load in rhesus macaques immunized with recombinant gp160 and challenged with simian immunodeficiency virus AIDS Res Hum Retroviruses. **10:**195-204.
4. **Altmeyer, R., M. Girard, S. van der Werf, V. Mimic, L. Seigneur, and M. F. Saron** 1995. Attenuated Mengo virus: a new vector for live recombinant vaccines Journal of Virology. **69:**3193-6.
5. **Andino, R., D. Silvera, S. D. Suggett, P. L. Achacoso, C. J. Miller, D. Baltimore, and M. B. Feinberg** 1994. Engineering poliovirus as a vaccine vector for the expression of diverse antigens Science. **265:**1448-51.
6. **Baba, T. W., V. Liska, R. Hofmann-Lehmann, J. Vlasak, W. Xu, S. Ayehunie, L. A. Cavacini, M. R. Posner, H. Katinger, G. Stiegler, B. J. Bernacky, T. A. Rizvi, R. Schmidt, L. R. Hill, M. E. Keeling, Y. Lu, J. E. Wright, T. C. Chou, and R. M. Ruprecht** 2000. Human neutralizing monoclonal antibodies of the IgG1 subtype protect against mucosal simian-human immunodeficiency virus infection Nat Med. **6:**200-6.
7. **Baba, T. W., V. Liska, A. H. Khimani, N. B. Ray, P. J. Dailey, D. Penninck, R. Bronson, M. F. Greene, H. M. McClure, L. N. Martin, and R. M. Ruprecht** 1999. Live attenuated, multiply deleted simian immunodeficiency virus causes AIDS in infant and adult macaques [see comments] [published erratum appears in Nat Med 199 May;5(5):590] Nat Med. **5:**194-203.
8. **Barnett, S. W., J. M. Klinger, B. Doe, C. M. Walker, L. Hansen, A. M. Duliège, and F. M. Sinangil** 1998. Prime-boost immunization strategies against HIV Aids Research and Human Retroviruses. **14 Suppl 3:**S299-309.
9. **Barouch, D. H., S. Santra, J. E. Schmitz, M. J. Kuroda, T. M. Fu, W. Wagner, M. Bilska, A. Craiu, X. X. Zheng, G. R. Krivulka, K. Beaudry, M. A. Lifton, C. E. Nickerson, W. L. Trigona, K. Punt, D. C. Freed, L. Guan, S. Dubey, D. Casimiro, A. Simon, M. E. Davies, M. Chastain, T. B. Strom, R. S. Gelman, D. C. Montefiori, and M. G. Lewis** 2000. Control of viremia and prevention of clinical AIDS in rhesus monkeys by cytokine-augmented DNA vaccination [In Process Citation] Science. **290:**486-92.
10. **Beard, M. R., L. Cohen, S. M. Lemon, and A. Martin** 2001. Characterization of Recombinant Hepatitis A Virus Genomes Containing Exogenous Sequences at the 2A/2B Junction J Virol. **75:**1414-1426.
11. **Benson, J., C. Chougnet, M. Robert-Guroff, D. Montefiori, P. Markham, G. Shearer, R. C. Gallo, M. Cranage, E. Paoletti, K. Limbach, D. Venzon, J. Tartaglia, and G. Franchini** 1998. Recombinant vaccine-induced protection against the highly pathogenic simian immunodeficiency virus SIV(mac251): dependence on route of challenge exposure Journal of Virology. **72:**4170-82.

12. **Berglund, P., M. Quesada-Rolander, P. Putkonen, G. Biberfeld, R. Thorstensson, and P. Liljestrom** 1997. Outcome of immunization of cynomolgus monkeys with recombinant Semliki Forest virus encoding human immunodeficiency virus type 1 envelope protein and challenge with a high dose of SHIV-4 virus AIDS Res Hum Retroviruses. **13:**1487-95.
13. **Bledsoe, A. W., C. A. Jackson, S. McPherson, and C. D. Morrow** 2000. Cytokine production in motor neurons by poliovirus replicon vector gene delivery [In Process Citation] Nat Biotechnol. **18:**964-9.
14. **Buge, S. L., E. Richardson, S. Alipanah, P. Markham, S. Cheng, N. Kalyan, C. J. Miller, M. Lubeck, S. Udem, J. Eldridge, and M. Robert-Guroff** 1997. An adenovirus-simian immunodeficiency virus *env* vaccine elicits humoral, cellular and mucosal immune responses in rhesus macaques and decreased viral burden following vaginal challenge J. Virol. **71:**8531-8541.
15. **Crotty, S., B. L. Lohman, F. X. Lu, S. Tang, C. J. Miller, and R. Andino** 1999. Mucosal immunization of cynomolgus macaques with two serotypes of live poliovirus vectors expressing simian immunodeficiency virus antigens: stimulation of humoral, mucosal, and cellular immunity J Virol. **73:**9485-95.
16. **Crotty, S., D. Maag, J. J. Arnold, W. Zhong, J. Y. Lau, Z. Hong, R. Andino, and C. E. Cameron** 2000. The broad-spectrum antiviral ribonucleoside ribavirin is an RNA virus mutagen Nat Med. **6:**1375-1379.
17. **Daniel, M. D., G. P. Mazzara, M. A. Simon, P. K. Sehgal, T. Kodama, D. L. Panicali, and R. C. Desrosiers** 1994. High-titer immune responses elicited by recombinant vaccinia virus priming and particle boosting are ineffective in preventing virulent SIV infection AIDS Res Hum Retroviruses. **10:**839-51.
18. **Davis, N. L., I. J. Caley, K. W. Brown, M. R. Betts, D. M. Irlbeck, K. M. McGrath, M. J. Connell, D. C. Montefiori, J. A. Frelinger, R. Swanstrom, P. R. Johnson, and R. E. Johnston** 2000. Vaccination of macaques against pathogenic simian immunodeficiency virus with Venezuelan equine encephalitis virus replicon particles [published erratum appears in J Virol 2000 Apr;74(7):3430] J Virol. **74:**371-8.
19. **Dittmer, U., D. M. Brooks, and K. J. Hasenkrug** 1999. Requirement for multiple lymphocyte subsets in protection by a live attenuated vaccine against retroviral infection Nat Med. **5:**189-93.
20. **Dove, A. W., and V. R. Racaniello** 1997. The polio eradication effort: should vaccine eradication be next? Science. **277:**779-80.
21. **Emini, E. A., W. A. Schleif, J. C. Quintero, P. G. Conard, J. W. Eichberg, G. P. Vlasuk, E. D. Lehman, M. A. Polokoff, T. F. Schaeffer, L. D. Schultz, and et al.** 1990. Yeast-expressed p55 precursor core protein of human immunodeficiency virus type 1 does not elicit protective immunity in chimpanzees AIDS Res Hum Retroviruses. **6:**1247-50.
22. **Giavedoni, L. D., V. Planelles, N. L. Haigwood, S. Ahmad, J. D. Kluge, M. L. Marthas, M. B. Gardner, P. A. Luciw, and T. D. Yilma** 1993. Immune response of rhesus macaques to recombinant simian immunodeficiency virus gp130 does not protect from challenge infection J Virol. **67:**577-83.
23. **Gohara, D. W., S. Crotty, J. J. Arnold, J. D. Yoder, R. Andino, and C. E. Cameron** 2000. Poliovirus RNA-dependent RNA Polymerase ($3D^{pol}$): Structural,

biochemical, and biological analysis of conserved structural motifs A and B Journal of Biological Chemistry. **275:**25523-25532.

24. **Hanke, T., V. C. Neumann, T. J. Blanchard, P. Sweeney, A. V. Hill, G. L. Smith, and A. McMichael** 1999. Effective induction of HIV-specific CTL by multi-epitope using gene gun in a combined vaccination regime Vaccine. **17:**589-96.
25. **Hanke, T., R. V. Samuel, T. J. Blanchard, V. C. Neumann, T. M. Allen, J. E. Boyson, S. A. Sharpe, N. Cook, G. L. Smith, D. I. Watkins, M. P. Cranage, and A. J. McMichael** 1999. Effective induction of simian immunodeficiency virus-specific cytotoxic T lymphocytes in macaques by using a multiepitope gene and DNA prime- modified vaccinia virus Ankara boost vaccination regimen J Virol. **73:**7524-32.
26. **Hirsch, V. M., T. R. Fuerst, G. Sutter, M. W. Carroll, L. C. Yang, S. Goldstein, M. Piatak, Jr., W. R. Elkins, W. G. Alvord, D. C. Montefiori, B. Moss, and J. D. Lifson** 1996. Patterns of viral replication correlate with outcome in simian immunodeficiency virus (SIV)-infected macaques: effect of prior immunization with a trivalent SIV vaccine in modified vaccinia virus Ankara J Virol. **70:**3741-52.
27. **Hofling, K., S. Tracy, N. Chapman, K. S. Kim, and J. Smith Leser** 2000. Expression of an antigenic adenovirus epitope in a group B coxsackievirus [In Process Citation] J Virol. **74:**4570-8.
28. **Hoxie, J. A., B. S. Haggarty, S. E. Bonser, J. L. Rackowski, H. Shan, and P. J. Kanki** 1988. Biological characterization of a simian immunodeficiency virus-like retrovirus (HTLV-IV): evidence for CD4-associated molecules required for infection J Virol. **62:**2557-68.
29. **Hull, H. F., N. A. Ward, B. P. Hull, J. B. Milstien, and C. de Quadros** 1994. Paralytic poliomyelitis: seasoned strategies, disappearing disease Lancet. **343:**1331-7.
30. **Imaoka, K., C. J. Miller, M. Kubota, M. B. McChesney, B. Lohman, M. Yamamoto, K. Fugihashi, K. Someya, M. Honda, J. R. McGhee, and H. Kiyono** 1998. Nasal immunization of nonhuman primates with simian immunodeficiency virus p55gag and cholera toxin adjuvant induces Th1/Th2 help for virus specific immune responses in reproductive tissues J. Immunol. **161:**5952-5958.
31. **Johnson, R. P., and R. C. Desrosiers** 1998. Protective immunity induced by live attenuated simian immunodeficiency virus Curr Opin Immunol. **10:**436-43.
32. **Kestler, H., T. Kodama, D. Ringler, M. Marthas, N. Pedersen, A. Lackner, D. Regier, P. Sehgal, M. Daniel, N. King, and R. Desrosiers** 1990. Induction of AIDS in rhesus monkeys by molecularly cloned simian immunodeficiency virus [see comments] Science. **248:**1109-12.
33. **Kohara, M., S. Abe, S. Kuge, B. L. Semler, T. Komatsu, M. Arita, H. Itoh, and A. Nomoto** 1986. An infectious cDNA clone of the poliovirus Sabin strain could be used as a stable repository and inoculum for the oral polio live vaccine Virology. **151:**21-30.
34. **Lehner, T., Y. Wang, M. Cranage, L. A. Bergmeier, E. Mitchell, L. Tao, G. Hall, M. Dennis, N. Cook, R. Brookes, L. Klavinskis, I. Jones, C. Doyle, and**

R. Ward 1996. Protective mucosal immunity elicited by targeted iliac lymph node immunization with a subunit SIV envelope and core vaccine in macaques [see comments] Nature Medicine. **2**:767-75.

35. **Letvin, N. L., J. E. Schmitz, H. L. Jordan, A. Seth, V. M. Hirsch, K. A. Reimann, and M. J. Kuroda** 1999. Cytotoxic T lymphocytes specific for the simian immunodeficiency virus Immunol Rev. **170**:127-34.
36. **Lifson, J. D., J. L. Rossio, R. Arnaout, L. Li, T. L. Parks, D. K. Schneider, R. F. Kiser, V. J. Coalter, G. Walsh, R. J. Imming, B. Fisher, B. M. Flynn, N. Bischofberger, M. Piatak, Jr., V. M. Hirsch, M. A. Nowak, and D. Wodarz** 2000. Containment of simian immunodeficiency virus infection: cellular immune responses and protection from rechallenge following transient postinoculation antiretroviral treatment J Virol. **74**:2584-93.
37. **Lohman, B. L., J. Higgins, M. L. Marthas, P. A. Marx, and N. C. Pedersen** 1991. Development of simian immunodeficiency virus isolation, titration, and neutralization assays which use whole blood from rhesus monkeys and an antigen capture enzyme-linked immunosorbent assay J Clin Microbiol. **29**:2187-92.
38. **Lu, F. X., Z. Ma, T. Rourke, S. Srinivasan, M. McChesney, and C. J. Miller** 1999. Immunoglobulin concentrations and antigen-specific antibody levels in cervicovaginal lavages of rhesus macaques are influenced by the stage of the menstrual cycle Infect Immun. **67**:6321-8.
39. **Lu, S., J. Arthos, D. C. Montefiori, Y. Yasutomi, K. Manson, F. Mustafa, E. Johnson, J. C. Santoro, J. Wissink, J. I. Mullins, J. R. Haynes, N. L. Letvin, M. Wyand, and H. L. Robinson** 1996. Simian immunodeficiency virus DNA vaccine trial in macaques J Virol. **70**:3978-91.
40. **Lü, X., H. Kiyono, D. Lu, S. Kawabata, J. Torten, S. Srinivasan, P. J. Dailey, J. R. McGhee, T. Lehner, and C. J. Miller** 1997. Targeted lymph-node immunization with whole inactivated simian immunodeficiency virus (SIV) or envelope and core subunit antigen vaccines does not reliably protect rhesus macaques from vaginal challenge with SIVmac251 AIDS. **12**:1-10.
41. **Mandl, S., L. Hix, and R. Andino** 2001. Preexisting immunity to poliovirus does not impair the efficacy of recombinant poliovirus vaccine vectors [In Process Citation] J Virol. **75**:622-7.
42. **Mandl, S., L. J. Sigal, K. L. Rock, and R. Andino** 1998. Poliovirus vaccine vectors elicit antigen-specific cytotoxic T cells and protect mice against lethal challenge with malignant melanoma cells expressing a model antigen Proceedings of the National Academy of Sciences of the United States of America. **95**:8216-21.
43. **Marthas, M. L., R. A. Ramos, B. L. Lohman, K. K. Van Rompay, R. E. Unger, C. J. Miller, B. Banapour, N. C. Pedersen, and P. A. Luciw** 1993. Viral determinants of simian immunodeficiency virus (SIV) virulence in rhesus macaques assessed by using attenuated and pathogenic molecular clones of SIVmac J Virol. **67**:6047-55.
44. **Mascola, J. R., G. Stiegler, T. C. VanCott, H. Katinger, C. B. Carpenter, C. E. Hanson, H. Beary, D. Hayes, S. S. Frankel, D. L. Birx, and M. G. Lewis** 2000. Protection of macaques against vaginal transmission of a pathogenic HIV-

1/SIV chimeric virus by passive infusion of neutralizing antibodies Nat Med. **6**:207-10.

45. **McAllister, A., A. E. Arbetman, S. Mandl, C. Pena-Rossi, and R. Andino** 2000. Recombinant Yellow Fever Viruses Are Effective Therapeutic Vaccines for Treatment of Murine Experimental Solid Tumors and Pulmonary Metastases J Virol. **74**:9197-9205.
46. **McChesney, M. B., J. R. Collins, D. Lu, X. Lü, J. Torten, R. L. Ashley, M. W. Cloyd, and C. J. Miller** 1998. Occult systemic infection and persistent simian immunodeficiency virus (SIV)-specific $CD4^+$-T-cell proliferative responses in rhesus macaques that were transiently viremic after intravaginal inoculation of SIV J. Virol. **72**:10029-10035.
47. **Melnick, J. L.** 1996. Enteroviruses: Polioviruses, coxsackieviruses, echoviruses, and newer enteroviruses, p. 655-712. *In* B. N. Fields, D. M. Knipe, and P. M. Howley (eds), Fields virology, 3rd ed, vol. 1. Lippincott-Raven Publishers, Philadelphia.
48. **Miller, C. J., M. B. McChesney, X. Lü, P. J. Dailey, C. Chutkowski, D. Lu, P. Brosio, B. Roberts, and Y. Lu** 1997. Rhesus macaques previously infected with simian/human immunodeficiency virus are protected from vaginal challenge with pathogenic SIVmac239 J. Virol. **71**:1911-1921.
49. **Minor, P. D.** 1997. Poliovirus, p. 555-574. *In* N. Nathanson, and R. Ahmed (eds), Viral pathogenesis. Lippincott-Raven, Philadelphia.
50. **Montefiori, D. C., T. W. Baba, A. Li, M. Bilska, and R. M. Ruprecht** 1996. Neutralizing and infection-enhancing antibody responses do not correlate with the differential pathogenicity of SIVmac239delta3 in adult and infant rhesus monkeys J Immunol. **157**:5528-35.
51. **Morrow, C. D., M. J. Novak, D. C. Ansardi, D. C. Porter, and Z. Moldoveanu** 1999. Recombinant viruses as vectors for mucosal immunity Current Topics in Microbiology and Immunology. **236**:255-73.
52. **Mueller, S., and E. Wimmer** 1998. Expression of foreign proteins by poliovirus polyprotein fusion: analysis of genetic stability reveals rapid deletions and formation of cardioviruslike open reading frames Journal of Virology. **72**:20-31.
53. **Murphy, C. G., W. T. Lucas, R. E. Means, S. Czajak, C. L. Hale, J. D. Lifson, A. Kaur, R. P. Johnson, D. M. Knipe, and R. C. Desrosiers** 2000. Vaccine protection against simian immunodeficiency virus by recombinant strains of herpes simplex virus [In Process Citation] J Virol. **74**:7745-54.
54. **Nomoto, A., T. Omata, H. Toyoda, S. Kuge, H. Horie, Y. Kataoka, Y. Genba, Y. Nakano, and N. Imura** 1982. Complete nucleotide sequence of the attenuated poliovirus Sabin 1 strain genome Proc Natl Acad Sci U S A. **79**:5793-7.
55. **Ogra, P. L.** 1999. Mucosal immunology, 2nd ed. Academic Press, San Diego.
56. **Ogra, P. L., and D. T. Karon** 1971. Formation and function of poliovirus antibody in different tissues Progess in Medical Virology. **13**:156-193.
57. **Omata, T., M. Kohara, Y. Sakai, A. Kameda, N. Imura, and A. Nomoto** 1984. Cloned infectious complementary DNA of the poliovirus Sabin 1 genome: biochemical and biological properties of the recovered virus Gene. **32**:1-10.
58. **Ourmanov, I., C. R. Brown, B. Moss, M. Carroll, L. Wyatt, L. Pletneva, S. Goldstein, D. Venzon, and V. M. Hirsch** 2000. Comparative efficacy of

recombinant modified vaccinia virus Ankara expressing simian immunodeficiency virus (SIV) Gag-Pol and/or Env in macaques challenged with pathogenic SIV J Virol. **74:**2740-51.

59. **Paul, J. R., J. T. Riordan, and J. L. Melnick** 1951. Antibodies to three different antigenic types of poliomyelitis virus in sera from north Alaskan eskimos American Journal of Hygiene. **54:**275-285.
60. **Plotkin, S., and W. Orenstein** (eds.) 1999 Vaccines, 3rd ed. W. B. Saunders Company, Philadelphia.
61. **Polacino, P., V. Stallard, J. E. Klaniecki, D. C. Montefiori, A. J. Langlois, B. A. Richardson, J. Overbaugh, W. R. Morton, R. E. Benveniste, and S. L. Hu** 1999. Limited breadth of the protective immunity elicited by simian immunodeficiency virus SIVmne gp160 vaccines in a combination immunization regimen J Virol. **73:**618-30.
62. **Polacino, P., V. Stallard, D. C. Montefiori, C. R. Brown, B. A. Richardson, W. R. Morton, R. E. Benveniste, and S. L. Hu** 1999. Protection of macaques against intrarectal infection by a combination immunization regimen with recombinant simian immunodeficiency virus SIVmne gp160 vaccines J Virol. **73:**3134-46.
63. **Pollard, S. R., G. Dunn, N. Cammack, P. D. Minor, and J. W. Almond** 1989. Nucleotide sequence of a neurovirulent variant of the type 2 oral poliovirus vaccine J Virol. **63:**4949-51.
64. **Racaniello, V. R.** 2000. It is too early to stop polio vaccination [comment] Bull World Health Organ. **78:**359-60.
65. **Rezapkin, G. V., W. Alexander, E. Dragunsky, M. Parker, K. Pomeroy, D. M. Asher, and K. M. Chumakov** 1998. Genetic stability of Sabin 1 strain of poliovirus: implications for quality control of oral poliovirus vaccine Virology. **245:**183-7.
66. **Robert-Guroff, M.** 2000. IgG surfaces as an important component in mucosal protection [news] Nat Med. **6:**129-30.
67. **Robinson, H. L., D. C. Montefiori, R. P. Johnson, K. H. Manson, M. L. Kalish, J. D. Lifson, T. A. Rizvi, S. Lu, S. L. Hu, G. P. Mazzara, D. L. Panicali, J. G. Herndon, R. Glickman, M. A. Candido, S. L. Lydy, M. S. Wyand, and H. M. McClure** 1999. Neutralizing antibody-independent containment of immunodeficiency virus challenges by DNA priming and recombinant pox virus booster immunizations [see comments] Nat Med. **5:**526-34.
68. **Ruprecht, R. M.** 1999. Live attenuated AIDS viruses as vaccines: promise or peril? Immunol Rev. **170:**135-49.
69. **Schlienger, K., D. C. Montefiori, M. Mancini, Y. Riviere, P. Tiollais, and M. L. Michel** 1994. Vaccine-induced neutralizing antibodies directed in part to the simian immunodeficiency virus (SIV) V2 domain were unable to protect rhesus monkeys from SIV experimental challenge J Virol. **68:**6578-88.
70. **Schmitz, J. E., M. J. Kuroda, S. Santra, V. G. Sasseville, M. A. Simon, M. A. Lifton, P. Racz, K. Tenner-Racz, M. Dalesandro, B. J. Scallon, J. Ghrayeb, M. A. Forman, D. C. Montefiori, E. P. Rieber, N. L. Letvin, and K. A.**

Reimann 1999. Control of viremia in simian immunodeficiency virus infection by CD8+ lymphocytes Science. **283**:857-60.

71. **Schultz, A.** 1998. Using recombinant vectors as HIV vaccines, p. 1-4, IAVI Report, vol. 3.
72. **Sigal, L. J., S. Crotty, R. Andino, and K. L. Rock** 1999. Cytotoxic T-cell immunity to virus-infected non-haematopoietic cells requires presentation of exogenous antigen Nature. **398**:77-80.
73. **Singh, M., R. Cattaneo, and M. A. Billeter** 1999. A recombinant measles virus expressing hepatitis B virus surface antigen induces humoral immune responses in genetically modified mice J Virol. **73**:4823-8.
74. **Suryanarayana, K., T. A. Wiltrout, G. M. Vasquez, V. M. Hirsch, and J. D. Lifson** 1998. Plasma SIV RNA viral load determination by real-time quantification of product generation in reverse transcriptase-polymerase chain reaction AIDS Res Hum Retroviruses. **14**:183-9.
75. **Sutter, R. W., S. L. Cochi, and J. L. Melnick** 1999. Live attenuated poliovirus vaccines, p. 1230. *In* S. Plotkin, and W. Orenstein (eds), Vaccines, 3rd ed. W. B. Saunders, Philadelphia.
76. **Tang, S., R. van Rij, D. Silvera, and R. Andino** 1997. Toward a poliovirus-based simian immunodeficiency virus vaccine: correlation between genetic stability and immunogenicity Journal of Virology. **71**:7841-50.
77. **UNAIDS, and WHO** 1998. Report on the Global HIV/AIDS Epidemic. World Health Organization.
78. **Wang, S. W., P. A. Kozlowski, G. Schmelz, K. Manson, M. S. Wyand, R. Glickman, D. Montefiori, J. D. Lifson, R. P. Johnson, M. R. Neutra, and A. Aldovini** 2000. Effective induction of simian immunodeficiency virus-specific systemic and mucosal immune responses in primates by vaccination with proviral DNA producing intact but noninfectious virions [In Process Citation] J Virol. **74**:10514-22.
79. **Weeks-Levy, C., and P. L. Ogra** 1996. Polioviruses and mucosal vaccines. *In* H. Kiyono, P. Ogra, and J. McGhee (eds), Mucosal Vaccines, 1st ed. Academic Press, New York.
80. **Yasutomi, Y., S. Koenig, R. M. Woods, J. Madsen, N. M. Wassef, C. R. Alving, H. J. Klein, T. E. Nolan, L. J. Boots, J. A. Kessler, and et al.** 1995. A vaccine-elicited, single viral epitope-specific cytotoxic T lymphocyte response does not protect against intravenous, cell-free simian immunodeficiency virus challenge J Virol. **69**:2279-84.
81. **Yim, T. J., S. Tang, and R. Andino** 1996. Poliovirus recombinants expressing hepatitis B virus antigens elicited a humoral immune response in susceptible mice Virology. **218**:61-70.

Table 1. SabRV1/2-SIV vaccine library cocktails

Sabin1 virus name	Sabin2 virus name	Amino acid coverage
SabRV1-Gag1	SabRV2-Gag1	Gag 2-134 (p17)
SabRV1-Gag2	SabRV2-Gag2	Gag 92-263 (p17/p24)
	SabRV2-Gag3N	Gag 133-299
	SabRV2-Gag3C	Gag 266-432
SabRV1-Gag4	SabRV2-Gag4	Gag 362-509 (p24/p9)
SabRV1-Pol6		Pol (-)29-146 (protease)
SabRV1-Pol7	SabRV2-Pol7	Pol 97-266
SabRV1-Pol8	SabRV2-Pol8	Pol 218-330
SabRV1-Pol9	SabRV2-Pol9	Pol 290-472
SabRV1-Pol10	SabRV2-Pol10	Pol 397-530
SabRV1-Pol11	SabRV2-Pol11	Pol 490-631
SabRV1-Pol12		Pol 597-767
SabRV1-Pol14	SabRV2-Pol14	Pol 828-981
SabRV1-Env15		Env 18-164 (gp120)
	SabRV2-Env15C	Env 71-211 (gp120)
SabRV1-Env16M	SabRV2-Env16M	Env 148-249 (gp120)
SabRV1-Env17	SabRV2-Env17	Env 237-380 (gp120)
SabRV1-Env18	SabRV2-Env18	Env 335-498 (gp120)
SabRV1-Env20	SabRV2-Env20	Env 486-632 (gp120/gp41)
SabRV1-Env21L	SabRV2-Env21L	Env 526-698 (gp41, extra)
SabRV1-Env22		Env 712-879 (gp41, cyto)
SabRV1-Nef23	SabRV2-Nef23	Nef 1-145
SabRV1-Nef24	SabRV2-Nef24	Nef 126-262
	SabRV2-Tat25	Tat 1-130

Table 2. SIV virus isolation

week[a]	1	2	4	6	8	12	16
27244	—	—	—	—	—	—	—
27270	—	—	+	—	—	—	—
25231	+	+	+	+	+	+	+
27250	+	+	+	+	+	+	+
28508	+	+	+	+	+	+	—
27253	+	+	+	+	+	+	+
27273	+	+	+	+	+	+	+
26385	+	+	+	+	+	+	+
28118	+	+	+	+	+	+	+
26560	+	+	+	+	+	—	+
26383	—	+	+	+	+	+	+
26405	—	+	+	+	+	+	+
23414	—	+	+	+	+	+	+

[a] Upper seven monkeys are vaccinated, lower six are control monkeys

Table 3. SIV proviral DNA PCR

week[a]	1	2	4	8	12
27244	—	—	—	—	—
27270	—	—	—	—	—
25231	—	+	—	+	+
27250	—	—	+	+	+
28508	—	—	+	+	+
27253	—	—	+	+	+
27273	—	—	+	+	+
26385	—	—	—	+	+
28118	—	—	—	+	+
26560	—	+	+	+	+
26383	—	+	—	+	+
26405	—	—	—	+	+
23414	—	nd	+	+	+

[a] Upper seven monkeys are vaccinated, lower six are control monkeys
nd = not done
Nested PCR used gag specific primers.

Table 4. Neutralizing Antibodies

Monkey[a]	0[b]	30 (Ch+0)[c]	32 (Ch+2)	38 (Ch+8)
27244	—[d]	—	—	—
27270	—	—	—	—
25231	—	—	—	7673
27250	—	—	—	1130
28508	—	—	—	6386
27253	—	—	—	421
27273	—	—	—	8348
26385	—	—	—	613
28118	—	—	—	1215
26560	—	—	—	1994
26383	—	—	—	512
26405	—	—	—	1764
23414	—	—	—	1301

[a] Upper seven monkeys are vaccinated, lower six are control monkeys
[b] Day of initial SabRV1-SIV immunization
[c] Day of challenge. (Ch = challenge)
[d] (—) indicates undetectable levels of neutralizing antibodies. See Materials and Methods. Titers indicated are reciprocal dilutions.

Figure Legends

Figure 1

(A) Recombinant Sabin poliovirus vector plasmid clones. Grey boxes indicate 2A proteolytic cleavage sites (GLTTY/GFGH). In both the pSabRV1 and pSabRV2 vector the first proteolytic cleavage site coding sequence is followed by a 5 glycine spacer (not marked) and the in frame cloning sites (white boxes) immediately prior to the second proteolytic cleavage site. In total, 60-70 extra nts are added to the viral genome to create the vector.

(B) Plaque assay of cloned Sabin 1 virus (pS1 derived) and the Sabin 1 recombinant virus vector (SabRV1) at 32° C.

(C) Plaque assay of cloned Sabin 2 (pS2-10F derived) and the Sabin 2 recombinant virus vector (SabRV2) at 37° C.

(D) SabRV1-SIV plaque assays. All SabRV1-SIV viruses made were titered by plaque assay. Growth of several representative viruses at 32° C is shown here. SabRV1 without an insert is shown as a control.

(E) SabRV2-SIV plaque assays. All SabRV2-SIV viruses made were titered by plaque assay. Growth of several representative viruses at 37°C is shown here. SabRV2 without insert is shown as a control.

(F) Library schematic. Map of SIV antigens used in SabRV1-SIV and/or SabRV2-SIV vaccine cocktails (see also Table 1).

Figure 2 Propagation of vaccine viruses.

(A) Stability of SabRV2 recombinant viruses passaged as a cocktail. Nine SabRV2-SIV viruses were mixed in equal amounts and passaged five times at an MOI of 0.1, for a total of at least 10 generations of viral replication. The P_1 virus is conservatively estimated as generation 2. Cocktail stocks were tested for the presence of the SIV inserts by RT-PCR using primers within the poliovirus sequence flanking the SIV inserts. SabRV2 empty vector RT-PCR is indicated by (V). The size of the SabRV2 band (427 bp) is the size of the virus containing no insert. Throughout all five passages, inserts are fully retained.

(B) Composition of SabRV2 cocktail over a series of passages. The passaged cocktail stocks were checked for the presence of the individual viruses by RT-PCR with primers specific for each SIV insert. Generation 1 indicates the original cocktail in which the nine P_0 viral stocks obtained directly from high-efficiency transfection were mixed in equal proportion. The generation 1 stock contained all nine viruses by RT-PCR. The middle and right panel show the presence of all nine SabRV2-SIV viruses both at generation 6 and generation 10.

Figure 3 Timeline of vaccination and challenge.

Figure 4 Serum anti-SIV antibodies.

(A) Anti-SIV IgG titers in the sera of SabRV1/2-SIV immunized monkeys. Seven cynomolgus macaques were inoculated intranasally with SabRV1-SIV at week 0 and 2 (indicated by Δ) and boosted intranasally at week 19 and 21 with SabRV2-SIV (indicated by ▲). Monkeys are labelled as follows: 25231 (■), 27244 (●), 27250 (▲),

27253 (◆), 27270 (□), 27273 (○), 28508 (△). Titers indicated are reciprocal dilutions. A titer of 1 is stringently defined as an ELISA OD reading three standard deviations above the average OD of a group of negative control monkeys (see Materials and Methods).

(B) Anti-SIV IgA titers in the sera of SabRV1/2-SIV immunized monkeys. Symbols are as noted above. A clear anemnestic IgA response is visible in all seven macaques after SabRV2-SIV immunization at week 19.

Figure 5 Rectal anti-SIV antibodies

(A) Anti-SIV IgG titers in the rectal washes of SabRV1/2-SIV immunized monkeys. Vaccinated monkeys were divided into two groups (upper and lower panels) for easier viewing. Titers indicated are reciprocal dilutions. A titer of 1 is stringently defined as an ELISA OD reading three standard deviations above the average OD of a group of negative control monkeys (see Materials and Methods).

(B) Anti-SIV IgA titers in the rectal washes of SabRV1/2-SIV immunized monkeys. Vaccinated monkeys were divided into the same two groups (upper and lower panels) as in part A, for easier viewing. Monkeys are labeled as in Figure 4.

Figure 6 Vaginal anti-SIV antibodies

(A) Anti-SIV IgG titers in the vaginal secretions of SabRV1/2-SIV immunized monkeys. Vaccinated monkeys are divided into two groups (upper and lower panels) for easier viewing, as was done in Fig. 4,5.

(B) Anti-SIV IgA titers in the vaginal secretions of SabRV1/2-SIV immunized monkeys. Monkeys are labelled as before.

Figure 7 Western Blotting. All seven monkeys made anti-SIV and anti-poliovirus antibody responses detectable by western blotting. Each serum was immunoblotted against purified SIV virion (first lane) and poliovirus infected HeLa cell extract (second lane). Positive controls used were SIV^+ rhesus serum (SIV^+), and human polio-immune serum ($Polio^+$). Preimmune serum from monkey 27250 was used as a negative control (preimm.). SIV antigens recognized by each monkey are indicated by symbols on the left of the blot: RT (⇨), gag (—), gp120(●), and gp41(O). Poliovirus VP1, recognized by all monkeys, is indicated by (◀) to the right of each blot. Bands do not necessarily line up precisely, as several of the blots were done at different times, but SIV and polio positive controls were always run as markers.

Figure 8 SIV-specific cytotoxic T lymphocytes (CTLs).

(A) **SIV-specific CTLs after immunization with SabRV1-SIV.** SIV-specifc CTLs were detected using bulk PBMCs collected two weeks post-immunization with SabRV1-SIV. Monkeys 25231, 27244, and 27250 tested positive for SIV Env specific CTLs. Negative control target cells are indicated by (□), and Env-expressing target cells are indicated by (●).

(B) **SIV-specific CTLs after immunization with SabRV2-SIV.** SIV-specific CTLs were detected using bulk PBMCs collected six weeks post-immunization with SabRV2-SIV. Monkey 25231 tested positive for SIV Gag specific CTLs and possibly Env specific CTLs. Negative control target cells are indicated by (□), Gag-expressing target cells are indicated by (▲), and Env-expressing target cells are indicated by (●).

Figure 9 Serum anti-SIV IgG antibody responses post-challenge. Antibody titers are shown for all animals post-challenge. Vaccinated monkeys (right panel) are indicated by the symbols used in previous figures: 25231 (■), 27244 (●), 27250 (▲), 27253 (◆), 27270 (□), 27273 (○), 28508 (△). Control monkeys (left panel) are indicated by the symbols: 26383 (★), 26385 (✱), 23414 (✙), 26405 (◇), 26560 (▽), 28118 (◀).

Figure 10 SIV RNA loads. SIV RNA levels in plasma post-challenge. All seven vaccinated monkeys and six control monkeys were challenged with an intravaginal inoculation of highly virulent $SIV_{mac}251$ at week 30 of the experiment (challenge week 0). Vaccinated monkeys (right panel) are indicated by the symbols used in previous figures: 25231 (■), 27244 (●), 27250 (▲), 27253 (◆), 27270 (□), 27273 (○), 28508 (△). Control monkeys (left panel) are indicated by the symbols: 26383 (★), 26385 (✱), 23414 (✙), 26405 (◇), 26560 (▽), 28118 (◀). Vaccinated monkeys 27270 and 27244 were never positive for SIV RNA and appear completely protected. Threshold sensitivity of the assay is 100 RNA copy Eq/ml, indicated by a dashed line. Data points below threshold value are shown at 100. Dagger (†) indicates death of the animal between week 32-44 post-challenge.

Figure 11 Clinical outcomes of vaginal challenge with $SIV_{mac}251$

(A) Post-challenge $CD4^+$ T lymphocyte counts. $CD3^+$ $CD4^+$ T lymphocyte counts in the peripheral blood of naive control cynomolgus macaques (left) and SabRV1/2-SIV

vaccinated macaques (right), from day of challenge through 36 weeks post-challenge. Symbols are as used in Fig. 10.

(B) Body weight. Weight of control macaques (left) and SabRV1/2-SIV vaccinated macaques (right), from day of challenge through 44 weeks post-challenge. Weight is indicated as percentage of body weight on the day of challenge. Body weight change of vaccinate animals is significantly better ($p < 0.003$) than the control monkeys. Symbols used are same as in (A).

(C) Mortality curve. SabRV-SIV vaccinated animals (■); control animals (●).

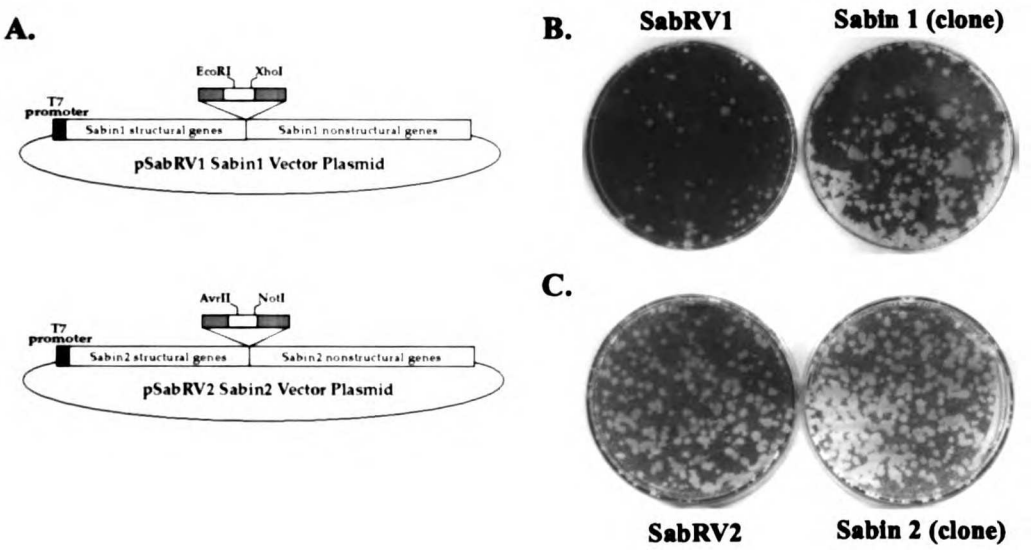
A.
EcoRI
XhoI
T7 promoter
Sabin1 structural genes
Sabin1 nonstructural genes
pSabRV1 Sabin1 Vector Plasmid
AvrII
NotI
T7 promoter
Sabin2 structural genes
Sabin2 nonstructural genes
pSabRV2 Sabin2 Vector Plasmid
B.
SabRV1
Sabin 1 (clone)
C.
SabRV2
Sabin 2 (clone)

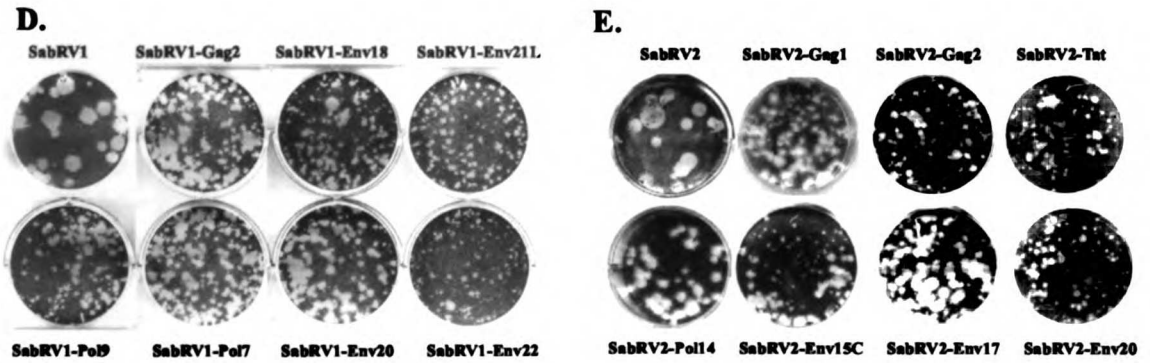
D.
SabRV1
SabRV1-Gag2
SabRV1-Env18
SabRV1-Env21L
SabRV1-Pol9
SabRV1-Pol7
SabRV1-Env20
SabRV1-Env22
E.
SabRV2
SabRV2-Gag1
SabRV2-Gag2
SabRV2-Tat
SabRV2-Pol14
SabRV2-Env15C
SabRV2-Env17
SabRV2-Env20

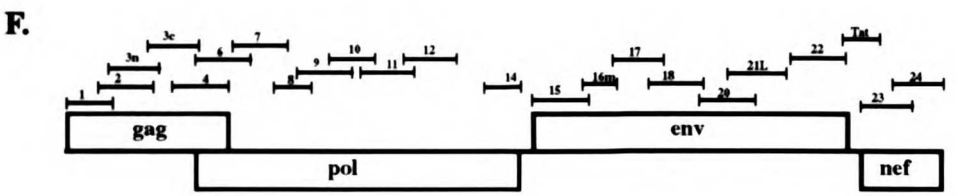
F.
3c
7
3n
6
9
10
11
12
17
Tat
22
21L
2
4
8
14
15
16m
18
20
24
1
23
gag
env
pol
nef

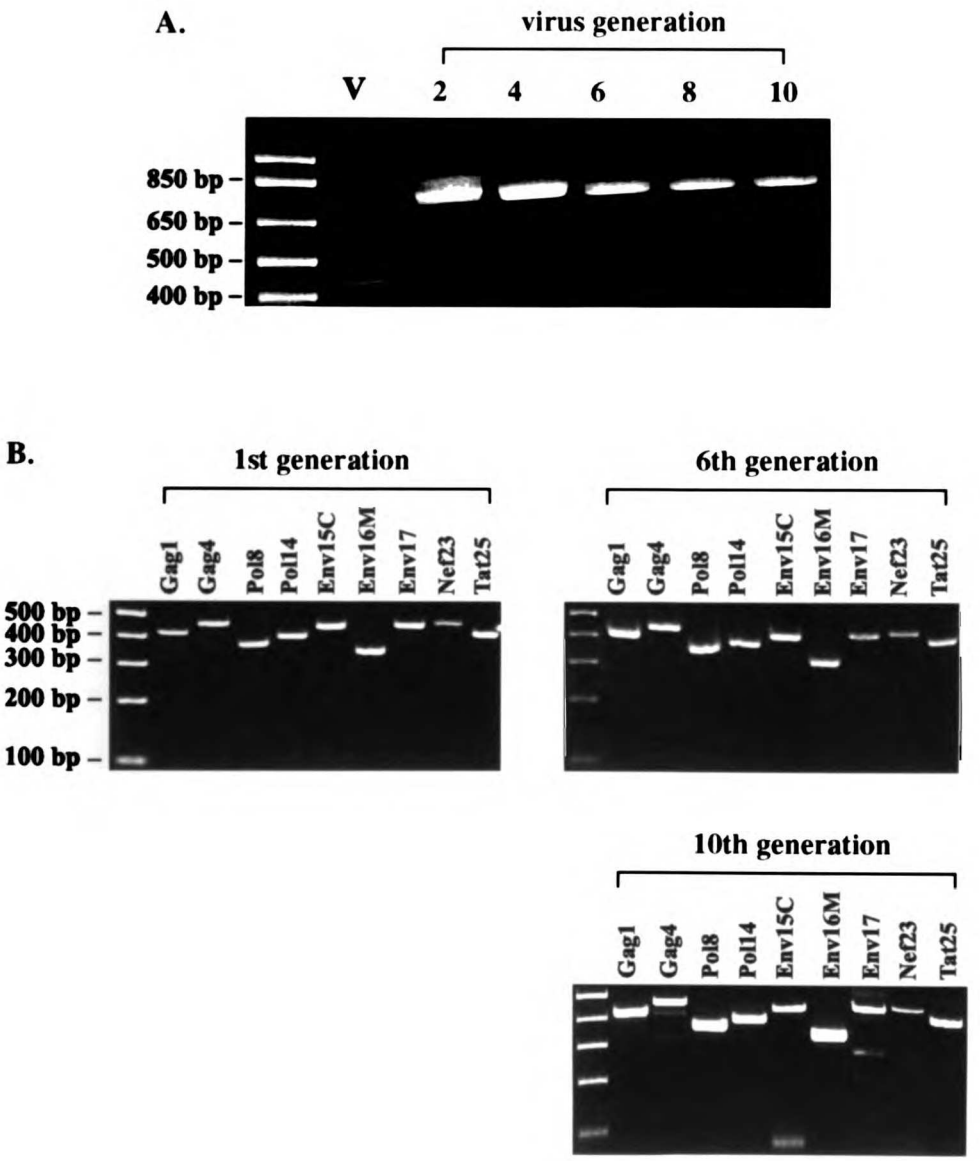
A.
virus generation
V
2
4
6
8
10
850 bp
650 bp
500 bp
400 bp
B.
1st generation
6th generation
10th generation
Gag1
Gag4
Pol8
Pol14
Env15C
Env16M
Env17
Nef23
Tat25
500 bp
400 bp
300 bp
200 bp
100 bp

Figure 3

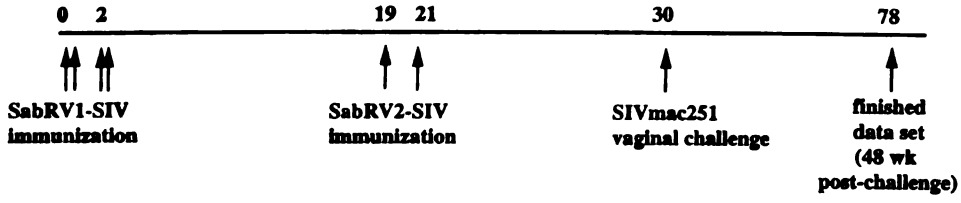
0
2
19
21
30
78
SabRV1-SIV immunization
SabRV2-SIV immunization
SIVmac251 vaginal challenge
finished data set (48 wk post-challenge)

Figure 4

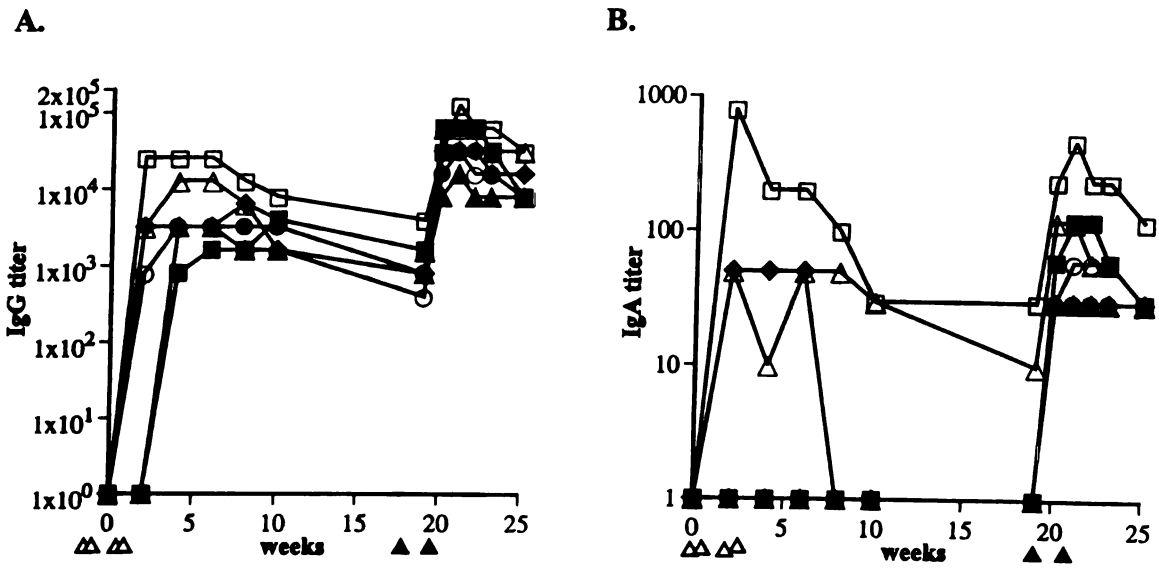

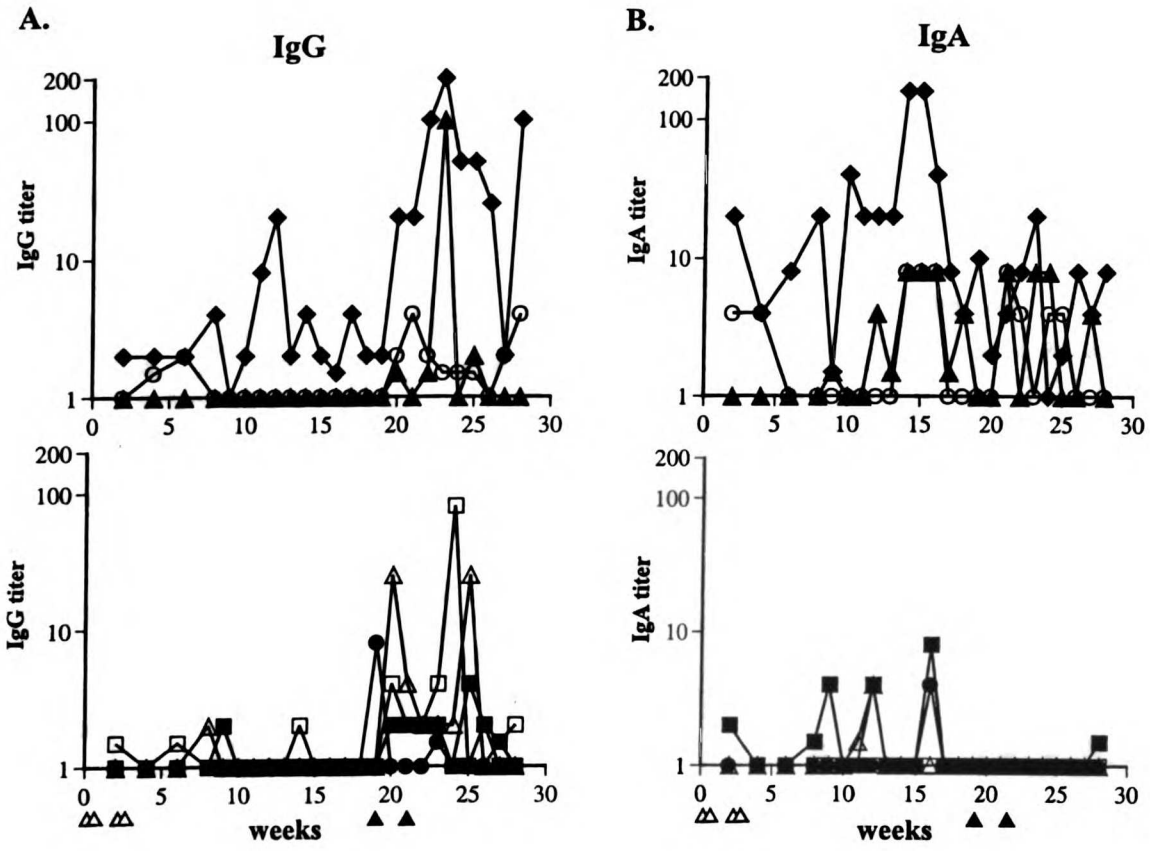
A.
IgG
IgG titer
200
100
10
1
0 5 10 15 20 25 30
IgG titer
200
100
10
1
0 5 10 15 20 25 30
weeks
B.
IgA
IgA titer
200
100
10
1
0 5 10 15 20 25 30
IgA titer
200
100
10
1
0 5 10 15 20 25 30
weeks

Figure 6

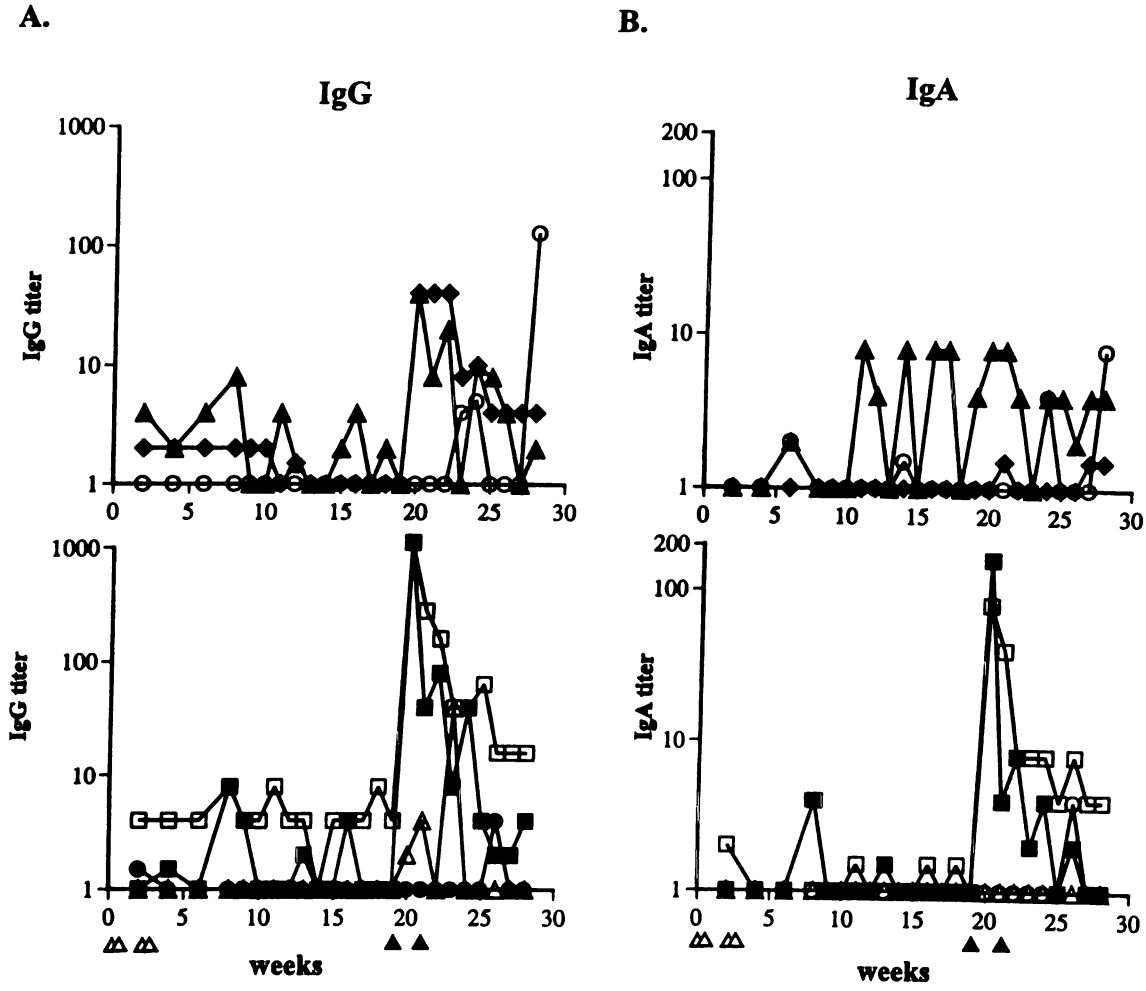
A.
IgG
IgG titer
1000
100
10
1
0 5 10 15 20 25 30
IgG titer
1000
100
10
1
0 5 10 15 20 25 30
weeks
B.
IgA
IgA titer
200
100
10
1
0 5 10 15 20 25 30
IgA titer
200
100
10
1
0 5 10 15 20 25 30
weeks

Figure 7

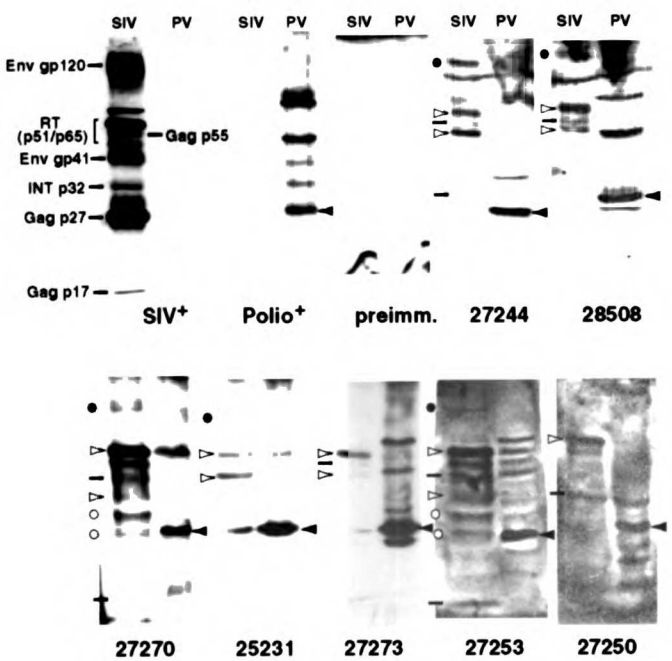
SIV PV SIV PV SIV PV SIV PV SIV PV
Env gp120
RT
(p51/p65)
Gag p55
Env gp41
INT p32
Gag p27
Gag p17
SIV+
Polio+
preimm.
27244
28508
27270
25231
27273
27253
27250

Figure 8

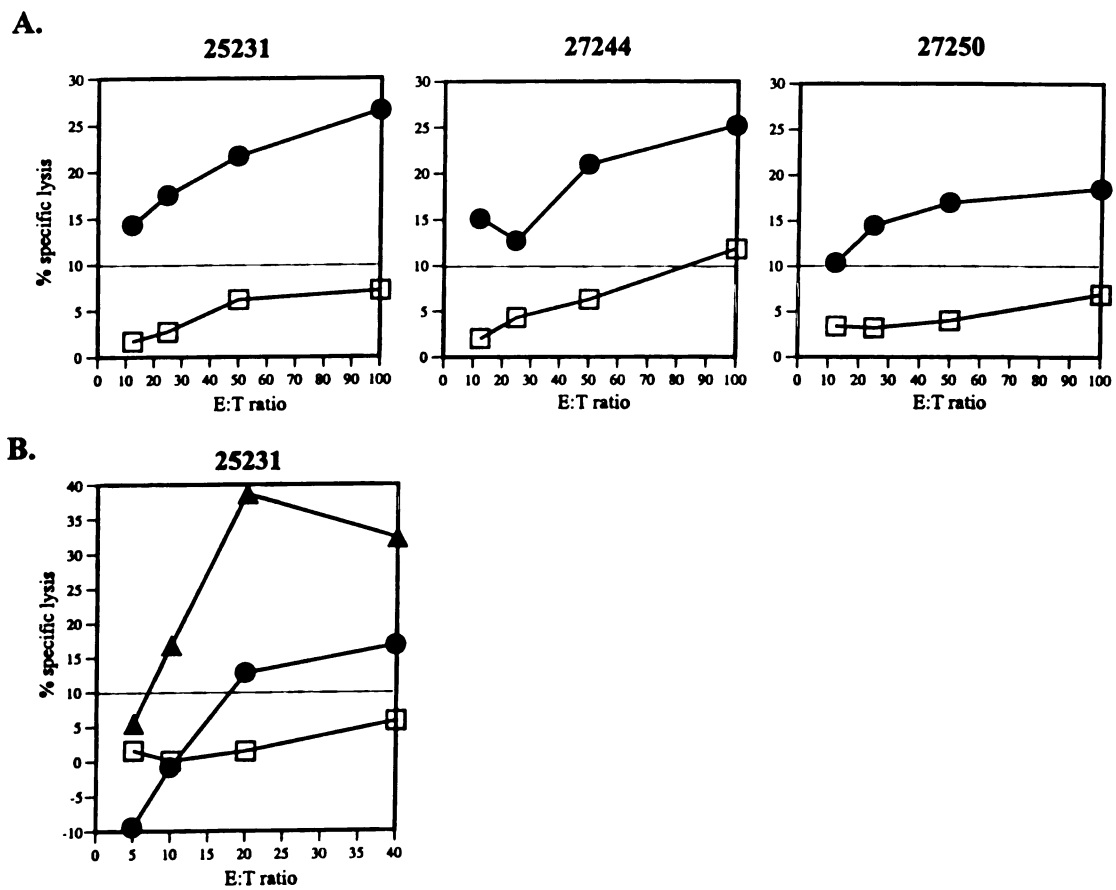
A.
25231
27244
27250
% specific lysis
E:T ratio
B.
25231
% specific lysis
E:T ratio

Figure 9

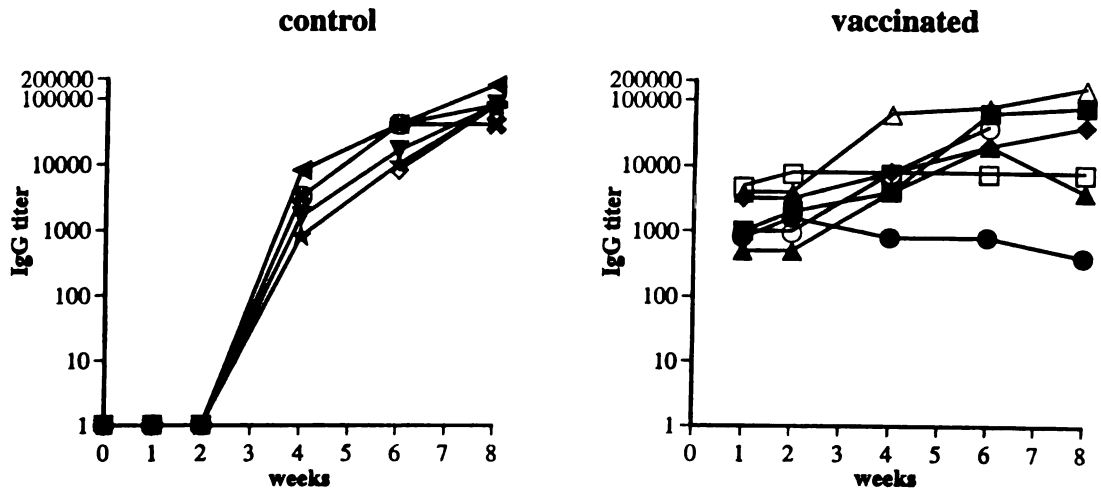
control
vaccinated
IgG titer
200000
100000
10000
1000
100
10
1
0 1 2 3 4 5 6 7 8
weeks

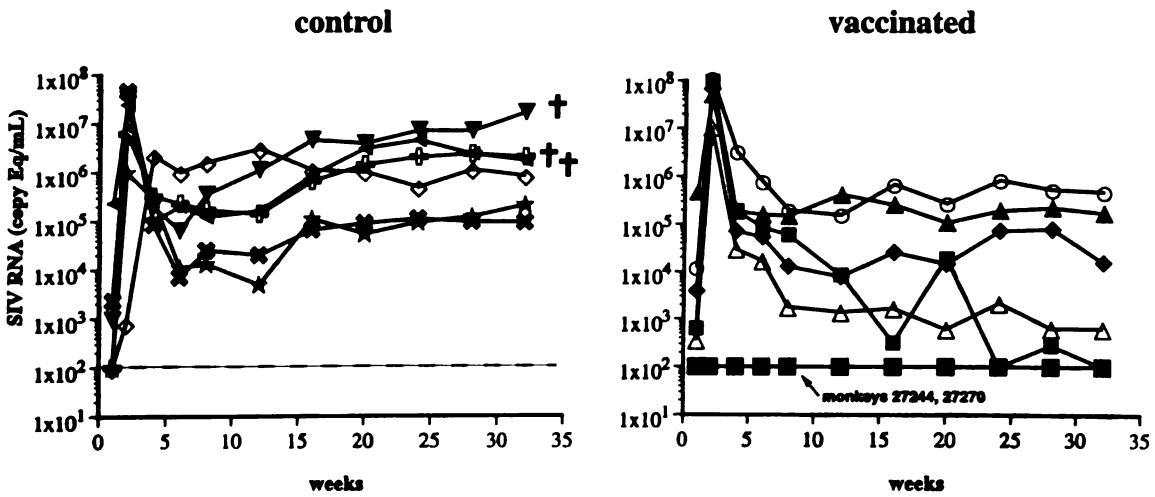
control
vaccinated
SIV RNA (copy Eq/mL)
1x10^8
1x10^7
1x10^6
1x10^5
1x10^4
1x10^3
1x10^2
1x10^1
0
5
10
15
20
25
30
35
weeks
†
†
†
monkeys 27244, 27270

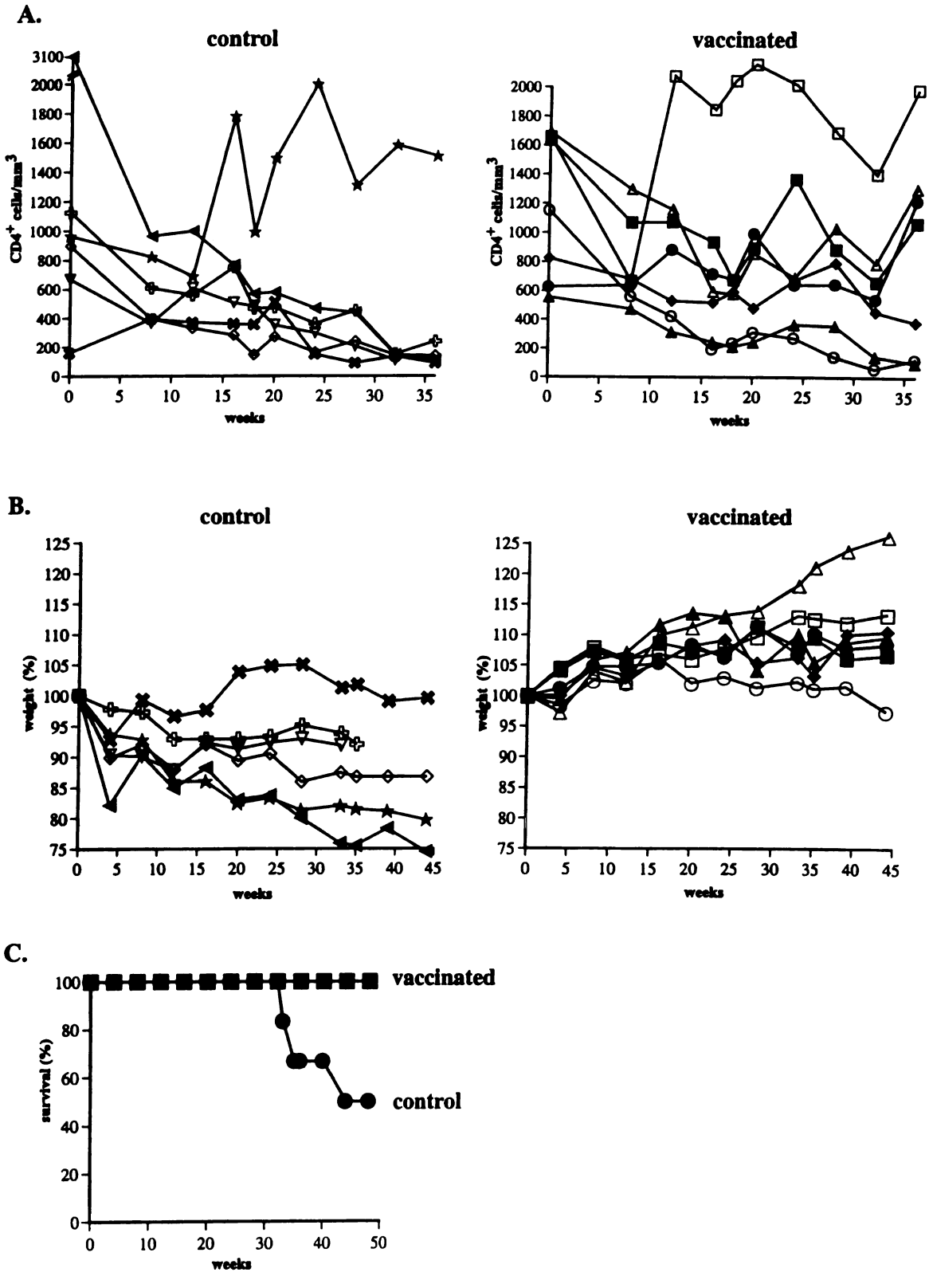
A.
control
vaccinated
CD4+ cells/mm3
weeks
B.
control
vaccinated
weight (%)
weeks
C.
vaccinated
control
survival (%)
weeks

Chapter 6

Discussion of section I: Poliovirus vector candidate AIDS vaccine

We find the results presented in Chapter 5 to be very encouraging. Our report of substantial protection of 4 out of 7 monkeys against a vaginal challenge with a virulent SIV virus is the first report of vaccine-mediated protection against a vaginal challenge with a virulent SIV. These important results validate the central premise of our approach. Furthermore, they place our recombinant poliovirus vaccine in the same league as a very small number of other approaches (such as MVA and alphavirus replicons) that elicit protective immunity against pathogenic uncloned strains of SIV. Given this data, there are two general poliovirus vector AIDS vaccine future directions being pursued: 1.) human trials, 2.) monkeys trials.

Human Trials

Raul is actively exploring the opportunities and resources available to conduct a human SabRV-HIV vaccine trial. There are many issues relevant to such a major undertaking, and I briefly review five of them below.

1.) Production of SabRV-HIV virus.

We propose two plausible strategies for the production of Sabin vectors for use in humans.

The first approach is to use our current vectors (SabRV1 and SabRV2) and a manufacturing strategy being considered for the production of replicons: high-throughput electroporation. Such a technique would effectively make P_0 stocks in a high-throughput manner. Then large quantities of P_1 stocks could be amplified from the P_0 stocks for use in humans. After vaccination, the viruses would eventually lose their inserts after multiple rounds of replication in the vaccinated individuals. However, that amount of replication *in vivo* before insert loss has proven to be sufficient to induce protective immunity in two different difficult challenge systems ((14) and dissertation chapter 5). Thus, after having served their purpose of stimulating a potent immune response against the desired target pathogen, insertless poliovirus could continue inducing anti-polio protective immunity until the infection is resolved.

The second approach to producing Sabin vectors for use in humans is to identify recombination-deficient (rec$^-$) polioviruses. It is believed that the inserted sequences in poliovirus are deleted by RNA recombination via a copy-choice mechanism (12) involving the RNA-dependent RNA polymerase (2, 6). It is not known whether mutations can effectively alter the capacity of poliovirus to recombine, but such mutations have been identified in the polymerase of another positive-strand RNA virus (7). Our hypothesis is that RNA recombination is a sophisticated process that the virus actively uses to improve its genetic fitness. As such, it is reasonable to propose that one can identify mutants defective for this complex biochemical process (rec$^-$ mutants). These

mutants, due to their deficiency at RNA recombination, will be genetically stable. Supporting this hypothesis is the observation that the recombination frequency of RNA virus species greatly varies. For example, for poliovirus, which has a high recombination frequency, up to 20% of progeny are products of recombination (4, 11). In the other side of the spectrum, it is very rare or impossible to find recombinants of flaviviruses like yellow fever virus and Kunjin virus (less than 0.01% recombination) (19). Identification of rec$^-$ polioviruses would greatly facilitate vector production.

2.) Safety of SabRV-HIV.

The oral poliovirus vaccine (OPV) is normally given as three doses of ~1 x 10^6 - 1 x 10^7 PFU (1), and that will probably be an appropriate dosage to use during SabRV-HIV human trials. The Sabin 1 poliovirus vaccine is one of the safest vaccines in existence, with significant side effects seen in fewer that 1 in 10 million individuals. It is notable that our recombinant polioviruses are even further attenuated than the vaccine strains in both mice and macaques. A recombinant poliovirus expressing a model antigen (GFP, the green fluorescent protein) is attenuated > 10^3 compared to the parental virus (S. Crotty, L. Hix, R. Andino unpublished data). Other researchers have observed substantial attenuation with a coxsackie recombinant picornavirus as well (9). If deemed necessary for political reasons, the wealth of molecular knowledge about poliovirus should allow us to create vector vaccine strains that are even safer still by, for example, changing the 5' UTR to prevent neurovirulence (> 10^5 attenuated) and that do not revert to wild-type (8, 10). Such strategies could be expedited by the recent approval of poliovirus receptor

(PVR) transgenic mice as WHO approved test animals for determining poliovirus vaccine attenuation (23).

3.) Communicability of SabRV-HIV.

The Sabin viruses used in OPV are communicable, and can provide "herd immunity" due to this communicability (21). This becomes an issue with SabRV-HIV because, though herd immunity has significant advantages during widespread use of a vaccine, it has disadvantages in a human trial. For example, in human trials a person who was not vaccinated with SabRV-HIV could potentially become infected with SabRV-HIV via close contact with a vaccinated family member. This 2° infected person could then seroconvert to HIV antigens in the SabRV-HIV and turn up false positive on an HIV test. Therefore, initial human trails most likely need to be performed on an inpatient basis, traking the shedding of SabRV-HIV in the vaccinated individuals until shedding ceases.

It is possible that, due to the deletion of inserts, no or inconsequential shedding of SabRV-HIV will be observed from inoculated individuals. Monkey studies will not be able to resolve this issue, because cynos do not replicate poliovirus in the gut to the high levels seen in humans. Therefore this shedding issue will need to be resolved in human trials.

4.) Immunogenicity of SabRV-HIV.

The monkey vaccination/challenge study reported in Chapter 5 was a proof of concept study. SabRV would probably be substantially more immunogenic and efficacious in humans, the natural host of poliovirus, as Sabin viruses are several orders

of magnitude more infectious in people (ID_{50} = 50 PFU) (16) than in cynomolgus macaques (ID_{100}= 10^6 PFU) (3), and could be expected to generate a significantly stronger immune response to SabRV expressed HIV antigens with fewer vaccine doses. OPV is normally given as three doses of ~1 x 10^6 - 1 x 10^7 PFU to obtain 100% seroconversion, and that will probably be an appropriate dosage to use during SabRV-HIV human trials.

5.) Pre-existing anti-polio immunity.

Several observers have expressed concern that the ongoing immunization of the global population with the poliovirus vaccine precludes the use of a poliovirus-based vaccine vector due to the presence of pre-existing anti-polio immunity. I disagree. Steffi Mandl has demonstrated that pre-existing immunity against poliovirus in mice does not block the efficacy of the polio-Ova tumor vaccine (13). Additionally, people immunized with OPV are protected from poliomyelitis for life, but they are only protected from poliovirus infection for a few years. The majority of OPV vaccinees can be re-infected with OPV several years later, leading to replication and shedding (20, 21). People immunized with the inactivated poliovirus vaccine (IPV) are protected from poliomyelitis, but they are not protected from poliovirus infection at any timepoint, and infection of IPV vaccinated individuals with OPV leads to virus replication and shedding (5, 17, 18). These observations indicate that the majority of the population should be infectable with SabRV-HIV.

Additionally, as mentioned above, Sabin viruses are several orders of magnitude more infectious in people than in cynomolgus macaques, and could be expected to

generate stronger immune responses to SabRV than monkeys do, even in the presence of pre-existing poliomyelitis immunity in humans.

Monkey Trials

There are multiple areas of poliovirus vaccine vector work worth extensive exploration in monkey trials.

1.) Use of purified vaccine virus.

We hope to facilitate the analysis of the immunological correlates of protection by using a purified poliovirus vector stock. The cocktail of recombinant viruses will be purified and concentrated by sucrose gradients. We observed strong, non-specific lymphoproliferative responses after vaccination with current unpurified SabRV1/2-SIV cocktails (Chapter 5). Due to this non-specific, high background we had difficulty assessing cellular immunity responses in the vaccinated animals. It has been observed in mice that viral preparations containing bovine serum could induce this type of non-specific proliferation. Since it is important to evaluate cellular responses to be able to analyze immunological correlates of protection, we will purify the viral stock before future inoculations in macaques.

2.) Assessment of vector replication in monkeys.

In the study reported in Chapter 5, we were quite interested in analyzing the replication of the viruses *in vivo*, and we therefore attempted to isolate virus from stool

samples taken from vaccinated animals at a series of timepoints post-vaccination. Virus was not detected in these samples. In retrospect, given that the virus was inoculated intranasally, and cynos appear to replicate the virus better in the nasopharyngeal region than in the gastrointestinal tract, it may have been more appropriate to isolate virus from nasal, mouth, or throat swabs. In our next round of primate experiments we expect to collect better data in this regard, as this is certainly an interesting issue.

Shedding of poliovirus in saliva and feces can be evaluated by plaque assay to determine the extent of viral replication in cynomolgus monkeys. Samples should probably be collected throughout the first 8 weeks post-inoculation. Viruses isolated from feces can be analyzed by RT-PCR and plaque assay immunodetection with anti-SIV antibodies (22). This would allow for the evaluation of the genetic stability of the recombinant virus *in vivo*, and may permit correlation between the *in vivo* viral replication of individual recombinants and their immunogenic capability. Because plaque assay hybridization can distinguish between different recombinant viruses (22), this assay also could determine the relative replication rates of different recombinants in the cocktail. That data could lead to changing the cocktail composition in an effort to normalize the replication of different cocktail component viruses.

3.) Simplification of the SabRV1 and SabR2 libraries.

Simplifying the Sabin libraries is an approach to to determine what cocktail components are responsible for the protective immunity observed. Our library is constituted of fragments that represent 90% of the SIV genome. One of the general hypotheses of the cocktail strategy is that, in an outbreed population, diverse antigens

derived from several SIV proteins are necessary to confer protection. However, it can be argued that not all the components of the library are necessary to induce protective immunity and that some may be actually detrimental for effective protection and thereby make the current approach unnecessarily complicated.

We have demonstrated that the two fully protected animals in our first challenge experiment presented high antibody titers directed against Env proteins. Therefore, one hypothesis is that anti-Env antibodies are responsible, at least in part, for protection. Separately, the two monkeys that exhibited strong control of SIV viremia post-challenge were probably protected by efficient anti-SIV CTL responses. Based on these hypotheses, we could divide the library into two new, smaller cocktails: one with Env, and one with Gag, Pol, Tat and Nef. This experiment is important because it may permit the identification of essential components of the vaccine and may allow formulation of simpler and more effective cocktails. Monkeys would be immunized with one of the two sub-cocktails, and then challenged with $SIV_{mac}239$. $SIV_{mac}239$ is a better challenge virus for this experiment, because it should allow for higher levels of protection than that observed against the uncloned $SIV_{mac}251$. Additionally, immunological data obtained after the vaccinations (but before the challenge) could be quite informative about the effects of giving smaller cocktails.

4.) Prime boost protocols.

Priming macaques first with a DNA vaccine, or boosting SabRV1/2-SIV vaccinated macaques with gp41/gp120 protein or a second vaccine vector may enhance the protective anti-SIV response. It would be interesting to determine if mucosal

immunity in vaccinated animals could be boosted by systemic inoculation using a different type of vaccine. A number of studies have demonstrated that the prime boost approach can elicit very strong and effective immunological responses. We propose to determine whether systemic inoculation with Yellow Fever Virus (YFV) vector carrying SIV antigens can effectively boost the SabRV-SIV elicited protective immunity. YFV vectors would be used because, in a parallel study, our laboratory has developed methods to genetically engineer virulence-attenuated yellow fever virus ((15) and A. Arbetman and L. Mathews, work in progress). Similarly to the poliovirus system, through these methods it is possible to create replication-competent recombinant yellow fever viruses (based on the extremely safe yellow fever vaccine strain virus, 17D) that carry and express genetic sequences derived from SIV and HIV. Important advantages of the live-attenuated yellow fever vaccine include its ability to induce long-lasting immunity and its safety, affordability, and documented efficacy in both developed and developing nations. We have already shown that immunity elicited by SabRV1 vectors is effectively boosted by SabRV2 vectors (Chapter 5). Thus, it is expected that a YFV vector boost will also enhance SIV immunity.

5.) New poliovirus vectors.

Additional insertion sites in the poliovirus genome are now being explored (M. Neagu and R. Andino). If one of those sites turns out to be significantly less prone to insert deletion, such a vector would warrant experiments in monkeys to assess its immunogenicity and replication.

Additional directions

Vaccine efforts using poliovirus vectors have now been expanded to other potential vaccine targets including cancer (13, 14), papilloma virus (W. Melchers and R. Andino, unpublished data), and respiratory syncytial virus (E. Simoes and R. Andino, unpublished data).

References

1. **AFHS** 1998. AFHS Drug Information. American Society of Hospital Pharmacists : SilverPlatter International, Bethesda, MD.
2. **Arnold, J. J., and C. E. Cameron** 1999. Poliovirus RNA-dependent RNA polymerase (3Dpol) is sufficient for template switching in vitro J Biol Chem. **274:**2706-16.
3. **Crotty, S., B. L. Lohman, F. X. Lu, S. Tang, C. J. Miller, and R. Andino** 1999. Mucosal immunization of cynomolgus macaques with two serotypes of live poliovirus vectors expressing simian immunodeficiency virus antigens: stimulation of humoral, mucosal, and cellular immunity J Virol. **73:**9485-95.
4. **Domingo, E., J. J. Holland, and P. Ahlquist** 1988. RNA genetics. CRC Press, Boca Raton, Fla.
5. **Faden, H., J. Modlin, M. L. Thoms, A. M. McBean, M. B. Ferdon, and P. L. Ogra** 1990. Comparative evaluation of immunization with live attenuated and enhanced-potency inactivated trivalent poliovirus vaccines in childhood: systemic and local immune responses The Journal of Infectious Diseases. **162:**1291-1297.
6. **Figlerowicz, M., P. D. Nagy, and J. J. Bujarski** 1997. A mutation in the putative RNA polymerase gene inhibits nonhomologous, but not homologous, genetic recombination in an RNA virus Proc Natl Acad Sci U S A. **94:**2073-8.
7. **Figlerowicz, M., P. D. Nagy, N. Tang, C. C. Kao, and J. J. Bujarski** 1998. Mutations in the N terminus of the brome mosaic virus polymerase affect genetic RNA-RNA recombination J Virol. **72:**9192-200.
8. **Gromeier, M., B. Bossert, M. Arita, A. Nomoto, and E. Wimmer** 1999. Dual stem loops within the poliovirus internal ribosomal entry site control neurovirulence Journal of Virology. **73:**958-64.
9. **Hofling, K., S. Tracy, N. Chapman, K. S. Kim, and J. Smith Leser** 2000. Expression of an antigenic adenovirus epitope in a group B coxsackievirus [In Process Citation] J Virol. **74:**4570-8.
10. **Iizuka, N., M. Kohara, K. Hagino-Yamagishi, S. Abe, T. Komatsu, K. Tago, M. Arita, and A. Nomoto** 1989. Construction of less neurovirulent polioviruses by introducing deletions into the 5' noncoding sequence of the genome Journal of Virology. **63:**5354-63.
11. **Jarvis, T. C., and K. Kirkegaard** 1991. The polymerase in its labyrinth: mechanisms and implications of RNA recombination Trends Genet. **7:**186-91.
12. **Kirkegaard, K., and D. Baltimore** 1986. The mechanism of RNA recombination in poliovirus Cell. **47:**433-43.
13. **Mandl, S., L. Hix, and R. Andino** 2001. Preexisting immunity to poliovirus does not impair the efficacy of recombinant poliovirus vaccine vectors [In Process Citation] J Virol. **75:**622-7.
14. **Mandl, S., L. J. Sigal, K. L. Rock, and R. Andino** 1998. Poliovirus vaccine vectors elicit antigen-specific cytotoxic T cells and protect mice against lethal

challenge with malignant melanoma cells expressing a model antigen Proceedings of the National Academy of Sciences of the United States of America. **95**:8216-21.

15. **McAllister, A., A. E. Arbetman, S. Mandl, C. Pena-Rossi, and R. Andino** 2000. Recombinant Yellow Fever Viruses Are Effective Therapeutic Vaccines for Treatment of Murine Experimental Solid Tumors and Pulmonary Metastases J Virol. **74**:9197-9205.
16. **Minor, P. D.** 1997. Poliovirus, p. 555-574. *In* N. Nathanson, and R. Ahmed (eds), Viral pathogenesis. Lippincott-Raven, Philadelphia.
17. **Onorato, I. M., J. F. Modlin, A. M. McBean, M. L. Thoms, G. A. Losonsky, and R. H. Bernier** 1991. Mucosal immunity induced by enhance-potency inactivated and oral polio vaccines J Infect Dis. **163**:1-6.
18. **Plotkin, S., A. Murdin, and E. Vidor** 1999. Inactivated polio vaccine, p. 1230. *In* S. Plotkin, and W. Orenstein (eds), Vaccines, 3rd ed. W. B. Saunders, Philadelphia.
19. **Rice, C. M.** 1996. Flaviviridae: The Viruses and their Replication, p. 2 v. (xxi, 2950). *In* B. N. Fields, D. M. Knipe, and P. M. Howley (eds), Fields virology, 3rd ed. Lippincott - Raven Press, New York.
20. **Smith, J. W., J. A. Lee, W. B. Fletcher, C. A. Morris, D. A. Parker, R. Yetts, D. I. Magrathe, and F. T. Perkins** 1976. The response to oral poliovaccine in persons aged 16-18 years Journal of Hygiene. **76**:235-47.
21. **Sutter, R. W., S. L. Cochi, and J. L. Melnick** 1999. Live attenuated poliovirus vaccines, p. 1230. *In* S. Plotkin, and W. Orenstein (eds), Vaccines, 3rd ed. W. B. Saunders, Philadelphia.
22. **Tang, S., R. van Rij, D. Silvera, and R. Andino** 1997. Toward a poliovirus-based simian immunodeficiency virus vaccine: correlation between genetic stability and immunogenicity Journal of Virology. **71**:7841-50.
23. **WHO** 1998. WHO Expert Committee on Biological Standardization. 46th Report World Health Organization Tech Rep Ser:1-90.

Section II

Ribavirin is an RNA virus mutagen

Chapter 7

Introduction to section II: Ribavirin is an RNA virus mutagen

Ribavirin (aka Virazole, or 1-ß-D-ribofuranosyl-1,2,4-triazole-3-carboxamide) was discovered in 1972 at ICN as a nucleoside analog that exhibited broad spectrum antiviral activity, primarily against RNA viruses (5). Since the 1980s, ribavirin has been used clinically to treat severe cases of respiratory syncytial virus (a negative strand RNA virus of the family paramyxoviridae) in infants (8). In the late 1980s ribavirin began to be used as the primary therapeutic intervention for lassa fever virus infections (3), a ambisense RNA virus of the family arenaviridae. In the late 1990s, ribavirin began to be used clinically in combination with interferon-alpha to treat chronic hepatitis C infections (2, 4). Hepatitis C virus (HCV), a positive-strand RNA virus of the pestivirus genus, is currently a significant public health problem, estimated to have chronically infected four million people. As chronic HCV infection can result in liver failure in a high percentage of individuals, a cure is highly desirable. Unfortunately, ribavirin plus interferon-alpha only cures ~30% of individual (2, 4).

Given the 30% HCV cure rate and the fact that ribavirin exhibits activity against very unrelated RNA viruses, pharmaceutical companies have been interested in developing better versions of ribavirin to try and cure 100% of HCV infections, and

possibly have activity against other RNA virus infections as well. The antiviral drug target of ribavirin has long been predicted to be the cellular enzyme inosine monophosphate dehydrogenase (IMPDH) (6). Ribavirin inhibits IMPDH with a K_i of 0.5 mM, which should lower the cytoplasmic nucleotide concentrations (6). This has been predicted to inhibit viral translation and replication. Schering-Plough spent upwards of $10 million developing new IMPDH inhibitors, and though some of those inhibitors block IMPDH activity 1000-fold better than ribavirin, the new drugs did not exhibit antiviral activity against BVDV (bovine viral diarheal virus), a model pestivirus (1). Additionally, data in the literature shows that ribavirin has only a modest effect on intracellular NTP concentrations (GTP concentrations drop to 65% normal levels), and that effect plateaus at ~10 μM ribavirin, while the antiviral effects of the drug continue to increase at higher doses (7).

So, perplexed, Schering-Plough was then fishing for the true drug target of ribavirin. Craig Cameron was consulting for Schering-Plough on HCV antiviral projects at the time, and he agreed to spend some time looking for ribavirin's drug target. That is where Chapter 8 begins.

Acknowledgements

The work in Chapter 8 was set up as a collaboration with Craig Cameron. The biochemistry experiments of Chapter 8 were done by David Maag and Jamie Arnold in the Cameron lab. Schering-Plough provided ribavirin for that work.

References

1. **Cameron, C. E.** 2000. *personal comm.*
2. **Davis, G. L., R. Esteban-Mur, V. Rustgi, J. Hoefs, S. C. Gordon, C. Trepo, M. L. Shiffman, S. Zeuzem, A. Craxi, M. H. Ling, and J. Albrecht** 1998. Interferon alfa-2b alone or in combination with ribavirin for the treatment of relapse of chronic hepatitis C. International Hepatitis Interventional Therapy Group [see comments] N Engl J Med. **339:**1493-9.
3. **McCormick, J. B., I. J. King, P. A. Webb, C. L. Scribner, R. B. Craven, K. M. Johnson, L. H. Elliott, and R. Belmont-Williams** 1986. Lassa fever. Effective therapy with ribavirin N Engl J Med. **314:**20-6.
4. **McHutchison, J. G., S. C. Gordon, E. R. Schiff, M. L. Shiffman, W. M. Lee, V. K. Rustgi, Z. D. Goodman, M. H. Ling, S. Cort, and J. K. Albrecht** 1998. Interferon alfa-2b alone or in combination with ribavirin as initial treatment for chronic hepatitis C. Hepatitis Interventional Therapy Group [see comments] N Engl J Med. **339:**1485-92.
5. **Sidwell, R. W., J. H. Huffman, G. P. Khare, L. B. Allen, J. T. Witkowski, and R. K. Robins** 1972. Broad-spectrum antiviral activity of Virazole: 1-beta-D-ribofuranosyl- 1,2,4-triazole-3-carboxamide Science. **177:**705-6.
6. **Streeter, D. G., J. T. Witkowski, G. P. Khare, R. W. Sidwell, R. J. Bauer, R. K. Robins, and L. N. Simon** 1973. Mechanism of action of 1-beta-D-ribofuranosyl-1,2,4-triazole-3-carboxamide (Virazole), a new broad-spectrum antiviral agent Proc Natl Acad Sci U S A. **70:**1174-8.
7. **Wray, S. K., B. E. Gilbert, M. W. Noall, and V. Knight** 1985. Mode of action of ribavirin: effect of nucleotide pool alterations on influenza virus ribonucleoprotein synthesis Antiviral Res. **5:**29-37.
8. **Wyde, P. R.** 1998. Respiratory syncytial virus (RSV) disease and prospects for its control Antiviral Research. **39:**63-79.

Chapter 8

The broad-spectrum antiviral ribonucleoside, ribavirin, is an RNA virus mutagen

Abstract

The ribonucleoside analog, ribavirin (1-ß-D-ribofuranosyl-1,2,4-triazole-3-carboxamide), exhibits antiviral activity against a variety of RNA viruses and is currently used in combination with interferon-a to treat hepatitis C virus infection. Here we show *in vitro* utilization of ribavirin triphosphate by a model viral RNA polymerase, poliovirus $3D^{pol}$. Ribavirin incorporation is mutagenic as it templates incorporation of cytidine and uridine with equal efficiency. Ribavirin reduces infectious poliovirus production by as much as 10^7-fold in cell culture. Importantly, the antiviral activity of ribavirin correlates directly with its mutagenic activity. Collectively these data suggest that ribavirin forces the virus into error catastrophe. We conclude that mutagenic ribonucleosides may represent an important class of anti-RNA virus agents.

Introduction

Ribavirin exhibits antiviral activity against a variety of RNA viruses (7, 31, 32) and is currently used in combination with interferon-a to treat hepatitis C virus infection (6, 24), and as monotherapy for lassa fever virus infection (23) and severe respiratory syncytial virus (RSV) infection (35). Since the discovery of the broad-spectrum antiviral activity of ribavirin in 1972 , it has been suggested that the active form of ribavirin is the monophosphate (RMP) (34). RMP inhibits inosine monophosphate dehydrogenase (IMPDH), causing a decrease in the intracellular concentration of GTP (32, 34). This decrease potentially diminishes viral protein synthesis and limits replication of viral genomes. However, inhibition of IMPDH may not be sufficient for antiviral activity (1, 13, 32, 33, 35). Other mechanisms of action have been proposed but not fully explored, including RMP inhibition of guanylyltransferase activity (16) and inhibition of viral transcription (5, 12).

Notably, ribavirin triphosphate (RTP) accumulates in cells after treatment with the nucleoside (25). Therefore, we explored the possibility that ribavirin's antiviral effect requires direct incorporation into viral RNA. Here we demonstrate utilization of RTP by the poliovirus polymerase ($3D^{pol}$) *in vitro* and potent mutagenesis of poliovirus by virtue of ribavirin incorporation *in vivo*.

Methods

Analysis of $3D^{pol}$ *in vitro*

$3D^{pol}$ was expressed and purified as described previously (15) and experiments employing sym/sub derivatives were performed as described previously (3). Briefly, $3D^{pol}$-sym/sub complexes were preassembled and then mixed with the appropriate nucleotide triphosphate to initiate the reaction. Reactions were quenched at various times by addition of EDTA. Product formation was monitored by phosphorimaging after denaturing polyacrylamide gel electrophoresis. In kinetics experiments, when the value for k_{pol} was greater than 1 s^{-1}, a rapid mixing/quenching device was employed. All RNA employed was synthetic and prepared by Dharmacon Research, Inc. (Boulder, Colorado). Ribavirin triphosphate was obtained from Moravek Biochemicals (Brea, California). Structural models (Fig. 2) were constructed by using WebLab Viewer.

Cells and viruses

HeLa S3 cells were propagated in OptiMEM (Life Technologies, Gaithersberg, Maryland) supplemented with 2% dialyzed fetal calf serum (DFCS) (Life Technologies). In most experiments, 5 x 10^5 cells were plated in each well of a 6-well dish 16-20 hours in advance. A final volume of 2 mL of the following was employed: OptiMEM supplemented with 0.2% DFCS and mutagen or drug (ribavirin and RIB4C (1-ß-D-ribofuranosyl-1,2,3-triazole-4-carboxamide) were provided by Schering-Plough; AZC, 5FU, and brefeldin A were purchased from Sigma). Under these conditions, 1 μM AZC was moderately toxic to cells, killing approximately 10% over a 4 day period. All viral infections were performed using a poliovirus stock grown from a plasmid-derived

Mahoney strain poliovirus (pXpA) (30). Mutagenesis experiments (Table 2) were performed using a viral inoculum of 100 pfu (± 3.5). Figure 3C (high MOI infections) used 1-2 x 10^7 pfu. Mutagenesis experiments employing 5FU (Table 2) were performed as described above except that mutagenized viral stocks were generated in cells grown in DMEM/F12 + 10% FCS and infected with an inoculum of 1 x 10^4 pfu. Replicon transfections and luciferase assays were performed using pRLucRA (aka, pRLuc rib+polyAlong) derived PolioLuc RNA as previously described (14), using HeLa cells grown as above. Translation experiment (Fig. 3B) was performed by using PolioLuc transfected cells in the presence of 2 μg/ml brefeldin A, which completely abolishes poliovirus replication (19, 22). Translation was assayed by luciferase assay at 2 hr post-transfection. PolioLuc replication assays (Fig. 3C, white bars) were done comparably, in the absence of BFA.

For direct quantitation of viral RNA, 5 x 10^6 cells were infected with 5 x 10^7 pfu poliovirus under growth and mutagen conditions described above. At 1, 6, 8, and 10 hrs post-infection, viral RNA was isolated using oligo dT_{25} DynaBeads (Oslo, Norway) and run on a non-denaturing 1.5% agarose gel in 1 x TAE in the presence of ethidium bromide. RNA from the timepoint of maximum viral replication was used in Fig. 3D (8 hrs for 0 and 100 μM ribavirin, and 10 hrs for 400 and 1000 μM ribavirin). Samples of virus from each timepoint were taken from cells prior to RNA isolation and quantified by plaque assay to determine the level of inhibition of infectious virus production.

Guanidine-resistance assay and genome sequencing

In our hands, 2 mM guanidine resistance is conferred by a single specific mutation: C to U at position 4605 of the poliovirus genome, in protein 2C (Pro to Ser at amino acid

161). The entire nonstructural genes of two independent gua^R mutants was sequenced to confirm that the C4605U mutation was the only change present. This mutation was additionally confirmed by sequencing the 2C gene of 20 independent gua^R virus isolates derived normally or in the presence of ribavirin or 5FU mutagen, all of which possessed the C4605U mutation. Gua^R virus was detected by plaque assay. HeLaS3 cells were plated 1 day in advance at 25% confluence in 10 cm dishes and were infected with 50 or 1 x 10^6 PFU of poliovirus (Fig. 3E) from the appropriate viral stock (previously grown in the presence or absence of ribavirin). Cells were covered with a 20 mL overlay of 1% agar and DMEM/F12 + 10% FCS supplemented with 2 mM L-glutamine, 100 U/mL penicillin, and 100 U/mL streptomycin (plus 2 mM guanidine hydrochloride (Sigma) in gua^R plaque assays). Plates were incubated at 37 °C for 72-80 hours and then developed using crystal violet staining. Other researchers, in two independent studies have identified several other specific gua^R mutations (4, 28), all of which occur in the same region of 2C (a.a. 142-248). The specific mutation selected for in those studies depended on the concentration of guanidine and the exact growth conditions used. Differences in the frequency of gua^R variants between our study and that of Holland et al. (18), in the presence of known RNA mutagens 5FU and AZC, likely depended on the fact that the two studies scored for different gua^R mutations (ours for a single C4605U, and theirs for different possible double point mutations) and used different growth conditions.

For sequence analysis, RNA was isolated using oligo dT_{25} DynaBeads from 1 x 10^6 cells (treated as described above) that had been infected at an MOI of 10 and then harvested at 10 hr post-infection. Random primed cDNA was synthesized from 1 μg RNA using Superscript II (Life Technologies), and VP1-coding sequence was PCR

amplified from $1/10^{th}$ of the cDNA using high fidelity PfuTurbo polymerase (Stratagene, California). An NheI-PstI fragment encompassing the VP1 gene was subcloned, and plasmid DNA prepared from independent bacterial colonies and was sequenced from position 2625-3400 of the poliovirus genome using BigDye terminator cycle sequencing and analyzed with DNASTAR. Virus capsid VP1 sequences were analyzed from 23 and 32 independent clones from "no ribavirin" and "1000 μM ribavirin" conditions, respectively. Results (Table 3) were analyzed for statistical significance using a two-tailed Student's *t*-test with unassumed variance.

Results

Ribavirin incorporation by the poliovirus RNA-dependent RNA polymerase ($3D^{pol}$)

Recently, we reported the development of a primer-extension assay for $3D^{pol}$ (3, 14). This assay employs a symmetrical primer/template substrate that we refer to as "sym/sub." Stable, elongation-competent complexes are formed after a brief incubation of $3D^{pol}$ with sym/sub. This system permits evaluation of the kinetics and thermodynamics of $3D^{pol}$-catalyzed nucleotide incorporation. By using this substrate we have shown that, in addition to correct ribonucleotides, $3D^{pol}$ utilizes incorrect ribonucleotides and deoxyribonucleotides (3).

The observation that $3D^{pol}$ utilizes a variety of nucleotides as substrates prompted us to determine whether ribavirin triphosphate (RTP) could act as a substrate for this enzyme. First we employed a sym/sub derivative containing cytidine as the first templating nucleotide (sym/sub-C, Fig. 1A). RTP was utilized by $3D^{pol}$ and incorporated into sym/sub-C (Fig. 1B). Prolonged reaction times permitted multiple cycles of ribavirin incorporation, suggesting that ribavirin incorporation did not terminate elongation of nascent RNA (+ 2 in Fig. 1B). We measured the observed rates of ribavirin monophosphate (RMP) incorporation at a variety of RTP concentrations (Fig. 1C) and used this information to determine the apparent dissociation constant (K_d) for RTP and the maximal rate of RMP incorporation (k_{pol}) (Fig. 1D). The K_d value was 430 μM and the k_{pol} value was 0.019 s^{-1} (Table 1). Consistent with this observation, RTP competitively inhibited correct nucleotide incorporation with a K_i value in the 400 μM

range (data not shown). In order to prove that ribavirin was not a chain terminator, we performed an experiment using the sym/sub-U derivative (see Table 1). In the presence of RTP, $3D^{pol}$ extended this substrate to produce 11-mer (Fig. 1E). When both RTP and UTP were present, $3D^{pol}$ extended this substrate to 12-mer without accumulation of 11-mer (Fig. 1E). The appearance of 13-mer in this experiment was a reflection of misincorporation.

Modeling studies showed that the pseudo base (1,2,4-triazole-3-carboxamide) of ribavirin was capable of basepairing equivalently with cytidine and uridine as long as rotation of the carboxamide moiety was not restricted (Fig. 2A-B). In order to test this prediction experimentally, we employed sym/sub-U instead of sym/sub-C. The efficiency of RMP incorporation opposite uridine was identical to that opposite cytidine (Table 1). While the efficiency of RMP incorporation was low relative to incorporation of correct nucleotides (e.g. GMP incorporation into sym/sub-C, Table 1), incorporation of RMP was equivalent to misincorporation of GMP (e.g. GMP incorporation into sym/sub-U, Table 1).

In order to determine the effect of incorporated ribavirin on subsequent rounds of RNA synthesis, we evaluated the kinetics of CMP and UMP incorporation into sym/sub-R, a template containing ribavirin (Table 1). CMP and UMP were incorporated equivalently opposite ribavirin (Table 1). Interestingly, CMP and UMP incorporation opposite ribavirin is, on average, 500-fold faster than incorporation of RMP opposite cytidine and uridine. The slow observed rate of RMP incorporation likely reflects isomerization of the pseudo base from the syn to the anti conformation (Fig. 2C). Once ribavirin is in the RNA, it is presumably trapped in the anti conformation and readily base

pairs with incoming pyrimidines. Taken together, these data demonstrate that RTP is a substrate for $3D^{pol}$ and predict that incorporation of ribavirin into RNA should be mutagenic to viral RNA, promoting A→G and G→A transitions.

Antiviral activity of ribavirin against poliovirus

We next established that ribavirin possesses antiviral activity against poliovirus. Pharmacokinetic studies have shown that ribavirin collects in the liver of patients treated with ribavirin for chronic hepatitis C virus infection, and the ribavirin reaches steady-state levels of approximately 250 μM in hepatocytes (unpublished data). Therefore, we tested ribavirin's antiviral activity against poliovirus by treating cells with concentrations of ribavirin in the 100-1000 μM range. Cells treated with 100 μM ribavirin and then infected with poliovirus at a low multiplicity of infection (MOI) showed a 2-fold reduction in virus production; treatment with 1000 μM ribavirin caused a striking 10^7-fold reduction in virus production (Table 2).

Ribavirin does not significantly inhibit translation or replication

We used a poliovirus replicon (PolioLuc), in which the capsid-coding sequence was replaced by a luciferase gene (17) (Fig. 3A), to evaluate the effects of ribavirin on poliovirus translation and RNA synthesis in cell culture. Transfection of HeLa cells with replicon RNA results in the production of a polyprotein containing luciferase that is processed by the viral 2A protease to liberate active luciferase, and the replicon translates and replicates comparably to wildtype poliovirus (2). First, an experiment was performed in the presence of 2 μg/ml brefeldin A (BFA), a drug which completely blocks poliovirus replication but not translation (22). In BFA treated cells, PolioLuc translation was not significantly inhibited by ribavirin (2-fold at 100, 400, or 1000 μM) (Fig. 3B).

Ribavirin only moderately reduced RNA replication in PolioLuc transfected cells (Fig. 3C, white bars, no BFA). 1000 μM ribavirin inhibited replication by 12-fold at 4 hrs after transfection (data not shown), with a recovery to 2.4-fold lower than wt levels by 6 hrs after transfection (Fig. 3C, white bars). In parallel with the replicon transfections, cells were infected with a high MOI of virus (10 plaque forming units per cell). While only modestly inhibiting replicon RNA replication, ribavirin reduced viable virus production in a single round of infection by up to 1,200-fold (Fig. 3C, black bars).

In order to confirm that ribavirin inhibited virus production without significantly affecting RNA synthesis, we determined the levels of poliovirus RNA accumulated in ribavirin-treated, poliovirus-infected cells. Consistent with the data obtained by using PolioLuc, peak viral replication in ribavirin-treated cells reached wildtype or near wildtype levels, while production of infectious virus from the cells was reduced by up to 1,200-fold (Fig. 3D). These results are consistent with our hypothesis that ribavirin incorporation induces mutations in the viral genomes during multiple rounds of RNA replication in the cell, resulting in a substantial increase in the production of defective genomes.

Ribavirin is a RNA virus mutagen

We measured the mutagenic potential of ribavirin on poliovirus by using a guanidine-resistance assay. Poliovirus multiplication is inhibited by the presence of 2 mM guanidine in the culture medium (Fig. 3E). Guanidine inhibits the $2C^{ATPase}$ protein(27); however, mutations in the 2C-coding sequence that confer resistance to guanidine have been identified (gua^R) (4, 28). In our hands, a specific single nucleotide mutation (C4605U) results in the guanidine resistant phenotype (gua^R), and this variant

exists in the natural population of poliovirus at a frequency of $\sim 10^{-5}$. The presence of this variant can be quantified by plaque assay in the presence of 2 mM guanidine (Fig. 3E). This assay provides a rapid method to evaluate the effect of different growth conditions on mutation frequencies, using gua^R as a genetic marker. The C→U mutation necessary for gua^R is consistent with incorporation of RTP as a GTP analog during negative strand genome synthesis. A dose-dependent increase in the frequency of gua^R virus was observed in poliovirus stocks grown in the presence of ribavirin (Fig. 3E and Table 2), thus confirming the mutagenic activity of ribavirin *in vivo*. Moreover, a direct correlation existed between the mutagenic activity of ribavirin and the antiviral activity of the compound (Table 2).

Control experiments were performed to demonstrate that known mutagens, such as 5-azacytidine (26, 29) and 5-fluorouracil (18, 20, 29) demonstrated dose-dependent antiviral activity at levels of mutagenesis comparable to that of ribavirin (AZC and 5FU in Table 2). Furthermore, an inosine monophosphate dehydrogenase (IMPDH) inhibitor that lacks antiviral activity (33) was not mutagenic (RIB4C in Table 2). Finally, a compound that inhibits poliovirus multiplication by a mechanism independent of both IMPDH and $3D^{pol}$ also lacked mutagenic activity (BFA in Table 2) (19, 22).

In order to evaluate the spectrum of mutations induced by ribavirin, we analyzed sequences derived from independently cloned cDNAs of poliovirus capsid VP1, from virus grown in the presence or absence of 1000 μM ribavirin. Ribavirin mutagenized genomes contained a striking 7-fold increase in G→A and C→U transition mutations (Table 3), confirming the G→A mutagenic activity predicted by our *in vitro* ribavirin experiments. The C→U mutations seen are consistent with G→A transitions induced by

incorporation of RTP as a GTP analog during negative-strand RNA synthesis. The increased frequency of G→A, C→U, and total mutations were all highly significant ($P < 0.0004$, $P < 0.0001$, and $P < 2 \times 10^{-7}$ respectively).

Discussion

RNA viruses live as quasispecies, creating extraordinary genetic diversity through mutation. Holland and Domingo have proposed that, due to this high mutation rate, RNA viruses exist on the threshold of "error catastrophe" (10, 11), and a moderate increase in mutation rate can kill a RNA virus population by causing a "genetic meltdown" (9, 18, 20). An extrapolation of our sequencing data would suggest that, on average, each poliovirus genome (7441 nt long) synthesized after multiple rounds of replication inside an infected cell normally contains ~2 point mutations. In the presence of 1000 μM ribavirin, each poliovirus genome synthesized contains ~15 points mutations. Thus, in our model RNA virus system, a surprisingly small increase (3- to 7-fold) in mutation rate produced a substantial antiviral effect (Table 2 and Table 3). Interestingly, prolonged growth of human immunodeficiency virus (HIV) in the presence of mutagenic deoxyribonucleoside analogs has been shown to inhibit HIV multiplication (21).

We conclude that the antiviral activity of ribavirin against poliovirus requires formation of RTP, that this nucleotide is utilized by the viral RNA polymerase, and that the incorporated ribavirin is mutagenic. The ability of ribavirin monophosphate to inhibit IMPDH and thereby decrease cellular GTP pools likely serves to potentiate the mutagenic/antiviral effect by decreasing the concentration of "competitor" nucleotide and thereby increasing the frequency of ribavirin incorporation. This unified model for the mechanism of action of ribavirin predicts that mutagenic ribonucleosides that can be incorporated by viral RNA-dependent RNA polymerases may represent an important class of antiviral agents for treatment of RNA virus infections.

References

1. 2000. AFHS Drug Information. American Society of Hospital Pharmacists : SilverPlatter International, Bethesda, MD.
2. **Andino, R., G. E. Rieckhof, P. L. Achacoso, and D. Baltimore** 1993. Poliovirus RNA synthesis utilizes an RNP complex formed around the 5'-end of viral RNA Embo Journal. **12:**3587-98.
3. **Arnold, J. J., and C. E. Cameron** 2000. Poliovirus RNA-dependent RNA polymerase (3D(pol)). Assembly of stable, elongation-competent complexes by using a symmetrical primer-template substrate (sym/sub) J Biol Chem. **275:**5329-36.
4. **Baltera, R. F., Jr., and D. R. Tershak** 1989. Guanidine-resistant mutants of poliovirus have distinct mutations in peptide 2C J Virol. **63:**4441-4.
5. **Cassidy, L. F., and J. L. Patterson** 1989. Mechanism of La Crosse virus inhibition by ribavirin Antimicrob Agents Chemother. **33:**2009-11.
6. **Davis, G. L., R. Esteban-Mur, V. Rustgi, J. Hoefs, S. C. Gordon, C. Trepo, M. L. Shiffman, S. Zeuzem, A. Craxi, M. H. Ling, and J. Albrecht** 1998. Interferon alfa-2b alone or in combination with ribavirin for the treatment of relapse of chronic hepatitis C. International Hepatitis Interventional Therapy Group N Engl J Med. **339:**1493-9.
7. **De Clercq, E.** 1993. Antiviral agents: characteristic activity spectrum depending on the molecular target with which they interact Adv Virus Res. **42:**1-55.
8. **Dea, P., M. P. Schweizer, and G. P. Kreishman** 1974. Nuclear magnetic resonance studies of the solution properties of the antiviral nucleoside, 1-beta-D-ribofuranosyl-1,2,4-triazole-3- carboxamide, the coresponding 5'-phosphate, and related triazole nucleosides Biochemistry. **13:**1862-7.
9. **Domingo, E.** 2000. Viruses at the Edge of Adaptation Virology. **270:**251-253.
10. **Domingo, E., and J. J. Holland** 1994. Mutation rates and rapid evolution of RNA viruses, p. xi, 353. *In* S. S. Morse (ed.), The Evolutionary biology of viruses. Raven Press, New York.
11. **Domingo, E., and J. J. Holland** 1997. RNA virus mutations and fitness for survival Annual Review of Microbiology. **51:**151-78.
12. **Eriksson, B., E. Helgstrand, N. G. Johansson, A. Larsson, A. Misiorny, J. O. Noren, L. Philipson, K. Stenberg, G. Stening, S. Stridh, and B. Oberg** 1977. Inhibition of influenza virus ribonucleic acid polymerase by ribavirin triphosphate Antimicrob Agents Chemother. **11:**946-51.
13. **Gilbert, B. E., and V. Knight** 1986. Biochemistry and clinical applications of ribavirin Antimicrob Agents Chemother. **30:**201-5.
14. **Gohara, D. W., S. Crotty, J. J. Arnold, J. D. Yoder, R. Andino, and C. E. Cameron** 2000. Poliovirus RNA-dependent RNA Polymerase ($3D^{pol}$): Structural, biochemical, and biological analysis of conserved structural motifs A and B Journal of Biological Chemistry. **275:**25523-25532.
15. **Gohara, D. W., C. S. Ha, S. Kumar, B. Ghosh, J. J. Arnold, T. J. Wisniewski, and C. E. Cameron** 1999. Production of "authentic" poliovirus RNA-dependent

RNA polymerase (3D(pol)) by ubiquitin-protease-mediated cleavage in Escherichia coli Protein Expression and Purification. **17:**128-38.

16. **Goswami, B. B., E. Borek, O. K. Sharma, J. Fujitaki, and R. A. Smith** 1979. The broad spectrum antiviral agent ribavirin inhibits capping of mRNA Biochem Biophys Res Commun. **89:**830-6.
17. **Herold, J., and R. Andino** 2000. Poliovirus requires a precise 5' end for efficient positive-strand RNA synthesis J Virol. **74:**6394-400.
18. **Holland, J. J., E. Domingo, J. C. de la Torre, and D. A. Steinhauer** 1990. Mutation frequencies at defined single codon sites in vesicular stomatitis virus and poliovirus can be increased only slightly by chemical mutagenesis Journal of Virology. **64:**3960-2.
19. **Irurzun, A., L. Perez, and L. Carrasco** 1992. Involvement of membrane traffic in the replication of poliovirus genomes: effects of brefeldin A Virology. **191:**166-75.
20. **Lee, C. H., D. L. Gilbertson, I. S. Novella, R. Huerta, E. Domingo, and J. J. Holland** 1997. Negative effects of chemical mutagenesis on the adaptive behavior of vesicular stomatitis virus Journal of Virology. **71:**3636-40.
21. **Loeb, L. A., J. M. Essigmann, F. Kazazi, J. Zhang, K. D. Rose, and J. I. Mullins** 1999. Lethal mutagenesis of HIV with mutagenic nucleoside analogs Proc Natl Acad Sci U S A. **96:**1492-7.
22. **Maynell, L. A., K. Kirkegaard, and M. W. Klymkowsky** 1992. Inhibition of poliovirus RNA synthesis by brefeldin A J Virol. **66:**1985-94.
23. **McCormick, J. B., I. J. King, P. A. Webb, C. L. Scribner, R. B. Craven, K. M. Johnson, L. H. Elliott, and R. Belmont-Williams** 1986. Lassa fever. Effective therapy with ribavirin N Engl J Med. **314:**20-6.
24. **McHutchison, J. G., S. C. Gordon, E. R. Schiff, M. L. Shiffman, W. M. Lee, V. K. Rustgi, Z. D. Goodman, M. H. Ling, S. Cort, and J. K. Albrecht** 1998. Interferon alfa-2b alone or in combination with ribavirin as initial treatment for chronic hepatitis C. Hepatitis Interventional Therapy Group N Engl J Med. **339:**1485-92.
25. **Miller, J. P., L. J. Kigwana, D. G. Streeter, R. K. Robins, L. N. Simon, and J. Roboz** 1977. The relationship between the metabolism of ribavirin and its proposed mechanism of action Ann N Y Acad Sci. **284:**211-29.
26. **Pathak, V. K., and H. M. Temin** 1992. 5-Azacytidine and RNA secondary structure increase the retrovirus mutation rate J Virol. **66:**3093-100.
27. **Pfister, T., and E. Wimmer** 1999. Characterization of the nucleoside triphosphatase activity of poliovirus protein 2C reveals a mechanism by which guanidine inhibits poliovirus replication J Biol Chem. **274:**6992-7001.
28. **Pincus, S. E., D. C. Diamond, E. A. Emini, and E. Wimmer** 1986. Guanidine-selected mutants of poliovirus: mapping of point mutations to polypeptide 2C Journal of Virology. **57:**638-46.
29. **Pringle, C. R.** 1970. Genetic characteristics of conditional lethal mutants of vesicular stomatitis virus induced by 5-fluorouracil, 5-azacytidine, and ethyl methane sulfonate J Virol. **5:**559-67.
30. **Racaniello, V. R., and D. Baltimore** 1981. Cloned poliovirus complementary DNA is infectious in mammalian cells Science. **214:**916-9.

31. **Sidwell, R. W., J. H. Huffman, G. P. Khare, L. B. Allen, J. T. Witkowski, and R. K. Robins** 1972. Broad-spectrum antiviral activity of Virazole: 1-beta-D-ribofuranosyl- 1,2,4-triazole-3-carboxamide Science. **177:**705-6.

32. **Smith, R. A., and W. Kirkpatrick** 1980. Ribavirin, a broad spectrum antiviral agent. Academic Press, New York.

33. **Smith, R. A., V. Knight, and J. A. D. Smith** 1984. Clinical applications of ribavirin. Academic Press, Orlando.

34. **Streeter, D. G., J. T. Witkowski, G. P. Khare, R. W. Sidwell, R. J. Bauer, R. K. Robins, and L. N. Simon** 1973. Mechanism of action of 1-beta-D-ribofuranosyl-1,2,4-triazole-3-carboxamide (Virazole), a new broad-spectrum antiviral agent Proc Natl Acad Sci U S A. **70:**1174-8.

35. **Wyde, P. R.** 1998. Respiratory syncytial virus (RSV) disease and prospects for its control Antiviral Research. **39:**63-79.

Table 1 The pseudo base of ribavirin pairs equally with cytosine and uracil

Substrates		Kinetic Parameters	
Nucleic Acid	Nucleotide	K_d μM	k_{pol} s^{-1}
sym/sub-C			
GAUCGGGCCC CCCGGGCUAG	RTP	430 ± 79	0.019 ± 0.002
	GTP	3.8 ± 0.7	56.7 ± 2.8
sym/sub-U			
GCAUGGGCCC CCCGGGUACG	RTP	496 ± 21	0.014 ± 0.001
	GTP	310 ± 30	0.013 ± 0.001
sym/sub-G			
CAUGCCCGGG GGGCCCGUAC	CTP	19.2 ± 3.2	157 ± 8
sym/sub-R			
CAURCCCGGG GGGCCCRUAC	CTP	493 ± 41	8.5 ± 0.3
	UTP	551 ± 127	7.6 ± 0.6

Table 2 Ribavirin is a mutagen of poliovirus, and the mutagenesis correlates directly with its antiviral activity

Mutagen	Viral titer produced[a] (pfu/ml)	Gua^R frequency[b] (gua^R/ 1×10^6 pfu)	**fold increase in Gua^R mutation frequency**
no mutagen	2×10^9	30	**1.0**
100 μM ribavirin	9×10^8	174	**5.8**
200 μM ribavirin	2×10^8	437	**14.6**
400 μM ribavirin	5×10^6	1243	**41.4**
1000 μM ribavirin	60	—[c]	—[c]
1 μM AZC[d]	1×10^9	63	**2.1**
400 μM RIB4C[d]	2×10^9	36	**1.2**
0.1 μg/ml BFA[d]	5×10^7	23	**0.8**
75 μM 5FU[d]	5×10^8	65	**2.5**
1900 μM 5FU	2×10^7	588	**22.7**
7500 μM 5FU	$< 1 \times 10^5$	—[c]	—[c]

[a] Viral titer after 4 days when 100% cytopathic effect (CPE) is apparent in all conditions shown except for 400 μM ribavirin (titered after 100% CPE at 6 days), and 1000 μM ribavirin (which showed no CPE after 7 days). Input virus was 100 pfu.

[b] Gua^R frequencies are the average of at least 3 experiments. Standard deviations are 10-20%.

[c] Mutation frequency could not be determined because viral titer was so severely reduced.

[d] AZC = 5-azacytidine, 5FU = 5-fluorouracil, RIB4C = 1-ß-D-ribofuranosyl-1,2,3-triazole-4-carboxamide, BFA = brefeldin A

Table 3 Sequence analysis of ribavirin treated poliovirus genomes

	G→A mutations /10^4 nts	C→U mutations /10^4 nts	**Total mutations / 10^4 nts[a]**
no ribavirin	0.6	1.7	**2.8**
1000 μM ribavirin	6.5*	11.8*	**20.3†**

[a] Total mutations is greater than the sum of the two columns, as a few other transition (U→C, A→G) and transversion (G→U, G→C, U→A) mutations were also detected.

* $P < 0.0004$ and, † $P < 2 \times 10^{-7}$ compared with no ribavirin (two-tailed, unpaired Student's *t*-test). A total of 42,335 nt was sequenced.

Figure Legends

Figure 1 Ribavirin triphosphate (RTP) utilization by poliovirus polymerase, $3D^{pol}$, *in vitro*.

(A) Primer/template (sym/sub-C) employed in the experiments shown in panels B, D and E.

(B) Denaturing polyacrylamide gel electrophoresis of the ^{32}P-labelled products from a timecourse of poliovirus polymerase catalyzed ribavirin incorporation into sym/sub-C.

(C) Kinetics of ribavirin incorporation at the following concentrations of RTP: 50 (●), 100 (○), 200 (■), 300 (□), 400 (▲), 600 (▼), 800 (Δ) and 1000 μM (×). The solid lines represent the fit of the data to a single exponential.

(D) RTP concentration dependence of the observed rate of ribavirin monophosphate (RMP) incorporation. The solid line represents a fit of the data to a hyperbola with a K_d value of 430 ± 79 μM and a k_{pol} value of 0.019 ± 0.002 s^{-1}.

(E) $3D^{pol}$-sym/sub-U complexes were preassembled and then mixed with either 1 mM RTP or 1 mM RTP and 10 μM UTP. All +1 product is chased to +2 and +3 in the presence of UTP.

Figure 2 Molecular modelling of ribavirin.

(A) RTP with the pseudo base in the anti conformation (left) basepairs with cytidine (right) in the template. Hydrogen bond distances are indicated in Ångstrøms.

(B) RTP also hydrogen bonds with uridine in the template after rotation of the carboxamide moiety.

(C) RTP with the pseudo base in the syn conformation is not within hydrogen bonding distance to the template base. The pseudo base of ribavirin nucleoside is known to exist primarily in the syn conformation, as determined by x-ray crystallography (8) and solution NMR analysis of RTP (data not shown). Atoms are colored as follows: N, blue; O, red; C, grey; P, orange.

Figure 3 Analysis of poliovirus translation and replication in the presence of ribavirin.

(A) Poliovirus replicon (PolioLuc) RNA has the capsid-coding sequence replaced by the luciferase gene.

(B) PolioLuc translation in the presence of ribavirin. Translation experiment was performed in the presence of 2 μg/ml brefeldin A, permitting direct analysis of the translation of the input replicon RNA (RLU, relative light units). (neg) indicates untransfected cells. Standard deviations are indicated.

(C) White bars show the RNA replication of PolioLuc in the presence of ribavirin (RLU, relative light units). In concomitant poliovirus infections (black bars) in the presence of ribavirin, a substantial reduction in the production of infectious virus is observed (PFU, plaque forming units).

(D) Direct determination of poliovirus RNA replication in the presence of ribavirin. PolyA$^+$ RNA was isolated from infected cells treated with ribavirin (100, 400, or 1000 μM) or untreated cells (0 μM) at the timepoint of maximal virus replication and analyzed on a non-denaturing agarose gel. RNA from uninfected cells (neg) was also analyzed.

Poliovirus RNA indicated is the ssRNA genomic form. RNA in each lane was loaded from a comparable number of cells, and 18S rRNA is shown as an internal loading control. Inhibition of infectious virus production (Titer reduction) in the ribavirin treated cells was also measured, and is indicated below each lane.

(E) Ribavirin is a mutagen to poliovirus. Virus stocks grown in the presence of increasing concentrations of ribavirin (0, 100, 200 μM) were plaque assayed for the presence of the gua^R genetic marker.

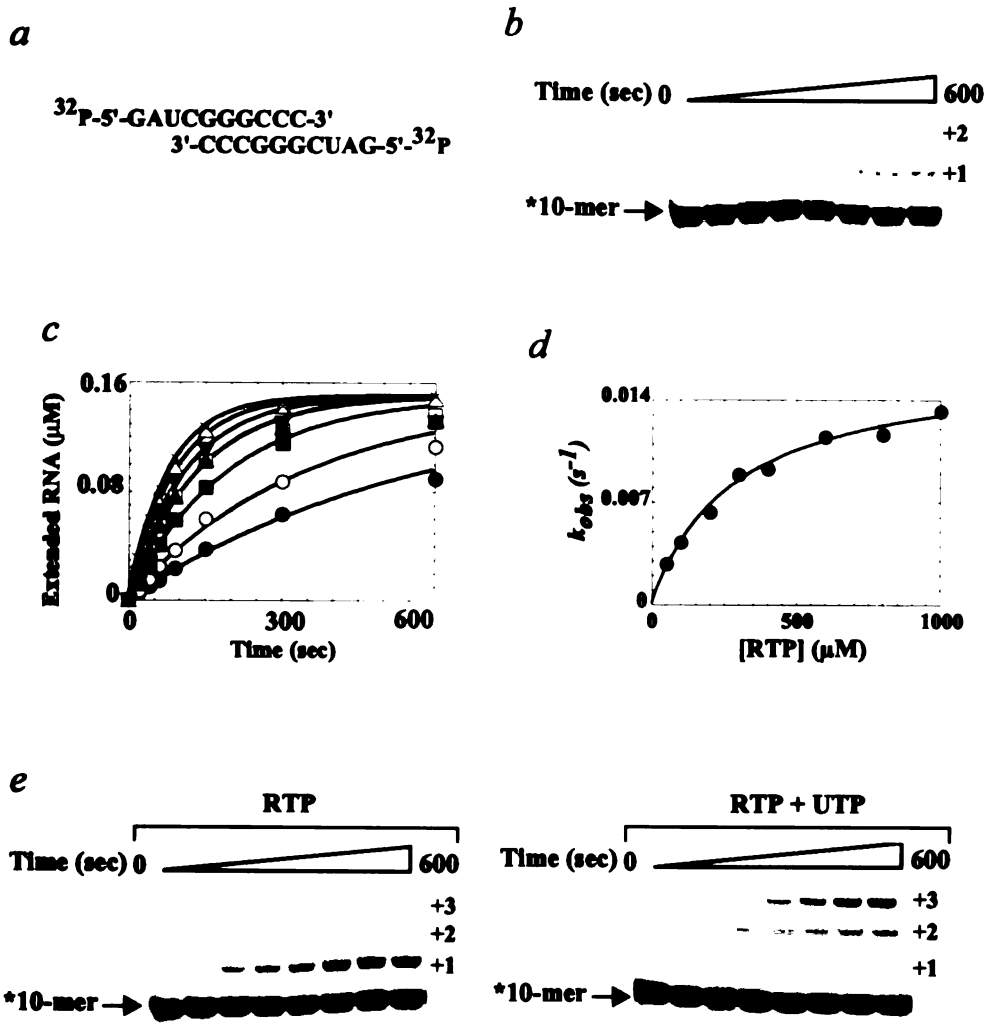
a
32P-5'-GAUCGGGCCC-3'
3'-CCCGGGCUAG-5'-32P
b
Time (sec) 0
600
+2
+1
*10-mer
c
Extended RNA (μM)
0.16
0.08
0
0
300
600
Time (sec)
d
kobs (s-1)
0.014
0.007
0
0
500
1000
[RTP] (μM)
e
RTP
Time (sec) 0
600
+3
+2
+1
*10-mer
RTP + UTP
Time (sec) 0
600
+3
+2
+1
*10-mer

Figure 2

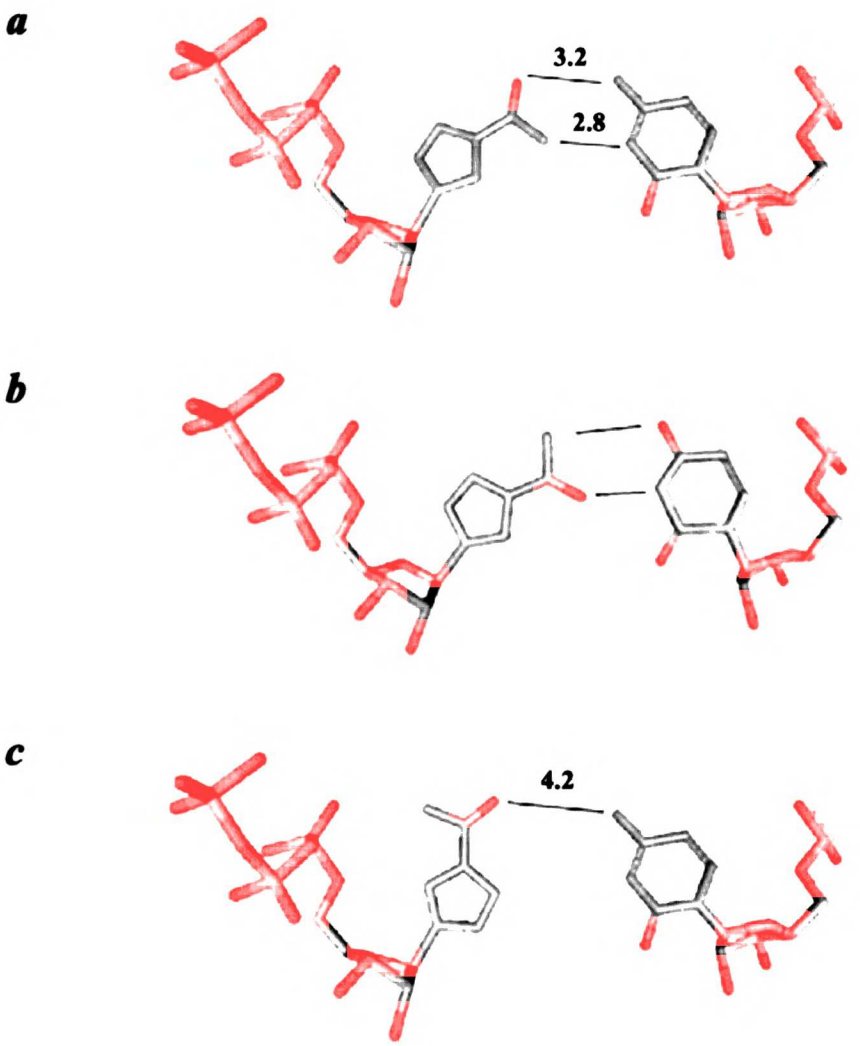

a

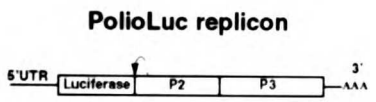
PolioLuc replicon
5'UTR
Luciferase
P2
P3
3'
AAA

b

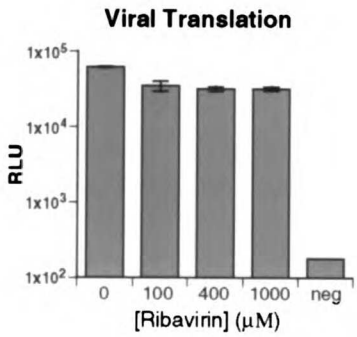
Viral Translation
RLU
1x10^5
1x10^4
1x10^3
1x10^2
0
100
400
1000
neg
[Ribavirin] (μM)

c

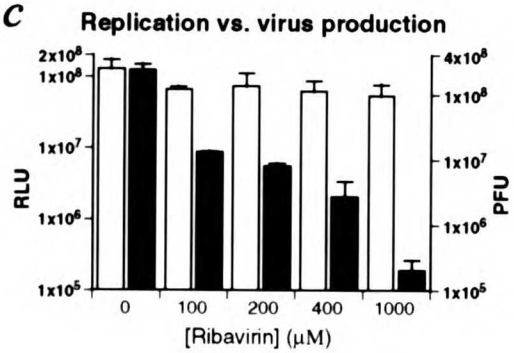
Replication vs. virus production
RLU
PFU
2x10^8
1x10^8
1x10^7
1x10^6
1x10^5
4x10^8
1x10^8
1x10^7
1x10^6
1x10^5
0
100
200
400
1000
[Ribavirin] (μM)

d

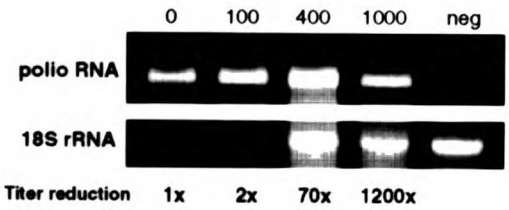
0
100
400
1000
neg
polio RNA
18S rRNA
Titer reduction
1x
2x
70x
1200x

e

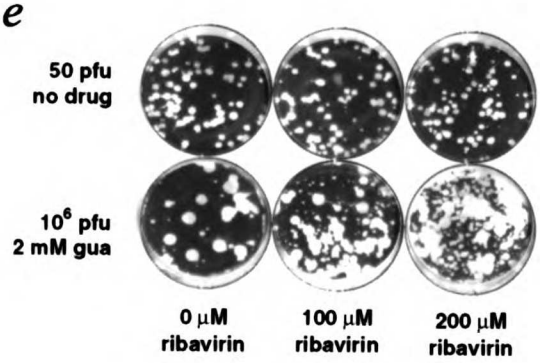
50 pfu
no drug
10^6 pfu
2 mM gua
0 μM
ribavirin
100 μM
ribavirin
200 μM
ribavirin

Supplementary Data

The complete replicon data set (abridged to produce Fig. 3C) is shown as Figure 4 on page 219. The figure legend is shown below.

(A) Ribavirin has a modest effect on RNA replication. Poliovirus replicon RLuc was transfected into HeLa cells, and poliovirus replication was assessed at various timepoints by measuring luciferase activity (RLU) in transfected cell lysates. Wildtype poliovirus replication (RLuc) is indicated by (■); and translation alone (RLuc plus 2 ug/ml brefeldin A) is indicated by (●). RNA replication in the presence of 100uM (Δ), 200uM (◇), 400uM (□), and 1000uM ribavirin (green ●) is shown.

(B) Ribavirin's inhibition of infectious virus production under one step growth kinetics (moi=5). Wildtype poliovirus growth is indicated by (■); completely inhibited growth (infection in the presence of 2 ug/ml brefeldin A) is indicated by (●). Virus production in the presence of 100uM (Δ), 200uM (◇), 400uM (□), and 1000uM ribavirin (green ●) is shown.

Erratum

Table 3 was misprinted by *Nature Medicine*. The number 10^4 was misprinted as 104, and the asterixes indicating statistical significance were misplaced. Their mistake is corrected in an erratum published in the February 2001 issue:

Table 3 Sequence analysis of ribavirin treated poliovirus genomes

	mutations[a]		
	G to A	C to U	**Total**
no ribavirin	0.6	1.7	**2.8**
1000 μM ribavirin	6.5*	11.8*	**20.3****

[a], per 10,000 nucleotides. Data for total mutations are greater than the sum of the two columns, as other transition (U to C, A to G) and transversion (G to U, G to C, and U to A) mutations were also detected. *, $P < 0.0004$ and **, $P < 0.0000002$ compared with no ribavirin (two-tailed, unpaired Student's *t*-test). A total of 42,335 nt was sequenced.

Figure 4

A.

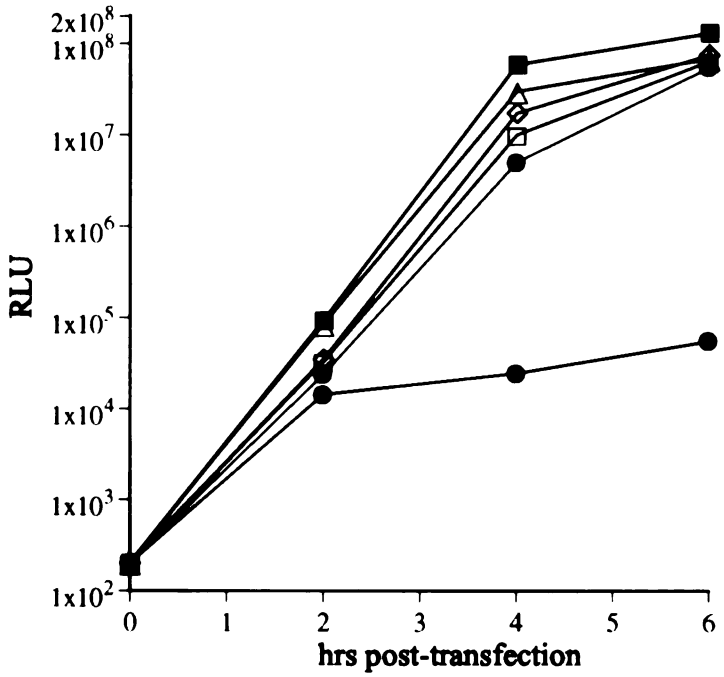
2x10^8
1x10^8
1x10^7
1x10^6
1x10^5
1x10^4
1x10^3
1x10^2
RLU
0
1
2
3
4
5
6
hrs post-transfection

B.

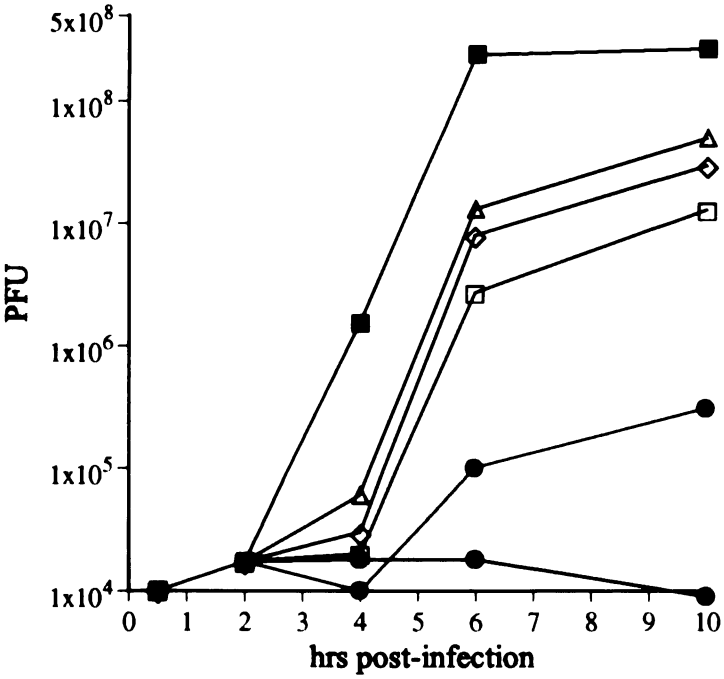
5x10^8
1x10^8
1x10^7
1x10^6
1x10^5
1x10^4
PFU
0
1
2
3
4
5
6
7
8
9
10
hrs post-infection

Chapter 9

RNA virus error catastrophe: direct molecular test using ribavirin

Abstract

RNA viruses evolve rapidly. One source of this ability to rapidly change is the apparently high mutation frequency in RNA virus populations. A high mutation frequency is a central tenet of the quasispecies theory. A corollary of the quasispecies theory postulates that, given their high mutation frequency, animal RNA viruses may be susceptible to error catastrophe, where they undergo a sharp drop in viability after a modest increase in mutation frequency. We recently showed that the important broad spectrum antiviral drug ribavirin (currently used to treat hepatitis C virus infections among others) is an RNA virus mutagen, and we proposed that ribavirin's antiviral effect is by forcing RNA viruses into error catastrophe. However, a direct demonstration of error catastrophe has not been made for ribavirin or any RNA virus mutagen. Here we describe a direct demonstration of error catastrophe using ribavirin as the mutagen and poliovirus as a model RNA virus. We demonstrate that ribavirin's full antiviral activity is

exerted through lethal mutagenesis of the viral genetic material. A 99.3% loss in viral genome infectivity is observed after a single round of virus infection in ribavirin concentrations sufficient to cause a 9.7-fold increase in mutagenesis. Compiling data on both the mutation levels and the specific infectivities of poliovirus genomes produced in the presence of ribavirin, we have constructed a graph of error catastrophe showing that normal poliovirus indeed exists at the edge of viability. This data suggests that RNA virus mutagens may represent a promising new class of antiviral drugs.

Introduction

The rapid evolution of RNA viruses is apparently powered by the high mutation frequency in RNA virus populations (1-6). The high mutation frequency of animal RNA viruses has been primarily inferred from genetic markers, and such assays may not be accurate enough to establish the exact mutation frequencies. Here we report data defining the high mutation frequency of poliovirus, a model RNA virus, and then we proceed to examine the implications of that high mutation frequency regarding mutagenic antiviral drug interventions that might exploit the high mutation frequency to destroy the virus.

The quasispecies theory states that an RNA virus population does not consist of a single "wildtype" genotype, but instead is an ensemble of related genotypes (7-11). This quasispecies is then capable of very rapid evolution in new environments, due to the large number of potentially beneficial mutations already present within the population. Maintaining such a high mutation frequency however is dangerous for the virus. There is an intrinsic limit to the maximum variability of viral genetic information before it loses meaning (7, 12), and if an RNA virus quasispecies goes beyond that mutation limit, the population will no longer be viable. The phenomenon that occurs when the loss of genetic fidelity results in a lethal accumulation of errors has been termed "error catastrophe" (Fig. 1) (3, 7). Most cellular organisms have evolved a number of sophisticated processes to maintain their genetic information with high fidelity and stay far away from the threshold of error catastrophe. In contrast, it has been predicted that RNA viruses with high mutation frequencies exist close to the edge of error catastrophe

and can be forced into error catastrophe by a moderate increase in mutation rate. Several indirect lines of evidence have been presented that support the existence of such an error catastrophe (13-17).

Our recent study demonstrated that the important broad spectrum antiviral drug ribavirin (currently used clinically to treat hepatitis C virus (HCV)(18, 19), respiratory syncytial virus (RSV)(20), and lassa fever virus infections (21)) is an RNA virus mutagen (15). In that study we observed a direct correlation between the mutagenic effect of ribavirin and the reduction of poliovirus titers, suggesting that ribavirin exerts its antiviral activity by lethally mutagenizing the virus population. However, a direct demonstration of error catastrophe/lethal mutagenesis has not been made for ribavirin or any RNA virus mutagen. That is to say, no study has provided direct proof that the antiviral effect of any drug is exerted via its mutagenic effects on the viral genetic material and not via secondary effects of the drug on cellular physiology or viability, or via inhibition of other aspects of the virus lifecycle.

Here we demonstrate that ribavirin's antiviral activity is exerted through lethal mutagenesis, specifically destroying the infectivity of the poliovirus genomic RNA. We also describe direct evidence that the error catastrophe theory applies to poliovirus. Compiling data from experiments using increasing levels of ribavirin mutagenesis, we are able to establish the relationship between mutation frequency and virus viability, showing a strikingly precipitous drop in virus viability at mutation levels only slightly higher than normal.

Materials and Methods

Cells and viruses. Human HeLa cells were propagated as previously described (15). All viral infections were performed using a poliovirus stock grown from a plasmid clone derived Mahoney strain poliovirus (pXpA). Inhibition of viral growth by ribavirin (1-ß-D-ribofuranosyl-1,2,4-triazole-3-carboxamide) was done in 3-12 x 10^6 HeLa cells in OptiMEM + 2% dialyzed FCS and pretreated with clinical grade ribavirin for 15 hrs. (kindly provided by Z. Hong, Schering-Plough) as previously described (15). Note that ribavirin obtained from Sigma is not sufficiently pure for in vivo experiments, as it causes significant toxicity at high concentrations (data not shown); clinical grade ribavirin is necessary for accurate experiments.

RNA and virus were harvested at the timepoint of maximum RNA accumulation (6 hrs post-infection for 0 and 100 μM ribavirin, and 10 hrs post-infection for 400 μM and 1000 μM ribavirin). PolyA+ RNA was collected using oligo dT_{25} DynaBeads on cytoplasmic lysates. Quantification of reduction in total poliovirus RNA at each condition (Fig. 2A, Table 2) was normalized to the number of HeLa cells harvested in each condition (previously published experiments normalized to 18S rRNA (15)). Total poliovirus titers (Table 2) were determined by plaque assay, as previously described (22). RNA infectivity (Figs. 3, 5) was determined by infectious center plaque assay, where the stated amount of RNA was electroporated into 1.2 x 10^6 HeLa cells, added to a 10cm plate of 50% confluent HeLa cells, let adhere for 2 hrs, then overlaid with medium/agar and let incubate for 48 hrs before staining the plate and counting plaques, using infectious

center assay techniques previously described (23). Control experiments were done to confirm that plaque formation after cell electroporation was linear with both RNA concentration and RNA infectivity (data not shown).

Molecular biology. In vitro transcribed poliovirus was generated using T7 RNA polymerase as previously described (23) on a pMoRA template (pXpA modified by a 5' ribozyme and long 3' polyA (24)). Plasmid DNA was destroyed by DNaseI (Ambion) treatment at 37 for 30', and RNA was then precipitated with 5M LiCl to eliminate any possible DNA contamination. Purity of all RNA samples (either in vitro transcribed or isolated from polio infected cells) was confirmed by a negative PCR for poliovirus capsid DNA (data not shown). Oligo dT primed cDNA was synthesized from 0.4 μg RNA from the appropriate source (T7 transcripts, normal viral RNA, or ribavirin-treated RNA) using Superscript II (Life Technologies), and VP1-coding sequence was PCR amplified from $1/10^{th}$ of the cDNA using high fidelity PfuTurbo polymerase (Stratagene, California) in a 25 cycle reaction. The VP1 gene was cloned and plasmid DNA was prepared from independent bacterial colonies. All DNA sequencing (Tables 1, 3) was done from position 2625-3400 of the poliovirus genome using BigDye terminator cycle sequencing and then analyzed with DNASTAR SeqManII (15). Sequence analysis of twenty-three (approximately half) of the normal poliovirus clones were published previously (15). Statistical analysis of significance (*P* values) of sequence data was done by Student's T-test. Plus or minus ranges indicated for sequence data are estimated at double (0.41 errors/10^4 nt) the frequency of RT-PCR introduced errors determined in Results (0.21 errors/10^4 nt).

Results

Mutation frequencies in normal poliovirus populations and in vitro generated genomes

One source of the impressive ability of RNA viruses to evolve is the apparently high mutation frequency in RNA virus populations. However, it has been argued that the available data does not accurately establish the mutation frequencies of animal RNA viruses, and the true mutation frequencies may be as low as 10^{-6} (25, 26). Most estimates of high RNA virus mutation frequencies have been based on genetic assays (1, 6, 27-34), which could give inaccurate estimates if the phenotypes are not completely tight. For example, the mutation frequency of poliovirus has been estimated at 2.1×10^{-4} by scoring for the presence of a single nucleotide mutation that confers a loss of dependence on guanidine (1). In that poliovirus strain, guanidine is necessary for poliovirus replication, but if that block is not absolute and the virus is capable of synthesizing ~100 new genomes in the absence of guanidine (instead of the normal 100,000 copies), the genetic marker would be overestimated in the population by 100x and the true mutation frequency would be 2×10^{-6}, not 2×10^{-4}. Therefore, direct molecular evidence (sequencing data) is necessary to precisely determine the mutation frequency.

As the mutation frequency is a basic parameter of RNA virus genetics, it is important to precisely establish this parameter. Therefore we set out to determine the mutation frequency in a poliovirus population by analyzing capsid gene sequences from a group of poliovirus clones. Poliovirus RNA was isolated from infected cells, and fifty-

five independent poliovirus cDNA clones were obtained. Those poliovirus cDNAs were generated from polio RNA by RT-PCR. As it was important to determine the number of mutations introduced during the RT-PCR reactions, we first performed a background control experiment where we sequenced the capsid VP1 genes of fifty-eight cDNA clones generated by RT-PCR reactions using as templates *in vitro* generated poliovirus genomes transcribed from a plasmid. We sequenced a total of 48,000 nts from the background control clones and observed an RT-PCR mutation frequency of 0.21 per 10,000 nts (Table 1). Then we analyzed the capsid VP1 gene sequences derived from the 55 independent normal poliovirus clones. We sequenced a total of 42,000 nts of clones from a normal poliovirus population, and observed a mutation frequency of 2.1 per 10,000 nts (Table 1), well above the background level ($P < 0.006$).

Direct antiviral effect of mutagenesis

Having established the high mutation frequency of a normal poliovirus population, we set out to test whether the virus exists near the threshold of error catastrophe. Several studies have shown a correlation between increased concentration of mutagen and loss of viral titer (13, 15-17), but not a direct demonstration that the antiviral effect was exerted via the mutagenesis of the viral RNA genetic material. The loss of titer could be due to inhibition of other virus processes (i.e. translation or RNA packaging) or secondary effects on cellular physiology/viability.

We recently demonstrated that ribavirin is an RNA virus mutagen (15). Here we have now carried out experiments designed to prove that lethal mutagenesis is the mechanism of action of ribavirin. We infected cells with poliovirus in the presence or

absence of ribavirin. At the timepoint of maximum viral RNA replication we measured viral titer by plaque assay and also isolated viral RNA. The amount of infectious virus was reduced 3.2-fold by 100μM ribavirin, 71-fold by 400μM ribavirin, and 2000-fold by 1000μM ribavirin. Additionally, we quantified the amount of viral RNA isolated from infected cells in each condition by spectrophotometry and gel electrophoresis of purified viral RNA (Fig. 2A).

The specific infectivity of the poliovirus genomic RNA was then determined for each condition, by transfection of isolated poliovirus genomic RNA into HeLa cells. Specific infectivity of genomic viral RNA is a direct measure of genome viability. Natural poliovirus genomic RNA had a specific infectivity of 1.5×10^6 plaque forming units (PFU) per μg genomes (Fig. 2B). Poliovirus RNA from cells treated with 100 μM ribavirin had a specific infectivity of 4.6×10^5 PFU/μg genomes, a 3.3-fold reduction from wildtype levels. Poliovirus RNA from cells treated with 400 μM ribavirin had a specific infectivity of 8.4×10^4 PFU/μg genomes, an 18-fold reduction from wildtype levels. Poliovirus RNA from cells treated with 1000 μM ribavirin had a specific infectivity of 1.1×10^4 PFU/μg genomes, a 140-fold reduction from wildtype levels, indicating that fewer than 1% of the viral genomes produced in the presence of 1000 μM ribavirin were viable. This data demonstrates that treatment with ribavirin has a potent direct effect on the viral genetic material.

Strikingly, the full antiviral effect of ribavirin can be attributed to lethal mutagenesis of the viral genetic material. In the presence of 100 μM ribavirin there was a 3.3-fold reduction in genome viability (Fig. 2B, Table 2), which can fully account for the 3.2-fold inhibition of infectious poliovirus titer (Table 2). In the presence of 400 μM

ribavirin there was an 18-fold reduction in genome viability (Fig. 2B, Table 2). Additionally, there was a 6-fold reduction in total genomic RNA (Fig. 2A, Table 2), which was likely due to the inactivation of many replicating viral genomes in the ribavirin-treated cells during the multiple rounds of replication and mutagenesis occurring in a single infectious cycle. The combined effects of the mutagen on loss in genome viability (18-fold) and reduction in genomic RNA production (6-fold) would result in an anticipated total reduction in infectious virus titer of ~100-fold, which indeed accounts for the full loss of titer observed (71-fold, Table 2). In the presence of 1000 μM ribavirin, there was a 140-fold reduction in genome viability (Fig. 2B, Table 2). Also there was a 16-fold reduction in total genomic RNA (Fig. 2A, Table 2), which again was likely due to the inactivation of many replicating viral genomes in the ribavirin-treated cells during the infectious cycle. The combined total of the loss in genome viability (140-fold) and the reduction in genomic RNA (16-fold) would result in an anticipated total reduction in infectious virus titer of ~2200-fold due to the direct effects of mutagenesis, which can account for the full loss of titer observed (2000-fold, Table 2).

Poliovirus replicates at the edge of the error catastrophe

DNA copies of viral RNA from each mutagen condition were sequenced to determine the increase in mutation frequency caused by ribavirin. The mutation frequency was increased 1.2-fold (± 0.2) in the presence of 100 μM ribavirin, 4.4-fold (± 0.2) in the presence of 400 μM ribavirin, and 9.7-fold (± 0.1) in the presence of 1000 μM ribavirin (Table 3). A wide range of G→A and C→T mutations were observed in the region sequenced, indicating that the clones were obtained independently. In addition,

G→A mutations are predicted to be induced by incorporation of ribavirin triphosphate as a GTP nucleoside analog during positive strand RNA synthesis, while C→T mutations are predicted to be the result of ribavirin incorporation during negative strand synthesis (15). There were no particular mutational hotspots (Fig. 3).

Plotting the data obtained above as genome infectivity versus the average number of errors per poliovirus genome would provide a graph of error catastrophe; but first, data elucidating the effect of a lower than normal mutation frequency was required. The specific infectivity of *in vitro* synthesized T7 genomic poliovirus transcripts, which have low (0.2×10^{-4}/nt) mutation levels, is comparable to that of natural poliovirus RNA (Fig. 4A). With the inclusion of that data, we then could construct a graph of error catastrophe based on our experimental observations (Fig. 4B). The graph illustrates several interesting features of the relationship between mutation levels and virus viability. First, there is no significant detrimental effect on the viability of poliovirus genomes at the normal mutation frequency (~10% in this particular experiment). Therefore, the poliovirus genetic information is flexible enough to absorb up to an average of approximately 1.5 mutations per genome without significant loss of function. Strikingly, a small increase in mutation frequency above the normal levels results in a large decline in viral infectivity (Fig. 4B). The LI_{50} (50% loss of infectivity), defined as the mutation frequency at which 50% of the viral genomes are lethally mutated, of poliovirus is ~2.0 mutations per genome, less than 2-fold higher than the natural mutation frequency. Furthermore, 95% of the genomes are lethally mutated when there is a 4-fold increase in mutation frequency. Thus, we conclude that the virus has evolved to exist near the edge of error catastrophe.

Discussion

The error catastrophe theory has existed as a corollary of the RNA virus quasispecies theory for over 20 years and several groups have previously published intriguing evidence that error catastrophe can occur in RNA virus populations (13-17). Using a potent RNA virus mutagen, ribavirin, here we have provided molecular evidence that poliovirus mutation frequencies are high (~2.1 x 10^{-4}), and we have described a direct molecular demonstration that error catastrophe exists and can be utilized as an effective antiviral strategy.

Mutation frequencies

A variety of genetic markers have been used to estimate the mutation frequencies of different RNA viruses. Given that the mutation frequency is a basic parameter of RNA virus genetics, it was valuable to firmly establish the mutation frequency of a model RNA virus, poliovirus, at the molecular level. We therefore carried out extensive sequence analysis of natural poliovirus genomes and background control *in vitro* generated genomes, and we have established that the mutation frequency is quite high, at ~2.1 x 10^{-4}. Using a different virus (FMDV), Domingo's group has recently published similar sequencing data (17), with an estimated mutation frequency of 2.8-5.9 x 10^{-4}. Although in that paper the frequency of reverse transcription and PCR errors was not determined, since they used similar experimental techniques to those used in this paper, the RT-PCR background control data presented here (Table 1) can probably be considered a reasonably accurate estimate of the RT-PCR induced mutations expected to be present in

their FMDV study. Therefore the FMDV mutation frequencies published by Domingo's group should be an accurate representation of the true mutation frequency. In both cases, the ability to sustain a 2.1-5.9 x 10^{-4} mutation frequency in virus populations of greater than 10^9 PFU/ml clearly depends on viral genomes that have evolved to consist of highly flexible genetic information.

Parvin et al. published data in 1986 that is in apparent contradiction to the poliovirus mutation frequency data we present here, as they stated that they observed no mutations out of 95,000 nts sequenced from 105 poliovirus VP1 gene clones (25). However, Parvin et al. stated in their methods section that, using the traditional Sanger dideoxy DNA sequencing technique, they were uncertain about mutations at 320 sites in the poliovirus clones (25). Even if only 10% of those 320 "uncertain" sites were true mutations, the data of Parvin et al. would be very similar to ours, and therefore we suggest that any apparent discrepancy between the two studies can likely be dismissed by simply accounting for our use of the more accurate fluorescent dye sequencing techniques now available.

Our 2.1 x 10^{-4} mutation frequency estimation by sequence analysis corroborates much of the available genetic marker-based literature on animal RNA virus mutation frequencies (3, 8). Therefore, genetic markers can be considered reasonable tools for estimating RNA virus mutation frequencies. In our study, the majority of natural mutations observed were transition mutations (C→U or G→A, Table 1). Genetic marker data is consistent with this observation, as genetic markers scoring for specific transitions were observed at high frequencies in several independent studies (3 x 10^{-5} (15), 2 x 10^{-4}

(1), 2 x 10^{-5} (32)), while a defined transversion event (A→C) was rarely detected in another study (26).

Error catastrophe

Ribavirin is an antiviral drug that is currently in widespread clinical use to treat hepatitis C, RSV, and lassa fever virus infections (18-21). The mechanism of action of ribavirin has been unclear since its discovery almost 30 years ago (20, 35-39). We previously proposed that ribavirin's antiviral activity is exerted through its potent RNA virus mutagenesis, as a nucleoside analog that becomes incorporated into newly synthesized genomes by the viral RNA-dependent RNA polymerase (15). Here we provide molecular proof that ribavirin exerts its antiviral action directly upon poliovirus's genetic material, lethally mutating the viral RNA genome (Fig. 2B). Most strikingly, ribavirin's mutagenic activity can fully account for its antiviral effect against poliovirus (Table 2).

Animal RNA viruses have been hypothesized to maintain themselves at the edge of error catastrophe (13). Figure 4B maps the relationship between mutation frequency and virus genome viability. The graph illustrates that the virus appears to have evolved to exist near the edge of error catastrophe, as small increases in mutation frequency above the normal levels results in a striking decline in viral infectivity, with a greater than 95% loss in genome infectivity upon a 4-fold increase in mutagenesis. Existing at the edge of error catastrophe is predicted to optimize the evolutionary fitness of the RNA virus quasispecies population by maximizing genetic variation without sacrificing viability (40). The data presented here demonstrates that high genetic variability, a biological

property that is normally a major advantage for an RNA virus, can be turned into a weapon against the virus by increasing that mutation rate beyond tolerable levels and causing a genetic meltdown.

Unlike RNA viruses, DNA based organisms generally have much lower mutation frequencies and do not exist near the error threshold. They appear to be able to absorb 300-5000 fold higher increases in mutation frequencies before significant loss of viability is seen (41, 42), though DNA viruses may be an exception (3, 42).

Implications for antiviral strategies

Ribavirin's activity as a nucleoside analog incorporated by the viral polymerase can explain the surprisingly broad spectrum action of ribavirin against members of almost all RNA virus families under laboratory cell culture conditions (39) (and clinical activity against three virus infections from diverse families), as the one common feature of RNA viruses is that they possess an RNA-dependent RNA polymerase. A high mutation frequency and a susceptibility to error catastrophe also appear to be common traits of most RNA viruses (3, 8, 40). The effectiveness of ribavirin *in vivo* as an RNA virus mutagen may be dependent on the accumulation of ribavirin and ribavirin triphosphate in some tissues (such as liver) but not others; alternatively, ribavirin may have different mechanisms of actions against different viruses (43, 44).

Ribavirin's lethal mutagenesis of poliovirus is probably enhanced by the well-characterized ability of ribavirin monophosphate to inhibit the cellular enzyme inosine monophosphate dehydrogenase (IMPDH) and thereby decrease cellular GTP pools (45-

47). The decrease in cellular GTP pools likely increases the frequency of ribavirin incorporation as a mutagenic GTP analog.

Several RNA virus mutagens are known, but they generally exhibit substantial cellular toxicity (as nucleoside analogs that are presumably incorporated by the cellular DNA and RNA polymerases) and are unacceptable for use in humans at the necessary doses (13, 14, 48, 49). Therefore, in the interest of developing new antiviral drugs that potentially exhibit activity against various RNA virus human pathogens, it may be possible to identify mutagenic nucleoside analogs that are highly specific for incorporation by viral RNA-dependent RNA polymerases. Such a drug development strategy should be plausible given the success in identifying and developing nucleoside analog anti-HIV therapies that are capable of specifically inhibiting that virus's RNA-dependent DNA polymerase.

References

1. de la Torre, J. C., Wimmer, E. & Holland, J. J. (1990) *Journal of Virology* **64,** 664-71.
2. Domingo, E., Holland, J. J. & Ahlquist, P. (1988) *RNA genetics* (CRC Press, Boca Raton, Fla.).
3. Domingo, E. & Holland, J. J. (1994) in *The Evolutionary biology of viruses*, ed. Morse, S. S. (Raven Press, New York), pp. xi, 353.
4. Domingo, E. (2000) *Virology* **270,** 251-253.
5. Domingo, E., Sabo, D., Taniguchi, T. & Weissmann, C. (1978) *Cell* **13,** 735-44.
6. Eggers, H. J. & Tamm, I. (1965) *Science* **148,** 97-98.
7. Eigen, M. & Biebricher, C. (1988) in *RNA genetics*, eds. Domingo, E., Holland, J. J. & Ahlquist, P. (CRC Press, Boca Raton, Fla.), pp. 3 v.
8. Domingo, E. & Holland, J. J. (1997) *Annual Review of Microbiology* **51,** 151-78.
9. Holland, J., Spindler, K., Horodyski, F., Grabau, E., Nichol, S. & VandePol, S. (1982) *Science* **215,** 1577-85.
10. Holland, J. J., De La Torre, J. C. & Steinhauer, D. A. (1992) *Current Topics in Microbiology and Immunology* **176,** 1-20.
11. Domingo, E., Holland, J. J., Biebricher, C. & Eigen, M. (1995) in *Molecular basis of virus evolution*, eds. Gibbs, A. J., Calisher, C. H. & Garcia-Arenal, F. (Cambridge University Press, Cambridge England ; New York, NY, USA), pp. xix, 603.
12. Eigen, M. (1971) *Naturwissenschaften* **58,** 465-523.
13. Holland, J. J., Domingo, E., de la Torre, J. C. & Steinhauer, D. A. (1990) *Journal of Virology* **64,** 3960-2.
14. Lee, C. H., Gilbertson, D. L., Novella, I. S., Huerta, R., Domingo, E. & Holland, J. J. (1997) *Journal of Virology* **71,** 3636-40.
15. Crotty, S., Maag, D., Arnold, J. J., Zhong, W., Lau, J. Y., Hong, Z., Andino, R. & Cameron, C. E. (2000) *Nature Medicine* **6,** 1375-1379.
16. Loeb, L. A., Essigmann, J. M., Kazazi, F., Zhang, J., Rose, K. D. & Mullins, J. I. (1999) *Proc Natl Acad Sci U S A* **96,** 1492-7.
17. Sierra, S., Davila, M., Lowenstein, P. R. & Domingo, E. (2000) *J Virol* **74,** 8316-23.
18. Davis, G. L., Esteban-Mur, R., Rustgi, V., Hoefs, J., Gordon, S. C., Trepo, C., Shiffman, M. L., Zeuzem, S., Craxi, A., Ling, M. H. & Albrecht, J. (1998) *N Engl J Med* **339,** 1493-9.
19. McHutchison, J. G., Gordon, S. C., Schiff, E. R., Shiffman, M. L., Lee, W. M., Rustgi, V. K., Goodman, Z. D., Ling, M. H., Cort, S. & Albrecht, J. K. (1998) *N Engl J Med* **339,** 1485-92.
20. Wyde, P. R. (1998) *Antiviral Research* **39,** 63-79.
21. McCormick, J. B., King, I. J., Webb, P. A., Scribner, C. L., Craven, R. B., Johnson, K. M., Elliott, L. H. & Belmont-Williams, R. (1986) *N Engl J Med* **314,** 20-6.

22. Crotty, S., Lohman, B. L., Lü, F. X., Tang, S., Miller, C. J. & Andino, R. (1999) *Journal of Virology* **73,** 9485-95.
23. Gohara, D. W., Crotty, S., Arnold, J. J., Yoder, J. D., Andino, R. & Cameron, C. E. (2000) *Journal of Biological Chemistry* **275,** 25523-25532.
24. Herold, J. & Andino, R. (2000) *J Virol* **74,** 6394-400.
25. Parvin, J. D., Moscona, A., Pan, W. T., Leider, J. M. & Palese, P. (1986) *J Virol* **59,** 377-83.
26. Sedivy, J. M., Capone, J. P., RajBhandary, U. L. & Sharp, P. A. (1987) *Cell* **50,** 379-89.
27. Blondel, B., Crainic, R., Fichot, O., Dufraisse, G., Candrea, A., Diamond, D., Girard, M. & Horaud, F. (1986) *J Virol* **57,** 81-90.
28. Lubeck, M. D., Schulman, J. L. & Palese, P. (1980) *Virology* **102,** 458-62.
29. Stec, D. S., Waddell, A., Schmaljohn, C. S., Cole, G. A. & Schmaljohn, A. L. (1986) *J Virol* **57,** 715-20.
30. Steinhauer, D. A., de la Torre, J. C. & Holland, J. J. (1989) *J Virol* **63,** 2063-71.
31. Holland, J. J., de la Torre, J. C., Steinhauer, D. A., Clarke, D., Duarte, E. & Domingo, E. (1989) *J Virol* **63,** 5030-6.
32. de la Torre, J. C., Giachetti, C., Semler, B. L. & Holland, J. J. (1992) *Proc Natl Acad Sci U S A* **89,** 2531-5.
33. Minor, P. D., Schild, G. C., Bootman, J., Evans, D. M., Ferguson, M., Reeve, P., Spitz, M., Stanway, G., Cann, A. J., Hauptmann, R., Clarke, L. D., Mountford, R. C. & Almond, J. W. (1983) *Nature* **301,** 674-9.
34. Sherry, B., Mosser, A. G., Colonno, R. J. & Rueckert, R. R. (1986) *J Virol* **57,** 246-57.
35. (2000) *AFHS Drug Information* (American Society of Hospital Pharmacists : SilverPlatter International, Bethesda, MD).
36. Gilbert, B. E. & Knight, V. (1986) *Antimicrob Agents Chemother* **30,** 201-5.
37. Smith, R. A. & Kirkpatrick, W. (1980) *Ribavirin, a broad spectrum antiviral agent* (Academic Press, New York).
38. Smith, R. A., Knight, V. & Smith, J. A. D. (1984) *Clinical applications of ribavirin* (Academic Press, Orlando).
39. Sidwell, R. W., Huffman, J. H., Khare, G. P., Allen, L. B., Witkowski, J. T. & Robins, R. K. (1972) *Science* **177,** 705-6.
40. Eigen, M. (1993) *Gene* **135,** 37-47.
41. Cupples, C. G. & Miller, J. H. (1989) *Proc Natl Acad Sci U S A* **86,** 5345-9.
42. Drake, J. W. & Holland, J. J. (1999) *Proceedings of the National Academy of Sciences of the United States of America* **96,** 13910-3.
43. Rankin, J. T., Jr., Eppes, S. B., Antczak, J. B. & Joklik, W. K. (1989) *Virology* **168,** 147-58.
44. Wray, S. K., Gilbert, B. E. & Knight, V. (1985) *Antiviral Res* **5,** 39-48.
45. Smith, R. A., Sidwell, R. W. & Robins, R. K. (1980) *Annu Rev Pharmacol Toxicol* **20,** 259-84.
46. Streeter, D. G., Witkowski, J. T., Khare, G. P., Sidwell, R. W., Bauer, R. J., Robins, R. K. & Simon, L. N. (1973) *Proc Natl Acad Sci U S A* **70,** 1174-8.
47. Wray, S. K., Gilbert, B. E., Noall, M. W. & Knight, V. (1985) *Antiviral Res* **5,** 29-37.

Table 1. Mutation frequency in a normal RNA virus population.

	transitions	transversions	Total mutation frequency[a]
RT-PCR background control	0	0.21	0.21
normal poliovirus population	1.88	0.24	2.12

[a] Mutations per 10,000 nts sequenced

Table 2. The antiviral effects of ribavirin can be directly attributed to lethal mutagenesis.

	normal	100μM ribavirin	400μM ribavirin	1000μM ribavirin
RNA infectivity loss	—	3.3	18	140
loss of total viral RNA	—	—	6	16
total predicted titer reduction	1	3.3	100	2200
Actual titer reduction[a]	**1**	**3.2**	**71**	**2000**

[a] Untreated ("normal") poliovirus titer in this experiment was 1.2×10^{10} PFU per plate of HeLa cells (6×10^6 cells). Data is to two significant digits.

Table 3. Mutation frequency in ribavirin treated RNA virus populations.

	G→A	C→T	Total mutation frequency[a]
normal population	0.5	1.2	2.1
100 μM ribavirin	—	1.3	2.5
400 μM ribavirin	4.4	5.0	9.3
1000 μM ribavirin	6.8	12.0	20.8

[a] Mutations per 10,000 nts sequenced

Figure Legends

Figure 1. Model of error catastrophe. The majority of viruses in a normal picornavirus population are viable (50). But a small increase in mutation frequency is predicted to push the virus population into error catastrophe (the mutagenized population on the right), where the number of errors per viral genome is sufficiently high to lethally mutate a majority of the virus population. White indicates live virus, red indicates dead virus. Most animal RNA virus genomes are approximately 10 kb long.

Figure 2.

A. Total poliovirus genomic RNA accumulation in infected cells, with and without ribavirin. On the left, normal poliovirus genomic RNA (Mo) isolated from infected cells is normalized to a known quantity (100 ng) of in vitro generated poliovirus genomes (TRX). On the right, quantities of poliovirus genomic RNA isolated from infected cells in 100 μM ribavirin (Mo^{100r}), cells in 400 μM ribavirin (Mo^{400r}), and cells in 1000 μM ribavirin (Mo^{1000r}), are normalized to amounts of poliovirus genomic RNA from infected untreated cells (Mo). Comparisons are tabulated in Table 2.

B. Direct antiviral effect of ribavirin on the viral genetic material. Large reductions in specific infectivity of ribavirin mutagenized RNA virus genomes. Genomic poliovirus RNA from (■) untreated cells, (●) 100 μM ribavirin-treated cells, (▲) 400 μM ribavirin-treated cells, (♦) 1000 μM ribavirin-treated cells. Data is shown with a linear curve fit for each series.

Figure 3. Distribution of mutations found in the VP1 capsid gene without ribavirin (Δ), with 400μM ribavirin mutagenesis (*), and 1000μM ribavirin mutagenesis (♦). Note that there are no particular mutational hotspots. Almost all mutations at C's were C→U and mutations at G's were G→A. Also note that in the presence of 400μM ribavirin an unusual 3 nt deletion (indicated by ---) was detected at a CCU sequence.

Figure 4.

A. Specific infectivity of T7 transcribed poliovirus genomes compared with natural poliovirus genomes. This illustrates that between 0.21 and 2.1 mutations per 10,000 nts there is no significant detrimental effect on the viability (specific infectivity) of poliovirus genomes. In vitro transcribed RNA (■) ; natural poliovirus RNA (●).

B. Relationship of mutation frequency to genomic RNA infectivity. Normal poliovirus RNA was set to 100%. The graph shows that poliovirus populations exist near the edge of error catastrophe, as there is a rapid decline in infectivity at levels of mutagenesis only slighly higher than normal. The LI_{50} (50% loss of infectivity) is defined as the mutation frequency at which 50% of the viral genomes are lethally mutated, indicated by the dashed line. Wildtype (wt or Mo) poliovirus genomes contain an average ~1.5 mutations/genome, based on data from Table 1. Poliovirus genomes from cells treated with 100 μM ribavirin (Table 3) contain an average ~1.9 mutations/genome. Poliovirus genomes from cells treated with 400 μM ribavirin (Table 3) contain an average ~6.9 mutations/genome. Poliovirus genomes from cells treated with 1000 μM ribavirin (Table 3) contain an average ~15.5 mutations/genome.

Figure 1

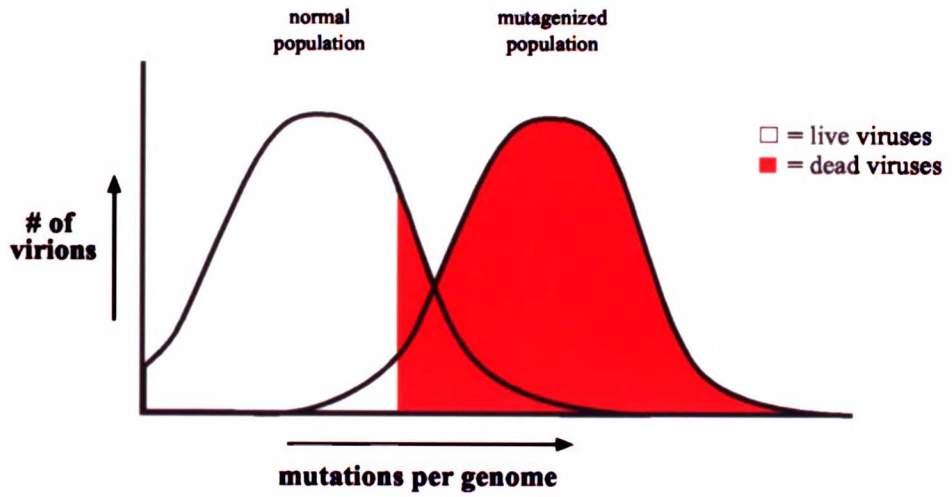
normal
population
mutagenized
population
□ = live viruses
■ = dead viruses
of
virions
mutations per genome

Figure 2

A.

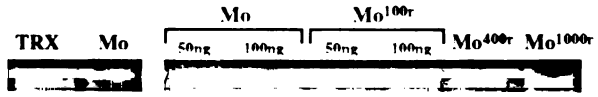
TRX
Mo
Mo
50ng
100ng
Mo100r
50ng
100ng
Mo400r
Mo1000r

B.

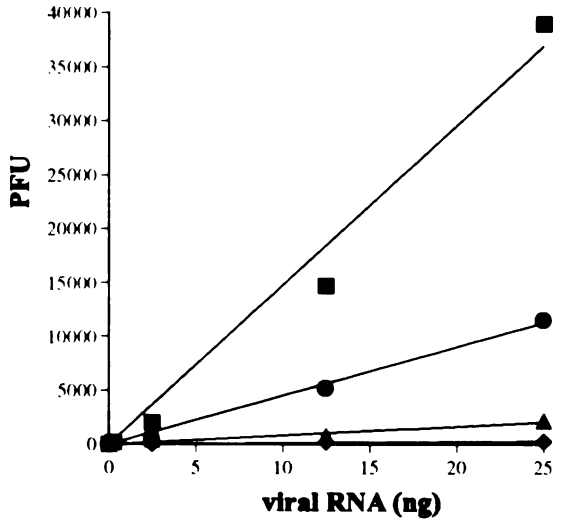
40000
35000
30000
25000
20000
15000
10000
5000
0
PFU
0
5
10
15
20
25
viral RNA (ng)


2625 CTGGGGCCACAAATCCACTAGTCCCTTCTGATACAGTGCAAACCAGACAT
GTTGTACAACATAGGTCAAGGTCAGAGTCTAGCATAGAGTCTTTCTTCGC
2725 GCGGGGTGCATGCGTGACCATTATGACCGTGGATAACCCAGCTTCCACCA
CGAATAAGGATAAGCTATTTGCAGTGTGGAAGATCACTTATAAAGATACT
2825 GTCCAGTTACGGAGGAAATTGGAGTTCTTCACCTATTCTAGATTTGATAT
GGAACTTACCTTTGTGGTTACTGCAAATTTCACTGAGACTAACAATGGGC
2925 ATGCCTTAAATCAAGTGTACCAAATTATGTACGTACCACCAGGCGCTCCA
GTGCCCGAGAAATGGGACGACTACACATGGCAAACCTCATCAAATCCATC
3025 AATCTTTTACACCTACGGAACAGCTCCAGCCCGGATCTCGGTACCGTATG
TTGGTATTTCGAACGCCTATTCACACTTTTACGACGGTTTTTCCAAAGTA
3125 CCACTGAAGGACCAGTCGGCAGCACTAGGTGACTCCCTTTATGGTGCAGC
ATCTCTAAATGACTTCGGTATTTTGGCTGTTAGAGTAGTCAATGATCACA
3225 ACCCGACCAAGGTCACCTCCAAAATCAGAGTGTATCTAAAACCCAAACAC
ATCAGAGTCTGGTGCCCGCGTCCACCGAGGGCAGTGGCGTACTACGGCCC
3325 TGGAGTGGATTACAAGGATGGTACGCTTACACCCCTCTCCACCAAGGATC
TGACCACATATGGATTCGGACACCAA

A.

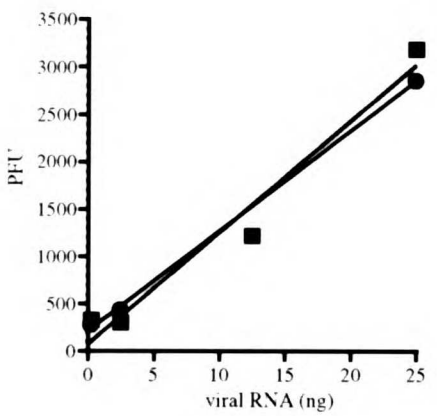
3500
3000
2500
2000
1500
1000
500
0
PFU
0
5
10
15
20
25
viral RNA (ng)

B.

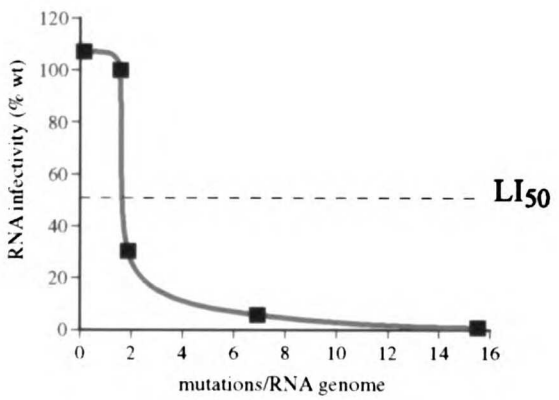
120
100
80
60
40
20
0
RNA infectivity (% wt)
LI50
0
2
4
6
8
10
12
14
16
mutations/RNA genome

Section III

Poliovirus receptor transgenic mice

Chapter 10

Introduction to section III: Poliovirus receptor (PVR) transgenic mice

Poliovirus is an excellent RNA virus model system. There excellent forward genetics, reverse genetics, biochemistry, and structural systems available, and the virus can be studied in cell culture, small animal models, large animal models (monkeys and chimps), and humans. One limitation of *in vivo* poliovirus studies has been that the small animal model system has significant limitations.

No small animals are naturally susceptible to poliovirus infection. There are mouse-adapted poliovirus strains, but those strains are strictly neurotropic and use an alternative receptor (5). The human poliovirus receptor (PVR) was identified in 1989 (3). A PVR transgenic mouse was the first transgenic mouse model of a human viral pathogen, which was a major accomplishment (5). Those PVR transgenic mice are susceptible to poliovirus infection, and succumb to lethal paralytic poliomyelitis after intracerebral, intraspinal, intramuscular, or intraperitoneal inoculation of wild type poliovirus. Several additional PVR transgenic mouse lines have since been generated, all of which have similar phenotypes (1, 2, 7). Unfortunately, none of these transgenic mice are susceptible to an oral route of infection with poliovirus (2, 5, 7), which is the natural route of poliovirus infection in humans. After oral infection poliovirus then replicates to

high titers in human small intestines (4), and no replication was detected at this site in the available mouse poliovirus models (2, 5, 7).

With that backdrop, we decided to develop a new PVR transgenic mouse model that might might mirror human poliovirus pathogenesis more accurately than previous poliovirus transgenic mouse models. The full description of that work constitutes Chapter 12.

PVR transgenic mice are valuable for a variety of studies, including the exploration of viral immunology. We took advantage of this avenue in a very fruitful collaboration with Luis Sigal and Kenneth Rock of the University of Massachusetts, Worchester. One specific advantage of working in the PVR mouse system is that it is possible to make chimeric mice expressing PVR in only a subset of tissues and therefore only susceptible to poliovirus infection in those tissues. This was used to great advantage in Chapter 11 to make a major immunological discovery (6).

Additional, the study done with Luis Sigal identified the first cytotoxic T lymphocyte (CTL) MHC class I epitope in the poliovirus genome that elicits a natural CTL response, providing more evidence that poliovirus elicits CTL responses. This issue is important for vaccine vector reasons discussed in section I, particularly in Chapter 5.

Acknowledgements

The work is Chapter 11 was primarily conceived and executed by Luis Sigal. I carried out the supporting role of determining the sites of poliovirus replication that could be contributing the antigens that were then taken up by professional antigen presenting cells (APCs) and used to inititate (CTL) responses. Laura Hix provided technical assistance on the work in Chapter 12.

References

1. **Deatly, A. M., R. E. Taffs, J. M. McAuliffe, S. P. Nawoschik, J. W. Coleman, G. McMullen, C. Weeks-Levy, A. J. Johnson, and V. R. Racaniello** 1998. Characterization of mouse lines transgenic with the human poliovirus receptor gene. Microbial Pathogenesis. **25**:43-54.
2. **Koike, S., C. Taya, T. Kurata, S. Abe, I. Ise, H. Yonekawa, and A. Nomoto** 1991. Transgenic mice susceptible to poliovirus. Proc Natl Acad Sci U S A. **88**:951-5.
3. **Mendelsohn, C. L., E. Wimmer, and V. R. Racaniello** 1989. Cellular receptor for poliovirus: molecular cloning, nucleotide sequence, and expression of a new member of the immunoglobulin superfamily. Cell. **56**:855-65.
4. **Minor, P. D.** 1997. Poliovirus, p. 555-574. *In* N. Nathanson, and R. Ahmed (eds), Viral pathogenesis. Lippincott-Raven, Philadelphia.
5. **Ren, R. B., F. Costantini, E. J. Gorgacz, J. J. Lee, and V. R. Racaniello** 1990. Transgenic mice expressing a human poliovirus receptor: a new model for poliomyelitis. Cell. **63**:353-62.
6. **Sigal, L. J., S. Crotty, R. Andino, and K. L. Rock** 1999. Cytotoxic T-cell immunity to virus-infected non-haematopoietic cells requires presentation of exogenous antigen. Nature. **398**:77-80.
7. **Zhang, S., and V. R. Racaniello** 1997. Expression of the poliovirus receptor in intestinal epithelial cells is not sufficient to permit poliovirus replication in the mouse gut. J Virol. **71**:4915-20.

Chapter 11

Anti-viral surveillance by CTLs requires professional APCs and MHC class I presentation of exogenous antigen

CTL are thought to detect viral infections by monitoring the surface of all cells for the presence of viral peptides bound to major histocompatibility complex (MHC) class I molecules. In most cells, MHC class I-presented peptides are derived exclusively from proteins synthesized by the antigen presenting cell (APC)[1]. Macrophages and dendritic cells also have an alternate MHC class I pathway that can present peptides derived from extracellular antigens, however the physiological role of this process is unclear [2]. Here we show that virally-infected non-hematopoietic cells are unable to directly stimulate primary CTL immunity. Instead, bone-marrow-derived cells are required as APCs to initiate anti-viral CTL responses. Moreover, in these cells the alternate (exogenous) MHC class I pathway is the obligatory mechanism for the initiation of CTL responses to viruses that exclusively infect non-hematopoietic cells.

The "classical" major histocompatibility complex (MHC) class I antigen presentation pathway is thought to be the major mechanism the immune system uses to detect viral infections in all cells. In this pathway, proteins synthesized by a cell are degraded in the cytoplasm into oligopeptides, a fraction of which are transported into the

endoplasmic reticulum (ER) by the transporter associated with antigen presentation (TAP). In the ER these peptides bind to new MHC class I molecules and the complexes are transported to the cell surface. Since peptide binding is required for the transport of MHC class I molecules to the plasma membrane, TAP is required for normal MHC class I expression at the cell surface and antigen presentation [1].

To test whether non-hematopoietic cells can function as APCs to initiate CTL responses to viruses, a model was required where the class I antigen presentation function of bone-marrow-derived cells was impaired, while that of other cells remained intact. For this purpose we constructed bone-marrow chimeras by lethally irradiating C57BL/6 mice (B6; H-2^b) and reconstituting them with bone-marrow from $TAP^{0/0}$ mice [3] (H-2^b; all bone-marrow chimeras will be referred to as bone-marrow donor → irradiated recipient). Since bone-marrow-derived cells in $TAP^{0/0}$ → B6 mice can not transfer peptides from the cytosol to the ER, they are unable to utilize the classical MHC class I pathway [3, 4].

The chimeric mice were assayed for the generation of CTL responses following infection with wild type vaccinia virus or with vaccinia-OVA, a vaccinia recombinant carrying chicken ovalbumin (OVA) as a full length non-structural protein [5]. Despite intact MHC class I antigen presentation in non-hematopoietic tissues, $TAP^{0/0}$ → B6 mice were unable to generate CTL responses to the antigens of wild type vaccinia virus (Fig. 1a) or to OVA in vaccinia-OVA (Fig. 1b). In contrast, robust CTL responses to vaccinia viral antigens and OVA were detected in control B6 → B6 mice. These results indicate that the generation of CTL to vaccinia virus requires bone-marrow-derived cells with functional TAP molecules.

Next, we evaluated whether the inability to generate CTL in $TAP^{0/0}$ → B6 mice was due to a defect in $CD8^+$ T cells or a failure of antigen presentation by bone-marrow-derived APCs. $TAP^{0/0}$ (non-chimeric) mice lack $CD8^+$ T cells almost completely because expression of MHC class I in epithelial thymic cells is necessary for the positive selection of $CD8^+$ T cells in the thymus [3]. However, when analyzed by flow cytometry, $TAP^{0/0}$ → B6 mice had normal numbers of $CD8^+$ T cells in peripheral blood and spleen (data not shown, and reference [4]) as a consequence of positive selection on wild type thymic epithelial cells (which are radioresistant and non-hematopoietic). In addition, these $CD8^+$ T cells were fully functional as shown in three different experiments. As seen in Figure 2a, $TAP^{0/0}$ → B6 mice generated a CTL response similar to B6 → B6 mice to vaccinia SS-SIINFEKL [5], a recombinant vaccinia construct expressing the antigenic peptide of OVA (SIINFEKL) [6] preceded by a signal sequence that delivers the peptide directly into the ER bypassing the need for TAP function. Also, $TAP^{0/0}$ → B6 chimeras generated anti-SIINFEKL CTL responses similar to control mice when injected intravenously with a graded numbers of B6 dendritic cells that had been pre-incubated with a single concentration of synthetic SIINFEKL (Fig. 2b) or when injected with $5x10^5$ B6 dendritic cells that had been incubated with graded concentrations of SIINFEKL (Fig. 2c).

These results indicate that the inability of $TAP^{0/0}$ → B6 mice to generate a CTL response to vaccinia virus is due to a failure of antigen presentation. This was not due to a failure of the $TAP^{0/0}$ → B6 chimeras to reconstitute bone-marrow-derived APCs because these mice generated MHC class II-restricted T cell responses to OVA which were at least as strong as those generated by B6 → B6 animals (Fig 3 a and b). Altogether, these data demonstrate that bone-marrow-derived professional APCs,

possessing a functional TAP, are required to initiate CTL responses to vaccinia, and that non-hematopoietic tissues infected with vaccinia cannot prime CTL. This is despite the ability of vaccinia to infect many different tissues, including respiratory organs, liver, kidney, spleen, ovaries, and central nervous system [7-9]. Several reasons may account for the inability of non-hematopoietic cells to stimulate a CTL response. Although non-hematopoietic cells are able to present antigenic peptides bound to MHC class I, they express low levels of these molecules in the absence of inflammation. Moreover, they do not express MHC class II molecules, essential for the stimulation of $CD4^+$ helper T cells, and lack adhesion and costimulatory molecules that might be required to stimulate *naïve* T cells. Furthermore, non-immune cells lack the ability to migrate to lymphoid organs where many immune responses are initiated [10]. On the other hand some bone-marrow-derived cells such as macrophages and dendritic cells express high levels of MHC class I and class II molecules and a variety of adhesion and costimulatory molecules, including B7.1 and B7.2 and can migrate to central lymphoid organs. However, after *naïve* CTLs are stimulated to become effectors, they no longer require costimulation or T cell help and can recognize lower levels of peptide MHC complexes. Therefore, once stimulated by professional APCs, the effector CTLs acquire the ability to migrate out of the lymphoid organs and can clear viral infections in all tissues.

In the experimental model described above, bone-marrow-derived APCs might acquire the viral antigens by becoming infected [11]. In fact, vaccinia virus does infect and its antigens are presented by dendritic cells and macrophages *in vitro* (not shown). However, it seems unlikely that professional APCs would express all the cellular factors needed to be infected by all viruses and therefore this mechanism would be unavailable to

detect infections with many tissue specific viruses. Alternatively the bone-marrow-derived APCs might acquire vaccinia viral antigens exogenously from other antigen-bearing cells and this mechanism could operate in all infections, as previously hypothesized [2, 12]. To determine whether the presentation of exogenous antigen is important in viral immunity, we developed a model where bone-marrow-derived cells could not be infected with a virus.

Poliovirus (polio) is a positive strand RNA virus with a host range that includes humans but not mice. This host range restriction is determined by the expression of a suitable poliovirus receptor (PVR)[13]. Cells from wild type mice are not infectable with polio, but mouse cells transfected with human PVR can be infected (data not shown and Reference [14]). In this study we used two human PVR transgenic mice. We constructed a transgenic mouse, (cPVR, in an ICR background) expressing a full length PVR cDNA (driven by the ß-actin promoter) in all tissues examined. They are susceptible to polio infection and die with poliomyelitis following injection with wild type polio (data not shown). Moreover, following intraperitoneal infection with the wild type strain of polio, we found much higher titers of virus (expressed as plaque forming units/gram of tissue) in skeletal muscle (12,000), brain (1,600), spinal cord (19,000), and to smaller degree in kidney (1.3) and liver (0.64) of cPVR mice, as compared to B6 mice (0.70, < 0.60, < 0.30, < 0.10, < 0.20 respectively). We mated cPVR mice with B6 mice, and their progeny [cPVR xB6]F1 mice (referred to here as cPVR B6) were used for this study. Another transgenic mouse strain (referred to here as gPVR B6) possesses the human PVR genomic locus, including the endogenous human promoter, backcrossed onto the B6 background. It also supports viral replication in skeletal muscle and central nervous system [13, 15]. To

examine the role of the exogenous MHC class I pathway in the initiation of CTL responses, we generated a series of bone-marrow chimeric mice, including two sets (B6 → cPVR and B6 → gPVR B6) that permitted infection only of non-bone-marrow-derived cells. In a previous study, we constructed a polio recombinant (polio-OVA) expressing the C-termini half of OVA (which includes the SIINFEKL epitope). In this construct the OVA fragment is synthesized as part of the viral polyprotein and released in the cytosol by viral proteinases. We demonstrated that this polio-OVA can induce anti-OVA CTL responses in gPVR B6 mice and cPVR B6 but not in B6 mice (Reference [14] and data not shown). Consistent with that result, cPVR B6 → cPVR B6 mice infected with polio-OVA generated anti-OVA CTLs (Fig. 3a, panel 3), but B6 → B6 mice did not (Fig. 3a, panel 4). Strikingly, B6 → cPVR B6 chimeric mice, which have non-infectable (PVR-negative) bone-marrow-derived cells, generated strong anti-OVA CTL responses when infected with polio-OVA (Fig. 3a, panel 1) but not when infected with a recombinant polio (polio-sp27) expressing an irrelevant protein (Fig. 3a, panel 5). Therefore, either the infected non-hematopoietic cells are stimulating CTL responses, or bone-marrow-derived cells are acquiring the polio expressed OVA from exogenous sources.

To distinguish between these two mechanisms we constructed chimeric mice using $TAP^{0/0}$ mice as bone-marrow donors and PVR^{+} transgenic mice as recipients. Remarkably, $TAP^{0/0}$ → cPVR B6 mice did not generate anti-OVA CTLs (Fig. 3a, panel 2) when infected with polio-OVA. As expected, their CTL were functional and generated a strong response to vaccinia SS-SIINFEKL (Fig. 3a, panel 6). In addition, similar results were obtained with gPVR B6 chimeric mice (Fig. 3b, all panels). As with the vaccinia virus experiments, these data indicate that non-hematopoietic cells are unable to stimulate

CTL immunity to a virus suggesting that this may be a general rule. Even more important, these results indicate that the bone-marrow-derived cells in B6 → c/gPVR B6 acquired antigen from exogenous sources. That $TAP^{0/0}$ → c/gPVR did not respond to polio-OVA also constitutes a control to demonstrate that the response in B6 → c/gPVR mice was not due to residual PVR^{+} bone-marrow-derived cells that survived irradiation.

Until now the physiological role of the exogenous MHC class I pathway has been unclear. Stimulation of CTL by this route has been shown to occur in several situations, such as transplantation ("crosspriming" for minor histocompatibility antigens) [16] and injection of particulate antigens [17], but it has been thought to make a minor contribution to overall responses. Two situations where this pathway has been shown to be important are generating CTL to a tumor [4] and for homing and tolerization of adoptively transferred T cells to a transgenic antigen expressed in pancreatic ß cells[18, 19]. However, in these cases it has been unclear whether the exogenous pathway might be dominant only because of the lack of inflammation (which stimulates antigen presentation and provides an adjuvant effect) and/or because these cells might be poor stimulators. Otherwise, it has also been suggested that the exogenous MHC class I pathway is inefficient and unlikely to play an important role in most physiological situations[20]. Our experiments with B6 → PVR mice contradict this view and indicate that this exogenous MHC class I pathway is essential for the initiation of CTL responses to viral infection confined to non-hematopoietic tissues. In fact, if this pathway did not exist viruses could escape immune surveillance by utilizing receptors that are not expressed on the critical bone-marrow-derived APCs. Interestingly, the magnitude of the CTL responses in PVR→ B6 mice are similar to those in B6 → PVR mice despite that polio virus can infect and be

presented by dendritic cells from gPVR mice (LJS and KLR, unpublished data). This suggests that the presentation of exogenous antigen is a major pathway in vivo and may contribute to the stimulation of CTL responses even in situations where viruses may infect bone-marrow-derived cells.

How do bone-marrow-derived cells acquire viral exogenous antigens? When infected cells die *in vivo,* they are very rapidly cleared by bone-marrow-derived phagocytes, which will import the viral antigens into both the exogenous MHC class I and class II pathways [21]. Interestingly, antigens from apoptotic cells have been shown to be avidly presented on class I molecules of dendritic cells [22]. Although our work does not specifically establish the identity of the bone-marrow-derived APCs responsible for initiating CTL responses through the exogenous pathway, macrophages and/or dendritic cells are again the likely candidates because they can present antigen *via* the exogenous MHC class I pathway *in vitro* [17, 23]. Also, these cells are able to ingest dying cells and cellular debris by phagocytosis and can thereby import viral antigens into the exogenous MHC class I pathway. Moreover, their migratory nature allows them to acquire antigen at a site of infection and then travel to the lymphoid tissues.

Two routes for the exogenous MHC class I pathway have been described *in vitro,* a TAP-independent pathway where antigen is hydrolyzed in endosomes [24], and a phagosome-to-cytosol pathway [25] that is TAP dependent. Our data provide indirect evidence that *in vivo*, vaccinia-OVA, and polio-OVA antigens follow the TAP-dependent exogenous MHC class I pathway.

In summary, our results show a strict requirement for professional APCs in the generation of anti-viral CTL immunity, and demonstrates that the exogenous pathway

plays a key role in the immune surveillance of non-hematopoietic tissues. These findings have implications for vaccine delivery and gene therapy as well as viral immune evasion. They suggest that to stimulate strong immunity, viral vectors or naked DNA must be expressed in professional APCs or deliver in a manner that will promote exogenous antigen presentation. Moreover, these mechanisms may limit the ability of viruses to block the generation of CTL by down-regulating MHC class I expression on infected cells[26] because this is unlikely to affect the exogenous pathway in uninfected APCs.

Methods

Media and cells

All cell lines used in this study have been described and were cultured as previously [27]. To obtain dendritic cells, bone-marrow cells obtained from B6 mice were incubated overnight in RPMI media (Irvine Scientific) supplemented with 10% fetal calf serum, (FCS; Atlanta Biologicals), $5x10^{-5}$ M 2-mercaptohethanol (Sigma) and 2 mM L-glutamine, antibiotics (Fungi-Bact), 0.01 M HEPES buffer and non-essential amino acids (all from Irvine Scientific). Non adherent cells were harvested and grown in the same media supplemented with 10 ng/ml GM-CSF and 5 ng/ml IL-4 (Pharmingen) for 5-6 days with further addition of cytokines every other day. Most cells in these cultures were dendritic cells as judged by morphology and expression of specific markers by flow cytometry. Before injecting into mice, $3x10^6$ dendritic cells where thoroughly washed in PBS resuspended in 1 ml PBS containing the indicated concentrations of SIINFEKL and 10 mg human b2m (Calbiochem) and incubated at 37 °C for 1 hour. Following incubation the cells were washed in PBS and injected intravenously into mice.

Recombinant viruses

The production and use of viruses was done as previously [14, 27] except that inoculation of mice with polio was performed IV rather than IP.

Mice

$TAP^{0/0}$ (B6,129-Tap $^{ltp\ 1Arp}$; Jackson Laboratory), and B6 (Taconic) mice were obtained at 6-8 weeks of age. cPVR mice were made by standard transgenic techniques using the

plasmid pPVR-9 that has already been described [14]. gPVR (a gift from Cyanamid) were bred at UMMC animal facilities.

Replication of Poliovirus in cPVR mice

Mice were inoculated intraperitoneally with 2 x 10^8 plaque forming units of poliovirus. Six paralyzed cPVR mice were sacrificed at days 4.5 - 6.5. Four control B6 mice were sacrificed at days 4.5-5.5. Tissue samples were homogenized, and poliovirus titers in each tissue were determined by plaque assay.

Preparation and use of Bone-marrow Chimeras

Bone-marrow cells from 1-3 month donor mice were treated with anti-Thy 1 antibody (M5/49.4.1; ATCC) and complement to eliminate mature T cells, washed twice and resuspended in PBS. Recipients were irradiated with 650 Rad followed by a second irradiation with 450 Rad four hours later. Irradiated mice were reconstituted by intravenous inoculation of 4-6 x 10^6 bone-marrow cells from the different donors. To avoid rejection of donor MHC class I-negative$TAP^{0/0}$ cells by host NK cells, chimeras also received an IP inoculation of 10 ml rabbit anti-asialo GM1 gammaglobulin (Wako Chemicals) on the day of the transplant, and a second inoculation three days later. Bone-marrow chimeras were rested for 4-6 month following reconstitution to allow for complete elimination of host derived APCs. Mice were inoculated with 2x10^7 plaque forming units of virus and CTL killing was measured from fresh spleen cells (wild type vaccinia) or from five days restimulation cultures using a ^{51}Cr release assay as previously described [27]. For MHC class II restricted responses mice were injected at the base of the tail with 100 mg OVA (Sigma) in PBS admixed 1/1 with complete Freund adjuvant (Gibco) in a final volume of 50ml. 10 days later mice were sacrificed and the cells

obtained from the para-aortic lymph node of 2 or 3 mice were pooled, and $2x10^5$ cells from each pool were incubated for 48 hours in triplicate wells of microtiter plates in the presence of OVA. Supernatants were assayed for the presence of IL-2 by measuring the incorporation of ^3H thymidine by the IL-2 dependent cell line CTLL. When indicated, antibodies were supplied as a 1/8 dilution of hybridoma culture supernatants. The antibodies M5/114 (ATCC TIB-120) Y-3 (ATCC HB-176) BBM.1 (ATCC HB-28) were used for anti-MHC Class II, anti-MHC Class I and control antibody respectively. All experiments in this paper were performed at least three times, except for Figure 3a which was done twice. Data points in all figures except 2c correspond to the averages ± SE for all the mice in a group. All experimental groups consisted of three mice, but some control groups (e.g. vaccinia SS-SIINFEKL, Polio-SP27) had two mice. In figure 2c,two mice were used per group and they are shown individually. All mice used in these experiments were housed at the UMMC animal facilities and experiments were conducted in compliance with NIH and institutional guidelines.

References

1. York, I.A. & Rock, K.L. Antigen processing and presentation by the class I major histocompatibility complex. *Ann. Rev. Immunol.* **14**, 369-96 (1996).
2. Rock, K.L. A new foreign policy: MHC class I molecules monitor the outside world. *Immunology Today.* **17**, 131-7 (1996).
3. Van Kaer, L., Ashton-Rickardt, P.G., Ploegh, H.L. & Tonegawa, S. TAP1 mutant mice are deficient in antigen presentation, surface class I molecules, and CD4-8+ T cells. *Cell.* **71**, 1205-14 (1992).
4. Huang, A.Y., Bruce, A.T., Pardoll, D.M. & Levitsky, H.I. In vivo cross-priming of MHC class I-restricted antigens requires the TAP transporter. *Immunity.* **4**, 349-55 (1996).
5. Restifo, N.P., *et al.* Antigen processing in vivo and the elicitation of primary CTL responses. *J Immunol.* **154**, 4414-22 (1995).
6. Rotzschke, O., *et al.* Exact prediction of a natural T cell epitope. *Eur J Immunol.* **21**, 2891-4 (1991).
7. Lee, M.S., *et al.* Molecular attenuation of vaccinia virus: mutant generation and animal characterization. *J Virol.* **66**, 2617-30 (1992).
8. Taylor, G., Stott, E.J., Wertz, G. & Ball, A. Comparison of the virulence of wild-type thymidine kinase (tk)- deficient and tk+ phenotypes of vaccinia virus recombinants after intranasal inoculation of mice. *J Gen Virol.* **72**, 125-30 (1991).
9. Buller, R.M., Smith, G.L., Cremer, K., Notkins, A.L. & Moss, B. Decreased virulence of recombinant vaccinia virus expression vectors is associated with a thymidine kinase-negative phenotype. *Nature.* **317**, 813-5 (1985).
10. Kundig, T.M., *et al.* Fibroblasts as efficient antigen-presenting cells in lymphoid organs. *Science.* **268**, 1343-7 (1995).
11. Zinkernagel, R.M., Kreeb, G. & Althage, A. Lymphohemopoietic origin of the immunogenic, virus-antigen-presenting cells triggering anti-viral T-cell responses. *Clin Immunol Immunopathol.* **15**, 565-76 (1980).
12. Bevan, M.J. Minor H antigens introduced on H-2 different stimulating cells cross-react at the cytotoxic T cell level during in vivo priming. *J Immunol.* **117**, 2233-8 (1976).
13. Ren, R.B., Costantini, F., Gorgacz, E.J., Lee, J.J. & Racaniello, V.R. Transgenic mice expressing a human poliovirus receptor: a new model for poliomyelitis. *Cell.* **63**, 353-62 (1990).
14. Mandl, S., Sigal, L.J., Rock, K.L. & Andino, R. Poliovirus vaccine vectors elicit antigen-specific cytotoxic T cells and protect mice against lethal challenge with malignant melanoma cells expressing a model antigen. *Proc Natl Acad Sci U S A.* **95**, 8216-21 (1998).
15. Ren, R. & Racaniello, V.R. Human poliovirus receptor gene expression and poliovirus tissue tropism in transgenic mice. *J Virol.* **66**, 296-304 (1992).

16. Bevan, M.J. Cross-priming for a secondary cytotoxic response to minor H antigens with H-2 congenic cells which do not cross-react in the cytotoxic assay. *J. Exp. Med.* **143**, 1283-1288 (1976).
17. Kovacsovics-Bankowski, M., Clark, K., Benacerraf, B. & Rock, K.L. Efficient major histocompatibility complex class I presentation of exogenous antigen upon phagocytosis by macrophages. *Proc. Natl. Acad. Sci. U.S.A.* **90**, 4942-6 (1993).
18. Kurts, C., Kosaka, H., Carbone, F.R., Miller, J.F. & Heath, W.R. Class I-restricted cross-presentation of exogenous self-antigens leads to deletion of autoreactive CD8(+) T cells. *J Exp Med.* **186**, 239-45 (1997).
19. Kurts, C., *et al.* Constitutive class I-restricted exogenous presentation of self antigens in vivo. *J Exp Med.* **184**, 923-30 (1996).
20. Reis e Sousa, C. & Germain, R.N. Major histocompatibility complex class I presentation of peptides derived from soluble exogenous antigen by a subset of cells engaged in phagocytosis. *J. Exp. Med.* **182**, 841-51 (1995).
21. Rock, K.L. & Clark, K. Analysis of the role of MHC class II presentation in the stimulation of cytotoxic T lymphocytes by antigens targeted into the exogenous antigen-MHC class I presentation pathway. *J Immunol.* **156**, 3721-6 (1996).
22. Albert, M.L., Sauter, B. & Bhardwaj, N. Dendritic cells acquire antigen from apoptotic cells and induce class I- restricted CTLs. *Nature.* **392**, 86-9 (1998).
23. Shen, Z., Reznikoff, G., Dranoff, G. & Rock, K.L. Cloned dendritic cells can present exogenous antigens on both MHC class I and class II molecules. *J. Immunol.* **158**, 2723-30 (1997).
24. Pfeifer, J.D., *et al.* Phagocytic processing of bacterial antigens for class I MHC presentation to T cells. *Nature.* **361**, 359-62 (1993).
25. Kovacsovics-Bankowski, M. & Rock, K.L. A phagosome-to-cytosol pathway for exogenous antigens presented on MHC class I molecules. *Science.* **267**, 243-6 (1995).
26. Ploegh, H.L. Viral strategies of immune evasion. *Science.* **280**, 248-53 (1998).
27. Sigal, L.J., Reiser, H. & Rock, K.L. The role of B7-1 and B7-2 costimulation for the generation of CTL responses in vivo. *J Immunol.* **161**, 2740-5 (1998).
28. Moore, M.W., Carbone, F.R. & Bevan, M.J. Introduction of soluble protein into the class I pathway of antigen processing and presentation. *Cell.* **54**, 777-85 (1988).

Figure Legends

Figure 1: The CTL responses to wild type vaccinia virus and OVA in recombinant vaccinia virus requires a bone-marrow-derived antigen presenting cell

a: CTL response to wild type vaccinia. The indicated bone-marrow chimeras were infected with $2x10^7$ plaque forming units of wild type vaccinia virus. One week later, mice were sacrificed and freshly explanted spleen cells were assayed in ^{51}Cr release assays on vaccinia infected MC57G cells (filled squares) or uninfected MC57G cells as controls (open circles). b: CTL response to OVA in vaccinia-OVA. The indicated bone-marrow chimeras were infected with $2x10^7$ plaque forming units of vaccinia-OVA. One week later, mice were sacrificed and their spleen cells were cultured in the presence of mitomycin C (MMC, Sigma) treated EG7 cells[28] (an EL-4 derived cell line stable transfected with OVA.) After five days cells were harvested an tested in ^{51}Cr release assays on EG7 targets (filled squares),or EL4 targets as controls(open circles).

Figure 2: $TAP^{0/0}$ → B6 mice can generate CTL responses comparable to those in B6 → B6 mice when antigen does not require processing

a: as in figure 1b but mice were infected with Vaccinia SS-SIINFEKL (for explanation of the construct see text). **b**: The indicated chimeric mice were immunized intravenously with the indicated numbers of B6-derived, *in vitro* cultured dendritic cells that had been incubated with 10 mg/ml SIINFEKL. CTL assays and symbols as in figure 1b. **c**: The

indicated chimeric mice were immunized intravenously with $5x10^5$ B6-derived, in vitro cultured dendritic cells that had been incubated with SIINFEKL peptide at the indicated concentrations. One week later mice were sacrificed and their spleen cells restimulated *in vitro* for four days with MMC treated EL4 cells that had been incubated with SIINFEKL. For each panel, symbol shapes represent individual mice. Targets were EL4 cells pre-incubated with SIINFEKL (filled symbols) or EL4 cells without peptide as controls (open symbols).

Figure 3: $TAP^{0/0}$ → B6 mice can generate MHC class II restricted responses comparable to those in B6 → B6 mice

a: production of IL-2 by lymph-node cells of immunized chimeras in response to different concentrations of OVA. Cells were from OVA immunized $TAP^{0/0}$ → B6 mice (filled squares) and B6 → B6 mice (open squares) or un-immunized controls (filled and open circles respectivelly). **b**: the same cells as in (**a**) were incubated with 0.5 mg/ml OVA in the prescence of the indicated antibody-containing supernatants. Only the results for immunized $TAP^{0/0}$ → B6 mice (filled columns) or B6 → B6 mice (open columns) are displayed.

Figure 4: Initiation of the CTL response to Polio-OVA requires the presence of bone-marrow-derived antigen presenting cells, but not their infection

Bone-marrow chimeras were infected with polio-OVA, polio-Sp27, or vaccinia SS-SIINFEKL as indicated. Three weeks later, mice were sacrificed and their spleen cells restimulated for five days in the presence of MMC treated EG7 cells and used in ^{51}Cr

release assays. **a**: Experiment using bone-marrow chimeras with cPVR B6 or B6 recipients as indicated. All panels correspond to a single experiment. Symbols as in Fig. 1b. **b**: Same as in (**a**), but using bone-marrow chimeras made with gPVR B6 mice as recipients.

Figure 1

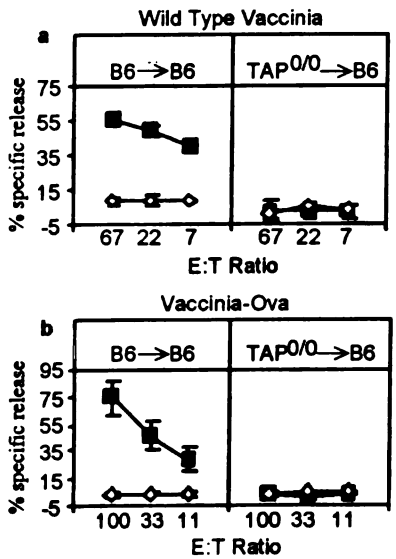
Wild Type Vaccinia
a
B6→B6
TAP0/0→B6
% specific release
75
55
35
15
-5
67 22 7
67 22 7
E:T Ratio
Vaccinia-Ova
b
B6→B6
TAP0/0→B6
% specific release
95
75
55
35
15
-5
100 33 11
100 33 11
E:T Ratio

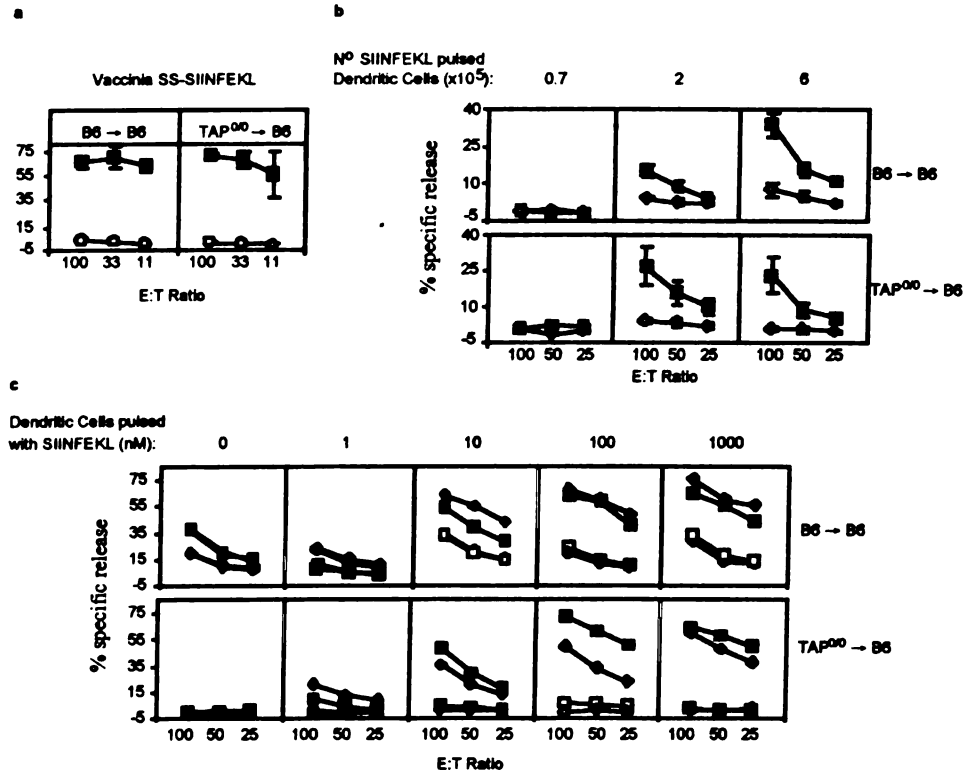
a
Vaccinia SS-SIINFEKL
B6 → B6
TAP0/0 → B6
75
55
35
15
-5
100 33 11
100 33 11
E:T Ratio
b
N° SIINFEKL pulsed
Dendritic Cells (x10^5):
0.7
2
6
% specific release
40
25
10
-5
B6 → B6
TAP0/0 → B6
100 50 25
E:T Ratio
c
Dendritic Cells pulsed
with SIINFEKL (nM):
0
1
10
100
1000
% specific release
75
55
35
15
-5
B6 → B6
TAP0/0 → B6
100 50 25
E:T Ratio

Figure 3

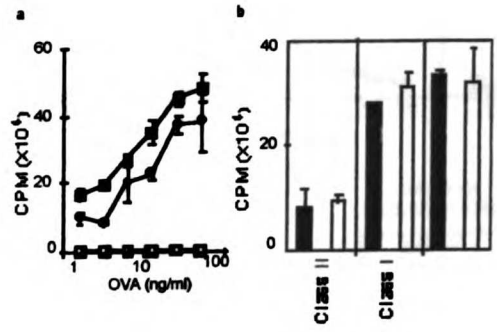
a
60
40
20
0
CPM (X10⁴)
1
10
100
OVA (ng/ml)
b
40
20
0
CPM (X10⁴)
Class II
Class I

Figure 4

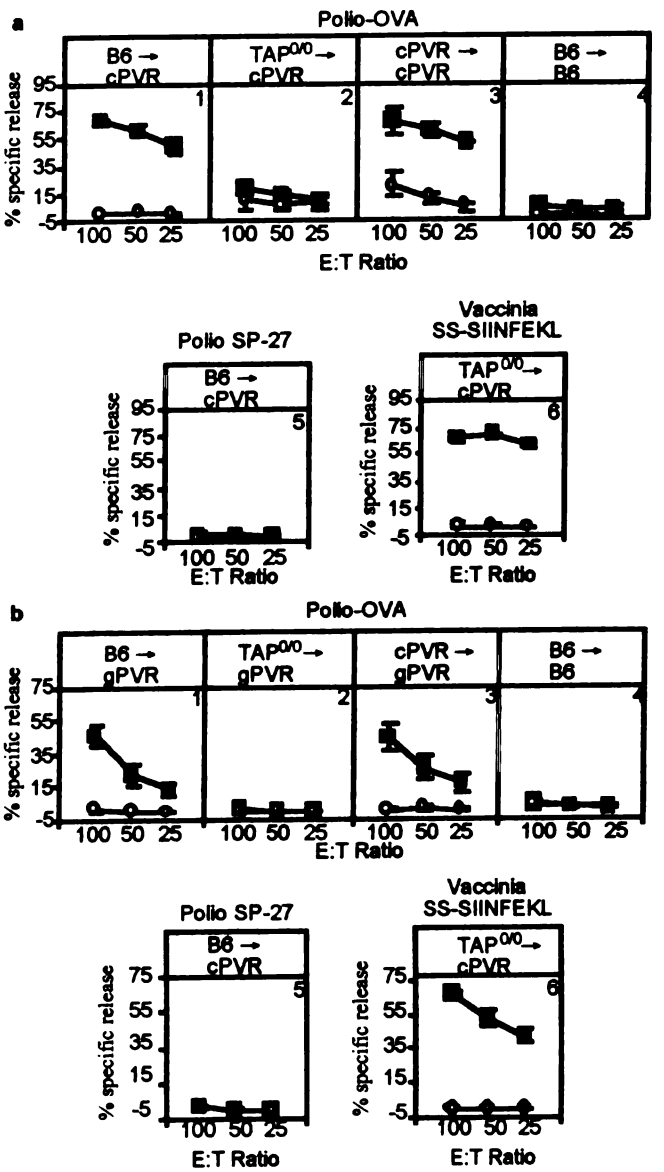
a
Polio-OVA
B6 → cPVR
TAP0/0 → cPVR
cPVR → cPVR
B6 → B6
% specific release
95
75
55
35
15
-5
100 50 25
E:T Ratio
Polio SP-27
Vaccinia SS-SIINFEKL
b
Polio-OVA
B6 → gPVR
TAP0/0 → gPVR
cPVR → gPVR
B6 → B6
Polio SP-27
Vaccinia SS-SIINFEKL

Chapter 12

A new poliovirus receptor (PVR) transgenic mouse susceptible to paralytic poliomyelitis via a mucosal route of infection

Abstract

Previously developed human poliovirus receptor (hPVR) transgenic mice are susceptible to poliovirus infection and develop paralytic poliomyelitis after intraperitoneal, intracerebral, or intramuscular inoculation. Viral replication is detectable in muscle, spinal cord, and brain. Notably and disappointingly, those transgenic mice are not susceptible to mucosal routes of infection, and do not replicate virus in the gastrointestinal tract of the mice. We hypothesized that limited tissue and cell type expression of Pvr protein in previously developed transgenic mice may have precluded mucosal infection. Therefore we constructed a PVR transgenic mouse line carrying a PVRδ cDNA driven by a β-actin promoter. We refer to this model as the cPVR mouse. The cPVR mice express Pvr in a variety of tissues (including small intestines, brain, spinal cord, muscle, blood, and liver) and are susceptible to infection after intraperitoneal, intracerebral, or intramuscular inoculation of poliovirus. After intraperitoneal inoculation, poliovirus replication is observed in cPVR muscle, brain, spinal cord, and notably small intestine. Surprisingly, cPVR mice are susceptible to paralysis following an intranasal

infection with poliovirus. After intranasal infection, virus replication is observed in the olfactory bulb, cerebrum, brain stem, and spinal cord, suggesting that intranasal infection of cPVR mice is a model for bulbar paralysis. Intranasally infected mice frequently display unusual neurological behaviors. The PVR transgenic mouse reported here provides the first available model for a mucosal route of infection with poliovirus.

Introduction

A PVR transgenic mouse was the first transgenic mouse model of a human viral pathogen (40). Those PVR transgenic mice are susceptible to poliovirus infection, and succumb to lethal paralytic poliomyelitis after intracerebral, intraspinal, intramuscular, or intraperitoneal inoculation of wild type poliovirus. Several additional PVR transgenic mouse lines have since been generated, all of which have similar phenotypes (13, 24, 53). Most experimental infections of PVR transgenic mice have been done using the Mahoney strain of type 1 poliovirus (24, 40, 53), but PVR transgenic mice are also susceptible to the other two serotypes of poliovirus: type 2 (41) and type 3 (1, 13). The PVR transgenic mice are much less susceptible to paralysis after inoculation with any of the Sabin poliovirus vaccine strain viruses, which mirrors viral pathogenesis in the natural human host (24, 40, 41). Unfortunately, none of these transgenic mice are susceptible to an oral route of infection with poliovirus (24, 40, 53), which is the natural route of poliovirus infection in humans.

Poliovirus infection in humans is characterized by fecal-oral transmission of the virus (though tracheal transmission is possible), with substantial viral replication in the gut of the infected individual, frequently for 4-8 weeks (29, 44). Most human poliovirus infections are subclinical, with a small percentage (10%) of infections resulting in flu-like symptoms, and infrequent cases of paralysis (~1%) (32, 44). Paralytic poliomyelitis is thought to occur when virus spreads to muscle tissue (possibly after a viremic phase), replicates, and then travels up motor neurons via retrograde transport. Paralytic

poliomyelitis is caused by destruction of motor neurons and is generally temporary. It is frequently characterized by paralysis in a single leg (in which presumably the most vigorous poliovirus infection of the musculature occurred). An acute phase of paralysis is observed for several weeks or months, normally subsequently followed by clearance of the poliovirus infection and recovery from paralysis (7, 14, 32, 44). Currently (as of 1999) 20,000 cases of paralytic poliomyelitis occur per year in the world, corresponding to an estimated two million total poliovirus infections annually (52). These numbers are rapidly decreasing due to extensive and heroic efforts by the World Health Organization to vaccinate the world population with the Sabin poliovirus vaccine (52).

Given that the natural route of human poliovirus transmission is fecal-oral, it has been disappointing that PVR transgenic mice are not susceptible to mucosal routes of infection. Additionally, though the PVR transgenic mice support poliovirus infection in most of the tissues that are thought to be susceptible in humans (namely, muscle, spinal cord, and brain), they do not support poliovirus infection in gut tissues (23, 38, 40, 53). In normal human poliovirus infections, however, the gut appears to be the site of greatest viral replication, as large quantities of virus are shed in human feces; and in experimentally inoculated chimpanzees the majority of infectious virus was isolated from the gastrointestinal tract (7, 32, 43, 44).

Studying transgenic mouse models of poliovirus infection and their reasons for inaccurately mimicking the disease in humans is important for several reasons. Poliovirus is a major virus model system, with excellent reverse genetics, biochemistry, and structural systems available; an accurate small animal model system would allow one to bring much more of this knowledge to bear on viral pathogenesis in vivo. Additionally, it

is important to develop a small animal model in which the natural replication and pathogenesis of the Sabin vaccine strain polioviruses can be studied in detail, as it is one of the best vaccines in the world and its cell type specific replication and immunogenicity are very poorly understood at the in vivo level. More generally, it has been difficult to generate accurate transgenic mouse models of any human infectious disease, as evidenced by the extensive efforts to develop mouse models of HIV and measles (6, 9, 19-21, 28, 31, 34, 37, 46). Experiences with PVR transgenic mice may shed light on generalities about the complexities of developing such model systems.

We therefore set out to generate a new PVR transgenic mouse line, which we refer to as cPVR mice, that might mirror human poliovirus pathogenesis more accurately than previous poliovirus transgenic mouse models.

Materials and Methods

DNA procedures and recombinant poliovirus construction. To construct pPVR7-1, human RNA was isolated from HeLa cells and RT-PCR was performed to generate PVR cDNA. The primers specifically amplified the shorter δ form membrane bound PVR isoform with a predicted 8 amino acid cytoplasmic tail. The δ PVR cDNA was cloned into the HindIII/SalI sites of a mammalian expression plasmid, pKS25, containing a 4.3 kb rat β-actin promoter, β-actin 5' UTR, and a 880 bp β-actin 3' UTR (Fig. 1A) in a pBluescript background (47, 49). This construct (pPVR7-1) was sequenced, and the PVRδ sequence was identical to that previously published (30). The XbaI-AflIII fragment of the plasmid was used for standard mouse embryonic stem cell microinjections (8).

Poliovirus stocks. Stocks of Mahoney type 1 poliovirus, Sabin 1 poliovirus, and Sabin 2 poliovirus were each generated from a molecular genomic cDNA clone in a plasmid. Mahoney type 1 poliovirus stocks were made from plasmid pXpA (36). Sabin 1 stocks were made from plasmid pS1, derived from Nomoto's molecular clone of Sabin 1 (33, 35), which we re-sequenced and modified the plasmid backbone in minor ways (S. Crotty et al., submitted). Sabin 2 stocks were made from plasmid pS2F, which was constructed and sequenced in our laboratory (S. Crotty et al., submitted) .

Poliovirus stocks were generated by linearization of the appropriate plasmid followed by T7 transcription and HeLa electroporation (18). Electroporated cells (P_0 viral stock) were grown on 6 cm plates in 3 ml of DMEM/F12 medium (Gibco) containing 10% FCS (Gibco), until lysis (approximately 12 h). Cells and supernatant were harvested,

freeze-thawed three times with dry ice-ethanol and 37° C baths, and supernatant was transferred to a fresh tube after the cellular debris was pelleted at 300g for 5 minutes. P_1 stocks were generated by infecting 50-80% confluent 10 cm dishes of HeLa cells with 1 x 10^4 PFU (MOI = 0.005). When 100% CPE was observed, cells and supernatant were harvested and freeze-thawed. Stocks were titered on HeLa cells as described (11). All passaging and titrations of Sabin 1 were done at 32° C; all passaging and titrations of Mahoney and Sabin 2 were done at 37° C.

Mice. cPVR mice were initially made and bred at the Gladstone Institute Transgenic Core facility in 1994, using standard microinjection techniques (8). The cPVR mice were later transferred to the UCSF specific-pathogen free Transgenic Mouse facility and have been continuously maintained there since. Currently the cPVR mice are at generation ~18. We will readily supply these cPVR mice to any research groups interested in using them. The cPVR mice are derived from an ICR outbred strain purchased from Simonsen (Gilroy, CA). Due to supply problems with Simonsen, we maintain our own colony of nontransgenic ICR mice (originally purchased from Simonsen) in the UCSF clean mouse facility as our controls. The gPVR mice (TgPVR1-17) (13, 38, 40) were the kind gift of V. Racaniello (Columbia University) and are maintained as a separate colony at UCSF. C57BL/6 mice were purchased from Charles River Laboratory, and CD1 mice were purchased from Jackson Laboratory (Bar Harbor, Maine). cPVR mice exhibited no unusual characteristics, physically or behaviorally, compared to nontransgenic ICR mice. cPVR mice are good breeders as both homozygotes (PVR^+/PVR^+) and heterozygotes (PVR^+/PVR^-), with normal litter sizes.

Genotyping and RT-PCR. Genomic DNA from tail bleeds (3) was used as template in PCR genotyping assays. PCR primers corresponding to positions 799-817 (GAGGCCACCCTGACCTGCG) and 983-1000 (GAGGTCCCTCTTTGACCT) (reverse complement) of the PVR open reading frame were used as forward and reverse primers respectively. PCR reactions used rTth polymerase (Perkin Elmer, Branchburg, NJ) with conditions as recommended by the manufacturer, with ~50 ng of template and 30 cycles of amplification.

For RNA analysis, tissues were removed from transgenic animals, snap frozen in a dry ice/EtOH bath, and frozen at -80 °C until ready for use. Tissues were then weighed, quickly thawed, and homogenized with an Ultra-Turrax T8 (IKA laboratory, USA) motorized disruptor, in cell lysis buffer (Qiagen). PolyA$^+$ RNA was isolated from homogenized tissue using a Qiagen polyA$^+$ RNA isolation kit. Approximately 10 μg RNA was isolated per 200 mg tissue, which was resuspended in 100 μl. Samples were DNase I (Roche) treated (10 U) at 37 °C for 1 hr to remove any contaminating genomic DNA. RNA quality was confirmed by gel electrophoresis. cDNA was synthesized using Superscript II (Life Technologies) with random hexamer primers and 1 μg RNA as template. PVR PCR was done as described above, except for 40 cycles. PCR for 18S RNA expression was done from the cDNA as a positive control, and from the polyA$^+$ RNA as a negative control, using mouse 18S primers obtained from Ambion, Inc. (Austin, Texas).

Fluorescence Activated Cells Sorting (FACS) analysis. Spleen cells from the indicated mice were depleted of red blood cells by hypotonic lysis. The remaining white cells were counted, and washed twice in FACS staining buffer (PBS containing 2% FCS and 0.04%

sodium azide). For primary labeling, the cells were incubated in 100 µl of FACS staining buffer containing the anti-PVR monoclonal antibody D171 (a kind gift from Dr. Eckard Wimmer) or, as controls, the MHC I anti-H-2K^b mAb Y3 or an irrelevant mouse anti-chicken ovalbumin. MC57G-PVR was a mouse cell line stably transfected with the pPVR7-1 expression construct, and this cell line was used as a positive control for Pvr expression on mouse cells. Following incubation with the primary antibody, the cells were washed twice and incubated in 100 µl of FACS staining buffer containing as secondary antibody FITC labeled goat anti-mouse IgG, gamma chain specific (KPL), at a final dilution of 1/300. Finally, the splenocytes where washed twice with PBS and resuspended in 200 µl of 0.5% paraformaldehyde in PBS. The stained cells were analyzed for fluorescence using a FacsCalibur apparatus and the Cellquest program (both from Beckton Dickinson).

Poliovirus infections. All of the poliovirus infections reported in this study used 6-8 week old adult mice, unless otherwise indicated.

Intramuscular inoculations were done as 50 µl injections into the thigh of the right hind leg using a 26 gauge syringe. Intraperitoneal inoculations were done as 100-300 µl injections using a 26 gauge syringe. Intracerebral inoculations were done in anesthesized animals (200 µl Avertin injected intraperitoneally in adult animals) as 15-30 µl injections into the mid-brain (between the ears of the mouse, along the skull midline) using a 27 3/4 gauge syringe. (In 10 week old mice, intracerebral inoculations were done into the same region from the left temple, on the side of the head, because the skullcap was too thick to penetrate consistently.) Intravenous inoculations were done as 200 µl tail vein injections using a 28 gauge syringe after warming the mice for 20' under a heating lamp and

topically treating the tail with 70% isopropanol. Intragastric inoculations of 100 µl were done using a steel 2" long round-balled gavage (a curved needle with a rounded end) attached to a syringe. The gavage tube was inserted down the throat of the mouse to the stomach, at which point the 100 µl volume was released and the gavage retracted from the mouse. Oral infections were done in a 50 µl volume by depositing the inoculum into the mouth using a standard 200 µl micropipetter. Intranasal inoculations were done in mice briefly sedated with Halothane (but not fully unconscious) (Halocarbon Laboratories, River Edge, NJ). 7.5 µl of virus inoculum was placed at the opening of each nostril sequentially using a micropipetter. The pipet tip was not inserted into the nostril, and generally did not come in direct contact with the skin. Rapid breathing of the mouse led to the 15 µl inoculum being rapidly sucked up into the nose. Mice were active and alert again within two minutes. Rectal inoculations were done as 100 µl (in cPVR mice) or 50 µl (in C57BL/6 and derivatives) injections using a micropipetter with a fine plastic tip ("yellow tip") coated with a thin layer of vaseline. Mice were fasted for 3-4 days and then anaesthetized with Avertin (see above) and the inoculating pipet tip was slowly inserted ~0.5-1.5 cm into the rectum of a prone animal. The inoculum was then slowly released and the tip withdrawn. This technique was pilot tested using trypan blue as an indicator. Trypan blue was injected rectally, and mice were sacrificed two hours later. Trypan blue was present throughout the colon and large intestine, though did not appear to go into the small intestines of the mice. No bleeding or tearing of the colon wall was observed, and the presence or absence of feces in the colon did not grossly affect the spread of the trypan blue.

A series of LD_{50} experiments (intracerebral, intramuscular, and intraperitoneal inoculations) was also done using cPVR x C57BL/6 F1 mice, with comparable LD_{50} results to that obtained when using homozygous cPVR mice (data not shown).

In pathogenesis experiments, all mice inoculated with poliovirus or PBS (control) were observed for at least 21 days for signs of disease: lethargy, ruffled fur, arched back, flaccid paralysis of a limb or back region, and death.

Tissue isolations and virus quantification. For tissue tropism experiments, mice were sacrificed every 24 hr and tissues were removed surgically. Whole tissues were stored at -80° C until a series of samples were collected. Tissues were weighed and then homogenized in phosphate-buffered saline containing penicillin/streptomycin using a Ultra-Turrax T8 (IKA laboratory, USA) motorized homogenizer. Samples were then frozen at -20° C for long term storage. Poliovirus was quantified in these tissue samples by plaque assay on HeLa cells in 6-well plates. Tissue from at least three cPVR mice and 2 ICR mice was used for each data point, and the graphed data (Fig. 3) represents the average titer from the multiple samples. At least six cPVR mice were used for most timepoints for tissues that exhibited poliovirus replication (muscle, spinal cord, brain, small intestine).

Results

cPVR mouse construction and transgene expression

Prior to this study, there were three previous major PVR transgenic mouse lines available. The laboratories of Racaniello and Nomoto each developed several lines of transgenic mice containing multiple copies of the human PVR locus integrated into the mouse genome (13, 24, 40). We currently refer to Racaniello's TgPVR-17 mice as gPVR mice and have used them in several studies (26, 27, 45, 48). The mouse lines based on the genomic PVR locus express all four isoforms of Pvr, two membrane bound and two soluble receptors, in varying amounts, driven by the natural human PVR promoter. In transgenic mice, the natural human PVR promoter drives substantial amounts of PVR RNA and Pvr protein expression in the brain, muscle, spinal cord, lung, and genitalia. Ten-fold lower levels are expressed in tissues such as small intestine, lung, and kidney, with undetectable amounts of RNA in liver and spleen (13, 24). It was reasoned that these lower levels of expression may limit poliovirus infection in some mouse tissues or cell types and prevent the mice from being orally susceptible to poliovirus. Therefore, Zhang and Racaniello developed a PVR transgenic mouse line (TgFABP-PVR) expressing Pvr from an intestinal epithelium specific promoter; but in spite of the good expression, that mouse was also unsusceptible to oral poliovirus infection (53). The authors did confirm that Pvr was expressed on the surface of M cells and gut epithelial cells in that mouse line, and that TgFABP-PVR mice were susceptible to intracerebral infection with poliovirus (53).

We reasoned that the lack of expression of membrane bound Pvr on certain unidentified intestinal or lymphatic cell types (i.e., peyer's patch residents) may be the reason that none of the previous PVR transgenic mice lines were orally susceptible to poliovirus infection. Therefore, we set out to generate a transgenic mouse that expresses membrane bound Pvr in a wide range of cell types. Human RNA was isolated and RT-PCR was performed to generate PVR cDNA. The primers specifically amplified the shorter δ form membrane bound PVR isoform with a predicted 8 amino acid cytoplasmic tail. The δ PVR cDNA was cloned into a mammalian expression plasmid containing a β-actin promoter, β-actin 5' UTR, and β-actin 3' UTR (Fig. 1A). This construct was sequenced and then used to generate an ICR transgenic mouse line using standard embryonic stem cell technology (8). Founder mice were screened for the presence of transgene by PCR, and two positive mice were used to generate a homozygous PVR^{+}/PVR^{+} mouse line which we call cPVR, referring to the fact that this mouse has the PVR gene as an intron-less cDNA. Mice are genotyped using PCR primers specific for PVRδ cDNA sequence (Fig. 1B).

The β-actin promoter was expected to drive near universal expression of the transgene. RT-PCR was done to determine the expression of PVR RNA in various tissues (Fig. 2A). PVR RNA was detected in brain, brain stem, spinal cord, blood, liver, small intestine, and muscle. Very low levels were detected in kidney. This distribution of expression was different than that for gPVR and Nomoto's PVRTg1 mice, notably the presence of PVR expression in liver (13, 23), spleen (13), and intestine (24). Though we did not attempt to identify Pvr protein in a series of different tissues, expression likely

closely parallels the RNA expression profile, as the cDNA is flanked by β-actin 5' and 3'UTRs.

We carried out a series of FACS analyses in F1 crosses of cPVR x C57BL/6 to show that Pvr was detectable in significant quantities on the surface of cPVR splenocytes, containing populations of lymphocytes and macrophages among other cell types (Fig. 2B). Expression of Pvr was detected on the surface of the splenocytes, with a median fluorescent intensity 11-fold higher than background staining in C57BL/6. MC57G-PVR, a mouse cell line stably transfected with PVR, was used as a positive control.

Poliomyelitis in cPVR mice

We tested all of the classic routes of inoculation of wild type poliovirus in these mice. The results are displayed in Table 1. The cPVR mice are susceptible to lethal poliomyelitis following intracerebral (i.c.), intramuscular (i.m.), intraperitoneal (i.p.), and intravenous (i.v.) infection. Disappointingly, these mice are not susceptible to poliomyelitis following oral or intragastric inoculation of up to 1×10^9 PFU. Unlike the other PVR transgenic mouse lines available, cPVR mice display greater susceptibility to intramuscular inoculation with poliovirus than to intracerebral inoculation. In adult mice (6 to 8 weeks old), after intramuscular inoculation the cPVR mice develop a rapid paralysis (2-5 days) and generally die within 3-6 days at the LD_{50} of 2×10^5 PFU. Paralysis was consistently seen in the leg that was inoculated. Intracerebral poliovirus inoculation of cPVR mice led to a slower paralysis with a 20-fold higher LD_{50} than intramuscular infection. Paralysis after intracerebral inoculation was generally observed in 5-13 days. Intraperitoneal infection had an LD_{50} of 1×10^8 in cPVR mice, with

paralysis and death seen in 3-7 days post-infection. Generally this paralysis presented as a flaccid uni- or bilateral paralysis of the hindlegs in conjunction with flaccid paralysis of the lower back. Intravenous poliovirus infection had a similar LD_{50} of 2×10^8, presenting as a flaccid paralysis of the lower back at approximately day 5 (Table 1). It was quite rare for any animal not to die within a couple of days of the onset of paralysis, but approximately 5% of paralyzed mice do survive the infection and can survive with permanent paralysis of a hindleg or the lower back for at least 6 more months in good health. This is in contrast to the pathogenesis of the virus in humans, where most cases of paralysis are transient (that is, the person regains use of the paralyzed limb) and few are permanent or lethal (32, 44).

We analyzed the tissue tropism of wild type poliovirus in cPVR mice after intraperitoneal inoculation. Mice were inoculated with 5×10^8 PFU wild type poliovirus (Mahoney strain) and then daily tissue samples were taken from a series of infected mice. The amount of poliovirus present in each tissue was quantified by plaque assay. After intraperitoneal infection with poliovirus, there is a rapid decline in circulating virus in non-transgenic ICR mice and the virus is completely cleared from most tissues by day 2 post-inoculation (Fig. 3). In the cPVR mice, poliovirus is readily detected in small intestine, spinal cord, muscle, and brain tissue beginning on days 1, 2, 2, and 3 post-infection respectively, and the virus is present in each of those tissues on all days thereafter (Fig. 3, A-D). We observed significant variability in muscle titers between individual mice (ranging from 3 PFU to 45,000 PFU/mg on day 4, data not shown), resulting in large daily variations in the average muscle titer (Fig. 3B). Virus was not detected at significant levels in kidney or blood (Fig. 3, E-F), or lung, heart, spleen, or

liver (data not shown). The maximum poliovirus titers (starting at day 2) detected in various cPVR and ICR mouse tissues after intraperitoneal inoculation are shown in Figure 4A for direct comparison. Spinal cord and muscle supported the highest levels of virus replication, with maximum titers (averaged across all animals on a given day post-infection) reaching 38,500 PFU/mg in spinal cord and 12,500 PFU/mg in muscle. Brain reached a maximum titer approximately 10-fold lower (1700 PFU/mg) and small intestine reached maximum titers 25% that of brain (501 PFU/mg).

We were intrigued by the presence of substantial poliovirus titers in cPVR small intestine, as this had not been reported with previous transgenic mice. Therefore we compared the poliovirus titers found in small intestine after intraperitoneal inoculation of cPVR, ICR, gPVR, and C57BL/6 (a nontransgenic control for gPVR) mice. We found that gPVR and C57BL/6 had comparable amounts of residual virus in small intestine on day 1 post-inoculation (10-100 PFU/mg), and no detectable level of virus on any day thereafter (< 1 PFU/mg). As in the previous experiment, we found substantially higher levels of poliovirus in cPVR mice than ICR mice, most strikingly on day 2, where cPVR mice had 500 PFU/mg, compared with background levels of 1.5 PFU/mg in nontransgenic ICR mice (Fig. 4B). For simplicity, the data is graphed as the amount of virus detected in the transgenic mice (cPVR or gPVR) after subtracting out the amount of virus detected in the nontransgenic control mice (ICR and C57BL/6 respectively).

Intranasal susceptibility

Interestingly, cPVR mice are susceptible to poliovirus infection via an intranasal route of inoculation. Adult cPVR mice develop a lethal paralysis within 5-8 days

following intranasal infection with 5 x 10^8 PFU poliovirus. These mice frequently display an atypical poliomyelitis, showing a highly arched back and neurological disorders in 4-8 days. Some mice become antisocial, display a lack of coordination, walk in tight circles, or exhibit head or forelimb twitches. We determined that the intranasal infection LD_{50} was 5 x 10^7 PFU (Fig. 5). cPVR mice are therefore more sensitive to paralysis following intranasal infection than intravenous infection.

We then examined poliovirus tissue tropism following intranasal inoculation, in two experiments. The first experiment involved intranasal inoculation of cPVR mice with a sublethal dose of poliovirus. High levels of virus were observed strictly in the olfactory bulb of the mice (Fig. 6A). Replication was not observed in the rest of the brain (cerebrum, cerebellum, brainstem), spinal cord, lungs, or intestines. Virus was observed for ~7 days before clearance.

In the second experiment, mice were intranasally inoculated with a lethal dose of poliovirus. Virus was observed at very high titers in the olfactory bulb early in infection (1 x 10^6 PFU/mg at day 3), with fairly constant levels of virus observed in the main body of the brain throughout the course of the experiment (1 x10^4 - 1 x 10^5 PFU/mg) (Fig. 6B). Strikingly, virus was not observed at all in the spinal cord until day 5 post-infection, after which very high titers were observed (1 x 10^7 PFU/mg) that closely correlated with the onset of clinical disease and paralysis in the animals.

Phenotype of Sabin poliovirus vaccine strains in cPVR mice

As anticipated, the attenuated Sabin poliovirus vaccine strains Sabin 1 and Sabin 2 are both highly attenuated in cPVR (Table 2). No adult cPVR mice were paralyzed at

the maximum dose of Sabin vaccine strain virus that we could inoculate by any route. The LD_{50} after intramuscular inoculation with Sabin 1 strain is at least 2000x higher than that for wild type poliovirus. The LD_{50} after intracerebral inoculation with Sabin 1 is at least 50x higher than wild type (Table 2). Sabin 2 was also highly attenuated, at least 150x less neurovirulent than wildtype after i.m. inoculation (Table 2).

Discussion

Pvr is expressed in a wide variety of tissues in cPVR mice, driven by a heterologous promoter, but poliovirus only replicates in select tissues in the cPVR mice. We found this somewhat surprising, and were further surprised to see, after intravenous or intraperitoneal inoculation, poliovirus replicated only in the tissues where it replicates in humans—muscle, spinal cord, brain, and intestine. This shows that the poliovirus receptor is necessary but not sufficient to confer susceptibility to poliovirus infection *in vivo*, and that there are additional cell type and tissue type specific post-entry blocks to translation, replication, and/or packaging. The cell tropism of HIV has been studied more extensively than any other virus, and it has been determined that, in the mouse, HIV requires the expression of at least four human proteins to allow a full HIV replication cycle, and three of those factors have been identified. CD4 (12, 22, 25) and the co-receptor CXCR4 or CCR5 are required for viral entry (10, 15). HIV also requires an intracellular factor, the TAR binding protein cyclin T1 (hCycT1), that is crucial for mediating Tat's activation of HIV transcription elongation (5, 50). As murine cells expressing CD4, CCR5, and hCycT1 do not support the full HIV life cycle (4, 17), there is at least one additional human factor missing in mice. Poliovirus appears to require the intracellular factors PCBP, La, Unr, PTB, and PABP for translation and replication (2, 16)(Herold and Andino, in press), but their tissue expression and effects on tissue tropism are unknown.

Oral resistance

We do not know why PVR transgenic mice continue to be resistant to oral infection with poliovirus. We attempted to infect the mice intrarectally to circumvent the possibility that the gastric environment of mice was somehow inhospitable to poliovirus (be it pH, the presence of a certain digestive enzyme, or the presence of an inactivating small molecule). But the mice (both cPVR and gPVR) were resistant to poliovirus infection following intrarectal inoculation (Table 1). The fact that we observed poliovirus titers in cPVR small intestine after intraperitoneal inoculation (Fig. 3, 4B) indicates that the problem may be the apical surface of the intestine. We propose three hypotheses to explain the failure of small intestine infection from the luminal/apical side: 1) Poliovirus may not infect human intestinal epithelium but simply be transported through human M cells, and mice lack factors required for efficient transcytosis of poliovirus particles through M cells; 2) Pvr does not receive a post-translational modification (i.e. glycosylation) necessary for poliovirus entry in the target gastrointestinal cell type; or 3) there may be cellular factors in mouse intestinal cells different than in human cells that either block or fail to support poliovirus replication. Data and theories of Zhang and Racaniello using TgFABP-PVR mice are consistent with these proposals (53). Additionally, it has recently been reported that the innate immune system can determine tissue tropism, as interferon α/β receptor knockout mice show a massive expansion in the tissue tropism of sindbis virus (42). Whether aspects of the innate immune system are important for poliovirus tissue tropism is unknown, but it is a possible factor in the resistance of PVR transgenic mice to oral infection.

The presence of poliovirus titers in cPVR mouse small intestine is significant because it would be valuable to have a small animal model where the replication and

tropism of the Sabin oral poliovirus vaccine (OPV) can be studied. Our results indicate that the mouse intestine can support poliovirus replication, and the cPVR mouse model should hopefully allow for an analysis of Sabin virus replication and spread in vivo.

Poliovirus spread

Data from all of our infection experiments was compiled and analyzed to develop a working model of poliovirus replication and spread in cPVR mice. Virus is first seen in the small intestine after intraperitoneal or intravenous inoculation. The virus then rapidly spreads to muscle, spinal cord, and brain. Paralysis and death is closely correlated with high viral titers in spinal cord. It does not appear that replication in muscle is obligatory for spread to the CNS in cPVR mice, as replication is detected in the CNS in several cPVR mice without any detectable titers in muscle (data not shown). However, this could be due to "hidden" replication in muscle tissue that we did not biopsy. Alternatively, the virus presumably may directly infect peripheral nerves accessible in the peritoneal cavity. Notably, cPVR mice are most susceptible to paralysis after intramuscular inoculation of poliovirus (Table 1).

Retrograde axonal transport appears to be very rapidly utilized by poliovirus (39), as evidenced in cPVR mice by the rapid paralysis and death after intramuscular inoculation. The virus likely replicates in the muscle tissue, infects neurons at the neuromuscular junctions, and then utilizes the cellular active retrograde transport system to quickly reach motor neurons of the spinal cord. Forward axonal transport appears to be poorly used, if at all, by poliovirus, as evidenced by the long lag time to paralysis after intracerebral or intranasal inoculation. The surprisingly difference in the time to paralysis between intramuscular and intracerebral infection suggests that virus in the cerebrospinal

fluid in the brain (deposited in the ventricles during injection of the virus inoculum) is unable to infect accessible cells in the spinal cord during circulation. Instead the virus uses cell to cell spread via neuronal dendrits and axons to move through the brain to the motor neurons of the spinal cord. But since the infection spreads so slowly in this direction it appears that the virus does not have the capacity to use active forward axonal transport and must instead rely on passive diffusion. This theory is supported by the observation that after intranasal inoculation the virus quickly spreads through the olfactory bulb to the cerebellum, but spreads slowly thereafter. Olfactory neurons are oriented such that transport from the nasal cavity to the cerebrum is retrograde axonal transport. Once the virus accesses the cerebrum after infection via the olfactory pathway, it is forced to use forward transport or diffusion to spread to the spinal cord. As mentioned above, given the long time lag to paralysis following intracerebral inoculation, though the virus efficiently uses active retrograde transport it does not appear to be able to utilize forward axonal transport mechanisms.

It is also possible that the virus accesses the CNS by entering the bloodstream after intraperitoneal inoculation and then trafficking across the blood-brain barrier, but that is unlikely for three reasons: 1) intracerebral inoculation (which accesses the cerebrospinal fluid) has a long time lag before paralysis; 2) the LD_{50} after intravenous inoculation is similar to the LD_{50} after intraperitoneal inoculation, therefore the quantity of virus in the blood does not appear to be an indicator for subsequent paralysis; and 3) we do not see a viremic phase of infection after intraperitoneal inoculation.

Mucosal route of infection

The cPVR mouse model reported here is the first description of a small animal model of poliovirus that is susceptible to a mucosal route of infection. This result is significant because poliovirus is transmitted mucosally in humans, and the very successful Sabin oral poliovirus vaccine (OPV) elicits a highly protective mucosal immune response that is poorly understood. Possessing a mouse susceptible to a mucosal route of poliovirus infection should allow us to examine and test aspects of OPV-elicited protective mucosal immunity.

Interestingly, the intranasal infection of cPVR mice appears to be comparable to intranasal infection of cynomolgus macaque monkeys, which leads to "bulbar paralysis" following rapid, extensive replication in the olfactory bulb. Whether this alternative route of infection exists in humans remains unclear. Though infection via the olfactory pathway has been predicted not to occur in humans (43), too few poliomyelitis autopsies examining the location of viral plaques in the brain have been performed to establish that olfactory pathway infection does not occur in a small minority of cases (14).

The cPVR mice are useful for a variety of studies. We have used these mice to identify poliovirus-specific CTLs (45), and we are pursuing additional immunological studies in these mice. These mice should also be a useful model system for studying poliovirus replication in the small intestines, and Sabin vaccine virus cell tropism and replication *in vivo*. Additionally, the World Health Organization has recently approved the use of transgenic mice to assess the safety of manufactured lots of live attenuated poliovirus vaccine, by direct intraspinal inoculation of Sabin vaccine samples (51). We are exploring the possibility that cPVR mice might be useful in similar assays.

References

1. **Abe, S., Y. Ota, Y. Doi, A. Nomoto, T. Nomura, K. M. Chumakov, and S. Hashizume** 1995. Studies on neurovirulence in poliovirus-sensitive transgenic mice and cynomolgus monkeys for the different temperature-sensitive viruses derived from the Sabin type 3 virus Virology. **210:**160-6.
2. **Andino, R., N. Boddeker, D. Silvera, and A. V. Gamarnik** 1999. Intracellular determinants of picornavirus replication Trends Microbiol. **7:**76-82.
3. **Ausubel, F. M.** 1995. Current protocols in molecular biology. Published by Greene Pub. Associates and Wiley-Interscience : J. Wiley, New York.
4. **Bieniasz, P. D., and B. R. Cullen** 2000. Multiple Blocks to Human Immunodeficiency Virus Type 1 Replication in Rodent Cells J Virol. **74:**9868-9877.
5. **Bieniasz, P. D., T. A. Grdina, H. P. Bogerd, and B. R. Cullen** 1998. Recruitment of a protein complex containing Tat and cyclin T1 to TAR governs the species specificity of HIV-1 Tat Embo J. **17:**7056-65.
6. **Blixenkrone-Moller, M., A. Bernard, A. Bencsik, N. Sixt, L. E. Diamond, J. S. Logan, and T. F. Wild** 1998. Role of CD46 in measles virus infection in CD46 transgenic mice Virology. **249:**238-48.
7. **Bodian, D.** 1955. Emerging concept of poliomyelitis infection Science. **122:**105-108.
8. **Brinster, R. L., H. Y. Chen, M. E. Trumbauer, M. K. Yagle, and R. D. Palmiter** 1985. Factors affecting the efficiency of introducing foreign DNA into mice by microinjecting eggs Proc Natl Acad Sci U S A. **82:**4438-42.
9. **Browning, J., J. W. Horner, M. Pettoello-Mantovani, C. Raker, S. Yurasov, R. A. DePinho, and H. Goldstein** 1997. Mice transgenic for human CD4 and CCR5 are susceptible to HIV infection Proc Natl Acad Sci U S A. **94:**14637-41.
10. **Choe, H., M. Farzan, Y. Sun, N. Sullivan, B. Rollins, P. D. Ponath, L. Wu, C. R. Mackay, G. LaRosa, W. Newman, N. Gerard, C. Gerard, and J. Sodroski** 1996. The beta-chemokine receptors CCR3 and CCR5 facilitate infection by primary HIV-1 isolates Cell. **85:**1135-48.
11. **Crotty, S., B. L. Lohman, F. X. Lu, S. Tang, C. J. Miller, and R. Andino** 1999. Mucosal immunization of cynomolgus macaques with two serotypes of live poliovirus vectors expressing simian immunodeficiency virus antigens: stimulation of humoral, mucosal, and cellular immunity J Virol. **73:**9485-95.
12. **Dalgleish, A. G., P. C. Beverley, P. R. Clapham, D. H. Crawford, M. F. Greaves, and R. A. Weiss** 1984. The CD4 (T4) antigen is an essential component of the receptor for the AIDS retrovirus Nature. **312:**763-7.
13. **Deatly, A. M., R. E. Taffs, J. M. McAuliffe, S. P. Nawoschik, J. W. Coleman, G. McMullen, C. Weeks-Levy, A. J. Johnson, and V. R. Racaniello** 1998. Characterization of mouse lines transgenic with the human poliovirus receptor gene Microbial Pathogenesis. **25:**43-54.

14. **Faber, H. K.** 1955. The pathogenesis of poliomyelitis, 1st ed. Charles C. Thomas, Springfield, Illinois.
15. **Feng, Y., C. C. Broder, P. E. Kennedy, and E. A. Berger** 1996. HIV-1 entry cofactor: functional cDNA cloning of a seven-transmembrane, G protein-coupled receptor [see comments] Science. **272**:872-7.
16. **Gamarnik, A. V., and R. Andino** 1996. Replication of poliovirus in Xenopus oocytes requires two human factors Embo Journal. **15**:5988-98.
17. **Garber, M. E., P. Wei, V. N. KewalRamani, T. P. Mayall, C. H. Herrmann, A. P. Rice, D. R. Littman, and K. A. Jones** 1998. The interaction between HIV-1 Tat and human cyclin T1 requires zinc and a critical cysteine residue that is not conserved in the murine CycT1 protein Genes Dev. **12**:3512-27.
18. **Gohara, D. W., S. Crotty, J. J. Arnold, J. D. Yoder, R. Andino, and C. E. Cameron** 2000. Poliovirus RNA-dependent RNA Polymerase ($3D^{Pol}$): Structural, biochemical, and biological analysis of conserved structural motifs A and B Journal of Biological Chemistry. **275**:25523-25532.
19. **Hanna, Z., D. G. Kay, N. Rebai, A. Guimond, S. Jothy, and P. Jolicoeur** 1998. Nef harbors a major determinant of pathogenicity for an AIDS-like disease induced by HIV-1 in transgenic mice Cell. **95**:163-75.
20. **Horvat, B., P. Rivailler, G. Varior-Krishnan, A. Cardoso, D. Gerlier, and C. Rarourdin-Combe** 1996. Transgenic mice expressing human measles virus (MV) receptor CD46 provide cells exhibiting different permissivities to MV infections J Virol. **70**:6673-81.
21. **Jamieson, B. D., and J. A. Zack** 1999. Murine models for HIV disease Aids. **13**:S5-11.
22. **Klatzmann, D., E. Champagne, S. Chamaret, J. Gruest, D. Guetard, T. Hercend, J. C. Gluckman, and L. Montagnier** 1984. T-lymphocyte T4 molecule behaves as the receptor for human retrovirus LAV Nature. **312**:767-8.
23. **Koike, S., H. Horie, Y. Sato, I. Ise, C. Taya, T. Nomura, I. Yoshioka, H. Yonekawa, and A. Nomoto** 1993. Poliovirus-sensitive transgenic mice as a new animal model Dev Biol Stand. **78**:101-7.
24. **Koike, S., C. Taya, T. Kurata, S. Abe, I. Ise, H. Yonekawa, and A. Nomoto** 1991. Transgenic mice susceptible to poliovirus Proc Natl Acad Sci U S A. **88**:951-5.
25. **Maddon, P. J., A. G. Dalgleish, J. S. McDougal, P. R. Clapham, R. A. Weiss, and R. Axel** 1986. The T4 gene encodes the AIDS virus receptor and is expressed in the immune system and the brain Cell. **47**:333-48.
26. **Mandl, S., L. Hix, and R. Andino** 2001. Preexisting immunity to poliovirus does not impair the efficacy of recombinant poliovirus vaccine vectors [In Process Citation] J Virol. **75**:622-7.
27. **Mandl, S., L. J. Sigal, K. L. Rock, and R. Andino** 1998. Poliovirus vaccine vectors elicit antigen-specific cytotoxic T cells and protect mice against lethal challenge with malignant melanoma cells expressing a model antigen Proceedings of the National Academy of Sciences of the United States of America. **95**:8216-21.
28. **McCune, J. M.** 1997. Animal models of HIV-1 disease Science. **278**:2141-2.

29. **Melnick, J. L.** 1996. Enteroviruses: Polioviruses, coxsackieviruses, echoviruses, and newer enteroviruses, p. 655-712. *In* B. N. Fields, D. M. Knipe, and P. M. Howley (eds), Fields virology, 3rd ed, vol. 1. Lippincott-Raven Publishers, Philadelphia.
30. **Mendelsohn, C. L., E. Wimmer, and V. R. Racaniello** 1989. Cellular receptor for poliovirus: molecular cloning, nucleotide sequence, and expression of a new member of the immunoglobulin superfamily Cell. **56:**855-65.
31. **Mrkic, B., J. Pavlovic, T. Rulicke, P. Volpe, C. J. Buchholz, D. Hourcade, J. P. Atkinson, A. Aguzzi, and R. Cattaneo** 1998. Measles virus spread and pathogenesis in genetically modified mice J Virol. **72:**7420-7.
32. **Nathanson, N., and R. Ahmed** 1997. Viral pathogenesis. Lippincott-Raven, Philadelphia.
33. **Nomoto, A., T. Omata, H. Toyoda, S. Kuge, H. Horie, Y. Kataoka, Y. Genba, Y. Nakano, and N. Imura** 1982. Complete nucleotide sequence of the attenuated poliovirus Sabin 1 strain genome Proc Natl Acad Sci U S A. **79:**5793-7.
34. **Oldstone, M. B., H. Lewicki, D. Thomas, A. Tishon, S. Dales, J. Patterson, M. Manchester, D. Homann, D. Naniche, and A. Holz** 1999. Measles virus infection in a transgenic model: virus-induced immunosuppression and central nervous system disease Cell. **98:**629-40.
35. **Omata, T., M. Kohara, Y. Sakai, A. Kameda, N. Imura, and A. Nomoto** 1984. Cloned infectious complementary DNA of the poliovirus Sabin 1 genome: biochemical and biological properties of the recovered virus Gene. **32:**1-10.
36. **Racaniello, V. R., and D. Baltimore** 1981. Cloned poliovirus complementary DNA is infectious in mammalian cells Science. **214:**916-9.
37. **Rall, G. F., M. Manchester, L. R. Daniels, E. M. Callahan, A. R. Belman, and M. B. Oldstone** 1997. A transgenic mouse model for measles virus infection of the brain Proc Natl Acad Sci U S A. **94:**4659-63.
38. **Ren, R., and V. R. Racaniello** 1992. Human poliovirus receptor gene expression and poliovirus tissue tropism in transgenic mice Journal of Virology. **66:**296-304.
39. **Ren, R., and V. R. Racaniello** 1992. Poliovirus spreads from muscle to the central nervous system by neural pathways Journal of Infectious Diseases. **166:**747-52.
40. **Ren, R. B., F. Costantini, E. J. Gorgacz, J. J. Lee, and V. R. Racaniello** 1990. Transgenic mice expressing a human poliovirus receptor: a new model for poliomyelitis Cell. **63:**353-62.
41. **Ren, R. B., E. G. Moss, and V. R. Racaniello** 1991. Identification of two determinants that attenuate vaccine-related type 2 poliovirus Journal of Virology. **65:**1377-82.
42. **Ryman, K. D., W. B. Klimstra, K. B. Nguyen, C. A. Biron, and R. E. Johnston** 2000. Alpha/beta interferon protects adult mice from fatal Sindbis virus infection and is an important determinant of cell and tissue tropism J Virol. **74:**3366-78.
43. **Sabin, A. B.** 1956. Pathogenesis of poliomyelitis Science. **123:**1151-1157.
44. **Sabin, A. B.** 1986. Poliomyelitis, p. xxv, 1620. *In* A. I. Braude, C. E. Davis, and J. Fierer (eds), Infectious diseases and medical microbiology, 2nd ed, vol. 2. Saunders, Philadelphia.

45. **Sigal, L. J., S. Crotty, R. Andino, and K. L. Rock** 1999. Cytotoxic T-cell immunity to virus-infected non-haematopoietic cells requires presentation of exogenous antigen Nature. **398:**77-80.
46. **Speck, R. F., M. L. Penn, J. Wimmer, U. Esser, B. F. Hague, T. J. Kindt, R. E. Atchison, and M. A. Goldsmith** 1998. Rabbit cells expressing human CD4 and human CCR5 are highly permissive for human immunodeficiency virus type 1 infection J Virol. **72:**5728-34.
47. **Sturm, K., M. Lafferty, and P. P. Tam** 1999. Pgk1 and Hprt gene activity in the peri-implantation mouse embryo is influenced by the parental origin of the X-chromosome Int J Dev Biol. **43:**69-73.
48. **Tang, S., R. van Rij, D. Silvera, and R. Andino** 1997. Toward a poliovirus-based simian immunodeficiency virus vaccine: correlation between genetic stability and immunogenicity Journal of Virology. **71:**7841-50.
49. **Trainor, P. A., S. X. Zhou, M. Parameswaran, G. A. Quinlan, M. Gordon, K. Sturm, and P. P. Tam** 1999. Application of lacZ transgenic mice to cell lineage studies Methods Mol Biol. **97:**183-200.
50. **Wei, P., M. E. Garber, S. M. Fang, W. H. Fischer, and K. A. Jones** 1998. A novel CDK9-associated C-type cyclin interacts directly with HIV-1 Tat and mediates its high-affinity, loop-specific binding to TAR RNA Cell. **92:**451-62.
51. **WHO** 1998. Forty-sixth Report World Health Organ Tech Rep Ser. WHO Expert Committee on Biological Standardization.
52. **WHO** 1998. Update on the Global Eradication of Poliovirus.
53. **Zhang, S., and V. R. Racaniello** 1997. Expression of the poliovirus receptor in intestinal epithelial cells is not sufficient to permit poliovirus replication in the mouse gut J Virol. **71:**4915-20.

Table 1. Classic susceptible routes of wild type poliovirus infection

route	LD_{50}[a]	day of paralysis[b]	inoculum used (PFU)	paralysis summary[c]
Intramuscular	2×10^5	2-6	$\geq 1 \times 10^7$	18/18
			1×10^6	5/6
			1×10^5	2/6
Intracerebral	4×10^6	5-13	5×10^7	4/6
			5×10^6	14/25
			5×10^5	2/16
			5×10^4	3/10
			5×10^3	0/10
Intraperitoneal	1×10^8	3-6	1×10^9	4/5
			2×10^8	12/15
			$\leq 5 \times 10^7$	2/17
Intravenous	2×10^8	5-7	2×10^8	3/5
			$\leq 1 \times 10^7$	0/10
Oral	$> 1 \times 10^{10}$	—	1×10^9	0/5
Rectal	$> 1 \times 10^{10}$	—	1×10^9	0/5
Intragastric	$> 1 \times 10^{10}$	—	1×10^9	0/5

a LD_{50} is in PFU of wild type poliovirus
b Numbers of days post-infection at which paralysis was observed
c mice paralyzed/total number of mice inoculated

Table 2. Attenuated phenotype of Sabin vaccine strain polioviruses in cPVR mice

Virus/ route	inoculum used (PFU)	paralysis summary[b]	LD_{50}[a]	attenuation
Sabin 1 Intramuscular	2×10^7	0/6	$> 2 \times 10^8$	> 2000x
Sabin 1 Intracerebral	1×10^7	0/6	$> 1 \times 10^8$	> 50x
Sabin 2 Intramuscular	8×10^6	0/6	$> 8 \times 10^7$	> 150x
Sabin 2 Intracerebral	2.5×10^6	0/6	$> 2.5 \times 10^7$	> 5x

a LD_{50} is in PFU of the appropriate virus
b mice paralyzed/total number of mice inoculated

Figure Legends

Figure 1

(A) Diagram of PVR transgene structure. The δ (also known as the short or B) isoform PVR cDNA was cloned downstream of a β-actin promoter, and is flanked by the β-actin 5' UTR and 3'UTR. The transmembrane domain of PVR is indicated by a gray box.

(B) PVR genotyping of cPVR mice, by PCR. Different DNA templates were used for the PCR reactions: (+) refers to a pPVR plasmid control template, (cPVR) refers to genomic DNA from a cPVR transgenic mouse, and (ICR) is genomic DNA from a normal ICR nontransgenic mouse. (Mk) are DNA molecular weight markers.

Figure 2 PVR expression in cPVR mice.

(A) RT-PCR analysis of PVR RNA expression in tissues from cPVR mice. RT-PCR for 18S RNA expression was done from the same cDNA as a positive control (middle). As a negative control (bottom), a reaction was done containing purified cPVR polyA$^+$ RNA, primer, and nucleotides, but lacking reverse transcriptase (RT-), to control for potential DNA contamination.

(B) Expression of Pvr on splenocytes. FACS analysis of whole spleen from cPVR x C57BL/6 F1 mice and nontransgenic C57BL/6 mice. MC57G-PVR cells were used as a positive control for Pvr expression. Binding of an irrelevant antibody (grey curve), anti-Pvr antibody (black line), and anti-MHC I antibody (green line) are all shown.

Figure 3 Poliovirus tissue tropism in cPVR mice after intraperitoneal inoculation

Timecourse of titer of poliovirus (PFU/mg) in cPVR mice (■) or syngenic nontransgenic control ICR mice (○) in the following tissues: **(A)** spinal cord, **(B)** muscle, **(C)** brain, **(D)** small intestine, **(E)** blood, **(F)** kidney. Mice were given intraperitoneal inoculations of 5 x 10^8 PFU poliovirus, and tissues were analyzed as described in Materials and Methods. For each timepoint the high and low data points (connected by a vertical line) indicate the range of titers among the mice tested. The center data points, which are connected across the timecourse, represent the average titer of the mice tested on each day post-infection.

Figure 4 Poliovirus titers

(A) Highest average poliovirus titers (PFU/mg) in cPVR mouse tissues after intraperitoneal inoculation, at day 2 post-infection or later.

(B) Comparison of small intestine viral titers in two PVR transgenic mouse lines. cPVR and gPVR mice were infected intraperitoneally with 2 x 10^8 poliovirus. Non-transgenic control mice (ICR and C57BL/6 mice, respectively) were given 2 x 10^8 poliovirus as well. Viral titers were determined from daily tissue samples. Data is graphed as poliovirus titer (PFU/mg) in the transgenic mouse tissue minus the titer in the appropriate control mouse tissue, to subtract out the background viral particles from the initial inoculum present during the first ~24 hours. Spleen and kidney are shown as representative negative control tissues. Both cPVR and gPVR mice had substantial replication in brain tissue (data not shown), demonstrating that productive infections

occurred in all transgenic animals used, consistent with our observation that 2 x 10^8 PFU is approximately the LD_{50} of poliovirus for both cPVR and gPVR adult mice.

Figure 5 **Mucosal route of poliovirus infection.** Survival curves of cPVR mice given intanasal inoculations of **(A)** 5 x 10^8 PFU, **(B)** 1 x 10^8 PFU, **(C)** 1 x 10^7 PFU, **(D)** 1 x 10^6 PFU poliovirus. Control, nontransgenic ICR mice exhibited no mortality or clinical symptoms at any intranasal dose of poliovirus (data not shown).

Figure 6 **Tissue tropism of poliovirus after intranasal infection**

(A) Poliovirus tissue tropism in cPVR mice after intranasal inoculation with a sublethal dose. cPVR mouse tissues are indicated by filled symbols: pharynx (■), olfactory bulb (●), cerebrum (▲). Control ICR mouse tissues are indicated by empty symbols: pharynx (□), olfactory bulb (○), cerebrum (△).

(B) Poliovirus tissue tropism in cPVR mice after intranasal inoculation with a lethal dose. cPVR mouse tissues are indicated by the symbols: pharynx (■), olfactory bulb (●), cerebrum (▲), spinal cord (◆), muscle (□), intestine (○), lungs (△). No significant virus titers were detected in any nontransgenic ICR mouse tissues (not shown).

Figure 1

A.

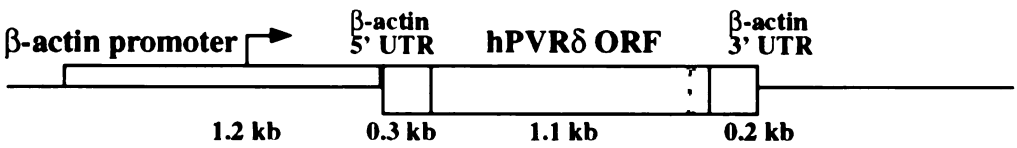
β-actin promoter
β-actin 5' UTR
hPVRδ ORF
β-actin 3' UTR
1.2 kb
0.3 kb
1.1 kb
0.2 kb

B.

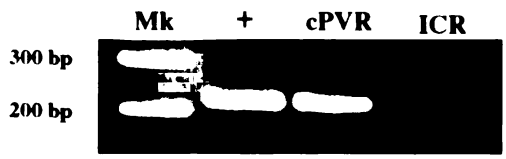
Mk
+
cPVR
ICR
300 bp
200 bp

A.

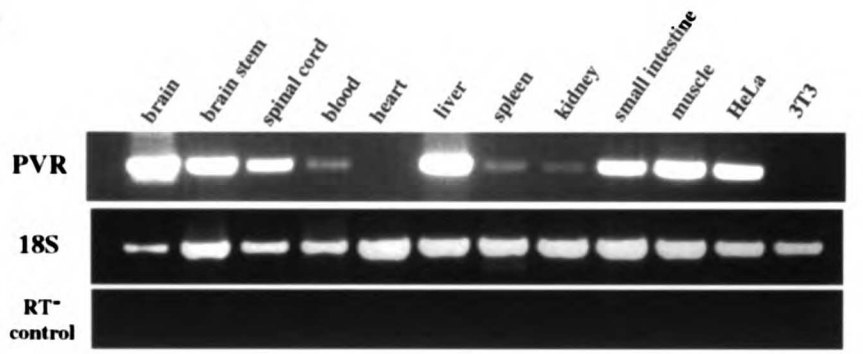
brain
brain stem
spinal cord
blood
heart
liver
spleen
kidney
small intestine
muscle
HeLa
3T3
PVR
18S
RT-
control

B.

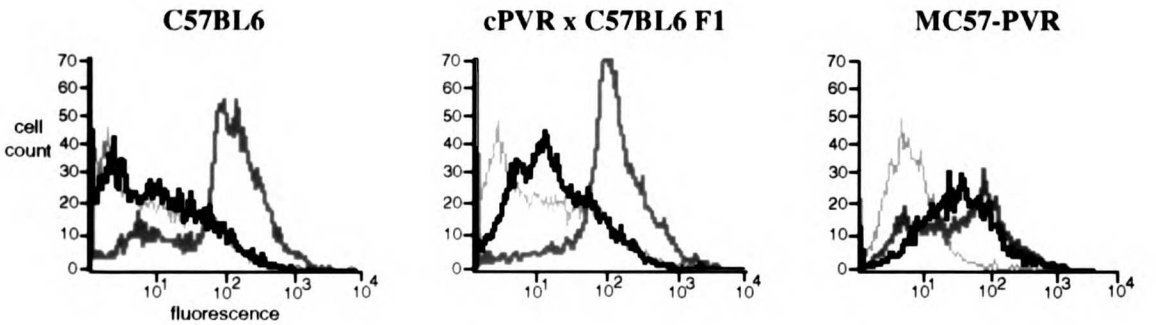
C57BL6
cPVR x C57BL6 F1
MC57-PVR
cell count
fluorescence

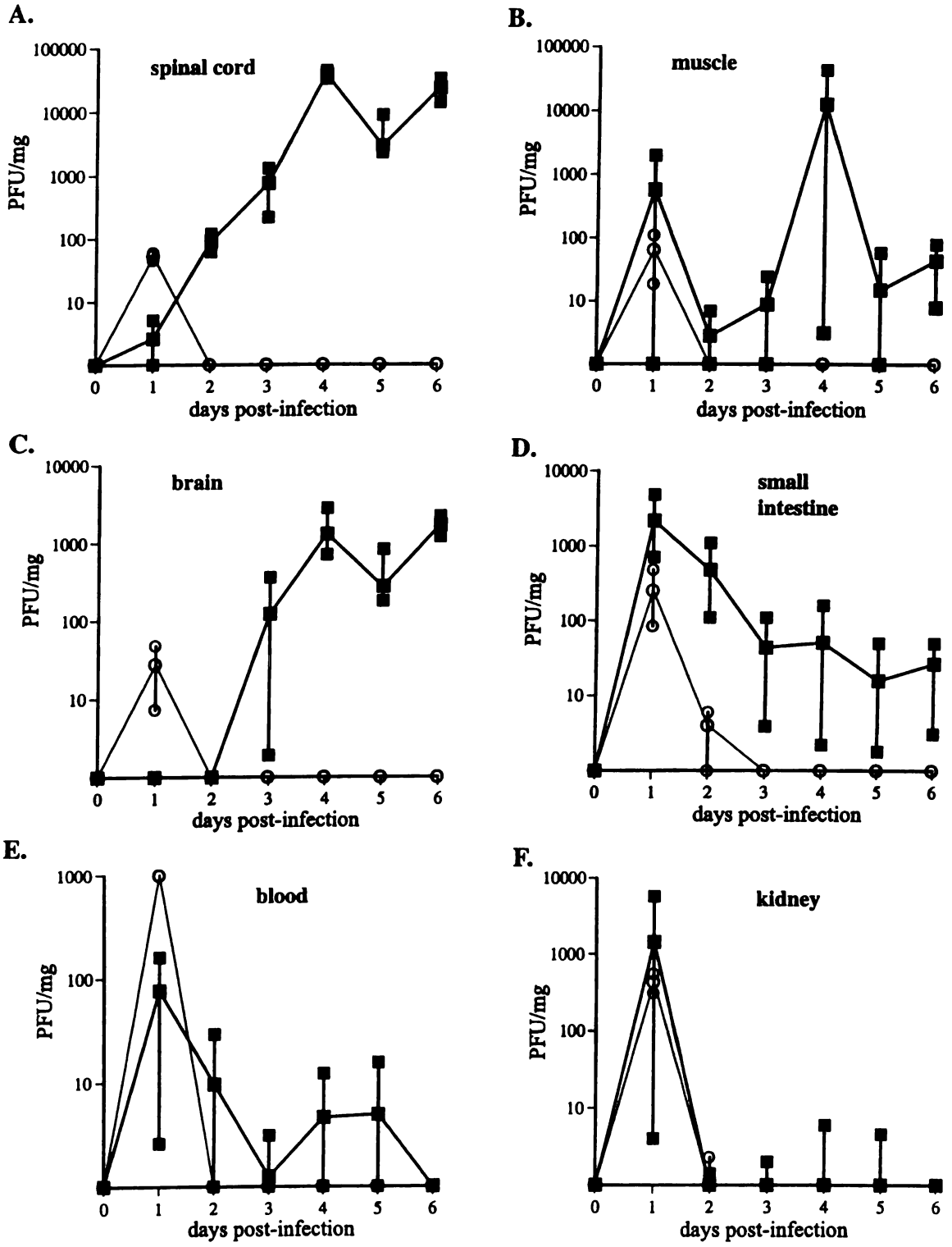
A.
spinal cord
PFU/mg
100000
10000
1000
100
10
0 1 2 3 4 5 6
days post-infection
B.
muscle
PFU/mg
100000
10000
1000
100
10
0 1 2 3 4 5 6
days post-infection
C.
brain
PFU/mg
10000
1000
100
10
0 1 2 3 4 5 6
days post-infection
D.
small intestine
PFU/mg
10000
1000
100
10
0 1 2 3 4 5 6
days post-infection
E.
blood
PFU/mg
1000
100
10
0 1 2 3 4 5 6
days post-infection
F.
kidney
PFU/mg
10000
1000
100
10
0 1 2 3 4 5 6
days post-infection

A.

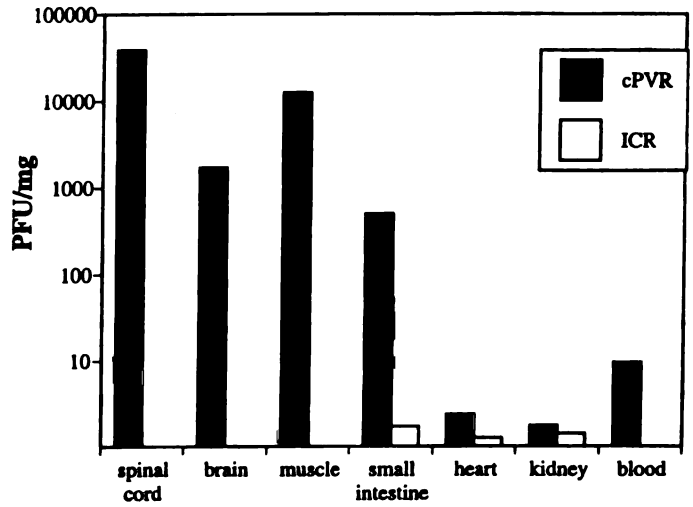
100000
10000
1000
100
10
PFU/mg
cPVR
ICR
spinal cord
brain
muscle
small intestine
heart
kidney
blood

B.

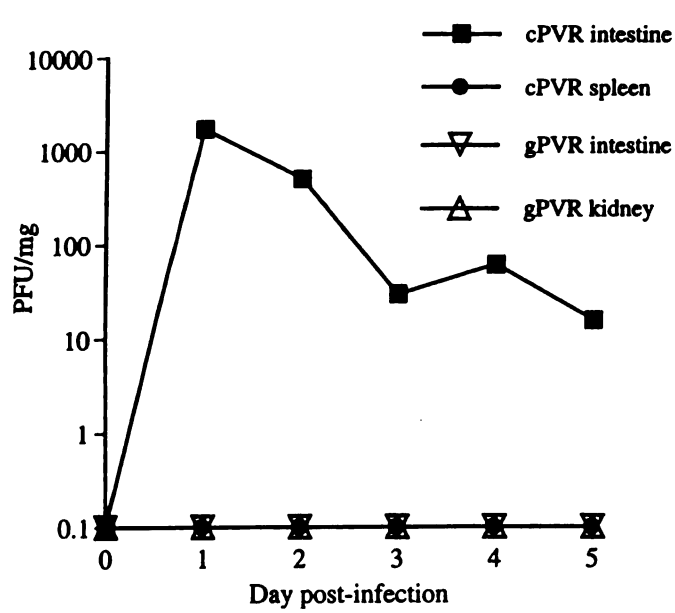
10000
1000
100
10
1
0.1
PFU/mg
cPVR intestine
cPVR spleen
gPVR intestine
gPVR kidney
0
1
2
3
4
5
Day post-infection

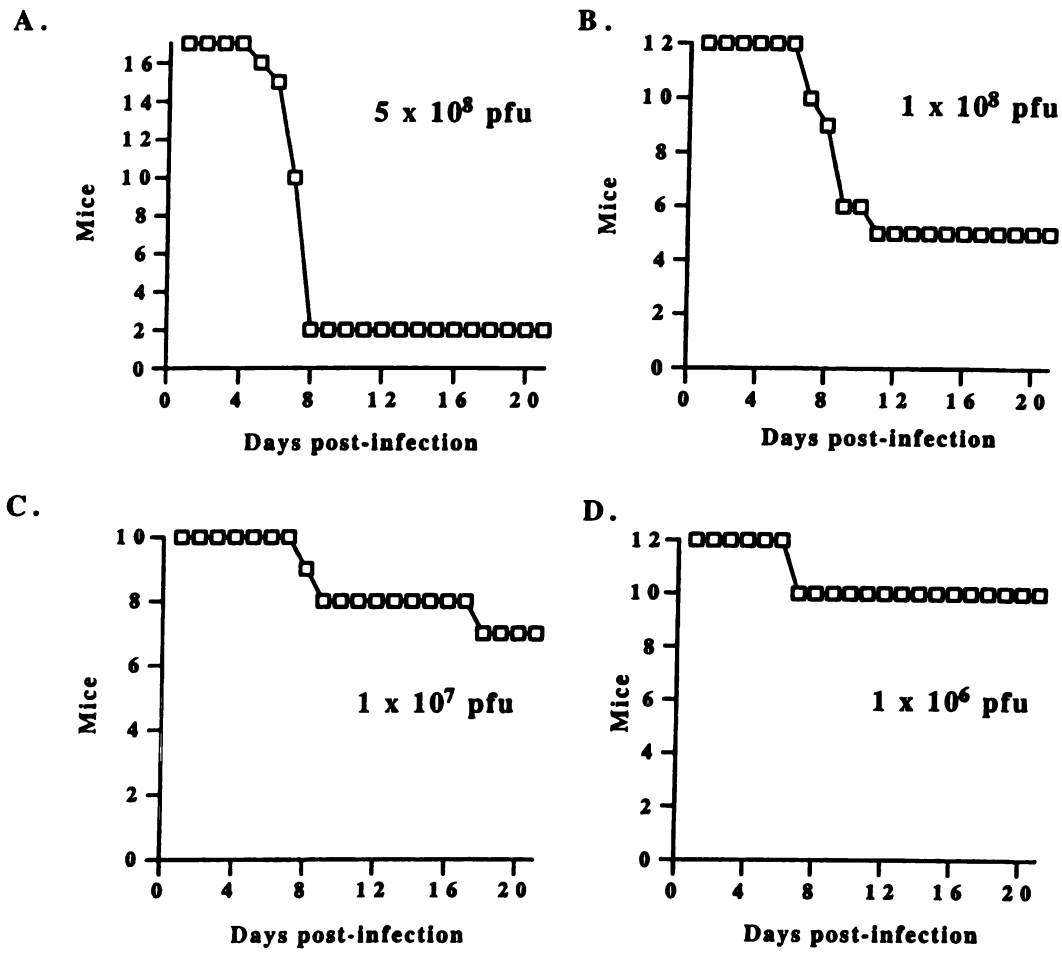
A.
5 x 10^8 pfu
Mice
Days post-infection
B.
1 x 10^8 pfu
Mice
Days post-infection
C.
1 x 10^7 pfu
Mice
Days post-infection
D.
1 x 10^6 pfu
Mice
Days post-infection

A.

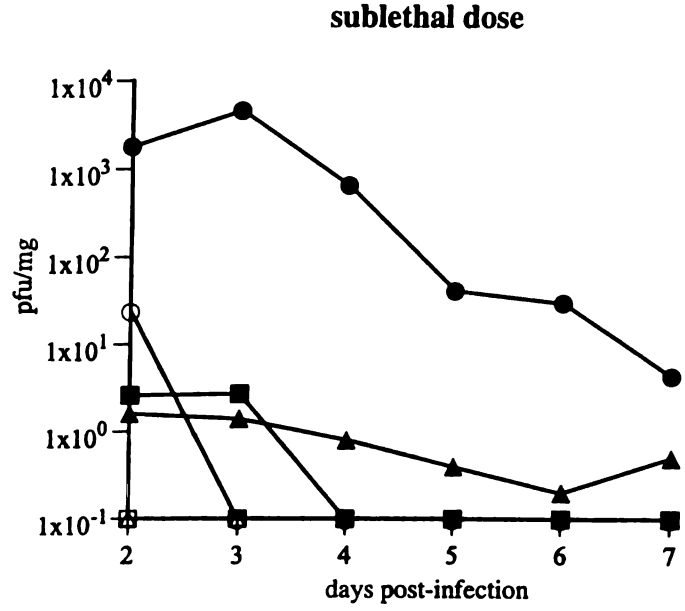
sublethal dose
1x10^4
1x10^3
1x10^2
1x10^1
1x10^0
1x10^-1
pfu/mg
2
3
4
5
6
7
days post-infection

B.

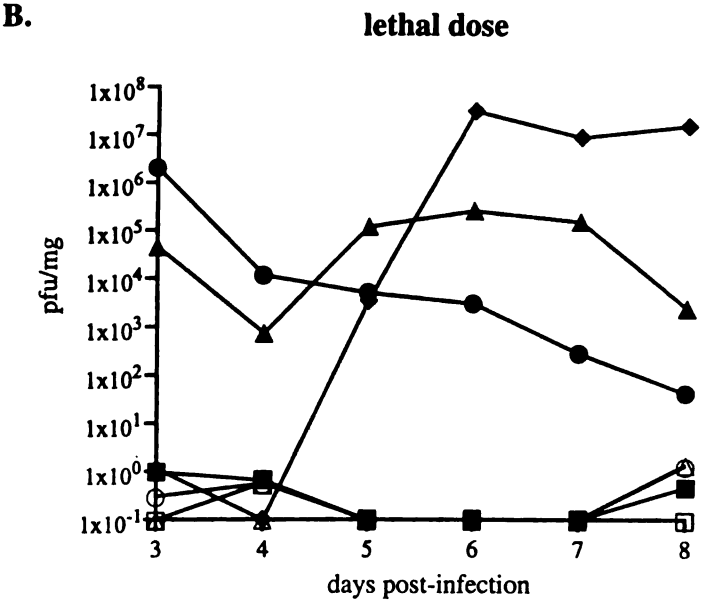
lethal dose
1x10^8
1x10^7
1x10^6
1x10^5
1x10^4
1x10^3
1x10^2
1x10^1
1x10^0
1x10^-1
pfu/mg
3
4
5
6
7
8
days post-infection

Supplementary Data

Tracking poliovirus spread after intracerebral inoculation

In the interest of tracking poliovirus replication and spread through cells in the central nervous system, we constructed a recombinant poliovirus expressing green fluorescent protein (Mov2.11-GFP). This virus grows well in tissue culture (Fig. 7A), and reaches reasonable titers of ~5 x 10^7.

We inoculated cPVR mice with 1 x 10^6 PFU of polio-GFP intracerebrally, and then followed the viral spread. GFP^+ cells were apparent by 12 hrs post-infection (data not shown). The infected cells frequently had neuronal morphology (Fig. 7B), with GFP fluorescence obvious in long and numerous cell processes (Fig. 7B-C). Spread of polio-GFP in the brain was apparent, as 1-2 infected cells in any given location at 24 hrs post-infection (Fig. 7B) became foci of 10-50 infected cells by 2-3 days post-infection (Fig. 7C).

As polio-GFP spread in the brain it exhibited genetic instability, reverting to a virus with GFP^- wildtype poliovirus characteristics. Such genetic instability is a hallmark of replication competent recombinant polioviruses, and is particularly pronounced with GFP, possibly because GFP's unusual protein fold interferes with poliovirus polyprotein folding and processing. However, we were able to track polio-GFP viral spread for 3-4 days post-infection in the brain, after which time GFP^+ cells were no longer visible, though viral plaques in the brain were apparent (data not shown), indicating that the poliovirus was still spreading, but was no longer expressing GFP. Infected cells were

seen broadly distributed in various regions of the grey matter in different mice, indicated no strict restriction of poliovirus infection and replication to a few discreet areas of the brain in cPVR mice. The virus did not spread extensively in the brain during the first 3-4 days post-infection (we did not observe any focus of polio-GFP$^+$ infected cells more than 2x the size of the one shown in Fig. 7C), corroborating our previous data that virus replication and/or spread was slow after intracerebral inoculation.

Age dependence of poliovirus susceptibility

All of the experiments described thus far were done using 6-8 week old adult mice. We next used cPVR mice at other ages to determine whether there was an age dependence to the susceptibility to poliovirus infection and paralysis in these transgenic animals. Ten to twelve week old cPVR mice were inoculated intracerebrally with wildtype poliovirus, and these mice exhibited comparable susceptibility to infection as six week old mice (Table 2). Two week old mice were then inoculated intracerebrally, and these younger mice exhibited greater susceptibility to paralysis, with an LD_{50} 25-fold lower than that of adult mice.

We then explored the intramuscular route of inoculation. Surprisingly, young mice were remarkably more susceptible to infection and paralysis after intramuscular inoculation, with an LD_{50} of 50 PFU, which is 10,000-fold lower than that for 6 wk old cPVR mice (Table 2). With such a highly enhanced susceptibility, two week old mice inoculated intramuscularly should be an excellent system for testing the attenuation of various poliovirus mutants in future *in vivo* studies using cPVR transgenic mice.

Table 3. Age dependence of poliovirus susceptibility

Age (wks)	Intramuscular			Intracerebral		
	Inoculum (PFU)	frequency of paralysis[a]	LD_{50}[b]	Inoculum (PFU)	frequency of paralysis	LD_{50}[b]
2	1×10^4 1×10^3 1×10^2 10	6/6 6/6 11/11 1/5	50	5×10^6 5×10^5 5×10^4	3/3 2/3 0/3	2×10^5
6	$\geq 1 \times 10^7$ 1×10^6 1×10^5	18/18 5/6 2/6	5×10^5	5×10^6 5×10^5 5×10^4	3/5 1/5 1/5	5×10^6
10	ND	ND	ND	5×10^6 5×10^5 5×10^4	3/5 2/5 0/5	5×10^6

a Six 2 wk old C57BL/6 control mice inoculated with 5×10^7 PFU of poliovirus intracerebrally had no paralysis or death.

b LD_{50} is in PFU of wildtype poliovirus

Figure 7. Tracking poliovirus spread after intracerebral inoculation.

A) Replication of polio-GFP in tissue culture cells. Plaque formation by polio-GFP shows that currently infected cells (along the outer rim of the plaque) express high levels of active GFP protein. Cells in the middle of the plaque have been killed by polio-GFP and are dark. Plaque was photographed at 48 hr post-infection.

B) Brain tissue section from a cPVR mouse 24 hr after intracerebral inoculation of 1 x 10^6 PFU of polio-GFP.

C) Brain tissue sections from a cPVR mouse 48 hr after intracerebral inoculation of 1 x 10^6 PFU of polio-GFP.

A.

B.

C.

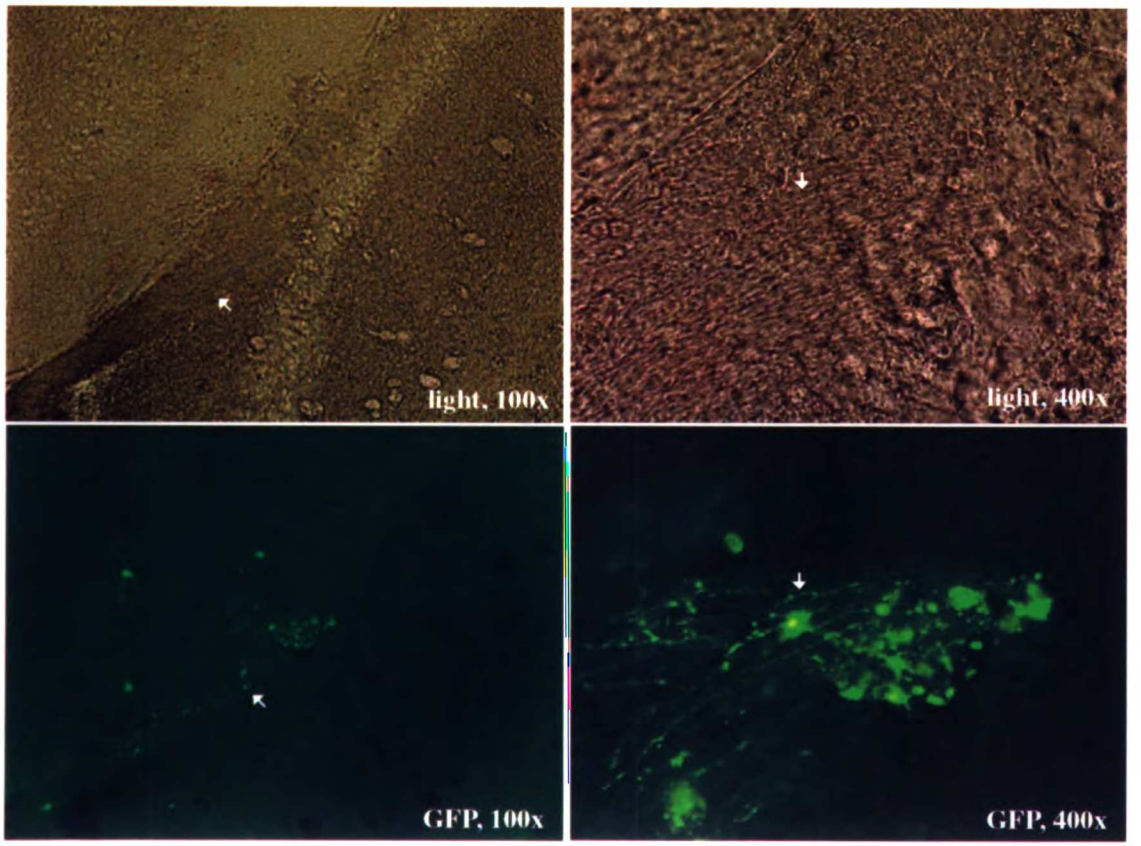

Chapter 13

Discussion of Section III: PVR transgenic mice

Most of the issues regarding PVR transgenic mice were discussed in Chapter 12. The flurry of recent activity regarding the "Anti-viral surveillance by CTL requires professional APCs and MHC class I presentation of exogenous antigen" *Nature* paper detailed in Chapter 11 is too much to generally review here, and it is much more Luis Sigal's field of expertise (though I can recommend references 1-3 as interesting starting points). However, I did have correspondence (~5/9/1999) with David Baltimore discussing one aspect of the experiments in Chapter 11, and I will recaptulate that discussion here. Baltimore wrote, "I was talking with Raul about it, and then happened to read more carefully the paper and I suddenly had a wonderment. If polio-infected cells are eaten by macrophages or dendritic cells, mightn't the virus start replicating anew in the new cellular milieu. Then the need for the TAP system becomes perfectly reasonable. It would change the interpretation of the experiments somewhat, although the general message that presentation requires professional cells would remain the same."

My response is below.

"Yes, you're definitely bringing up a real issue. When we were doing the experiments, Luis and I talked about the possibility that endocytosed viral RNA produced

the antigen in the macrophages or dendritic cells. We can't exclude that possibility, but there are several reasons we think it's unlikely. We've been unable to productively infect purified PVR^+ mouse dendritic cells with poliovirus. We've tried a number of times and have never observed replication (measured by infectious virus production) or even translation (measured by expression of GFP by polio-GFP) (4). So, viral RNA inside dendritic cells doesn't appear to be efficiently translated or replicated. This would be quite reasonable in light of the fact that our transgenic mice express the polio receptor in all tissues, but still I only detect replication in spinal cord, brain, small intestine, and muscle (5). There is a strong post-entry block to polio replication in most cell types. And experiments by Racaniello's laboratory showing that the wt polio IRES can drive translation in neuroblastoma cells but the Sabin IRES cannot (while they obviously both translate great in HeLa and other lines) shows that cell type specific factors can drastically affect polio translation (6).

"There is a caveat to this arguement. We have not shown that the virus gets into the PVR^+ dendritic cells in the cell culture infection experiments. We could try electroporating or lipofecting in the polio RNA, but we haven't had compelling reasons to try. And we haven't exhaustively tried to infect the DCs, maybe it's a technical problem (obviously culturing DCs results in significant developmental changes). Also, sometimes Luis could get a small amount of OVA class I antigen presentation by "infecting" cultured mouse dendritic cells with polio-OVA. Two reasonable interpretations: polio enters DCs, and translates a small amount—enough to show up in a sensitive CTL assay; or polio doesn't get in and get translated, but there is enough OVA protein contaminating

the viral stock (produced by previously infected cells) to get endocytosed and presented on class I in limited amounts, in some experiments.

"Regarding macrophages, I've been unable to infect fresh human PBMCs (mine and Raul's) with poliovirus (as measured by infectious virus production or GFP translation), even though macrophages appear to express the receptor (7). Again, these experiments were limited in scope, but human macrophages seem to be intransigent to polio infection/translation/replication. We haven't done any work with mouse macrophages.

"I do agree with you that if a polio RNA got transported into the cytoplasm of a receptor-minus cell and replicated it would be a potent source of antigen, in a TAP-dependent manner. We could certainly try to differentiate exogenous RNA vs. protein priming of professional APCs in vivo. We could inoculate the B6 → PVR bone marrow chimeric mice with UV-inactivated polio. If we saw (anti-polio) CTL stimulation, it would be due to protein acquired exogenously by professional APCs. That experiment could be done now that Luis has identified a polio capsid CTL epitope (8). It is known that the hepatitis B subunit vaccine can stimulate a CTL response in mice (by the endosomal pathway). Vice versa, if we could show that lipofected polio RNA into cultured dendritic cells generate significant amounts of polio translation (and possibily replication), we could then lipofect polio RNA into DCs and inject the DCs in mice and look for a CTL response. If it worked it would show that polio RNA transported into dendritic cell cytoplasm is sufficient to prime a CTL response, but like I said up at the top, we haven't had any luck with DC infections so far."

References

1. T. Schumacher. (1999) "Accessory to murder." *Nature* 398:26-27.
2. P. Machy, K. Serre, and L. Leserman. (2000) "Class I-restricted presentation of exogenous antigen acquired by Fcgamma receptor-mediated endocytosis is regulated in dendritic cells." *Eur. J. Immunology* 30:848-857.
3. J. Davoust and J. Banchereau. (2000) "Naked antigen-presenting molecules on dendritic cells." *Nature Cell Biology* 2:46-48.
4. S. Crotty and R. Andino. unpublished observations.
5. S. Crotty, L. Hix, L. Sigal, and R. Andino. submitted for publication.
6. N. La Monica and Racaniello, V. R. (1989) "Differences in replication of attenuated and neurovirulent polioviruses in human neuroblastoma cell line SH-SY5Y" *J. Virology* 63:2357-60.
7. S. Crotty and R. Andino. unpublished observations.
8. L. J. Sigal, S. Crotty, R. Andino, and K. Rock. (1999) "Anti-viral surveillance by CTL requires professional APCs and MHC class I presentation of exogenous antigen." *Nature* 398: 77-80.

Section IV

Novel poliovirus mutants

Chapter 14

Introduction to section IV: novel poliovirus mutants

This section consists of two studies, the first of which involves an analysis of amino acid residues critical for the function of the poliovirus polymerase $3D^{pol}$. Ever since David Baltimore made the original discovery of RNA-dependent RNA polymerase activity in poliovirus infected HeLa cells (4, 6), poliovirus has been the prototypic animal virus RNA-dependent RNA polymerase model. However, our understanding of RNA-dependent RNA polymerases has lagged far behind our understanding of the other three classes of polymerase: DNA-dependent DNA polymerases, DNA-dependent RNA polymerases, and RNA-dependent DNA polymerases. A major step in understanding RNA-dependent RNA polymerases was recently made with the solution of a crystal structure of the poliovirus polymerase (8). That structure has now been followed by the solution of the hepatitis C virus (HCV) polymerase, NS5B (5, 9), and the solution of a second picornavirus polymerase (James, unpublished data).

Craig Cameron's laboratory set out to finally determine the basic biochemical kinetic and thermodynamic parameters of the poliovirus polymerase. Their first studies focused on the use of homopolymeric templates (2, 3). But they then discovered that a symetrical short primer/template substrate allowed them to assemble polymerase-template complexes in a stoichiometric manner (1), and with the ability to assemble

stoichiometric complexes they could accurately assess the fundamental kinetic parameters of the polymerase, such as the incorporation rate (1). However, it was critical to know whether the biochemical data obtained with sym/sub is an accurate reflection of in vivo function. Craig Cameron and I therefore arranged a collaboration where I would test a series of polioviruses containing mutant polymerases for viability and RNA replication *in vivo* and compare those results with their biochemical sym/sub data. That collaboration resulted in Chapter 15, which was published in the Journal of Biological Chemistry in August of 2000 in a revised form as "Poliovirus RNA-dependent RNA Polymerase ($3D^{pol}$): Structural, Biochemical and Biological Analysis of Conserved Structural Motifs A and B" (7) (and also, see note on page 5334 of the Arnold et al. 2000 sym/sub publication (1)). The molecular modelling, thermodynamic analysis, kinetic analysis, and in vivo analysis presented in Chapter 15 represents a major advance in our understanding of RNA-dependent RNA polymerases.

Chapter 16 continues a genetic exploration of the function of $3D^{pol}$ asparagine 297 that begins in Chapter 15, and results in some very unexpected findings about the virus and the polymerase.

Chapter 17 is the second study described in this section, and it began as a simple bet. The bet was: It is not possible for poliovirus to become resistant to the drug brefeldin A, because brefeldin A targets cellular proteins and processes, not viral ones. I bet that the preceeding postulate was wrong. Viruses are incredibly clever, and I set out to identify a brefeldin A resistant poliovirus. The study resulted in the identification of an amazing mutant virus, and Chapter 17 is a testament to the incredible cleverness of

viruses. They can evolve and survive in even the most inhospitable of environments. And additionally, the identification of these brefeldin A mutations may open an important doorway to understanding the complex and confusing cell biology of poliovirus.

Acknowledgments

David Gohara performed all of the biochemical work in the study presented in Chapters 15, and that study was very much driven by his work and by Craig Cameron; my contribution to Chapter 15 was the *in vivo* analysis. I include the full story as it explains the rationale and value of the *in vivo* experiments. David Gohara also performed the biochemical analysis in Chapter 16. Oren Beske performed the immunofluorescence analysis in Chapter 17. Those contributions were essential to the success of these studies.

References

1. **Arnold, J. J., and C. E. Cameron** 2000. Poliovirus RNA-dependent RNA polymerase (3D(pol)). Assembly of stable, elongation-competent complexes by using a symmetrical primer-template substrate (sym/sub) J Biol Chem. **275:**5329-36.
2. **Arnold, J. J., and C. E. Cameron** 1999. Poliovirus RNA-dependent RNA polymerase (3Dpol) is sufficient for template switching in vitro J Biol Chem. **274:**2706-16.
3. **Arnold, J. J., S. K. Ghosh, and C. E. Cameron** 1999. Poliovirus RNA-dependent RNA polymerase (3D(pol)). Divalent cation modulation of primer, template, and nucleotide selection J Biol Chem. **274:**37060-9.
4. **Baltimore, D., and R. M. Franklin** 1962. Preliminary data on a virus-specific enzyme system responsible for the synthesis of viral RNA Biochemical and Biophysical Research Communications. **9:**388-392.
5. **Bressanelli, S., L. Tomei, A. Roussel, I. Incitti, R. L. Vitale, M. Mathieu, R. De Francesco, and F. A. Rey** 1999. Crystal structure of the RNA-dependent RNA polymerase of hepatitis C virus Proc Natl Acad Sci U S A. **96:**13034-9.
6. **Crotty, S.** 2001. Ahead of the Curve: David Baltimore's Life in Science. University of California Press, San Francisco, CA.
7. **Gohara, D. W., S. Crotty, J. J. Arnold, J. D. Yoder, R. Andino, and C. E. Cameron** 2000. Poliovirus RNA-dependent RNA Polymerase ($3D^{pol}$): Structural, biochemical, and biological analysis of conserved structural motifs A and B Journal of Biological Chemistry. **275:**25523-25532.
8. **Hansen, J. L., A. M. Long, and S. C. Schultz** 1997. Structure of the RNA-dependent RNA polymerase of poliovirus Structure. **5:**1109-22.
9. **Lesburg, C. A., M. B. Cable, E. Ferrari, Z. Hong, A. F. Mannarino, and P. C. Weber** 1999. Crystal structure of the RNA-dependent RNA polymerase from hepatitis C virus reveals a fully encircled active site Nat Struct Biol. **6:**937-43.

Chapter 15

Poliovirus RNA-dependent RNA Polymerase ($3D^{pol}$): Structural, Biochemical and Biological Analysis of Conserved Structural Motifs A and B

Abstract

We have constructed a structural model for poliovirus RNA-dependent RNA polymerase ($3D^{pol}$) in complex with primer/template and nucleotide. This model predicts that residues from conserved structural motifs A (Asp-238) and B (Asn-297) participate in nucleotide selection in a manner different than predicted by evaluation of the unliganded structure of $3D^{pol}$. We have engineered mutations into $3D^{pol}$-coding sequence that change Asp-238 or Asn-297 to a variety of residues. Asp-238 derivatives were 10- to 400,000-fold less active than wild-type enzyme *in vitro*, and these derivatives did not support virus multiplication owing to a defect in RNA synthesis. Asn-297 derivatives were 1.3- to 5-fold less active than wild-type enzyme based upon poly(rU) polymerase activity and 2.5- to 70-fold less active than wild-type enzyme based upon kinetics of AMP incorporation into sym/sub. The Ala-238 derivative utilized rNTPs and dNTPs with equal efficiency. The Ala-297 derivative exhibited a 20-fold preference for rNTPs, a 10-fold reduction relative to wild-type $3D^{pol}$. A direct correlation existed between

activity on sym/sub and biological phenotypes; a 2.5-fold reduction in polymerase elongation rate produced virus with a temperature sensitive growth phenotype. These data support our structural model for nucleotide selection by $3D^{pol}$ and confirm the biological relevance of the sym/sub system.

Introduction

All nucleic acid polymerases, with the exception of mammalian DNA polymerase ß, have the same overall topology [1]. As suggested first by Steitz in his description of the Klenow fragment of DNA polymerase I (KF)[1] [2], these enzymes resemble a cupped, right hand with fingers, palm and thumb subdomains. The fingers and thumb subdomains contribute to substrate binding, especially to regions of primer and template remote from the catalytic center [3,4,5,6,7]. The palm subdomain of all classes of polymerase contains structural elements necessary for phosphoryl transfer and binding to primer, template and nucleotide [8,9,10,11,12]. The overall structure and, to some extent, sequence of palm subdomains are also highly homologous. Thus, the functional similarity between the kinetic and chemical mechanism of nucleic acid polymerases is not surprising [13,14,15,16].

Nucleic acid polymerases are categorized based upon their specificity for template and nucleotide. Of course, specificity is a relative term as it is quite dependent upon reaction conditions [17,18,19]. At physiologically relevant values of pH and ionic strength and in the presence of magnesium ions, most DNA-dependent DNA polymerases (DdDPs) prefer to utilize DNA templates and deoxyribonucleotides (dNTPs) as substrates rather than RNA and ribonucleotides (rNTPs) [17,18,19]. The converse is true for RNA-dependent RNA polymerases (RdRPs) [20].

However, even under physiological conditions, exceptions to polymerase specificity have been noted, especially for primer and/or template utilization. For

example, KF utilizes RNA templates [21], T7 DNA-dependent RNA polymerase (DdRP) utilizes RNA templates [22] and poliovirus RdRP utilizes DNA primers [20]. Template preference becomes even more ambiguous when alternative divalent cations, such as manganese, are employed [20]. This "identity crisis" of polymerases regarding template utilization is not too surprising given the existence of enzymes like reverse transcriptases (RTs) which bridge both worlds [23]. Moreover, the ease of polymerases to move from one template type to another was likely a driving force for the evolution of specific protein-nucleic acid and protein-protein interactions as an obligatory step in the initiation process of transcription, replication and repair [24].

In contrast to template selection, nucleotide selection is more stringent under physiological conditions. For example, T7 DdRP exhibits an 80-fold preference for rNTPs relative to dNTPs [25]. KF exhibits a 10^3-10^6-fold preference for dNTPs [26,27,28]. The RTs from human immunodeficiency virus (HIV-1) and Moloney murine leukemia virus (MMLV) exhibit a 10^5-fold preference for dNTPs [29,30]. The use of manganese as divalent cation permits all classes of polymerase to incorporate one or two nucleotides of the incorrect sugar configuration [31,32,33,34,35,36]. However, processive incorporation of nucleotides of the incorrect sugar configuration is not tolerated [37,38].

The molecular basis for nucleotide selection by polymerases has been a topic of considerable interest recently [39,40,41,42,43]. This interest has resulted from the development of structural models for DdDPs and a DdRP in complex with various substrates (e.g. primer, template and nucleotide). These studies have uncovered interactions between the enzyme and nucleotide that may be important during the

selection process [5,6,7,8,9]. Construction and characterization of site-directed mutants of KF, HIV-1 RT and MMLV RT have confirmed the structural predictions by altering the dNTP/NTP preference of these enzymes. Essentially, the dNTP-utilizing enzymes use a steric-gating mechanism to decrease the affinity of the enzyme for rNTPs [28,29,40]. The steric gate is formed, in part, by a residue found in structural motif A (motif designations are as defined by Hansen *et al.* [1]) of the palm subdomain (KF E710, HIV-1 RT Y115, MMLV RT F155). Structural motif B of the palm subdomain may also participate in this process [43].

The mechanism employed by rNTP-utilizing enzymes is not fully understood. A steric-gating mechanism has been proposed for T7 DdRP. Succinctly, it has been suggested that a water molecule bound to Y639, a residue that occludes the nucleotide-binding pocket, is displaced as a consequence of rNTP binding. Displacement of this water results in movement of Y639 out of the pocket thereby permitting productive rNTP binding. The absence of a 2'-hydroxyl would not permit induction of this conformational transition thereby creating a steric block to productive binding of dNTPs [25,45]. Although this model is based upon steady-state kinetic analysis of T7 RNA polymerase derivatives, a water molecule and movement of Y639 have been observed crystallographically [44,45,46].

An alternative model has been proposed recently for rNTP selection by T7 DdRP based solely upon structural observations. Selection for rNTP binding appears to be mediated by a hydrogen-bonding network consisting of the 2'-hydroxyl and side chains of the enzyme (H784 and Y639). Such a network is more consistent with the 80-fold preference of this enzyme for rNTPs [25,47]. One might expect a greater difference by

employing a steric mechanism [27,40]. Aspects of these two models are mutually exclusive. Analysis of H784 derivatives under conditions in which dNTP incorporation by the wild-type enzyme is observed should help to distinguish between these two models [45].

Currently, information regarding the mechanism of nucleotide selection by the RdRP is not available. Our previous work has shown that the RdRP from poliovirus utilizes rNTPs 121-fold more efficiently than dNTPs [48]. This value is similar to that determined for T7 DdRP. In addition, Hansen *et al.* have predicted the use of a hydrogen-bonding network to select for rNTP binding based upon the unliganded structure of this enzyme [1]. In this report, we have used the structure for the ternary complex of HIV-1 RT to develop a model for the ternary complex of poliovirus RNA polymerase. In addition, we use biochemical and biological analysis of site-directed mutants of $3D^{pol}$ to test predictions of this model. This analysis demonstrates a role for conserved structural motifs A and B in rNTP/dNTP selection by the RdRP that is different than suggested previously [1]. In addition, we provide additional support for the biological relevance of the primer/template (sym/sub) system developed to study the RdRP from poliovirus *in vitro* [48].

Materials and Methods

Materials - [α-^{32}P]UTP (>6,000 Ci/mmol) was from NEN Life Science Products; [γ-^{32}P] ATP (> 7,000 Ci/mmol) was from ICN; nucleoside 5'-triphosphates (ultrapure solutions) were from Amersham Pharmacia Biotech, Inc.; all DNA oligonucleotides and T4 DNA ligase were from Life Technologies, Inc.; all RNA oligonucleotides were from Dharmacon Research, Inc. (Boulder, CO); Restriction enzymes, T4 polynucleotide kinase and Deep Vent DNA polymerase were from New England Biolabs, Inc.; polyethyleneimine-cellulose TLC plates were from EM Science; 2.5 cm DE81 filter paper discs were from Whatman. All other reagents were of the highest grade available from Sigma or Fisher.

Construction of the 3D^{pol} Ternary-Complex Model - The coordinates for the HIV-1 RT ternary complex (1rtd) and 3D^{pol} (1rdr) are available from the Research Collaboratory for Structural Bioinformatics, RCSB. Superpositioning of the two structures was performed using lsqkab from the CCP4 suite of programs [49]. Structural alignments were initially performed using the thumb and palm subdomains. Final superpositioning of the two structures was confined to structural motifs A (3D^{pol} residues 233-240), B (287-302), C (324-331) and E (368-380). The final positions of Cα atoms in the four structural motifs had an r.m.s. deviation ranging from 0.9-1.8 Å.

3D^{pol} residues were inserted into the structurally analogous positions of HIV-1 RT using the program O [50]. Residues having the same identity in both structures were not altered from those observed in the HIV-1 RT structure. Amino acids unique to 3D^{pol} were manually set in position based on their orientation in the unliganded 3D^{pol} structure.

In some instances the side chains were adjusted to eliminate steric contact with neighboring residues. 2'-hydroxyls were inserted into both the primer and template strands of the nucleic acid within the polymerase active site as well as the incoming nucleotide. Bond angles for the 2'-hydroxyls were adopted from various RNA structures determined using NMR and X-ray crystallography obtained from the RCSB. Within the vicinity of the active site, DNA in the HIV-1 RT structure adopts an A-form conformation causing the sugar pucker to switch from C2'-endo to C3'-endo, hence modification of the sugar geometry was not necessary. Nucleotide bases of the RNA were modified to correspond to that of sym/sub [48], 5'-GCAUCCCGGG-3', and the incoming nucleotide modified to ATP, the first nucleotide incorporated into sym/sub. Two additional regions (residues 163-202) were modeled into the structure based on a partial structural and sequence alignment. Region I, residues 175-202, was identified by superpositioning of the $3D^{pol}$ and HIV-1 RT structures and consists of an extended α-helix that runs underneath the 3' end of the template strand. Region II comprises residues 163-174 (which are absent from the $3D^{pol}$ structure) and represents the active-site side of the fingers subdomain.

Energy minimizations were performed on the entire structure, comprising both modified and unmodified regions, using the program CNS SOLVE [51]. Initial attempts at energy minimization were performed on the modified region of the structure only; however, upon completion of the first cycle, gross distortions of the molecule were observed. The modified region was reinserted into the entire HIV-1 RT structure and energy minimizations repeated. The additional structure eliminated distortions in the molecule allowing the protein side chains to relax into positions void of unfavorable,

steric contact. Iterative cycles of minimization, a total of 10, were performed using the constant temperature algorithm. The final settings for energy minimizations follow. The Cartesian (restrained) molecular dynamics algorithm was utilized at a constant temperature (298 K) using the coupled temperature control method [52]. 10,000 molecular dynamics steps were performed at 0.0005 ps intervals. The dielectric was set to 1 (the default value) and the number of trials utilizing different initial velocities set to 1. The output files from each cycle were superimposed to observe side chain and nucleic acid motions, which were most apparent for side chains and nucleotides not involved in protein or nucleic acid interactions. Upon completion of the final cycle of minimization, the modified region was removed from the structure and side chain geometry checked using the program PROCHECK [53]. Finally, the modified regions of the HIV-1 RT structure, nucleic acid, nucleotide as well as Mg^{++} ions were removed from the file and used to generate a new PDB file (3DRTSS).

Construction, Expression and Purification of $3D^{pol}$ Derivatives - Mutations were introduced into a modified $3D^{pol}$-coding sequence by using overlap-extension PCR [54] and expressed in *Escherichia coli* by using a ubiquitin fusion system. The ubiquitin fusion system, PCR conditions and modified gene have been described previously [55]. The D238F clone was engineered such that it contained a silent Nhe I site, the sequence of the forward oligo is: 5'-GAC TAC ACA GGG TAT TTC GCT AGC CTC AGC CCT-3', the Asp to Phe substitution is underlined, the Nhe I site is in bold. A wild-type reverse oligo was employed (oligo 10, Table 1). Briefly, two separate PCR reactions were performed: one reaction with the pET-Ub-Sac II for oligo and the D238 WT rev; the other with D238F for and pET-3D-BamH I rev. Both reactions employed pET26b-Ub-

3D [55] as template. Products were purified by agarose gel electrophoresis and used as the template in the next round of PCR with a 1:10 molar ratio of the wild-type:D238F modified fragments. The Afl II for and Avr II rev oligos were used as the sole primers for this cycle of PCR. Product was purified, digested with Avr II and Afl II and ligated into pET26b-Ub-3D that had been digested with the same restriction enzymes. Plasmids were screened for the presence of the Nhe I site. The remaining $3D^{pol}$ genes were constructed by using PCR as described above and subcloned into the D238F vector between the Afl II and Avr II restriction sites and screened for the loss of the Nhe I site. Mutations were confirmed by DNA sequencing (Nucleic Acid Facility, Pennsylvania State University). $3D^{pol}$ derivatives were expressed and purified as previously described [55] with the following modifications. 100 mL cultures were lysed by using a French press, nucleic acid removed by precipitation with polyethyleneimine and supernatants clarified by ultracentrifugation [55]. $3D^{pol}$ was precipitated by addition of solid ammonium sulfate to 40% saturation. Recovered pellets were suspended and passed over a 3 mL phosphocellulose column. Bound protein was eluted from the phosphocellulose column by using 1/6 column volumes (500μL) of 50 mM HEPES pH 7.5, 10 mM DTT, 20% glycerol, 0.1% NP-40 and 200 mM NaCl. The proteins were > 90% pure based upon SDS-PAGE analysis. Two of the derivatives (D238A and N297A) were purified using the complete purification procedure [55] to > 95% purity. The concentration of all $3D^{pol}$ derivatives was determined by absorbance at 280 nm using a calculated extinction coefficient of 71,480 M^{-1} cm^{-1} [56]. The concentration of enzyme stocks prepared by using the abbreviated procedure ranged from 43 to 51 μM.

Purity of [α-^{32}P] UTP - [α-^{32}P] UTP was diluted to 0.1 μCi/μL in ddH_2O, and 1 μL spotted in triplicate onto TLC plates. TLC plates were developed in 0.3 M potassium phosphate, pH 7.0, dried and exposed to a phosphorimager screen. Imaging and quantitation were performed by using the ImageQuant software from Molecular Dynamics. The purity was used to correct the specific activity of UTP in reactions in order to calculate accurate concentrations of product.

Poly(rU) Polymerase Activity Assays - Reactions contained 50 mM HEPES pH 7.5, 10 mM 2-mercaptoethanol, 5 mM $MgCl_2$ or $MnCl_2$, 60 μM $ZnCl_2$, 500 μM UTP, 0.4 μCi/μL [α^{32} P] -UTP, 1.8 μM dT_{15}/2 μM rA_{30} primer/template and $3D^{pol}$. Reactions were carried out in a total volume of 25 μL with 250 ng of enzyme at 30 °C for 5 min. Reactions were quenched by the addition of 5 μL of 0.5 M EDTA. 10 μL of the quenched reaction was spotted onto DE81 filter paper discs and dried completely. The discs were washed 3 times for 10 min in 250 mL of 5% dibasic sodium phosphate and rinsed in absolute ethanol. Bound radioactivity was quantitated by liquid scintillation counting in 5 mL of EcoScint scintillation fluid (National Diagnostics).

5'-^{32}P Labeling of Oligonucleotides - RNA oligonucleotides were end-labeled using [γ-^{32}P]ATP and T4 polynucleotide kinase essentially as specified by the manufacturer. Reactions typically contained 11 μM [γ-^{32}P]ATP, 10 μM RNA oligonucleotide, and 0.4 units/μL T4 polynucleotide kinase. Unincorporated nucleotide was removed by passing the sample over two consecutive 1 mL Sephadex G-25 (Sigma) spun columns.

Kinetics of Single Ribo- and Deoxyribonucleotide Incorporation - Rates of nucleotide incorporation were determined using a synthetic RNA oligonucleotide primer/template (sym/sub) [48]. Reactions were performed either on the bench top or in an RQF-3 rapid

quenching/mixing device (KinTek Corp, Austin, TX) [57]. Enzyme/nucleic acid complexes were preformed by incubating 2 μM end-labeled sym/sub and 2 μM enzyme for 90-200 seconds at 30 °C in 50 mM HEPES pH 7.5, 5 mM $MgCl_2$ or $MnCl_2$, 10 mM β-mercaptoethanol, 60 μM $ZnCl_2$. Reactions were initiated by the addition of an equal volume of nucleotide in the above buffer. At indicated times, the reaction was quenched by addition of 0.5 M EDTA to a final concentration of 0.3 M.

Denaturing PAGE - Ten μL of the quenched reaction was added to 10 μL of loading buffer: 90% formamide, 50 mM Tris borate, 0.025% bromophenol blue, 0.025% xylene cyanol. Samples were heated to 70 °C for 2-5 min prior to loading 5 μL on a 23% polyacrylamide, 1.5% bisacrylamide, 7 M urea gel. Electrophoresis was performed in 1X TBE (89 mM Tris, pH 8.0, 10 mM boric acid, 2 mM EDTA) at 75 W. Gels were visualized by using the Phosphorimager (Molecular Dynamics, Inc) and quantitated by using the ImageQuant software (Molecular Dynamics, Inc).

Data Analysis - Data were plotted using the program Kaleidagraph (Synergy Software, Reading, PA). The rate of nucleotide incorporation (k_{obs}) was determined by fitting the data to a single exponential, $k_{obs} = A*\exp^{-kt}$, where A is the maximum amplitude, k is the observed rate of nucleotide incorporation and t is time. The maximum rate of nucleotide incorporation (k_{pol}) as well as the apparent binding constant (K_d) were determined by replot of k_{obs} versus [nucleotide] and fit to the following equation: $k_{obs} = ((k_{pol}*[\text{nucleotide}])/(K_d + [\text{nucleotide}]))$.

Construction of Mutated Viral cDNA Clones (pMo-3D) - Cloning of mutated $3D^{pol}$-coding sequence into the plasmid containing the full-length cDNA of poliovirus (pMoRA, also known as pXpA-rib$^+$polyAlong [58]) required subcloning into an

intermediate pUC plasmid due to conflicting restriction sites in the pMoRA plasmid. Bgl II and Sca I restriction sites were introduced into a pUC18 plasmid by insertion of a synthetic linker between the BamH I and EcoR I sites of this vector. The linker oligos (oligos 17 and 18, Table 1) were annealed prior to ligation. Sca I was used to screen clones for the presence of the linker. The cDNA encoding the 3CD region of the wild-type Mahoney strain of poliovirus was PCR amplified from pMoRA using the DNA oligonucleotides: pMo-EcoR I-rev (oligo 19, Table 1) and pMo-Bgl II-for (oligo 20, Table 1). The PCR product was ligated into the modified pUC18 vector using the Bgl II and EcoR I restriction sites. The entire insert was sequenced, and this construct was designated pUC-3CD.

Each mutated $3D^{pol}$-coding sequence was PCR amplified from the appropriate pET26b-Ub-3D plasmid using the DNA oligonucleotides: N-Term-Ub (oligo 21, Table 1) and 3D-rev-pET (oligo 22, Table 1). The PCR product was digested with BstB I and Mfe I and ligated into appropriately digested pUC-3CD. The mutated viral cDNA clones were constructed by subcloning the Bgl II-EcoR I fragment from pUC-3CD into pMovRA. These final constructs were sequenced from the BstB I site through the Mfe I site.

Construction of Mutated Replicons (pRLuc-3D) - The pRLuc-3D clones were constructed by subcloning the Bgl II-Apa I fragment from pMo-3D constructs containing the mutated 3D genes into pRLucRA (also known as pRLuc31-rib$^+$polyAlong) [58].

Cells and Transfections - HeLa S3 (ATCC stock + 10-30 passages) were propagated in DMEM/F12 (Gibco/Life Technologies) supplemented with 10% fetal calf serum (Gibco/Life Technologies), always keeping the cultures between 20-80% confluence. For

infectious center assays, viral RNA was produced by *in vitro* transcription of linearized plasmids (pMoRA wt plasmid, or the appropriate pMo-3D^{pol} derivative) using T7 RNA polymerase as described [59]. 10 μg of each viral RNA transcript was electroporated into 1.2 x 10^6 HeLa cells in 400 μl in a 0.2 cm cuvette using the electroporation settings: 950 μF, 24 Ω, 130 V on a BTX electroporator, giving an average pulse length of 5 msec. Electroporated cells were separately diluted (10-fold) in phosphate buffered saline (PBS), and 100 μl of appropriate dilutions (10^{-1}-10^{-5}) were plated on 2 x 10^5 HeLa cells (prepared one day in advance) in 6-well dishes (a total volume of 0.5 mL.) The remainder of the undiluted electroporated cells were also plated. Cells were allowed to adsorb to the plate for 1-2 hrs at 37 °C or 32 °C then the medium/PBS was aspirated and the cells were overlaid with 3 mL of a mixture of 1x DMEM/F12 + 10% FCS and 1% agar. Infectious center assays were then incubated at 37 °C or 32 °C for 2 days (wt at 37 °C), 3 days (wt at 32 °C), or 7 days (3D^{pol} mutant viruses). Plates were stained with the vital dye crystal violet and viral plaques were counted.

Replicon transfections were performed using polioLuc RNA transcribed from the plasmid pRLucRA [58] or the pRLuc-3D derivatives detailed above, using electroporation conditions described above. 1 x 10^5 cells were added per well to 6-well dishes in pre-warmed (37 °C or 32 °C) DMEM/F12 + 10% FCS medium. Cells were harvested at various times by centrifugation at 14,000g for 2 minutes in an Eppendorf microfuge, lysed in 100 μl 1x cell culture lysis reagent (Promega, Madison, WI) on ice for 2 minutes, and cellular debris and nuclei were removed away by centrifugation by 14,000g for 1 minutes in the microfuge. Lysates were left on ice at 4 °C until all timepoints were collected. Lysates were diluted 1:100 in H_2O and assayed for luciferase

activity after mixing 10 μl lysate with 10 μl luciferase assay substrate (Promega, WI) in an OptocompI luminometer (MGM, USA).

Results and Discussion

Model for the Ternary Complex of $3D^{pol}$ - As a first step towards elucidating the structure-function relationships of the RNA-dependent RNA polymerase from poliovirus ($3D^{pol}$), we constructed a model of a complex comprising the enzyme, primer/template and nucleotide. The final structural model consists of structural motifs A, B, C and E, nucleic acid primer/template, incoming nucleotide and magnesium ions. In addition, an extended α-helix that supports the template strand, the loop leading into motif B and the active site portion of the fingers subdomain were constructed. The latter two elements were missing in the $3D^{pol}$ structure [1] (Figure 1).

This model contains features that offer insight into the roles of conserved residues of the RdRP. RdRPs contain a signature GDD motif (structural motif C) consisting of a strictly conserved glycine (G327) as well as an aspartic acid (D328). A structurally analogous aspartic acid has been observed at this position in all nucleic acid polymerases studied to date; however, the role of the conserved glycine in the RdRP remains unclear. Comparison of the $3D^{pol}$ ternary complex model with the HIV-1 RT ternary complex structure offers insight into the functional significance of a glycine at this position. In the $3D^{pol}$ model, the presence of a bulky side chain, such as methionine, would clash with the 2'-OH on the primer strand.

The structurally analogous residue in HIV-1 RT, M184, lines the underside of the sugar on the 3' end of the DNA primer. Recently, Vaccaro *et al.* have shown that initiation of minus-strand DNA synthesis by HIV-1 RT is 12- to 33-fold slower when

utilizing an RNA primer/template instead of a DNA/RNA or DNA/DNA primer/template [60]. This slow initiation is likely due to a steric clash between M184 and the 2'-OH at the 3'-end of the RNA primer. Steric problems should be overcome following multiple rounds of dNMP incorporation that permit movement of the RNA primer out of the enzyme active site [61,62]. Consistent with this observation, mutational analysis of G327 of $3D^{pol}$ has shown that smaller side chains, such as alanine or serine, are accommodated to some extent while substitution of larger residues at this position are inhibitory based upon poly(rU) polymerase activity [63]. Interestingly, in T7 RNAP a histidine (H811) is present at the structurally analogous position to G327 of $3D^{pol}$. In the crystal structure of a transcribing T7 RNAP, H811 makes a hydrogen bond to the furanose ring oxygen of the nucleotide at the 3' end of the primer [46]. In order to preclude steric problems with the 2'-OH on the primer strand, the side-chain of H811 is positioned away from this hydroxyl group by interactions with charged side-chains of the enzyme [46].

Conserved residues involved in active site metal coordination (D233, motif A and D328, motif C) are present in the model. Mutational analysis of either residue in $3D^{pol}$, as well as in other polymerase systems, has demonstrated that an aspartic acid at both positions is required for polymerase activity [63]. $3D^{pol}$ derivatives containing glutamic acid, histidine, asparagine, or glutamine in place of D328 lack poly(rU) polymerase activity [63].

By analogy to the HIV-1 RT structure, two conserved basic residues, K167 and R174 of $3D^{pol}$, are predicted to make contact with the phosphate moiety of the incoming nucleotide. While the fingers subdomain is not present in the unliganded structure for $3D^{pol}$, superpositioning of the two structures reveals an α-helix ($3D^{pol}$ residues 183-202)

in close proximity to the beta-strand segment of HIV-1 RT leading into the active-site side of the fingers subdomain. Sequence homology permitted the assignment of $3D^{pol}$ residues corresponding to the beta flap of HIV-1 RT (β3-β4). Recently, the complete structure for the RdRP from hepatitis C virus (HCV NS5B) was determined [10,11]. Structural comparisons of the fingers region of NS5B and HIV-1 RT identified a new structural motif (motif F) [11]. The assignment of residues 163-174 of $3D^{pol}$ to motif F are in agreement with structural information now available for NS5B.

Nucleotide crosslinking studies with $3D^{pol}$ have suggested that another conserved residue, K66, is required for activity both *in vitro* and *in vivo* and may be in direct contact with the incoming nucleotide [64]. While the K66 side chain is disordered in the $3D^{pol}$ structure, structural and sequence homology to NS5B would place this residue at the border of the NTP channel leading to the polymerase active site. Modeling of nucleic acid and nucleotide into the NS5B structure places the analogous residue to K66, K56, approximately 3.0 Å away from the incoming nucleoside triphosphate (data not shown). K66 may therefore be required to direct the incoming nucleotide into the active site and/or stabilize the triphosphate moiety by making contact with oxygens on the γ phosphate.

DNA polymerases most likely select for 2'-deoxyribonucleotides by using a steric gating mechanism that excludes the bulky 2'-OH present on ribonucleotides. Residues in conserved structural motifs A and B appear to be important mediators of the selection against rNTP binding [27,29,65]. Mutation of E710 (KF) and F155 (MMLV RT) to alanine and valine, respectively, has revealed that these derivatives are less likely to discriminate against a ribonucleotide when compared to the wild-type enzyme [27,30].

While these enzymes are capable of incorporating a ribonucleotide more efficiently than their wild-type counterparts, multiple cycles of NMP incorporation may be prohibited by the steric problems with motif C discussed above.

Based upon structural homology to residues in DNA polymerases, it was put forward that D238 and N297 of $3D^{pol}$ are important for nucleotide selection at the 2'-position of the ribonucleotide [1]. Specifically, it was suggested that selection for the presence of a 2'-OH is mediated by a hydrogen bonding network between D238, N297 and the 2'-OH of the incoming ribonucleotide [1]. In contrast to the unliganded structure, the final model for the ternary complex of $3D^{pol}$ shows D238 hydrogen bonding to a highly conserved threonine (T293) while N297 is interacting with the 2'-OH of the incoming nucleotide (Figure 2). Given the difference between the unliganded structure and the model, substitutions were made at both positions to determine the functional significance of a hydrogen bond between these two residues. Furthermore, because both residues are strictly conserved in the supergroup I and III polymerases and highly conserved in the supergroup II polymerases [66], functional analysis of these amino acids is important to begin to understand the roles of these conserved side chains which line the nucleotide-binding pocket.

Rationale for Mutations - In order to test the functional significance of the hydrogen-bonding interaction between D238 and N297 (Figure 2), a series of mutations were introduced into $3D^{pol}$-coding sequence. These mutations changed D238 to alanine, asparagine, glutamic acid, phenylalanine or valine, or changed N297 to alanine, aspartic acid, glutamine, phenylalanine or valine. Alanines were substituted at either position

(D238A or N297A) such that a hydrogen bond between D238 and N297 would be disrupted. The structurally analogous residues of the DNA-dependent DNA polymerases (D238E or N297Q) and reverse transcriptases (D238F or N297F) were substituted. If a steric interaction and not a hydrogen bond is important for activity then substitution of valine may be sufficient for $3D^{pol}$ activity (D238V or N297V). Finally, substitution of the pairing partner of either two residues (D238N or N297D) may be sufficient to retain the hydrogen bond and have little effect on activity. If a hydrogen bond between D238 and N297 is required for ribonucleotide selection then substitutions at either position that would disrupt hydrogen bonding should result in $3D^{pol}$ derivatives that have equivalent phenotypes.

Activity on Homopolymeric Primer-Templates - In order to assess the effects of substitutions at positions 238 and 297 on polymerase activity, we evaluated the $(dT)_{15}$-primed poly(rU) polymerase activity of each $3D^{pol}$ derivative. If a hydrogen bond between D238 and N297 is required for polymerase function, then substitutions at either position should equally impair polymerase activity. However, an equivalent phenotype was not observed. Substitutions at position 238 almost completely abolished activity (1-7% wild-type) while those at position 297 had only moderate effects (20-80% wild-type) (Table 2).

Derivatives containing substitutions that mimic the nucleotide-binding site of DNA polymerases (D238F, D238E and N297Q) were analyzed for poly(dT) polymerase activity. Incorporation of dTMP was not observed with any of the derivatives by using this assay (data not shown). It was possible that incorporation of dNMPs required

"proper" positioning of the enzyme on the primer/template. In the previous experiments, a DNA primer was employed. Perhaps an RNA primer could support dNMP incorporation. To test this possibility, incorporation of rNMPs and dNMPs was evaluated by using an $(rU)_{15}$ primer. Again, dNMP incorporation was not observed (data not shown).

Changing D225 of NS5B (D238 homologue) to glycine or asparagine resulted in a complete loss of activity [67]. Changing D240 of EMCV $3D^{pol}$ to glutamic acid produced an enzyme with a 33-fold reduction in activity [68]. However, based upon poly(rU) polymerase activity, substitutions at the N297 equivalent of $3D^{pol}$ resulted in either a complete loss of activity or significantly reduced activity (6 % wild-type) for NS5B and EMCV $3D^{pol}$, respectively. While these results are in partial agreement with our observations, alternative substrates were not available to evaluate these substitutions further, making interpretation of these differences difficult.

It is possible that substitutions at D238 may have resulted in large rearrangements of the nucleotide-binding pocket. To test the catalytic competence of the $3D^{pol}$ derivatives, manganese was substituted for magnesium in the poly(rU) polymerase assays because manganese is known to stimulate wild-type activity [20]. All of the derivatives could be stimulated in the presence of manganese, albeit to various degrees (Table 2). Substitutions at N297 could be stimulated to wild-type levels or greater than the wild-type levels observed in magnesium. For three of the five substitutions at D238, approximately 75% of the wild-type activity could be restored by using manganese. Two of the derivatives: D238F and D238V showed only a slight increase in poly(rU) polymerase activity suggesting that the presence of larger hydrophobic residues at this

position is not suitable for activity, possibly due to the presence of large and/or charged residues in the pocket. Taken together, these results suggest that in most instances major structural rearrangements do not occur when substitutions are made at positions 238 and 297 and a hydrogen bond between D238 and N297 is not absolutely required for polymerase activity.

Activity on sym/sub - While evaluation of poly(rU) polymerase and related activities of $3D^{pol}$ derivatives is useful as a first step, the fact that the rate-limiting step for this reaction reflects template switching limits the utility of the resulting data [19]. We recently reported the development of a symmetrical primer/template substrate (sym/sub) suitable for evaluation of the kinetics and mechanism of $3D^{pol}$-catalyzed RNA synthesis [48]. We have used this system to characterize further each $3D^{pol}$ derivative. The kinetics of AMP incorporation were evaluated for each $3D^{pol}$ derivative at two concentrations of ATP: 100 μM and 1000 μM. The K_d value of wild-type $3D^{pol}$ for ATP is approximately 100 μM (JJ Arnold and CE Cameron, manuscript in preparation).

The position 238 derivatives had the following order of activity: D238A>D238E=D238N>D238F/D238V (Table 3). The D238A derivative was 400- to 900-fold less active than the wild-type enzyme. This reduction in activity could not be attributed to defects in nucleotide binding for this derivative (or any other) because a 10-fold increase in ATP concentration never produced more than a two-fold increase in the observed rate of AMP incorporation.

The position 297 derivatives had the following order of activity: N297D> N297V>N297A>N297Q (Table 3), representing a 2- to 70-fold reduction in activity

relative to wild-type $3D^{pol}$. This range of activity relative to wild-type $3D^{pol}$ is significantly different from the 2- to 5-fold decrease in activity observed by using the poly(rU) polymerase assay. This difference likely reflects a change in the rate-limiting step measured using the different assays: template switching (poly(rU) polymerase assay) [19] and elongation (sym/sub assay) [48].

The rates of single nucleotide incorporation were also determined by using Mn^{++} as the metal-ion cofactor at a single concentration of ATP (100 μM). Mn^{++} also stimulated AMP incorporation into sym/sub for each derivative analyzed. The relative order of activity of both position 238 and 297 derivatives was consistent with that observed in magnesium. However, the extent of the Mn^{++} rescue was not as substantial with the sym/sub assay as with the poly(rU) polymerase assay. By using preassembled $3D^{pol}$-sym/sub complexes, the effect of Mn^{++} reflects changes in the rate of nucleotide incorporation only (DW Gohara and CE Cameron, manuscript in preparation). By using dT_{15}/rA_{30}, the effect of Mn^{++} reflects both an increase in the rate of nucleotide incorporation and a decrease in the K_d value for $3D^{pol}$ binding to dT_{15}/rA_{30} [19,20].

By using sym/sub it is possible to determine the kinetic parameters, k_{pol} and K_d, for nucleotide incorporation and calculate the specificity constant, k_{pol}/K_d. This analysis permits a direct evaluation of the role of these residues in nucleotide selection. Two derivatives were selected for analysis: D238A and N297A. For this analysis, these two derivatives were purified by using the complete purification procedure [55].

The wild-type enzyme utilizes AMP 220-fold better than dAMP (Table 4). The selection by the enzyme for the ribonucleotide occurs primarily during incorporation (108-fold) rather than binding (2-fold) (Table 4). The D238A derivative was incapable of

distinguishing dATP from ATP. The k_{pol} value of this enzyme for both nucleotides was decreased 2000-fold relative to wild-type $3D^{pol}$. This difference may reflect a change in the rate-limiting step for this derivative, perhaps the chemical step is now rate-limiting for incorporation. If the rate of the chemical step is decreased, then the apparent reduction in the K_d value for nucleotides may reflect the constant for a different species (intermediate) in the reaction pathway rather than an increase in the affinity of the enzyme for nucleotide [48].

These data are consistent with observations made by Joyce and colleagues with Klenow fragment [26,27,28]. Mutation of E710 in this enzyme to alanine, resulted in an enzyme capable of incorporating ribonucleotides [27,28]. Furthermore, the maximal rate of incorporation of dNMPs was dramatically reduced relative to wild-type enzyme, suggesting a more direct role for this residue in nucleotidyl transfer [27,28].

In contrast to the complex phenotype of the D238A derivative, the phenotype of the N297A derivative is more easily interpreted. This enzyme had a 10-fold reduction in the ability to distinguish ribonucleotides from deoxyribonucleotides (Table 4). This reduction in specificity is due to a decrease in the efficiency of ribonucleotide incorporation rather than a decrease in the affinity of the enzyme for ribonucleotides (Table 4). It is possible that an interaction between N297 and the 2'-OH of the ribonucleotide, as indicated in the structural model (Figure 2), stabilizes the catalytically-competent ternary complex. If this complex "opens" more frequently in the absence of this interaction, then the observed rate of incorporation would be reduced. A similar argument can be used to explain the reduced rate of dNMP incorporation relative to rNMP incorporation for the wild-type enzyme (Table 4). The finding that the N297A

derivative is only 10-fold slower than the wild-type enzyme instead of 100-fold suggests that an additional residue may interact with the 2'-OH of the incoming rNTP. It is possible that another motif B residue, for example S288, has this function.

For the T7 RNAP system, Steitz and colleagues have suggested that H784 (N297 homologue) is in the proper orientation for selection at the 2'-position based upon their structural studies [44]. However, Sousa and co-workers have suggested that Y639 is involved in 2'-OH contacts based upon biochemical analysis of polymerase derivatives [25,45]. When the Y639F substitution was analyzed, relaxed specificity towards dNMP incorporation was observed compared to the wild-type enzyme. This result was interpreted as evidence that Y639 is directly involved in 2'-OH selection. More recently, the structure of an elongating T7 RNAP complex was solved with an incoming nucleotide bound at the active site [46]. In this structure it is observed that H784 and another residue, R425, interact with 2'-OH groups of both the incoming nucleotide and primer terminus. While these results seem to contradict each other, it is possible that the role of Y639 may be to increase the stringency of nucleotide binding as discussed in the "Introduction" rather than a direct interaction with the 2'-OH of the incoming ribonucleotide. The role of N297 in 2'-OH selection is probably very similar to that of H784 in T7 RNAP--that is, to provide a direct hydrogen bond.

Activity *in vivo*. The poly(rU) polymerase assay showed that the N297A, N297D and N297Q derivatives retained 80%, 60% and 20% of the wild-type activity, respectively. If these values reflect the biological activity, then it is reasonable to predict that the N297A and N297D derivatives might support virus multiplication while the

N297Q might exhibit a delayed growth phenotype or not support any virus growth. In contrast, the sym/sub assay showed that the N297A, N297D and N297Q derivatives retained 10%, 40% and 1% of the wild-type activity, respectively. Based upon these data it is reasonable to predict that virus containing a $3D^{pol}$-N297D substitution might be viable, but a virus containing $3D^{pol}$-N297A or $3D^{pol}$-N297Q might not. A series of poliovirus variants were constructed containing these specific alterations in $3D^{pol}$ to determine which of the two *in vitro* polymerase assays is more relevant biologically.

The viability of the mutant polioviruses were determined by transfecting cells at high efficiency with *in vitro* transcribed poliovirus RNA. 5×10^4 cells were infected per 1.2×10^6 cells transfected with wild-type poliovirus RNA or the MoΔNde I variant at 37 °C (Table 5), as scored in an infectious center assay (see Materials and Methods). Mo-$3D^{pol}$238A, Mo-$3D^{pol}$297A, Mo-$3D^{pol}$297D, and Mo-$3D^{pol}$297Q were all inviable at 37 °C (Table 5). Transfections were repeated at 32 °C and showed that only Mo-$3D^{pol}$297D was viable (Table 5). Interestingly, Mo-$3D^{pol}$297D was temperature sensitive and only formed small plaques at 6 days post-transfection, 4 days slower than wild-type virus (Fig. 3A).

To determine more directly the effect of these substitutions on RNA synthesis, a poliovirus replicon (polioLuc) that consists of a full-length poliovirus genome with the capsid genes replaced by a luciferase reporter gene was employed (Fig. 3B). Upon transfection into HeLa cells, polioLuc translates and replicates at levels comparable to wild-type poliovirus [58]. The appropriate $3D^{pol}$ mutations were cloned into this construct and translation and replication of the mutants observed at 37 °C and 32 °C (Fig. 3C and 3D). Poliovirus replication is inhibited by 2 mM guanidine. Therefore, luciferase activity obtained from polioLuc transfection in the presence of 2 mM guanidine is a measure of

the direct translation of the input RNA. All constructs translated at wild-type levels. PolioLuc-3D^{pol}238A completely failed to replicate as expected. PolioLuc-3D^{pol}297A replicated to levels slightly above background at both 37 °C and 32 °C, demonstrating a serious defect for replication *in vivo*. PolioLuc-3D^{pol}297D clearly replicated both at 32 °C and 37 °C, but was 10-fold down from wild-type replication levels at its peak at 37 °C, whereas 50% of the wild-type replication level was observed at 11 hrs post-transfection at 32 °C (Fig. 3C and 3D).

Taken together, these data demonstrate a direct correlation between the kinetics of elongation on sym/sub *in vitro* and the kinetics of RNA synthesis *in vivo* as judged by using the poliovirus replicon. Moreover, a 3-fold reduction in the elongation rate of 3D^{pol} confers a temperature sensitive growth phenotype upon the virus. Changes at position 297 should also affect nucleotide selection and may also change the overall fidelity of this derivative relative to wild-type 3D^{pol}. Therefore, additional studies with other derivatives will be necessary to prove that the biological phenotype associated with the virus containing the N297D substitution in 3D^{pol} is due solely to a defect in the rate of elongation. However, these results support the hypothesis that sym/sub recapitulates the biologically relevant elongation reaction.

Conclusions

Guided by the structural data for a complex of HIV RT with primer/template and nucleotide [7], we have constructed a structural model for a $3D^{pol}$-sym/sub-ATP elongation complex. This model makes several predictions regarding the function of conserved structural motifs found in the three RdRP supergroups. Here we show that the model is valid to a first approximation by using kinetic analysis of site-directed mutants of $3D^{pol}$ engineered to test predictions unique to the model—that is, aspects of the model that differ from structural data [1]. Residues found in conserved structural motifs A (Asp-238) and B (Asn-297) are involved in nucleotide selection. Asp-238 appears to couple binding of nucleotides with the correct sugar configuration to catalytic efficiency at the active site of the enzyme. Asn-297 is important for selection of rNTPs over 2'-dNTPs; a role mediated most likely via a hydrogen bond between the side chain of this residue and 2'-OH of the rNTP (Fig. 2). A more rigorous kinetic analysis of position 238 and 297 derivatives should provide greater insight into the molecular mechanism that requires these residues for nucleotide selection.

Mutational analysis of residues at positions 238 and 297 of $3D^{pol}$ produced derivatives exhibiting a range of catalytic efficiencies when assayed *in vitro* for poly(rU) polymerase activity or sym/sub elongation activity. We exploited this observation by subcloning a series of mutations into the poliovirus genome and a poliovirus replicon in order to address the following: (1) to determine whether poly(rU) polymerase activity or sym/sub elongation activity was a better prognostic for the biological polymerase

reaction; and (2) to determine the level of polymerase activity required to support virus multiplication. These data show a direct correlation between the activity of $3D^{pol}$ on sym/sub *in vitro* and the efficiency of RNA synthesis *in vivo*. In addition, a 30% reduction in the elongation rate of $3D^{pol}$ measured by using sym/sub produced virus with a temperature sensitive growth phenotype. Taken together, it is reasonable to conclude that complete inhibition of viral RNA transcription and replication is not necessary to reduce significantly virus production. Although additional studies will be necessary to understand the molecular basis for this observation, it is intriguing to speculate that the observed defect is related to the kinetic coupling of RNA synthesis and downstream processes such as packaging [69].

References

1. Hansen, J.L., Long, A.M., Schultz, S.C. (1997) *Structure* **5,** 1109-22.

2. Ollis, D.L., Kline, C., Steitz, T.A. *Nature* (1985) **313,** 818-9.

3. Eick, D., Wedel, A., Heumann, H. *Trends Genet.* (1994) 292-6.

4. Hermann, T., Meier, T., Gotte, M., Heumann, H. *Nucleic Acids Res.* (1994) **22,** 4625-33.

5. Doublie, S., Tabor, S., Long, A.M., Richardson, C.C., Ellenberger, T. *Nature* (1998) **391,** 251-8.

6. Kiefer, J.R., Mao, C., Braman, J.C., Beese, L.S. (1998) *Nature* **391,** 304-7.

7. Huang, H., Chopra, R., Verdine, G.L., Harrison, S.C. (1998) *Science* **282,** 1669-75.

8. Doublie, S., Ellenberger, T. (1998) *Curr. Opin. Struct. Biol.* **8,** 704-12.

9. Boyer, P.L., Ferris, A.L., Clark, P., Whitmer, J., Frank, P., Tantillo, C., Arnold, E., Hughes, S.H. (1994) *J. Mol. Biol.* **243,** 472-83.

10. Ago, H., Adachi, T., Yoshida, A., Yamamoto, M., Habuka, N., Yatsunami, K., Miyano, M. (1999) *Structure Fold. Des.* **7,** 1417-26.

11. Lesburg, C.A., Cable, M.B., Ferrari, E., Hong, Z., Mannarino, A.F., Weber, P.C. (1999) *Nat. Struct. Biol.* **6,** 937-43.

12. Steitz, T.A., Steitz, J.A. (1993) *Proc. Natl. Acad. Sci. U S A.* **90,** 6498-502.

13. Steitz, T.A. (1999) *J. Biol. Chem.* **274,** 17395-8.

14. Kuchta, R.D., Mizrahi, V., Benkovic, P.A., Johnson, K.A., Benkovic, S.J. (1987) *Biochemistry* **26,** 8410-7.

15. Patel, S.S., Wong, I., Johnson, K.A. (1991) *Biochemistry* **30,** 511-25.

16. Reardon, J.E. (1993) *J. Biol. Chem.* **268,** 8743-51.

17. Jia, Y., Patel, S.S. (1997) *J. Biol. Chem.* **272,** 30147-53.

18. Jia, Y., Patel, S.S. (1997) *Biochemistry* **36,** 4223-32.

19. Arnold, J.J., Cameron, C.E. (1999) *J. Biol. Chem.* **274,** 2706-16.

20. Arnold, J.J., Ghosh, S.K., Cameron, C.E. (1999) *J. Biol. Chem.* **274,** 37060-9.

21. Ricchetti, M., Buc, H. (1993) *EMBO J.* **12,** 387-96.

22. Arnaud-Barbe, N., Cheynet-Sauvion, V., Oriol, G., Mandrand, B., Mallet, F. (1998) *Nucleic Acids Res.* **26,** 3550-4.

23. Kati, W.M., Johnson, K.A., Jerva, L.F., Anderson, K.S. (1992) *J. Biol. Chem.* **267,** 25988-97.

24. Mosig, G. (1998) *Annu. Rev. Genet.* **32,** 379-413.

25. Huang, Y., Eckstein, F., Padilla, R., Sousa, R. (1997) *Biochemistry* **36,** 8231-42.

26. Minnick, D.T., Astatke, M., Joyce, C.M., Kunkel, T.A. (1996) *J. Biol. Chem.* **271,** 24954-61.

27. Astatke, M., Grindley, N.D., Joyce, C.M. (1998) *J. Mol. Biol.* **278,** 147-65.

28. Astatke, M., Ng, K., Grindley, N.D., Joyce, C.M. (1998) *Proc. Natl. Acad. Sci. U S A.* **95,** 3402-7.

29. Gao, G., Orlova, M., Georgiadis, M.M., Hendrickson, W.A., Goff, S.P. (1997) *Proc. Natl. Acad. Sci. USA* **94,** 407-11.

30. Gao, G., Goff, S.P. (1998) *J. Virol. 72,* 5905-11.

31. Rienitz, A., Grosse, F., Blocker, H., Frank, R., Krauss, G. (1985) *Nucleic Acids Res.* **13,** 5685-95.

32. Tabor, S., Richardson, C.C. (1989) *Proc. Natl. Acad. Sci. USA* **86,** 4076-80.

33. Beard, W.A., Minnick, D.T., Wade, C.L., Prasad, R., Won, R.L., Kumar, A., Kunkel, T.A., Wilson, S.H. (1996) *J. Biol. Chem.* **271,** 12213-20.

34. Astatke, M. Grindley, N. D. F., Joyce,C. M. (1995) *J. Biol. Chem.* **270,** 1945

35. Spence, R.A., Kati, W.M., Anderson, K.S., Johnson, K.A. (1995) *Science* **267,** 988-93.

36. Brandis, J.W., Edwards, S.G., Johnson, K.A. (1996) *Biochemistry* **35,** 2189-200.

37. Lewis, D.A., Bebenek, K., Beard, W.A., Wilson, S.H., Kunkel, T.A. (1999) *J. Biol. Chem.* **274,** 32924-30.

38. Tabor, S., Richardson, C.C. (1989) *Proc. Natl. Acad. Sci. USA* **86,** 4076-80.

39. Joyce, C.M. (1997) *Proc. Natl. Acad. Sci. USA* **94,** 1619-22.

40. Bonnin, A., Lazaro, J.M., Blanco, L., Salas, M. (1999) *J. Mol. Biol.* **290,** 241-51.

41. Harris, D., Kaushik, N., Pandey, P.K., Yadav, P.N., Pandey, V.N. (1998) *J. Biol. Chem.* **273,** 33624-34.

42. Kaushik, N., Harris, D., Rege, N., Modak, M.J., Yadav, P.N., Pandey, V.N. (1997) *Biochemistry* **36,** 14430-8.

43. Gutierrez-Rivas, M., Ibanez, A., Martinez, M.A., Domingo, E., Menendez-Arias, L. (1999) *J. Mol. Biol.* **290,** 615-25.

44. Cheetham, G.M., Jeruzalmi, D., Steitz, T.A. (1999) *Nature* **399,** 80-3.

45. Brieba, L.G., Sousa, R. (2000) *Biochemistry* **39,** 919-23.

46. Cheetham, G.M., Steitz, T.A. (1999) *Science* **286,** 2305-9.

47. Rechinsky, V. O.. Kostyuk, D. A., Tunitskaya, V. L., Kochetkov, S. N. (1992) *FEBS Lett.* **306,** 129

48. Arnold, J.J., Cameron, C.E. *J. Biol. Chem.* (2000) **275,** 5329-36.

49. Bailey, S. (1994) Acta Crystallogr. D **50,** 760-763.

50. T. A. Jones, J.-Y. Zhou, S. W. Cowan, M. Kjeldgaard, (1991) *Acta Crystallogr. D Biol. Crystallogr.* **A47,** 110 .

51. Brunger, A.T. (1998) *Acta Crystallogr. D Biol. Crystallogr.* **54,** 905-21.

52. Berendsen, R. (1984) *J. Chem. Phys.* **81,** 3684-3690.

53. Laskowski, R. A., McArthur, M. W., Moss, D. S., Thornton, J. M. (1993) *J. Appl. Crystallogr.* **26,** 283-291.

54. Aiyar, A., Xiang, Y., Leis, J. (1996) *Methods Mol. Biol.* **57,** 177-91.

55. Gohara, D.W., Ha, C.S., Ghosh, S.K.B., Arnold, J.J., Wisniewski, T.J., Cameron, C.E. (1999) *Protein Expr. Purif.* **17,** 128-38.

56. Gill, S.C., and von Hippel, P.H. (1989) *Anal. Biochem.* **182,** 319-326.

57. Johnson, K.A. (1986) *Methods Enzymol.* **134,** 677-705.

58. Herold, A and Andino, R. (2000) *J. Virol.* in press.

59. Crotty, S., Lohman, B.L., Lu, F.X., Tang, S., Miller. C.J., Andino, R. (1999) *J. Virol.* **73,** 9485-95

60. Vaccaro, J.A., Singh, H.A., Anderson, K.S. (1999) *Biochemistry.* **38,** 15978-85.

61. Wohrl, B.M., Krebs, R., Goody, R.S., Restle, T. (1999) *J. Mol. Biol.* **292,** 333-44.

62. Thrall, S.H., Krebs, R., Wohrl, B.M., Cellai, L., Goody, R.S., Restle, T. (1998) *Biochemistry* **37,** 13349-58.

63. Jablonski, S.A., Morrow, C.D. (1995) *J. Virol.* **69,** 1532-9.

64. Richards, O.C., Ehrenfeld, E. (1997) *J. Biol. Chem.* **272,** 23261-4.

65. Esteban, J.A., Salas, M., Blanco, L. (1993) *J. Biol. Chem.* **268,** 2719-26.

66. Koonin, E.V. (1991) *J. Gen. Virol.* **72,** 2197-206.

67. Lohmann, V., Korner, F., Herian ,U., Bartenschlager, R. (1997) *J. Virol.* **71,** 8416-28.

68. Sankar, S., Porter, A.G. (1992) *J. Biol. Chem.* **267,** 10168-76.

69. Nugent, C.I., Johnson, K.L., Sarnow, P., Kirkegaard, K. (1999) *J. Virol.* **73,** 427-35.

Figure Legends

Figure 1. Structural Model for the Ternary Complex of $3D^{pol}$. Structural model for $3D^{pol}$ complex with RNA primer/template (sym/sub), ATP and Mg^{++}. Model construction is described in the Materials and Methods. Structural motifs are color coded according to Hansen *et. al.*: motif A (residues 233-240), red; motif B (287-302), green; motif C (324-331), yellow; and motif E (368-380), purple. The proposed active site portion of the fingers subdomain (motif F, 175-202) as well as the alpha helical extension (163-174) are colored gray. Primer, template and ATP are shown as stick models and color coding is as follows: red, oxygen; blue, nitrogen; orange, phosphorus; gray, carbon. Metal ions A and B are shown as magenta spheres. For clarity only the last two nucleotides on the 3' end of the primer are shown. All structural diagrams were generated using the program WebLabViewer (Molecular Simulations Inc., San Diego, CA).

Figure 2. Analysis of the unliganded structure and ternary complex model of $3D^{pol}$. **A)** Asp-238 (motif A) and Asn-297 (motif B) are shown interacting at a distance of 3.0 Å, based on a modified version (see below) of the coordinate file for the unliganded structure of 3D pol (1); Thr-293 (motif B) is approximately 4.5 Å away from Asp-238. Superpositioning of the unliganded 3D pol structure onto the ternary complex structure of HIV-1 RT shows steric clash between Asp-238 and the 2'- and 3'-OHs of the nucleotide. To avoid unfavorable steric contact, either the side chain of Asp-238 must move relative

to the incoming nucleotide or the position of the nucleotide itself must be altered. However, the position of the nucleotide in the active site is constrained by hydrogen bonds between the phosphate moiety and the protein backbone, the position of the 3'-OH of the primer relative to the a-phosphate, and hydrogen bonding/stacking interactions of the base. A similar motion of Asp-225 (Asp-238 homologue) in NS5B is also required given the above constraints.

B) The ternary complex model indicates that Asp-238 is a distance of 2.8 Å from Thr-293, while Asn-297 is within hydrogen bonding distance (3.3 Å) of the 2'-OH of the incoming nucleotide (ATP). The 3'-OH and an oxygen of the b-phosphate are within hydrogen bonding distance.

C) Superposition of the unliganded 3D pol structure (dark gray) with the ternary complex model (light gray) predicts a conformational change of the enzyme after rNTP binding.

D) Proposed model for rNTP selection. Asn-297 hydrogen bonds to the 2'-OH of the incoming rNTP. Asp-238 is within hydrogen bonding distance of the 2'-OH of the incoming nucleotide in a conformation that is stabilized by hydrogen bonds to Thr-293 as well as the backbone amide of Ser-288. The 3'-OH of the incoming nucleotide makes contact with the backbone amide of Asp-238 and is within hydrogen bonding distance of the oxygen on the b-phosphate, thus providing a link between the nucleotide-binding pocket and the catalytic center of $3D^{pol}$.

Figure 3. ***In vivo*** **analysis of $3D^{pol}$ variants.** (A) Infectious center assay. HeLa cells were transfected with viral RNA (Mo or Mo-$3D^{pol}$297D) and then serially diluted and plated on a monolayer of untransfected HeLa cells. Plates were overlaid with an agar-

medium mixture (see "Material and Methods") as in traditional plaque assays, and incubated at 32 °C. Plates were developed on Day 3 or Day 6 post-transfection. Plates containing transfected cells plated at a 1 x 10^3 dilution are shown. Pinpoint plaques are visible on the Mo-3D^{pol}297D plate by day 6, when a comparable Mo transfected plate has been completely lysed. Plaque assays were repeated numerous times. (B) Schematic of polioLuc. PolioLuc is a poliovirus replicon that consists of a full-length poliovirus genome with the capsid genes replaced by a luciferase reporter gene. Upon translation, the active luciferase protein is cleaved away from the viral polyprotein by the viral protease 2A. (C) PolioLuc replicons at 37 °C. This experiment was performed in triplicate, a representative experiment is shown. Symbols are: wild-type polioLuc (■), wt polioLuc + 2mM guanidine (●), polioLuc-3D^{pol}238A (Δ), polioLuc-3D^{pol}297A (◊), and polioLuc-3D^{pol}297D (□). (D) PolioLuc replicons at 32 °C. Experiment was performed in triplicate, a representative experiment is shown. Symbols are as in (C)

Table 1 Oligonucleotides used in this study.

Oligo	Oligo Name	Sequence
1	pET-Ub-Sac II for	5' GCG GAA TTC CCG CGG TGG AGG TGA AAT CCA GTG G 3'
2	pET-Ub-BamH I rev	5' GCG TCT AGA GGA TCC ACC GCG GAG 3'
3	3D Afl II for	5' AAA AAC GAT CCC AGG CTT AAG ACA GAC TTT3'
4	3D Avr II rev	5' CCT GAG TGT TCC TAG GAT CTT TAG T 3'
5	D238A for	5' GAC TAC ACA GGG TAT GCT GCA TCT CTC AGC CCT 3'
6	D238E for	5' GAC TAC ACA GGG TAT GAA GCA TCT CTC AGC CCT 3'
7	D238F Nhe I for	5' GAC TAC ACA GGG TAT TTC GCA TCT CTC AGC CCT 3'
8	D238N for	5' GAC TAC ACA GGG TAT AAC GCA TCT CTC AGC CCT 3'
9	D238V for	5' GAC TAC ACA GGG TAT GTT GCA TCT CTC AGC CCT 3'
10	D238 wild-type rev	5' AGG GCT GAG AGA TGC ATC ATA CCC TGT GTA GTC 3'
11	N297A for	5' GGC ACT TCA ATT TTT GCT TCA ATG ATT AAC AAC 3'
12	N297D for	5' GGC ACT TCA ATT TTT GAC TCA ATG ATT AAC AAC 3'
13	N297F for	5' GGC ACT TCA ATT TTT TTC TCA ATG ATT AAC AAC 3'
14	N297Q for	5' GGC ACT TCA ATT TTT CAG TCA ATG ATT AAC AAC 3'
15	N297V for	5' GGC ACT TCA ATT TTT GTT TCA ATG ATT AAC AAC 3'
16	N297 wild-type rev	5' GTT GTT AAT CAT TGA GTT AAA AAT TGA AGT GTT3'
17	pUC18-Bsl II-top	5' GAT CCA GAT CTA GTA CTG 3'
18	pUC18-Bgl II-bot	5' AAT TCA GTA CTA GAT CTG 3'
19	pMo-EcoR I-rev	5' GAA TTA AAT CAT CGA TGA ATT CGG GCC C 3'
20	pMo-Bgl II-for	5' GAA GTG GAG ATC TTG GAT GCC AAA GCG 3'
21	N-term-Ub	5' ACG CTG TCT GAT TAC AAC 3'
22	3D-rev-pET	5' TTG GCT TGA CTC ATT TTA GTA AGG ATC CGA ATT CCG C 3'

Table 2. Poly(rU) Polymerase Activity of Wild-type $3D^{pol}$ and $3D^{pol}$ Derivatives

Specific activities were determined as described under "Materials and Methods."

Enzyme	Specific Activity[a] (*pmol UMP incorporated/min/μg*)	
	Mg^{++}	Mn^{++}
Wild-type	10	90
D238A	0.8	40
D238E	0.4	40
D238F	0.2	4
D238N	0.1	40
D238V	0.4	10
N297A	8	80
N297D	6	80
N297Q	2	30
N297V	4	50

[a] Specific activity values reported have been rounded to one significant figure.

Table 3. Kinetics of AMP Incorporation into Sym/sub Catalyzed by Wild-type $3D^{pol}$ and $3D^{pol}$ Derivatives.

Rates were determined as described under "Materials and Methods."

Enzyme	Rate (s^{-1})		
	Mg^{++}		Mn^{++}
	100 μM ATP	1000 μM ATP	100 μM ATP
Wild-type	17 ± 2	40 ± 5[a]	118 ± 12
D238A	0.040 ± 0.002	0.044 ± 0.003	2.3 ± 0.2
D238E	0.007 ± 0.001	0.013 ± 0.001	0.87 ± 0.02
D238F	< 0.0001	< 0.0001	-
D238N	0.009 ± 0.001	0.015 ± 0.002	0.94 ± 0.05
D238V	< 0.0001	< 0.0001	-
N297A	1.9 ± 0.4	3.4 ± 0.2	5.4 ± 0.6
N297D	6.5 ± 0.8	16.3 ± 1.2	25 ± 5
N297Q	0.25 ± 0.01	0.59 ± 0.02	0.84 ± 0.13
N297V	2.6 ± 0.2	7.3 ± 0.6	5.8 ± 1.1

[a]The two-fold difference in wild-type $3D^{pol}$ activity compared to Table 4 is due to the increased ionic strength of these enzyme preparations compared to those purified by using the complete protein purification procedure.

Table 4. Kinetic Parameters for Wild-type $3D^{pol}$ and $3D^{pol}$ Derivatives at 30 °C.

Parameters were determined as described under "Materials and Methods."

Enzyme	Nucleotide Substrate			
	ATP		dATP	
	k_{pol} (s^{-1})	K_d (μM)	k_{pol} (s^{-1})	K_d (μM)
WT[a]	86.7 ± 3.7	133 ± 18.1	0.80 ± 0.06	284 ± 59.1
D238A	0.044 ± 0.002	41 ± 5	0.037 ± 0.001	30 ± 2
N297A	4.6 ± 0.2	176 ± 31	0.22 ± 0.03	256 ± 29

[a]Values taken from Arnold and Cameron (manuscript in preparation).

Table 5. Poliovirus Mutants at $3D^{pol}$ Residues 238 or 297

virus	37 °C pfu/transfection[a]	32 °C pfu/transfection[b]
Mo	5×10^4	5×10^4
MoΔNde1	5×10^4	5×10^4
MoΔNde1—$3D^{pol}$D238A	0[c]	0[c]
MoΔNde1—$3D^{pol}$N297A	0	0
MoΔNde1—$3D^{pol}$N297D	0[d]	2×10^4
MoΔNde1—$3D^{pol}$N297Q	0	0

[a]37 °C plaque assays were observed for up to 7 days post-transfection. Wild-type virus was scored on day 2.
[b]32 °C plaque assays were observed for up to 8 days post-transfection. Wild-type virus was scored on day 3.
[c]Rare (2/transfection) plaques were recovered. These viruses were sequenced to confirm that they had reverted from 238A (codon GCT) to the wt 238D (codon GAT), and still possessed the MoΔNde1 silent marker mutations. The single point mutations were most likely generated during the *in vitro* T7 RNA transcription reactions.
[d]Rare (~10/transfection) plaques were recovered. By plaque appearance, these viruses fell into two classes: wild-type revertants (1-3 wt size plaques/transfection), and second site suppressor mutants (8-10 small plaques/transfection).

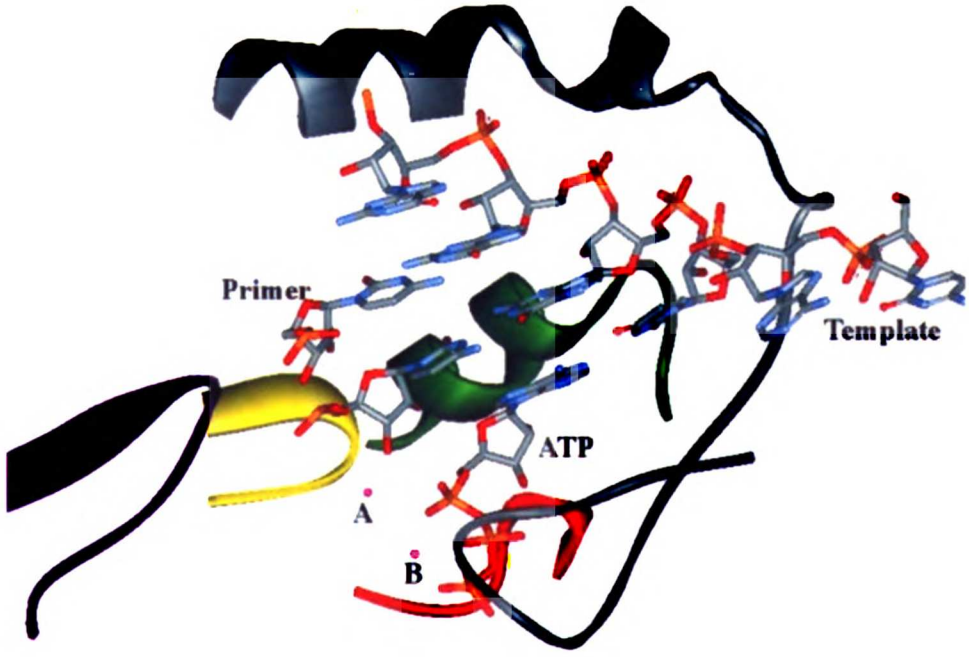
Primer
Template
ATP
A
B

Figure 2

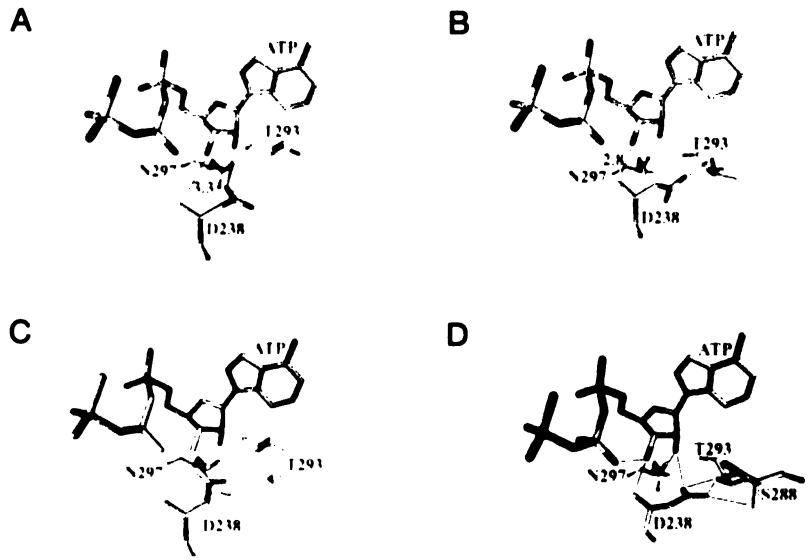
A
ATP
T293
N297
3.34
D238
B
ATP
T293
2.8
N297
D238
C
ATP
T293
N297
D238
D
ATP
T293
N297
S288
D238

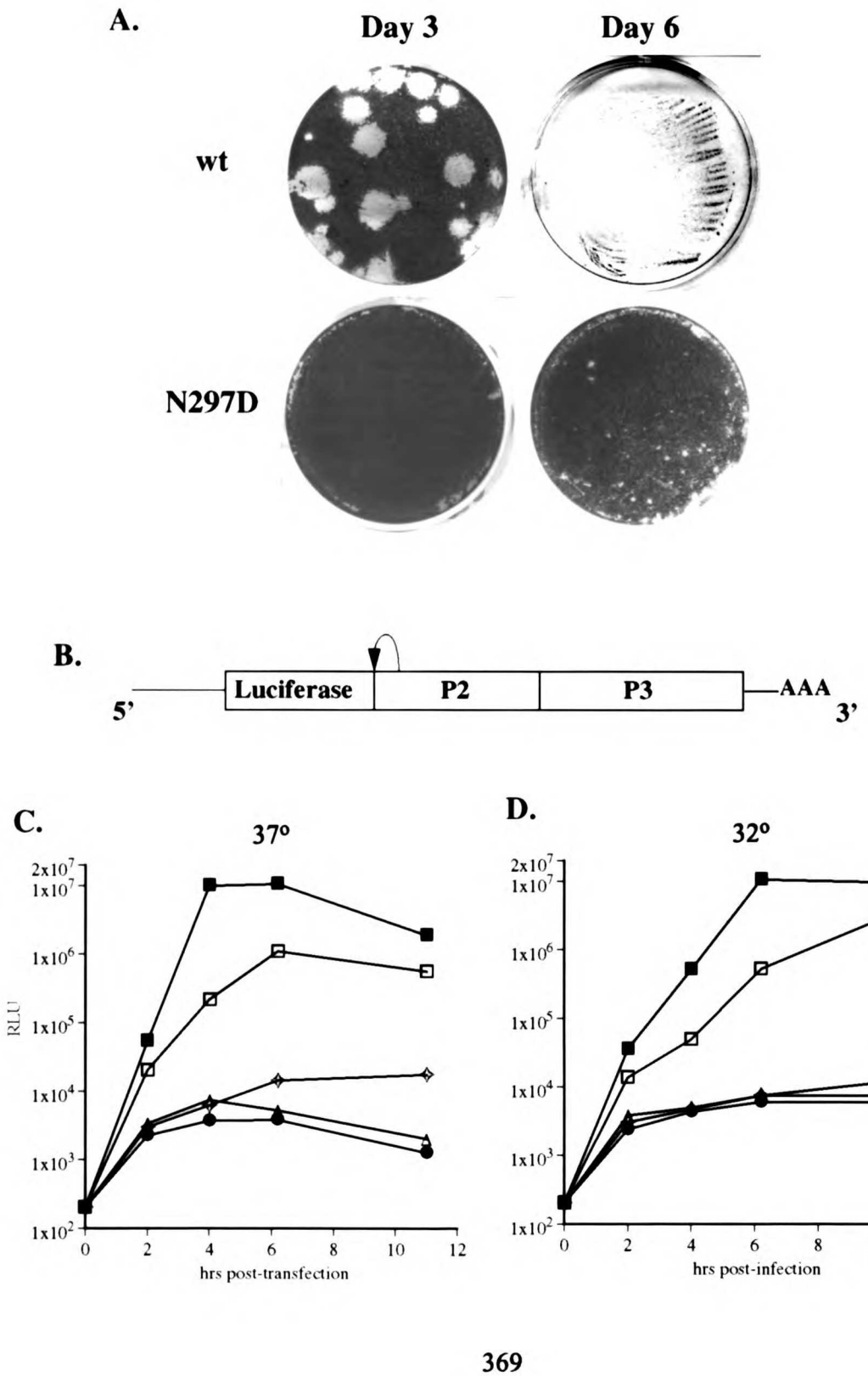
A.
Day 3
Day 6
wt
N297D
B.
Luciferase
P2
P3
AAA
5'
3'
C.
37°
RLU
2x10^7
1x10^7
1x10^6
1x10^5
1x10^4
1x10^3
1x10^2
0
2
4
6
8
10
12
hrs post-transfection
D.
32°
2x10^7
1x10^7
1x10^6
1x10^5
1x10^4
1x10^3
1x10^2
0
2
4
6
8
10
12
hrs post-infection

Chapter 16

Viable manganese dependent poliovirus RNA-dependent RNA polymerases with mutations involving a highly conserved NTP binding site asparagine

Introduction

RNA viruses exhibit extreme genetic diversity and an extraordinary ability to evolve in new environmental conditions. The genetic diversity of RNA viruses is most evident when the protein-coding sequences of related family members is analyzed, for example the positive strand RNA viruses of eukaryotes. The RNA-dependent RNA polymerase is the only protein coding sequence with clear sequence homology across this family of viruses (11, 12). Even within the RNA-dependent RNA polymerase protein coding sequence (~300-500 a.a. in the core catalytic domain), there is an enormous variety of sequences, with only six residues being conserved across all species of positive strand RNA viruses of eukaryotes (11). Using the poliovirus polymerase $3D^{pol}$ sequence as a reference, those six completely conserved amino acids are lysine 159, glycine 289, aspartic acid 233, aspartic acid 238, asparagine 297 (Fig. 1A), and the two aspartic acids (pos. 328-329) of the canonical GDD motif (the SDD motif in coronaviruses). Lysine 159 likely interacts with and stabilizes the triphosphate moity of the incoming nucleotide (NTP). Glycine 289 is part of the NTP binding pocket. Aspartic acids 233, 328, and 329 are involved in the coordination of the two magnesium cations (Mg^{++}) essential for catalyzing the incorporation of the incoming NTP (6)(Cameron et al., in prep.). Aspartic acid 238 binds to and positions the 3' OH of the incoming NTP (6). Asparagine 297 appears to assist in NTP binding (likely at the 2' OH) and descrimination between NTPs and dNTPs (6) (Fig. 1B).

As these residues are the only six amino acids conserved across all species of positive strand RNA viruses of eukaryotes, they are each expected to be critical for the function of the polymerase. Mutations engineered into these positions of the poliovirus polymerase $3D^{pol}$ have generally resulted in dead viruses, as expected (6, 9, 10, 13). The one exception was the most conservative possible change at position 297, changing the asparagine to an aspartic acid, which resulted in a highly temperature sensitive virus that produced pinpoint plaques after 6 days at 32°C (compared to 1 day for wildtype poliovirus) (6).

We therefore were surprised to discover, in the study reported here, that an asparagine at position 297 is not essential for growth at 37°C. The virus appears to have genetic flexibility even at this extremely conserved locus, as a glycine 297 mutation was viable, and two double mutations involving an alanine at 297 were also viable. We were even more surprised to observe that two of these viruses containing mutant polymerases exhibited manganese dependent growth.

Materials and Methods

Mutation identification. Candidate mutant viruses were used to infect HeLa cells at an moi of 0.1, incubated in medium the presence of 1 mM manganese at 37°C for 8 hrs, and total RNA was then harvest from the cells by RNeasy (Qiagen). Oligo dT primed cDNA of each candidate mutant was made using Superscript II. The $3D^{pol}$ coding sequence was PCR amplified from cDNA, and the entire length of the $3D^{pol}$ coding region was sequenced using BigDye terminator cycle sequencing and an ABI 310 DNA sequencer, and the data was analyzed with DNASTAR SeqManII.

Plasmids and molecular biology. Desired mutations were introduced into the polymerase coding region by oligo-directed mutagenesis using PCR. Primers 3DPST1 and 3D297G.R were used to amplify up PCR fragment G5 from a pMoBPKN template (6). Primers 3D297G.F and 3DNHE1 were used to amplify up PCR fragment G3. G5 and G3 products were then used as the combined template in a hybrid PCR reaction to produce fragment 297Gh, which was spin purified, digested with Pst1 and Nhe1, and cloned into Pst1-Nhe1 digested subcloning plasmid pLIT-3CD-BPKN. All PCR reactions were done using PfuTurbo under the manufacturer's recommended conditions. Sequence of the resulting pLIT-3CD-297G was confirmed by DNA sequencing. The BglII-EcoRI fragment of pLIT-3CD-297G was then cloned into a BglII-EcoRI digested pMoRA backbone. The $3D^{pol}$ coding sequence of the resulting plasmid, pMo-$3D^{pol}$297G, was sequenced to confirm the presence of the desired 297G mutation and the absence of any spurious mutations. A comparable cloning strategy was used to make pMo-

$3D^{pol}$286L/297A. Primers 3DPST1 and 3DMnD1.R were used to amplify PCR fragment D5 from a pMoBPKN template. Primers 3DMnD1.F and 3DNHE1 were used to amplify PCR fragment D3. Fragments D3 and D5 were used to template a hybrid PCR reaction, and the resulting product was cloned into pLIT-3CD-BPKN using the Pst1-Nhe1 sites as described above, and then then the appropriate BglII-EcoRI pLIT-3CD-286L/297A fragment was used to make pMo-$3D^{pol}$286L/297A, which was then sequenced across the $3D^{pol}$ coding region to confirm the presence of the two desired mutations and the absence of any spurious mutations. The cloning strategy for making pMo-$3D^{pol}$239G/297A required an additional level of complexity. Primers 3DPST1 and 3D236G.R were used to amplify PCR fragment 13.N from a pMoBPKN template. Primers 3D239G.F and 3D297A.R were used to amplify PCR fragment 13.M. Primers 3D297A.F and 3DNHE1 were used to amplify PCR fragment 13.C. The three fragments 13.N, 13.M, and 13.C were used as a combined template for a hybrid PCR reaction, and the resulting product MnD13h was cloned into pLIT-3CD-BPKN using the Pst1-Nhe1 sites as described above, and then the appropriate BglII-EcoRI pLIT-3CD-239G/297A fragment was used to make pMo-$3D^{pol}$286L/297A, which was sequenced across the $3D^{pol}$ coding region to confirm the presence of the two desired mutations and the absence of any spurious mutations. All of those plasmids contain an Amp^R selectable marker.

Subcloning plasmid pLIT-3CD-BPKN was made by cloning the BglII-EcoRI fragment of pMoRA-BPKN into a BglII-EcoRI digested pLIT28S backbone. pLIT28S was made by taking the plasmid pLITMUS28 (New England Biolabs, MA) and removing the PstI-AflII region of the polylinker. Those plasmids also contained Amp^R selectable markers.

Replicon clones were made by cloning the BglII-ApaI fragments of pLIT-3CD-297G, pLIT-3CD-286L/297A, and pLIT-3CD-239G/297A into BglII-ApaI digested pRLucRA (aka pRLucrib+polyAlong (5, 8)) to produce the respective plasmids pRLucRA-297G, pRLucRA-286L/297A, and pRLucRA-239G/297A. Each of those resulting mutant pRLucRA derivatives was sequenced across the $3D^{pol}$ coding region to confirm the presence of the appropriate mutations. Replicon plasmids each contain an Amp^R selectable marker.

$3D^{pol}$ expression vectors were constructed by cloning the Pst1-Nhe1 fragments of pLIT-3CD-297G, pLIT-3CD-286L/297A, and pLIT-3CD-239G/297A into Pst1-Nhe1 digested pET26-Ub-3D-BPKN-I92T (6) to produce the respective plasmids pET-3D-286L/297A (a.k.a. pET-3D-MnD1), pET-3D-297G, and pET-3D-239G/297A (a.k.a. pET-3D-MnD13). Each plasmid was sequenced across the entire region cloned to confirm the introduction of the desired mutations. pET-$3D^{pol}$ expression plasmids each contain a Kan^R selectable marker.

Oligonucleotides.

3DPST1 = GATAACAGGTTCTGCAGT

3D297G.R = TAATCATTGATCCAAAAATTGAGGTACCTGAG

3D297G.F = CCTCAATTTTTGGATCAATGATTAACAACTTGAT

3DNHE1 = TTCCTGATTGGGCTAGC

3DMnD1.F =

CAAGGGCGGTTTGCCATCTGGCTGCTCAGGTACCTCAATTTTTGCTTCAATGA

TTAACAACTTGAT

3DMnD1.R =

TAATCATTGAAGCAAAAATTGAGGTACCTGAGCAGCCAGATGGCAAACCGCC

CTTGACACAGTATG

3D239G.F = AGGGTATGATGGATCTCTCAGCCCTGCTTG

3D239G.R = GGCTGAGAGATCCATCATACCCTGTGTAGT

3D297A.F = CCTCAATTTTTGCTTCAATGATTAACAACTTGAT

3D297A.R = TAATCATTGAAGCAAAAATTGAGGTACCTGAG

Cells and Transfections. HeLa S3 (ATCC stock + 10-30 passages) were propagated in DMEM/F12 (Gibco/Life Technologies) supplemented with 10% fetal calf serum (Gibco/Life Technologies), always keeping the cultures between 20-80% confluence. For infectious center assays, viral RNA was produced by *in vitro* transcription of linearized plasmids using T7 RNA polymerase as described (4). 10 μg of each viral RNA transcript was electroporated into 1.2 x 10^6 HeLa cells in 400 μl in a 0.2 cm cuvette using the electroporation settings: 600 μF, 24 Ω, 130 V on a BTX electroporator, giving an average pulse length of 5 msec. Electroporated cells were plated on 2 x 10^5 HeLa cells in a six-well dish in a total volume of 1.0 ml.

The original Mo297A infectious center assay was done by electroporating cells as described above, then plating the electroporated cells on 3 x 10^6 HeLa cells (prepared one day in advance) in a 10 cm dish in a total volume of 3.0 mL.) Cells were allowed to adsorb to the plate for 1-2 hrs at 37°C then the medium/PBS was aspirated and the cells were overlaid with 20 mL of a mixture of 1x DMEM/F12 + 10% FCS and 1% agar as described (6). Infectious center assays were then incubated at 37 °C, and plaques were identified and picked at day 5.

Plaque assays were done as described (4, 5), with manganese added to the medium as necessary.

Replicon transfections and luciferase assays were performed using pRLucRA derived PolioLuc RNA, or RNA from clones pRLucRA-$3D^{pol}$286L/297A, pRLucRA-$3D^{pol}$297G, and pRLucRA-$3D^{pol}$239G/297A as previously done and described (5, 6), using electroporation conditions described above. 1 x 10^5 cells were added per well to 6-well dishes in pre-warmed 37 °C DMEM/F12 + 10% FCS medium. Cells were harvested at various times by centrifugation at 14,000g for 2 minutes in an Eppendorf microfuge, lysed in 100 µl 1x cell culture lysis reagent (Promega, Madison, WI) on ice for 2 minutes, and cellular debris and nuclei were removed away by centrifugation by 14,000g for 1 minute in the microfuge. Lysates were left on ice at 4 °C until all timepoints were collected. Lysates were diluted 1:100 in H_2O and assayed for luciferase activity after mixing 10 µl lysate with 10 µl luciferase assay substrate (Promega, WI) in an Optocompl luminometer (MGM, USA). Luciferase assays were not done in the presence of manganese because manganese inhibited the luciferase.

Biochemistry. $3D^{pol}$ expression and purification was done as previously described. Polymerase activities in Table 1 and Table 2 were measured using reagents and methods as previously described (2, 6, 7). dT_{15}/$polyA_{460}$ extension reactions contained 1 mM dT_{15}, 0.15 mM $polyA_{460}$, 0.4 mCi/mL [α-32 P]-UTP, 500 mM UTP in 50 mM HEPES pH 7.5, 5 mM $MgCl_2$, 10 mM ß-Mercaptoethanol and 60 mM $ZnCl_2$ (final). Reactions were initiated by the addition of $3D^{pol}$ to a final concentration of 0.5 mM and allowed to proceed for 5 minutes at 30°C. Reactions were stopped by the addition of an equal volume of 0.5 M EDTA. For pulse chase/pulse quench experiments, $3D^{pol}$ was added to

the above reaction mix in the absence of unlabeled UTP for three minutes. Initially labeled products were either quenched (PQ) or chased into long products (PC) by the addition of unlabeled UTP and heparin-3000 to final concentrations of 500 mM and 10 mM, respectively. A single time point was taken 5 min after the addition of unlabeled UTP/heparin and stopped as described above. The reaction products were resolved on a 15 % denaturing polyacrylamide gel as previously described (6). Template switching assay (Fig. 6) was done similarly to that previously described (3) except that the final concentration of rA_{30} was 1 mM and the reactions contained either $MgCl_2$ or $MnCl_2$ to final concentration of 5 mM. Upon the addition of unlabeled UTP/heparin, time points were taken at 3 and 7 min and the reactions quenched as described above.

Results

In a previous study (6), we analyzed the biological phenotypes of polioviruses containing a series of mutations in the nucleotide binding pocket. Several of these mutations were changes at position 297 in $3D^{pol}$ (Fig. 1A). The mutations tested all resulted in dead viruses at 37° C, including mutant Mo-$3D^{pol}$297A (6). Because RNA-dependent RNA polymerase activity in vitro can be stimulated by manganese (2, 3), we experimented with mutant virus growth conditions by supplementing infectious center assays with 0.5 mM manganese (Mn) after transfection with Mo-$3D^{pol}$297A RNA, an inviable virus possessing a polymerase with marginal *in vitro* activity (6). We were intrigued to observe that a few (~20) plaques appeared in the presence of 0.5 mM manganese five days after transfection. Those plaques were picked and classified into three complementation groups based on plaque size in the absence of manganese. Two clones from each complementation group were sequenced. Both clones from the first complementation group contained a single point mutation converting the methionine at position 286 of $3D^{pol}$ to a leucine (M286L), and they retained the 297A mutation. Both clones from the second complementation group contained a single point mutation that changed the mutant alanine at position 297 of $3D^{pol}$ into a glycine (N/A297G); no other mutations were observed in the second complementation group clones. Both clones from the third complementation group contained a single point mutation changing the wildtype alanine at position 239 of $3D^{pol}$ to a glycine (A239G), and they retained the 297A mutation. All three of these mutant virus classes contained highly unexpected sequences

at position 297 of the polymerase. Since the asparagine at position 297 of $3D^{pol}$ is completely conserved and is situated in an apparently critical position in the nucleotide binding pocket, we explored the phenotypes of these mutant viruses further.

The $3D^{pol}$ mutations were introduced into poliovirus plasmid clones by site-directed mutagenesis. All three mutant plasmid clones—pMo-$3D^{pol}$286L/297A, pMo-$3D^{pol}$297G, and pMo-$3D^{pol}$239G/297A—were sequenced to confirm the presence of the appropriate mutations, and then viral stocks were produced from the molecular clones. Plaque assays of virus produced from the plasmid clones of the $3D^{pol}$297 mutants are shown, with wildtype virus (Mo) as a positive control (Fig. 1A). Small plaques were observed for Mo-$3D^{pol}$286L/297A. Only pinpoint plaques were visible for Mo-$3D^{pol}$ 297G and Mo-$3D^{pol}$239G/297A after three to four days in culture (Fig. 1A).

All three viruses had severely defective growth kinetics under one step growth conditions (Fig. 1B). While wildtype virus had reached maximum virus production of 1.5 x 10^9 PFU by six hours post-infection, no virus production was detectable for the three mutants at six hours post-infection. Virus production for Mo-$3D^{pol}$286L/297A, Mo-$3D^{pol}$297G, and Mo-$3D^{pol}$239G/297A began appearing at 8 hrs (data not shown) and reached maximum titers by 12 hours post-infection (Fig. 1B). Mo-$3D^{pol}$286L/297A and Mo-$3D^{pol}$297G grew to relatively high titers of 1-3 x 10^8 PFU/ml under these conditions. Mo-$3D^{pol}$239G/297A was highly defective for virus production, generating only 3 x 10^6 PFU/ml, a 500-fold decrease from wildtype levels.

We used a poliovirus replicon (PolioLuc) to evaluate the RNA replication levels mediated by the mutant polymerases in cell culture. PolioLuc is a poliovirus replicon that consists of a full-length poliovirus genome with the capsid genes replaced by a luciferase

reporter gene (1, 8). Transfection of HeLa cells with replicon RNA results in the production of a polyprotein containing luciferase that is processed by the viral 2A protease to liberate active luciferase, and the replicon translates and replicates comparably to wildtype poliovirus (1, 8). Sequences from the three polymerase mutants were cloned into the pRLucRA luciferase replicon plasmid backbone, and PolioLuc-3D^{pol}286L/297A, PolioLuc-3D^{pol}297G, and PolioLuc-3D^{pol}239G/297A RNA was produced from each respective plasmid clone. Upon transfection of the RNA into HeLa cells, replication rates were compared against PolioLuc replicon RNA containing the wildtype poliovirus polymerase, and a separate replicon containing a completely defective polymerase, PolioLuc-3D^{pol}238A, which has no detectable RNA replication activity in cell culture (7).

PolioLuc-3D^{pol}238A never reached luciferase levels higher than seen with translation alone (~6 x 10^3 RLU, Fig. 3). Wildtype PolioLuc rapidly replicated to levels 1000-fold higher than the negative control PolioLuc-3D^{pol}238A by 4 hours post-transfection (7 x 10^6 RLU), levelling off at ~1.1 x 10^7 RLU by 6 hours post-transfection (Fig. 3). PolioLuc-3D^{pol}286L/297A replicated to levels ~90% that of wildtype PolioLuc, but with two hour slower kinetics. PolioLuc-3D^{pol}239G/297A replicated to comparable levels, but with a four hour time lag before maximum replication levels were reached. PolioLuc-3D^{pol}297G replicated to levels equal that of wildtype PolioLuc, but with a two hour time lag, comparable to that of PolioLuc-3D^{pol}286L/297A.

An additional construct, PolioLuc-3D^{pol}297D was also tested, as this construct was previously demonstrated to replicate to levels approximately 30% that of wildtype virus. That level of replication, in the context of the full length viral clone Mo3D^{pol}297D,

is not sufficient to produce visible plaques at 37° C (7). In the context of this experiment, PolioLuc-3D^{pol}297D replicated with very slow kinetics to maximum levels ~15% that of wildtype PolioLuc, as expected. All three of the viable 297 mutants replicated to significantly higher levels than PolioLuc-3D^{pol}297D in this replicon assay (Fig. 3). This confirmed that the kinetics of RNA replication observed in the replicon assay are a relatively good indicator of the polymerase activity necessary for viability, as PolioLuc-3D^{pol}286L/297A replicated better than PolioLuc-3D^{pol}239G/297A which replicated better than PolioLuc-3D^{pol}297D. The equivalence of PolioLuc-3D^{pol}286L/297A and PolioLuc-3D^{pol}297G was reflective of the growth of those two respective viruses under one-step growth conditions (Fig. 2B), but was not tightly correlated with the plaque assay phenotypes observed, as PolioLuc-3D^{pol}297G had a significantly smaller plaque phenotype (Fig. 2A).

As these mutant viruses were originally observed in an infectious center assay in the presence of 0.5 mM manganese, we assessed the growth phenotypes of Mo-3D^{pol}286L/297A, Mo-3D^{pol}297G, and Mo-3D^{pol}239G/297A in the presence of supplemental manganese. Plaque assays were performed in the absence or presence of 0.7 mM manganese. The presence of manganese had no obvious effect on wildtype poliovirus plaque formation (Fig. 4A). Mo-3D^{pol}286L/297A made plaques approximately 40% larger in the presence of manganese, and made twice as many plaques. Mo-3D^{pol}297G and Mo-3D^{pol}239G/297A had significantly stronger phenotypes, making easily visible plaques at day three in the presence of manganese, but no or pinpoint plaques in the absence of manganese (Fig. 4A). The most striking phenotype was the growth of Mo-3D^{pol}239G/297A in the presence of 1.0 mM manganese, where 75 plaques

were visible at day three, but only 3 pinpoint plaques were observed in the absence of manganese (Fig. 4B).

Given these unusual manganese-dependent phenotypes observed by plaque assay, we tested the effect of supplemental manganese on the replication of these mutant viruses under one step growth conditions. 0.5 μM manganese had no effect on any of the mutant viruses, or on wildtype virus (Fig. 5B). However, 0.5 mM manganese had a dramatic effect on Mo-3D^{pol}239G/297A growth: virus production increased 80-fold. Mo-3D^{pol}297G exhibited a more modest 5-fold increase in virus production in the presence of 0.5 mM manganese (Fig. 5B). PolioLuc-3D^{pol}286L/297A did not show a manganese dependent increase in virus production (data not shown).

Biochemical analysis of polymerase mutants

We then characterized the mutant polymerases biochemically. All three biologically selected mutant 3D^{pol} polymerases had faster nucleotide incorporation rates than 3D^{pol}297A under single turnover conditions using a sym/sub template (2, 5, 6) in the presence of magnesium, and lower incorporation rates than wildtype polymerase (Table 1). 3D^{pol}297D incorporation rates were 17 s^{-1} using the sym/sub template, comparable to that of 3D^{pol}286L/297A and 3D^{pol}297G, and higher than that of 3D^{pol}239G/297A (Table 1). Given that Mo-3D^{pol}297D is inviable at 37°C (and even at 32°C, Mo-3D^{pol}286L/297A, Mo-3D^{pol}297G, and Mo-3D^{pol}239G/297A each grew substantially better than Mo-3D^{pol}297D, data not shown) there was not a direct correlation between the *in vivo* viability of position 297 polymerase mutants and their polymerase single turnover nucleotide incorporation rates *in vitro*. Since Mo-3D^{pol}297G and Mo-3D^{pol}286L/297A

both exhibited manganese dependent growth phenotypes *in vivo*, we tested the incorporation rates of the $3D^{pol}$ mutants in the presence of manganese. Mo-$3D^{pol}$286L/297A, Mo-$3D^{pol}$297G, and Mo-$3D^{pol}$286L/297A had incorporation rates 30-50% that of wildtype polymerase in the presence of manganese, better than that of $3D^{pol}$297A (10% of wildtype levels, Table 1). However, $3D^{pol}$297D had similar or higher single turnover incorporation rates in manganese.

Seperately, the mutants showed no obvious differences in nucleoside misincorporation rates compared to wildtype on sym/sub-U in the presence of ATP (data not shown).

We then assessed the primer elongation capabilities of the polymerase mutants on long templates. To do this we utilized homopolymeric RNA templates rA_{460} or rA_{30}, with a dT_{15} primer. Using the rA_{460} template, $3D^{pol}$286L/297A, $3D^{pol}$297G, and $3D^{pol}$239G/297A all exhibited higher activity than $3D^{pol}$297A or $3D^{pol}$297D in the presence of magnesium (Table 2). The differences were even stronger when the rA_{30} template was used (Table 2). Additionally, $3D^{pol}$286L/297A, $3D^{pol}$297G, and $3D^{pol}$239G/297A exhibited higher activity than $3D^{pol}$297A or $3D^{pol}$297D on the rA_{30} template in the presence of manganese (Table 2).

We explored the rA_{460} extension results in greater detail by performing pulse-quench and pulse-chase analyses of product formation in the presence of magnesium (Fig. 6). For pulse-chase experiments, $3D^{pol}$ was added to a reaction mix containing 0.2 μM [α-^{32}P]-UTP and dT_{15}/rA_{460} primer-template, in the absence of unlabeled UTP, for a three minute pulse. Products labelled during the pulse period were chased into long products (PC lanes in Fig. 6) by the addition of unlabeled 500 μM UTP and heparin.

Pulse-quench experiments were quenched immediately after the three minute pulse by the addition of 0.5 M EDTA (PQ lanes in Fig. 6).

If the various mutant polymerases differed in their extension activity due to poor processivity, we would anticipate that a pulse-chase experiment would result in the formation of products of various lengths. If the mutant polymerases differed in the extension activity instead due to an inability to initiate synthesis, we would anticipate that the total amount of radioactivity incorporated into products during the pulse (as observed in the pulse-quench experiments) would be equivalent to the amount of radioactivity incorporated into the long products visible after a pulse-chase experiment.

We observed that the polymerases exhibited clear differences in their ability to initiate synthesis, as fewer products were observed in reactions primed with $3D^{pol}$297A and $3D^{pol}$297D than in reactions primed with $3D^{pol}$286L/297A, $3D^{pol}$297G, or wildtype, and all of the products formed during the pulse were compentent for extension into full length product, as the total amount of radioactivity detected after the pulse was equivalent to that detected in the long products after the chase (Fig. 6). Additionally, all mutants had no change in off rates (data not shown).

Pulse-chase and pulse-quench experiments were then done using template rA_{30} to assess the template switching ability of these polymerases, as formation of long products by $3D^{pol}$ in the presnce of an rA_{30} template requires template switching (3). On this template the polymerases again exhibited clear differences in their ability to initiate synthesis in the presence of magnesium (Fig. 7). The polymerases did not exhibit any obvious differences in template switching capacity, as long products were formed by all of the polymerases in proportion to the amount of radiolabelled nucleotide incorporated

during the pulse (Fig. 7). These experiments were also performed in the presence of manganese, and all of the polymerases exhibited an increased rate of initition in manganese.

Discussion

The viable mutants obtained were counterintuitive, as we predicted that any polymerase with an alanine at position 297 would be dead, much less a glycine at 297. This result attests to the extreme evolutionary flexibility of the virus's RNA-dependent RNA polymerase, as two point mutations are able to replace the function of an amino acid residue that is completely conserved across the entire family of positive strand RNA viruses of eukaryotes, one of only six such amino acid positions in the polymerase (11).

Mutation 286L/297A

The most fit of the selected viruses, Mo-3D^{pol}286L/297A, grows to titers of 3 x 10^8 PFU/ml under normal conditions. Biochemical analysis of 3D^{pol}286L/297A revealed that the polymerase has a reasonable rate of NTP incorporation (20 s^{-1}), but not significantly faster than 3D^{pol}297D (17 s^{-1}) which exhibits slower and 10-fold lower RNA replication *in vivo* (Fig. 3) such that Mo-3D^{pol}297D cannot form plaques at 37°C. This may be an issue of temperature sensitivity of 3D^{pol}297D, as the *in vitro* assays are done at 30°C, and higher temperatures might potentially cause a peculiar problem with this derivative (though even at 32°C Mo-3D^{pol}286L/297A grows much better than Mo-3D^{pol}297D by plaque assay). A primer elongation assay indicates that the issue is not temperature sensitvity, but instead a generally poor initiation of synthesis by 3D^{pol}297D, and 3D^{pol}297A (Fig. 6), which is greatly improved by the M286L second site mutation in conjunction with N297A.

Modelling and biochemical data indicates that N297 and D238 may interact with the 2' OH of the incoming NTP to correctly position the NTP and select against dNTPs (6). Molecular modelling suggests that S288 and T293 are part of a hydrogen bond network that stabilizes the positions of D238 and N297. Mutating the asparagine at 297 to an alanine completely eliminates any direct interactions that residue could have with the 2'OH of the incoming NTP. A compensatory M286L mutation could possibly reposition S288 and/or T293 to interact directly with the 2'OH, or encourage a stronger D238 interaction with the 2'OH.

Mutation 297G

$3D^{pol}$297G appears to replicate RNA *in vivo* with comparable efficiency to $3D^{pol}$286L/297A (Fig. 3), and to grow to fairly similar titers (1 x 10^8 PFU/ml, 3-fold less than Mo-$3D^{pol}$286L/297A), but it generally has a significantly smaller plaque phenotype than Mo-$3D^{pol}$286L/297A. Biochemically, the two polymerases $3D^{pol}$297G and $3D^{pol}$286L/297A behave quite similarly, in good correlation to the RNA replication data obtained. The one exception in that there is no obvious biochemical explanation for the 5-fold manganese dependent viral titer increase of Mo-$3D^{pol}$297G. This phenotype may be related to the higher rate of polymerase initiation seen *in vitro* in the presence of manganese and depend on an *in vivo* mixture of magnesium and manganese not easy to reproduce *in vitro*. Alternatively, it may depend on subtle NTP vs. dNTP fidelity improvements in the presence of supplementary manganese that are difficult to observe. Molecular modelling suggests that a glycine at position 297 should leave a sufficiently large pocket for a water molecule. Therefore, glycine may substitute for asparagine by

recruiting a water molecule to become the hydrogen bonding partner for the NTP 2'OH. Manganese liganded NTPs are thought to be bound more tightly in the polymerase binding pocket [REF], lowering the stringency of incorporation by allowing more time to appropriately position the NTP for catalysis. The presence of manganese may lower constraints on $3D^{pol}$297G initiation *in vivo* by allowing time for the appropriate positioning of the H_2O asparagine 297 surrogate and the NTP. The normal plaque phenotype of Mo-$3D^{pol}$297G is variable (compare Fig. 2 with Fig. 4), which is possibly a reflection of the sensitivity of $3D^{pol}$297G to environmental conditions. For example, $3D^{pol}$297G may possibly have a requirement for trace manganese that is variable in the medium and serum used.

Mutation 239G/297A

This mutant had the most severe growth defect of the three viable mutants observed. Nevertheless, Mo-$3D^{pol}$239G/297A is capable of plaque formation at 37°C under normal conditions. Luciferase replicon experiments demonstrated that $3D^{pol}$239G/297A is 10-fold better at RNA replication than $3D^{pol}$297D (Fig. 3). However, biochemical analysis revealed that $3D^{pol}$239G/297A had a three-fold worse single turnover NTP incorporate rate than $3D^{pol}$297D (6.0 versus 17, Table 1). Therefore, the single turnover NTP incorporation rate does not appear to be the factor determining viability of these polymerases.

$3D^{pol}$297A has minimal activity in magnesium. The glycine mutation at position 239 makes the polymerase viable in the context of Mo-$3D^{pol}$239G/297A *in vivo*. This virus is not as viable as Mo-$3D^{pol}$286L/297A. We posited that $3D^{pol}$286L/297A

compensated for the loss of the asparagine at position 297 by repositioning S288 and/or T293 to interact with the 2'OH of the incoming NTP. Mo-3D^{pol}239G/297A may solve the same problem by strengthening the interaction of D238 with the 2'OH of the incoming NTP. Mutating the alanine at position 239 to a glycine may let the aspartic acid at 238 slip into a more optimal position for interacting with the 2'OH. However, since D238 also appears to have important interactions with the 3'OH of the incoming NTP, the glycine mutation at position 239 may hinder that 3'OH interaction.

The mutant polymerase of Mo-3D^{pol}239G/297A resulted in a striking 80-fold manganese dependent growth phenotype *in vivo*. This demonstrates that a viable polymerase can depend on a cation besides magnesium. That requirement could indicate that 3D^{pol}239G/297A primarily depends on manganese for catalysis *in vivo*, or that 3D^{pol}239G/297A primarily uses magnesium *in vivo* but requires manganese as a supplemental metal ion for certain critical functions--possibly initiation. We posit that this could be due to the stabilizing effects of manganese on the incoming NTP. This may be important with a glycine at position 239, as the role of D238 in positioning of the NTP may be strained. Alternatively, 3D^{pol}239G/297A may have an increased dNTP incorporation rate *in vivo*, which may result in chain termination (Cameron et al., in prep). The presence of manganese may allow the polymerase to overcome the block in replication caused by dNTP incorporation. The manganese could be doing the same thing for 3D^{pol}286L/297A and 3D^{pol}297G, but presuming that these polymerases have lower dNTP incorporation rates they would have chain termination events less frequently than 3D^{pol}239G/297A and therefore the manganese would have less of an effect on Mo-3D^{pol}286L/297A and Mo-3D^{pol}297G virus growth.

The identification of viable mutants after transfection of Mo-3D^{pol}297A RNA in the presence of manganese could have been dependent on the presence of mutated T7 polymerase-derived *in vitro* transcripts only capable of significant plaque formation after transfection in manganese (e.g. Mo-3D^{pol}239G/297A). Alternatively, manganese is an RNA virus mutagen (S. Crotty and R. Andino, unpublished data), and the presence of manganese could encourage the synthesis of mutated Mo-3D^{pol}297A derivatives during the low-level Mo-3D^{pol}297A replication that occurs post-transfection, and several of those new mutants were viable for plaque formation. Jablonski and Morrow reported that they were able to recover infectious poliovirus in the presence of iron ($FeSO_4$) after transfection of a plasmid containing a mutant poliovirus genome possessing a GDN sequence instead of the canonical GDD motif (10). Unfortunately, they were never able to detect viral genomes of the viable virus or sequence that virus, and so they could not determine the polymerase sequence of the virus that appeared or characterize the RNA replication of the virus (10).

Our results with Mo-3D^{pol}239G/297A clearly demonstrate that a viable virus can have a requirement for an alternative cation. This may be of particular relevance to the RNA-dependent RNA polymerases of plant viruses, as plants generally contain significant intracellular stores of manganese. We speculate that certain plant viruses may have polymerases with a requirement for manganese.

If polioviruses with several alternative mutations involving N297 are viable, why then is N297 completely conserved across positive strand RNA viruses? Though a poliovirus containing 3D^{pol}286L/297A, 3D^{pol}297G, or 3D^{pol}239G/297A is viable, there

may be significant fitness problems with such polymerases over the course of multiple passages. And certainly any virus that managed to mutate back to N297 would have a large growth advantage, as the wildtype sequence replicates substantially faster than even the best of the mutants, 286L/297A, and to 10-fold higher titers. Nevertheless, if for example the presence of an antiviral drug "forced" a mutation at residue 297 for the virus to escape drug selection, it appears that the virus could effectively mutate around such a drug even at this completely conserved site.

References

1. **Andino, R., G. E. Rieckhof, P. L. Achacoso, and D. Baltimore** 1993. Poliovirus RNA synthesis utilizes an RNP complex formed around the 5'-end of viral RNA Embo Journal. **12**:3587-98.
2. **Arnold, J. J., and C. E. Cameron** 2000. Poliovirus RNA-dependent RNA polymerase (3D(pol)). Assembly of stable, elongation-competent complexes by using a symmetrical primer-template substrate (sym/sub) J Biol Chem. **275**:5329-36.
3. **Arnold, J. J., and C. E. Cameron** 1999. Poliovirus RNA-dependent RNA polymerase (3Dpol) is sufficient for template switching in vitro J Biol Chem. **274**:2706-16.
4. **Crotty, S., B. L. Lohman, F. X. Lu, S. Tang, C. J. Miller, and R. Andino** 1999. Mucosal immunization of cynomolgus macaques with two serotypes of live poliovirus vectors expressing simian immunodeficiency virus antigens: stimulation of humoral, mucosal, and cellular immunity J Virol. **73**:9485-95.
5. **Crotty, S., D. Maag, J. J. Arnold, W. Zhong, J. Y. Lau, Z. Hong, R. Andino, and C. E. Cameron** 2000. The broad-spectrum antiviral ribonucleoside ribavirin is an RNA virus mutagen Nat Med. **6**:1375-1379.
6. **Gohara, D. W., S. Crotty, J. J. Arnold, J. D. Yoder, R. Andino, and C. E. Cameron** 2000. Poliovirus RNA-dependent RNA Polymerase ($3D^{Pol}$): Structural, biochemical, and biological analysis of conserved structural motifs A and B Journal of Biological Chemistry. **275**:25523-25532.
7. **Gohara, D. W., C. S. Ha, S. Kumar, B. Ghosh, J. J. Arnold, T. J. Wisniewski, and C. E. Cameron** 1999. Production of "authentic" poliovirus RNA-dependent RNA polymerase (3D(pol)) by ubiquitin-protease-mediated cleavage in Escherichia coli Protein Expr Purif. **17**:128-38.
8. **Herold, J., and R. Andino** 2000. Poliovirus requires a precise 5' end for efficient positive-strand RNA synthesis J Virol. **74**:6394-400.
9. **Jablonski, S. A., M. Luo, and C. D. Morrow** 1991. Enzymatic activity of poliovirus RNA polymerase mutants with single amino acid changes in the conserved YGDD amino acid motif J Virol. **65**:4565-72.
10. **Jablonski, S. A., and C. D. Morrow** 1995. Mutation of the aspartic acid residues of the GDD sequence motif of poliovirus RNA-dependent RNA polymerase results in enzymes with altered metal ion requirements for activity J Virol. **69**:1532-9.
11. **Koonin, E. V.** 1991. The phylogeny of RNA-dependent RNA polymerases of positive-strand RNA viruses J Gen Virol. **72**:2197-206.
12. **Koonin, E. V., and V. V. Dolja** 1993. Evolution and taxonomy of positive-strand RNA viruses: implications of comparative analysis of amino acid sequences Crit Rev Biochem Mol Biol. **28**:375-430.
13. **Richards, O. C., S. Baker, and E. Ehrenfeld** 1996. Mutation of lysine residues in the nucleotide binding segments of the poliovirus RNA-dependent RNA polymerase J Virol. **70**:8564-70.

Table 1. Rates of AMP incorporation into sym/sub-U by wild-type $3D^{pol}$ and $3D^{pol}$ derivatives

	Rates (s^{-1})	
Enzyme	Mg^{++}	Mn^{++}
wildtype	45 ± 4	11 ± 2
N297A	3.3 ± 0.3	1.4 ± 0.1
N297D	17 ± 1	5.3 ± 0.2
N297G	14 ± 2	3.0 ± 0.2
M286L/N297A	20 ± 4	4.5 ± 0.5
A239G/N297A	6.0 ± 0.6	3.3 ± 0.3

Table 2. Extension activities of wild-type $3D^{pol}$ and $3D^{pol}$ derivatives

	Activity (pmol UMP incorporated/min/μg protein)		
	$dT_{15}/poly(rA)_{460}$	dT_{15}/rA_{30}	
Enzyme	Mg^{++}	Mg^{++}	Mn^{++}
wildtype	1477	10	80
N297A	550	2	32
N297D	228	1	30
N297G	1064	10	50
M286L/N297A	514	4	64
A239G/N297A	1013	6	60

Figure Legends

Figure 1. Conserved asparagine 297

A. The asparagine at position 297 of the poliovirus RNA-dependent RNA polymerase ($3D^{pol}$) is absolutely conserved among all eukaryotic positive stranded RNA viruses, in all three supergroups. Viruses indicated are from Koonin (11).

B. Asparagine 297 is postulated to play an important role in nucleotide selection in the NTP binding site. By hydrogen bonding with the 2' hydroxyl of incoming NTPs, the asparagine positively selects for NTPs and discriminates against incorrect dNTPs (6). The NTP is labelled magenta, the primer strand is yellow, template is blue, magnesium ions are grey spheres, and $3D^{pol}$ residues are indicated in grey, with oxygens labelled red and nitrogens labelled blue.

Figure 2. Viable $3D^{pol}$297 mutants

A. Viable polioviruses with mutations at $3D^{pol}$ position 297. Three day plaque assays are shown. Approximately 50 pinpoint plaques (and 1 small plaque) are visible in the Mo-$3D^{pol}$ 239G/297A well.

B. Virus production from high moi (10 PFU/cell) infections with wt, Mo-$3D^{pol}$286L/297A, Mo-$3D^{pol}$297G, and Mo-$3D^{pol}$239G/297A. Wildtype virus reached maximum titers of 1×10^9 PFU/ml by six hours post-infection. Mo-$3D^{pol}$ 286L/297A, Mo-$3D^{pol}$ 297G, and Mo-$3D^{pol}$ 239G/297A viruses reached maximum titers of 3×10^8, 2×10^8, and 5×10^6 PFU/ml respectively, by twelve hours post-infection.

Figure 3. We used a poliovirus replicon (PolioLuc) to evaluate RNA replication by the mutant polymerases in cell culture. PolioLuc is a poliovirus replicon that consists of a full-length poliovirus genome with the capsid genes replaced by a luciferase reporter gene []. Wildtype polymerase (Mo) is shown as a positive control (□), and Mo-3D^{pol}238A (O), which has no detectable RNA replication activity in cell culture (6), is shown as a negative control. Mo-3D^{pol}297D (●) replicates at 37° C, but not sufficiently to produce plaques in the context of full length virus (6). Mo-3D^{pol}286L/297A (▲), Mo-3D^{pol}297G (◆), and Mo-3D^{pol}239G/297A (■) all replicate to within 80% of wildtype levels, though with a 2-4 hr time lag.

Figure 4. Plaque assays were supplemented with manganese to tested for possible manganese dependent growth phenotype of the mutant viruses. **(A)** Three day plaque assays done in the absence of manganese (no Mn), or the presence of 0.7 mM manganese or 0.8 mM manganese. Significant increases in plaque size and the number of plaques were seen for Mo-3D^{pol} 297G and Mo-3D^{pol} 239G/297A. No change was seen for wt virus. **(B)** A 3 day plaque assays of Mo-3D^{pol} 239G/297A in the absence or presence of 1.0 mM Mn^{++}. One pinpoint plaque is visible in the absence of manganese, while ~75 plaques are visible in the presence of 1.0 mM Mn^{++}.

Figure 5. Manganese dependent virus growth

A. Virus production in Mn^{++}. High moi (10 PFU/cell) infections with wt, Mo-$3D^{pol}$ 297G, and Mo-$3D^{pol}$ 239G/297A, in the presence of different concentrations of Mn. Graph is stimulation of virus production over levels seen with no Mn supplement. We saw no stimulation of virus production with 0.5 uM Mn supplement. We observed a 5-fold stimulation of Mo-$3D^{pol}$ 297G virus production in the presence of 0.5 mM Mn, and we observed a striking 80-fold stimulation of Mo-$3D^{pol}$ 239G/297A virus production in the presence of 0.5 mM Mn.

B. Viral titers in the presence or absence of 0.5 mM Mn.

Figure 6. dT_{15}/polyA$_{460}$ pulse-chase and pulse quench polymerase extension reactions. $3D^{pol}$ was added to the reaction mix (containing 0.2 μM [α-^{32}P]-UTP, see Materials and Methods) in the absence of unlabeled UTP for three minutes. Initially labeled products were either quenched (PQ) or chased into long products (PC) by the addition of 500 μM unlabeled UTP and 10 μM heparin-3000 for 5 minutes. The reaction products were resolved on a 15 % denaturing polyacrylamide gel as previously described (6).

Figure 7. Pulse-chase/Pulse-quench on dT_{15}/rA_{30}. Reactions were performed as described above, except the final concentration of rA_{30} was 1 μM and the reactions contained either $MgCl_2$ or $MnCl_2$ to final concentration of 5 mM. Upon the addition of unlabeled UTP/heparin, time points were taken at 3 and 7 min and the reactions quenched as described in Figure 6.

Absolutely conserved asparagine (3D^{pol} pos. 297)

A.

group 1	polio	KGGMPSGCSGTSIF**N**SMIN-NLIIRTLL
	FMDV	EGGMPSGCSATGII**N**TILN-NIYVLYAL
	HAV	CGSMPSGSPCTALL**N**SIIN-NVNLYYVF
	TBRV	NCGLPSGFALTVVM**N**SIFNEEILIRYAY
	EAV	RGGLSSGDPITSIS**N**TIYSLVLYTQHML
group 2	HCV	RASRASGVLTTSCG**N**TLICYIKARAA-C
	BVDV	NGQRGSGQPDTSAG**N**SMLNVLTMMYAFC
	YFV	RDQRGSGQVVTYAL**N**TITNLKVQLIRMA
	TBSV	EGCRMSGDINTSLG**N**YLL-MCAMVHGYM
	PEMV2	KGRRMSGDMDTSLG**N**CVL-MVLLTRNLC
group 3	TMV	WYQRKSGDVTTFIG**N**TVIIAACLASMLP
	TRV	WYQQKSGDADTYNA**N**SDRTLCALLSELP
	RuBV	GCERTSGEPATLLH**N**TTVAMCMAMRMVP
	ASGV	AIMRFTGEFCTFLF**N**TFANMLFTQLKYK

B.

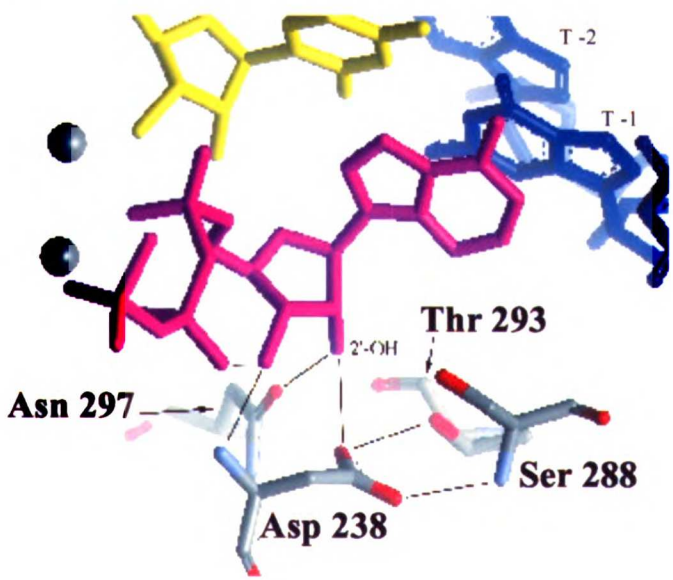

A.

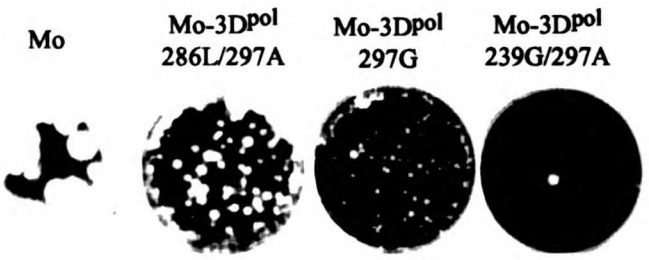
Mo
Mo-3D^pol 286L/297A
Mo-3D^pol 297G
Mo-3D^pol 239G/297A

B.

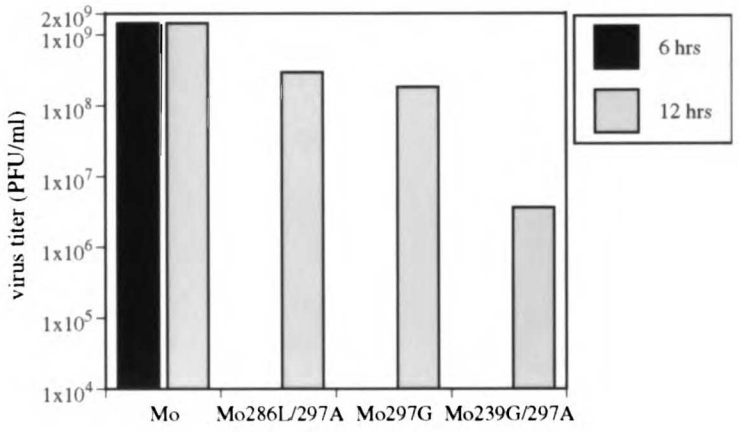
virus titer (PFU/ml)
2x10^9
1x10^9
1x10^8
1x10^7
1x10^6
1x10^5
1x10^4
6 hrs
12 hrs
Mo
Mo286L/297A
Mo297G
Mo239G/297A

Figure 3

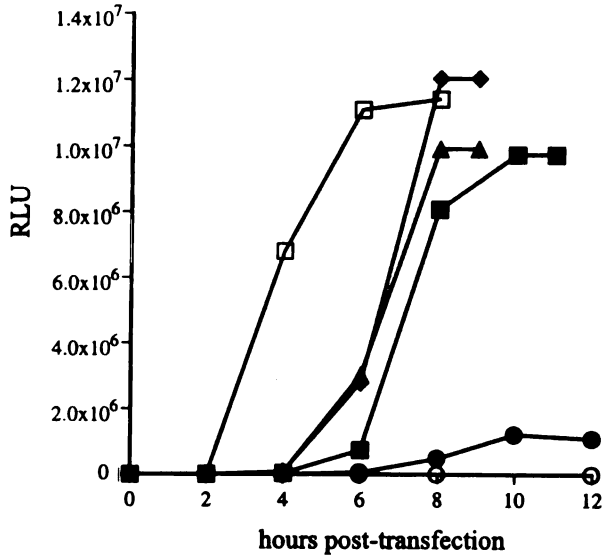
1.4x10^7
1.2x10^7
1.0x10^7
8.0x10^6
6.0x10^6
4.0x10^6
2.0x10^6
0
RLU
0
2
4
6
8
10
12
hours post-transfection

A.

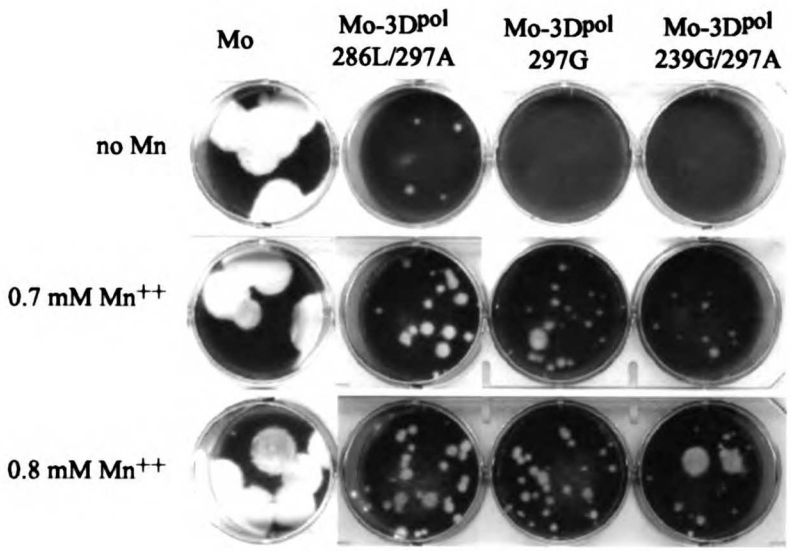
Mo
Mo-3D^pol 286L/297A
Mo-3D^pol 297G
Mo-3D^pol 239G/297A
no Mn
0.7 mM Mn++
0.8 mM Mn++

B.

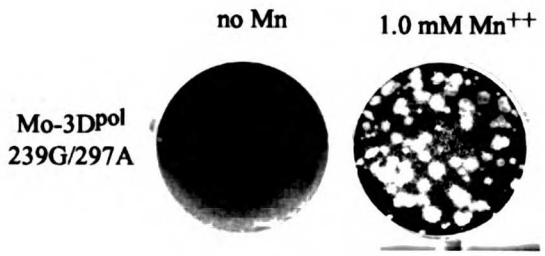
no Mn
1.0 mM Mn++
Mo-3D^pol 239G/297A

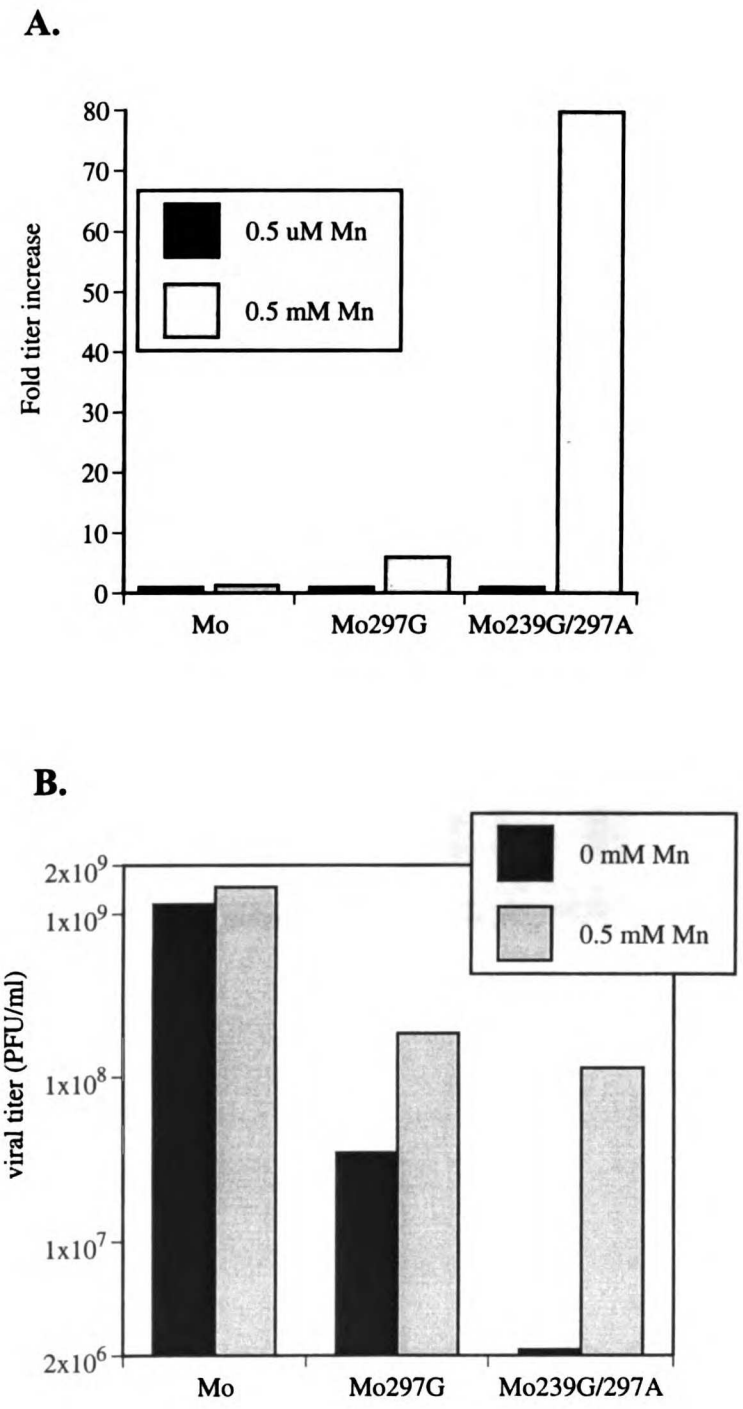
A.
Fold titer increase
80
70
60
50
40
30
20
10
0
0.5 uM Mn
0.5 mM Mn
Mo
Mo297G
Mo239G/297A
B.
viral titer (PFU/ml)
2x10^9
1x10^9
1x10^8
1x10^7
2x10^6
0 mM Mn
0.5 mM Mn
Mo
Mo297G
Mo239G/297A

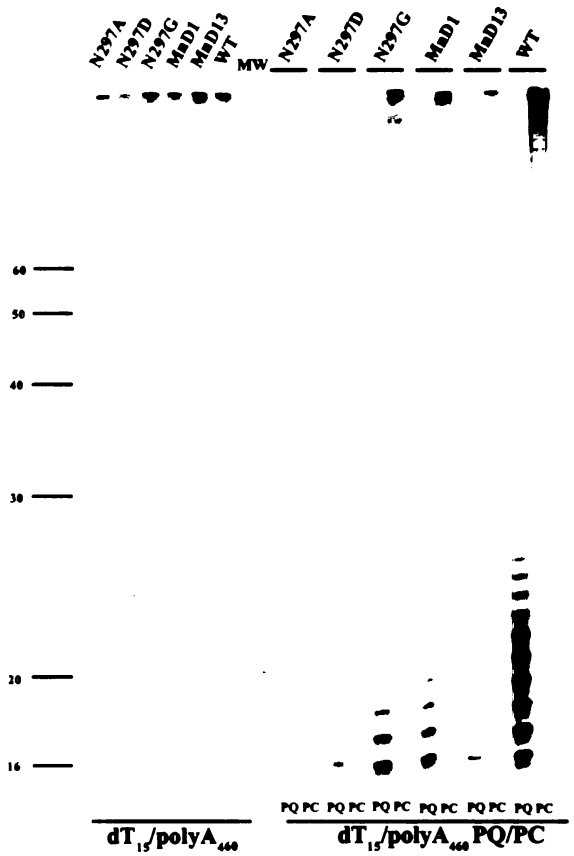
N297A
N297D
N297G
MaD1
MaD13
WT
MW
N297A
N297D
N297G
MaD1
MaD13
WT
60
50
40
30
20
16
PQ PC PQ PC PQ PC PQ PC PQ PC PQ PC
dT15/polyA440
dT15/polyA440 PQ/PC

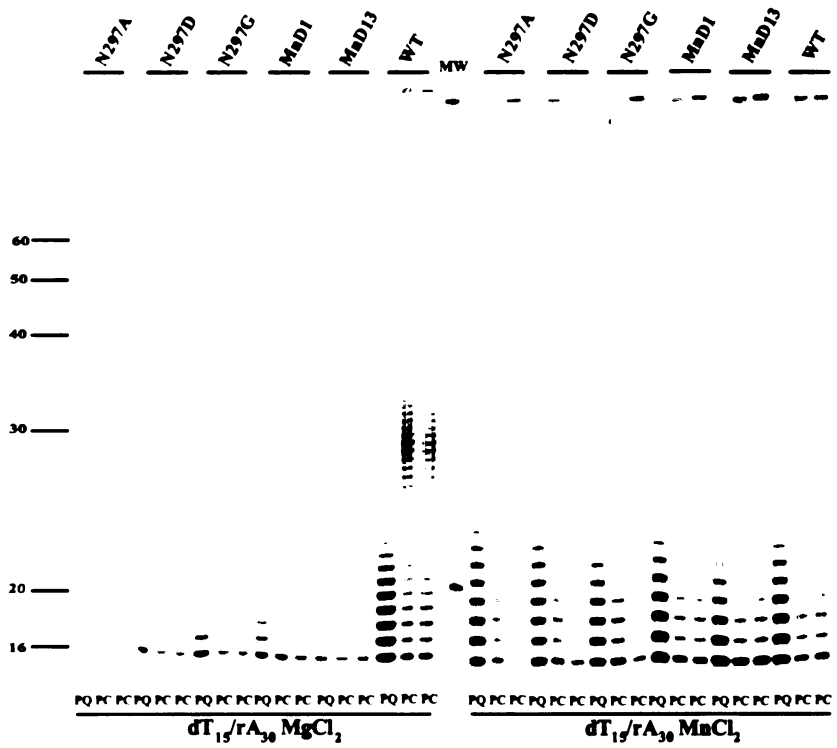
N297A
N297D
N297G
MnD1
MnD13
WT
MW
N297A
N297D
N297G
MnD1
MnD13
WT
60
50
40
30
20
16
PQ PC PC PQ PC PC PQ PC PC PQ PC PC PQ PC PC PQ PC PC
PQ PC PC PQ PC PC PQ PC PC PQ PC PC PQ PC PC PQ PC PC
dT15/rA30 MgCl2
dT15/rA30 MnCl2

Chapter 17

Viral escape from a drug with a cellular protein target: brefeldin A resistant poliovirus

Abstract

Brefeldin A is a potent inhibitor of poliovirus RNA replication. Brefeldin A's inhibition of poliovirus is not via direct interaction with viral proteins, but via inhibition of cellular proteins, probably leading to a block in the ability of poliovirus to generate membranous vesicles on which poliovirus replication occurs (poliovirus replication complexes). Brefeldin A is the only known anti-poliovirus compound for which no drug resistant virus mutant is known. It has been presumed that the virus could not become resistant to brefeldin A because the drug targets a cellular host protein, not the virus directly. Most efforts to develop effective antiviral drugs specific for a given viral protein are nullified by the high mutation/escape rates of viruses, and therefore developing drugs that instead inhibit viruses by blocking cellular factors is an appealling strategy to avoid drug resistance. Since the strategy of using cellular proteins as antiviral drug targets is a potentially powerful approach, we assessed the general feasibility of such an approach by further exploring the relationship between poliovirus and brefeldin A. We were surprised to discover that poliovirus is capable of developing full resistance to brefeldin A after

only two point mutations. Strikingly, the brefeldin A resistant virus appears to replicate in a different subcellular compartment in the presence of the drug. In the absence of brefeldin A, the resistant virus replicates in the normal poliovirus manner on poliovirus induced cytoplasmic vesicles. Implications of these results for viral RNA replication and antiviral drug strategies are discussed.

Introduction

Though much effort has been devoted to developing antiviral drugs, very few effective antiviral drugs exist. Why? One of the major reasons is that viruses rapidly mutate into drug resistant variants. The vast and rapid capacity of viruses to develop drug resistance is extraordinary. For most known antiviral drugs capable of completely inhibiting their target virus (> 99.9% inhibition of virus production), the virus can become fully resistant to the drug with a single point mutation. HIV is the most well-known virus to exhibit this stupifying level of genetic flexibility, but other viruses are comparably flexible (Domingo et al., 1988; Morse, 1994). One strategy to combat virus drug resistance has been to use multiple antiviral drugs in combination, to reduce the possibility that the virus can generate the necessary combination of mutations before being eliminated. This strategy has been used with some success, particularly in the case of HIV highly active anti-retrovirus therapy (HAART), which combines three anti-HIV drugs in a single cocktail (Finzi et al., 1997; Harrington and Carpenter, 2000; Pillay et al., 2000; Vandamme et al., 1999).

A second approach being explored is to identify cellular proteins that are essential for virus replication but not cellular viability and use those proteins as "anti-host" drug targets. This approach should potentially avoid the problem of drug resistance. Presumably the virus cannot become resistant to the "anti-host" drug because the virus is not the drug target. This strategy is currently being explored with some success in several

systems, including the use of cell cycle inhibitors that block CMV or herpes virus replication (Meijer et al., 1999; Schang et al., 2000).

Because of the powerful virological, biochemical, and genetic tools available to study poliovirus replication, poliovirus has long been a model RNA virus system for studying antiviral drugs and the development of drug resistance. Strikingly, drug resistant poliovirus mutants have been identified for all anti-poliovirus drugs except for one: brefeldin A. This is interesting because brefeldin A (BFA) is a well-characterized small molecule that targets the interaction of cellular proteins ARF1 and Sec7, inhibiting GTP cycling and causing the dissolution of the golgi complex (Chardin and McCormick, 1999; Klausner et al., 1992; Peyroche et al., 1999). Brefeldin A does not directly inhibit any poliovirus proteins, as cell types resistant to brefeldin A's inhibition of ARF1 are capable of replicating poliovirus with wildtype kinetics even in the presence of brefeldin A (Doedens et al., 1994). Poliovirus replication is associated with small cytoplasmic membranous vesicles induced by poliovirus infection (Bolten et al., 1998; Egger et al., 1996). Brefeldin A has been postulated to inhibit the formation of poliovirus-induced vesicles (Cuconati et al., 1998; Doedens et al., 1994; Irurzun et al., 1992; Maynell et al., 1992). Brefeldin A also inhibits poliovirus replication in a cell-free system (Cuconati et al., 1998). In the cell-free replication system, ARF1 dominant negative peptides that are capable of inhibiting in vitro vesicular transport are also able to block poliovirus replication (Cuconati et al., 1998). Therefore, the inability of the virus to become resistant to brefeldin A makes intuitive sense, as brefeldin A appears to inhibit the function of a cellular protein that poliovirus requires for replication (Doedens et al., 1994).

As the strategy of using cellular proteins as antiviral drug targets is a potentially powerful approach, we assessed the general feasibility of such an approach by further exploring the relationship between poliovirus and brefeldin A.

Results

Poliovirus growth is completely inhibited by brefeldin A (Fig. 1A, and (Irurzun et al., 1992; Maynell et al., 1992)). The inhibition occurs by blocking poliovirus RNA replication (Fig. 1B, and (Maynell et al., 1992)). We show that brefeldin A specifically inhibits RNA replication and has no effect on poliovirus translation by observing the translation and replication of the poliovirus replicon PolioLuc (containing the luciferase gene instead of the poliovirus capsid genes) in the presence or absence of brefeldin A. As a control for poliovirus translation alone, we included a mutant poliovirus replicon, PolioLuc-3D^{pol}238A, with an inactive polymerase (Gohara et al., 2000). No effect on poliovirus translation was seen in the presence of brefeldin A (Fig. 1B). In the absence of drug, a 10,000-fold increase in PolioLuc luciferase activity is observed between 2 and 6 hours, due to rapid viral RNA replication; but in the presence of 2.0 ug/ml brefeldin A, RNA replication was completely inhibited (Fig. 1B).

We then attempted to isolate brefeldin A resistant poliovirus mutants. First we titrated the concentration of brefeldin A necessary to inhibit poliovirus in HeLa cells. Brefeldin A concentrations of 0.1 ug/ml are sufficient to inhibit poliovirus production ≥ 99%, 0.5 ug/ml brefeldin A inhibits poliovirus production 10^4-fold, and 2.0 ug/ml completely inhibits poliovirus production with a greater than 10^7-fold reduction in titer (Fig. 1C). The concentrations of brefeldin A necessary to inhibit poliovirus replication were consistent with the concentrations of brefeldin A necessary to disrupt the golgi complexes in a population of HeLa cells.

Poliovirus was then passaged once in 0.1 ug/ml brefeldin A (P_1), once in 0.2 ug/ml brefeldin A (P_2), once in 0.4 ug/ml (P_3), once in 0.6 ug/ml brefeldin A (P_4), and then once in 1.0 ug/ml brefeldin A (P_5). The titer of the 5th passage virus was 5 x 10^6 PFU/ml, well above the background level of 1 x 10^4 PFU/ml of virus expected in 1.0 ug/ml brefeldin A.

At this point we isolated individual virus clones from the P_5 population and assessed their growth in the presence of brefeldin A. HeLa cells were infected at a low MOI (0.001 PFU/cell) and then incubated for two days in the presence or absence of 0.5 ug/ml brefeldin A. All of the viruses grew similar to wildtype (wt) in the absence of drug (Fig. 2A). One viral clone (dr1) exhibited some resistance to brefeldin A, partially lysing the infected plate of HeLa cells in the presence of drug (Fig. 2A). Several other clones exhibited a pronounced resistance to brefeldin A, rapidly spreading throughout the plate and completely lysing the HeLa cells (Fig. 2A, viruses dr3 and dr4). One viral clone (dr3) was sequenced in its entirity and two point mutations were identified in the genome: G→A at nt 4361, and C→T at nt 5190. The G4361A mutation results in a valine to isoleucine change at amino acid 80 of poliovirus nonstructural protein 2C (Fig. 2B). The C5190T mutation results in an alanine to valine change at amino acid 27 of poliovirus nonstructural protein 3A (Fig. 2B). The 2C and 3A genes were sequenced in seven additional viral clones, and six of the clones contained both the 2C and 3A mutations, while the one clone exhibiting partial resistance (dr1) contained just the 2C mutation.

These two mutations were reintroduced (together and separately) into plasmid clones of the poliovirus genome. Mutant viruses were generated from the plasmid clones. The three molecularly-derived mutant viruses—Mo4361A, Mo5190T, and MoBFA^r

(containing both mutations, a.k.a. Mo4361A/5190T)—were analyzed under one-step growth conditions. All three mutants grew with wildtype kinetics in the absence of drug (Fig. 3). Wildtype poliovirus replication was fully inhibited by 2.0 ug/ml brefeldin A, as expected (Fig. 3A). But MoBFA^r replication was almost completely unaffected by brefeldin A, growing rapidly and to high titers (5 x 10^8 PFU/ml) (Fig. 3B). Viruses containing the 2C mutation alone or the 3A mutation alone had an intermediate phenotype, growing to levels 1000x higher than background in the presence of 2 ug/ml brefeldin A, but with slower kinetics than the double mutant virus MoBFA^r (Fig 3. C-D). Interestingly, the mutant virus with the single change in 3A, Mo5190T, is substantially more cytopathic in tissue culture under low MOI conditions than mutant Mo4361A (dr2 versus dr1 in Fig. 2A). Mutations in 3A have been associated with changes in cytopathogenicity in other picornaviruses (Beneduce et al., 1995; Graff et al., 1994; Lama et al., 1998; Morace et al., 1993).

Given that MoBFA^r grew to high titers both in the presence and absence of brefeldin A, we were curious about the golgi phenotype of MoBFA^r infected cells. Poliovirus infection normally causes a rapid dissolution of the golgi via an unknown mechanism (Cho et al., 1994)(Beske and Andino, submitted). We wondered if the development of brefeldin A resistance would somehow alter this phenotype in MoBFA^r infected cells under normal conditions. We observed the condition of the golgi complex both in wildtype infected cells and MoBFA^r infected cells and saw no difference; both viruses caused a rapid dissolution of the golgi upon infection (Fig. 4).

Poliovirus replication occurs on small membranous vesicles of uncertain origin, and poliovirus 2C and 3A are both membrane associated proteins that are components of

the poliovirus replication complex ((Schlegel and Kirkegaard, 1995; Tershak, 1984) and see Discussion). Brefeldin A appears to prevent the formation of the poliovirus-induced vesicles necessary for replication (Maynell et al., 1992). We therefore analyzed the intracellular distribution of poliovirus replication complexes in cells infected with wildtype or MoBFA^r viruses. Immunofluorescent staining for poliovirus protein 2C is a standard marker for poliovirus replication complexes (Bienz et al., 1992; Bolten et al., 1998; Egger et al., 2000). The 2C staining was identical in both wt and MoBFA^r virus infected cells in the absence of brefeldin A (Fig. 5). This indicates that under standard growth conditions MoBFA^r proteins 2C and 3A traffic, form vesicles, and replicate polio RNA on vesicles in the same manner as wildtype virus. Normally 2C staining is seen on ER early in infection ((Bienz et al., 1992) and Beske and Andino, submitted). As large numbers of poliovirus replication vesicles form, the 2C staining becomes strongly concentrated in a perinuclear zone where the poliovirus replication vesicles accumulate (Bolten et al., 1998; Egger et al., 2000), as seen in Figure 5 at seven hours and eight hours post-infection (wildtype and MoBFA^r in the absence of drug; leftmost column and middle column).

No 2C staining was seen in wildtype virus infected cells in the presence of brefeldin A, because replication is completely inhibited (data not shown). In contrast, high levels of 2C expression were seen in MoBFA^r infected cells in the presence of brefeldin A (Fig. 5, rightmost column), as brefeldin A has only minor effects on MoBFA^r replication. Early in infection (3-5 hrs), 2C was seen in a diffuse ER-like staining pattern. Surprisingly, later in infection strong 2C staining remained spread throughout the cell, apparently part of large membranous structures, suggesting that MoBFA^r 2C may remain

ER-associated throughout the course of infection (7-8 hrs, Fig. 5). No perinuclear accumulation of polio-induced vesicles was seen in the majority of cells (> 90%); but a few cells did have a perinuclear concentration of 2C in the presence of brefeldin A (< 10%, data not shown). Nevertheless, the majority of MoBFA^r infected cells exhibited an unusual diffuse or tubular subcellular distribution of 2C not observed before (additional examples shown in Figure 7), indicating that MoBFA^r appears to have adapted its membrane requirements to replicate in a different subcellular compartment in the presence of brefeldin A.

To futher assess the intracellular location of MoBFA^r replication in the presence of brefeldin A, we co-stained MoBFA^r infected cells for poliovirus 2C and the endoplasmic reticulum resident protein calnexin (Fig. 6). In the presence of brefeldin A, MoBFA^r 2C almost completely co-localizes with ER early in infection (Fig. 6A, 5 hrs post-infection). At later timepoints, when many large 2C-staining structures are visible, 2C partially co-localizes with ER throughout infected cells (Fig. 6A, 7 hrs post-infection). No cellular protein marker has been identified that tightly co-localizes with poliovirus replication complexes (Bolten et al., 1998; Schlegel et al., 1996). Current models of poliovirus replication propose that the paucity of co-localization may be due to the exclusion of cellular proteins from the membrane site of poliovirus replication (Suhy et al., 2000), the possible replication of poliovirus on membranes from multiple subcellular sources (Schlegel et al., 1996; Suhy et al., 2000; Teterina et al., 1997), or the partial staining of subcellular compartments by markers such as calnexin.

We completed similar immunofluorescence experiments with brefeldin A resistant mutants Mo4361A and Mo5190T. At early timepoints of Mo4361A and

Mo5190T viral replication (5-7 hrs post-infection), extensive co-localization of 2C and calnexin was observed (Fig. 6B-C). ER morphology was not affected by BFA resistant poliovirus replication in the presence of brefeldin A (Fig. 6B and data not shown), unlike wildtype replication which causes a collapse of the ER into a perinuclear zone (Beske and Andino, unpublished data). Similarly to the MoBFA^r experiments, large 2C-staining structures were seen distributed throughout the Mo4361A and Mo5190T infected cells in the presence of brefeldin A at peak viral replication (Fig. 6B-C, 9 hrs), exhibiting partial co-localization with calnexin.

Discussion

All eukaryotic RNA viruses that have been examined carry out their replication in association with cellular membranes. The reason for this is unclear, as many of these viruses (including poliovirus) are not enveloped and have no virion membrane components. Presumably, for the non-enveloped viruses, the association with membranes facilitates the establishment of an environment advantageous for viral replication. For example, membrane associated replication may provide an increased local concentration of viral proteins. Poliovirus replication is physically associated with poliovirus induced vesicles (Bienz et al., 1992). The source of poliovirus-induced vesicles remains unclear, though ER (Bienz et al., 1987; Suhy et al., 2000), golgi (Bienz et al., 1983; Bolten et al., 1998; Sandoval and Carrasco, 1997), and mixed or varied membrane sources (Egger et al., 1996; Schlegel et al., 1996) have all been postulated. Poliovirus proteins 2C and 3A are major components of the poliovirus replication complex (Bolten et al., 1998; Egger et al., 2000; Schlegel et al., 1996; Tershak, 1984). When expressed individually they are each membrane associated (Cho et al., 1994; Doedens et al., 1997), and 2C is capable of inducing vesicle formation (Cho et al., 1994). Expression of 2C and 3A together is sufficient to produce vesicles similar in appearance to the poliovirus-induced vesicles seen in infected cells (Suhy et al., 2000).

Brefeldin A appears to block the formation of poliovirus-induced vesicles that become poliovirus replication complexes, thereby blocking viral RNA replication (Doedens et al., 1994; Maynell et al., 1992). Brefeldin A blocks the function of cellular

protein ARF1 (among other ARFs), and ARF1 function is necessary for COPI-coated vesicle formation. We have identified a brefeldin A resistant poliovirus that rapidly replicates to high titers even in the presence of 2 ug/ml brefeldin A. The identification of brefeldin A resistance mutations in 2C and 3A is quite intriguing. The functions of 2C and 3A remain unclear, and these mutations may be useful for identifying cellular membrane-associated proteins that 2C and 3A interact with and that are necessary for induction of vesicle formation and RNA replication. MoBFA^r, containing both a 2C mutation and the 3A mutation, appears to induce normal poliovirus vesicles in the absence of brefeldin A. But in the presence of brefeldin A, the MoBFA^r virus appears to change its subcellular location of replication, apparently no longer replicating on vesicles but instead exhibiting an unusual reticulated subcellular distribution, perhaps remaining ER-associated.

The ability of viruses to rapidly mutate and evade antiviral drugs is one of the truisms of virology. But since RNA viruses have stringent restrictions on their genetic coding capacity, they carry only the most essential replication components in their genomes and rely on a large set of cellular proteins to accomplish their full cycle of replication. It has therefore been presumed that targetting antiviral drugs at cellular proteins necessary for virus replication could avoid the problem of drug resistance, because it was thought that the virus cannot become resistant to the drug since the virus is not the direct target of the drug. We have shown here that this is an erroneous assumption. We discovered that poliovirus can become completely resistant to brefeldin A. The viral replication machinery seems to be astoundingly flexible, as the virus's strategy to develop full resistance to brefeldin A required only two point mutations and

allows the virus to replicate in either of two subcellular compartments. It is intriguing to consider that similar changes in the subcellular location of viral replication may occur *in vivo* as part of normal viral pathogenesis as the virus spreads in different cell types with differing subcellular compartments and/or cellular protein factors.

Regarding antiviral drug strategies, our results indicate that development of cellular protein targetted antiviral drugs will not be a panacea for the problem of viral drug resistance, but our results do not state that such a drug strategy cannot work in specific instances. Presumbly there are some scenarios where viral protein-cellular protein interactions cannot be bypassed or replaced by viral point mutants. Given that our study has identified a drug resistant poliovirus mutant that is completely immune to the effects of a potent poliovirus inhibitor targetted to a host cell protein, situations where RNA viruses cannot mutate around an antiviral drug may be exceedingly rare.

Methods

Cells and Viruses. HeLa cells were used in all experiments, grown under conditions previously described (Crotty et al., 1999). Brefeldin A was obtained from Sigma and stock solutions were 2.0 mg/ml in 70% ethanol. Starting poliovirus wildtype stock was a Mohoney stock derived from pMoRA (also called pMo rib+polyAlong) (Herold and Andino, 2000), which was derived from the pXpA plasmid (Racaniello and Baltimore, 1981). One step growth curves (Tang et al., 1997) and plaque assays (Crotty et al., 1999) were done as described.

Replicons. Replicon RNA was produced by *in vitro* transcription of linearized plasmids—pRLucRA wt plasmid (Crotty et al., 2000; Herold and Andino, 2000), or the pRLuc-3D^{pol}238A derivative (Gohara et al., 2000)—using T7 RNA polymerase as described (Crotty et al., 1999). 10 ug of each viral RNA transcript was electroporated into 1.2 x 10^6 HeLa cells, cells were incubated in complete medium at 37° C for the indicated period of time (in the presence or absence of 2 ug/ml brefeldin A), and the luciferase activity was measured as described (Gohara et al., 2000).

Selection conditions. Titration of brefeldin A (Fig. 1C) was done in 10 cm dishes of HeLa cells incubated in 10 mls DMEM/F12 + 10% FCS and the appropriate concentration of brefeldin A at 37° C (5-7% CO_2). Passaging of virus was done by infecting a 10 cm plate containing 3-5 x 10^6 HeLa cells with 1 x 10^4 PFU of virus for 15 minutes. Then, after one wash, 5 mls of medium containing the appropriate concentration of brefeldin A was added, and the dishes were incubated at 37° C until 100% lysis was

observed. Four control plates were always included: uninfected plate with no drug, uninfected plate with brefeldin A, passaged poliovirus infected plate without brefeldin A, and wildtype poliovirus stock infected plate with brefeldin A. Poliovirus was passaged once in 0.1 ug/ml brefeldin A to get the P_1 stock. Lysis of the P_1 plate was observed after 2 days, with a viral titer of 1×10^8 PFU/ml. The P_1 stock was then passaged in 0.2 ug/ml brefeldin A to obtain a P_2 stock. Lysis of the P_2 plate was observed after 3 days, with a titer of 5×10^6 PFU/ml. The P_2 stock was then passaged in 0.4 ug/ml brefeldin A to obtain a P_3 stock. Lysis of the P_3 plate was observed after 2 days, with a titer of 5×10^7 PFU/ml. The P_3 stock was then passaged in 0.6 ug/ml brefeldin A to obtain a P_4 stock. Lysis of the P_4 plate was observed after 2 days, with a titer of 1.2×10^8 PFU/ml. The P_4 stock was then passaged once in 1.0 ug/ml brefeldin A to obtain a P_5 stock. Lysis of the P_5 plate was observed after 2 days, with a titer of 5×10^6 PFU/ml.

Cloning and plasmids. RNA of potential brefeldin A resistant viruses was obtained from infected HeLa cells using Qiagen RNeasy. RNA was reverse transcribed using Superscript II RT, and poliovirus genome fragments were amplified by PCR using high fidelity PfuTurbo polymerase (Stratagene, California) in standard conditions for 30 cycles. The entire genome (pos. 20-7425) of clone dr3 was sequenced directly from the PCR products using BigDye terminator cycle sequencing and the electropherograms were analyzed with DNASTAR, as described (Crotty et al., 2000). Other clones were sequenced across the full length of genes 2C and 3A. The MoBFA^r double point mutation (4361A/5190T) was cloned into a full length poliovirus plasmid clone by digesting amplified PCR product with NheI and BglII and ligating the fragment (consisting of the poliovirus genome from pos. 2470-5601) into a NheI-BglII digested pMoRA plasmid.

After transformation and midiprepping, the resulting plasmid pMoBFA^r was sequenced from the NheI site through to the BglII site and confirmed to contain only the desired 4361A and 5190T mutations. To obtain pMo4361A and pMo5190T, the SnaBI-BglII fragment of pMoBFA^r was subcloned into pLITMUS28 (New England BioLabs, MA) to give pLITS-BAr-P2. The 1.0 kb BamHI-BglII fragment of wildtype poliovirus (from pMoRA) was then cloned into a BamHI-BglII digested pLITS-BAr-P2 to give pLITS-4361A. In parallel, the 1.6 kb SnaBI-BamHI fragment of wildtype poliovirus (from pMoRA, also digested with AatII to avoid an extra band) was gel purified and cloned into a SnaBI-BamHI digested pLITS-BAr-P2 to give pLITS-5190T. The SnaBI-BglII fragments from the pLITS-4361A and pLITS-5190T subcloning plasmids were then cloned into SnaBI-BglII digested pMoRA to get pMo4361A and pMo5190T containing full length poliovirus genomes containing the 4361A and 5190T mutations respectively. Each plasmid was sequenced across the full cloned region to confirm the presence of the desired mutation. All of these plasmids are readily available to any interested investigator. Infectious RNA is derived from these poliovirus plasmids by linearization with ClaI or ApaI, followed by T7 RNA polymerase transcription as described (Gohara et al., 2000; Herold and Andino, 2000). The T7 transcripts of the poliovirus genome are infectious upon transfection.

Immunofluorescence and microscopy. Anti-2C polyclonal antibodies were produced by the inoculation of the 2C C-terminal peptide (CNIGNCMEALFQ) conjugated to KLH into rabbits (HTI Bio-products, Ramona CA). The Calnexin antibody was purchased from Stressgen. GM130 antibody was purchased from Transduction Laboratories. HeLa cells were grown on cover-glass for microscopy experiments. Cells were infected with

the appropriate virus at an MOI of 1 and incubated in DMEM/F12 + 10% NCS, with or without 2.0 ug/ml brefeldin A for the indicated number of hours. Cells were fixed for 15 minutes with cold 3.5% paraformaldehyde in PBS. Incubation with the primary antibody was carried out in 2% newborn calf serum in PBS + 0.1% triton (PBST) solution for 1 hour. The cells were then washed 3X with PBST and subsequently incubated for 30 minutes with the secondary antibody in PBST. After 3 PBST washes, the slides were mounted with Vectashield (purchased from Vecta). Standard epifluorescent microscopy was performed at 40x and digital images were obtained using a CCD camera. All images were then imported to and processed in Adobe Photoshop and Adobe Illustrator.

References

Beneduce, F., Pisani, G., Divizia, M., Pana, A. and Morace, G. (1995) Complete nucleotide sequence of a cytopathic hepatitis A virus strain isolated in Italy. *Virus Res*, **36**, 299-309.

Bienz, K., Egger, D. and Pasamontes, L. (1987) Association of polioviral proteins of the P2 genomic region with the viral replication complex and virus-induced membrane synthesis as visualized by electron microscopic immunocytochemistry and autoradiography. *Virology*, **160**, 220-6.

Bienz, K., Egger, D., Pfister, T. and Troxler, M. (1992) Structural and functional characterization of the poliovirus replication complex. *J Virol*, **66**, 2740-7.

Bienz, K., Egger, D., Rasser, Y. and Bossart, W. (1983) Intracellular distribution of poliovirus proteins and the induction of virus-specific cytoplasmic structures. *Virology*, **131**, 39-48.

Bienz, K., Egger, D., Troxler, M. and Pasamontes, L. (1990) Structural organization of poliovirus RNA replication is mediated by viral proteins of the P2 genomic region. *J Virol*, **64**, 1156-63.

Bolten, R., Egger, D., Gosert, R., Schaub, G., Landmann, L. and Bienz, K. (1998) Intracellular localization of poliovirus plus- and minus-strand RNA visualized by strand-specific fluorescent In situ hybridization. *J Virol*, **72**, 8578-85.

Chardin, P. and McCormick, F. (1999) Brefeldin A: the advantage of being uncompetitive. *Cell*, **97**, 153-5.

Cho, M.W., Teterina, N., Egger, D., Bienz, K. and Ehrenfeld, E. (1994) Membrane rearrangement and vesicle induction by recombinant poliovirus 2C and 2BC in human cells. *Virology*, **202**, 129-45.

Crotty, S., Lohman, B.L., Lu, F.X., Tang, S., Miller, C.J. and Andino, R. (1999) Mucosal immunization of cynomolgus macaques with two serotypes of live poliovirus vectors expressing simian immunodeficiency virus antigens: stimulation of humoral, mucosal, and cellular immunity. *J Virol*, **73**, 9485-95.

Crotty, S., Maag, D., Arnold, J.J., Zhong, W., Lau, J.Y., Hong, Z., Andino, R. and Cameron, C.E. (2000) The broad-spectrum antiviral ribonucleoside ribavirin is an RNA virus mutagen. *Nat Med*, **6**, 1375-1379.

Cuconati, A., Molla, A. and Wimmer, E. (1998) Brefeldin A inhibits cell-free, de novo synthesis of poliovirus. *J Virol*, **72**, 6456-64.

Doedens, J., Maynell, L.A., Klymkowsky, M.W. and Kirkegaard, K. (1994) Secretory pathway function, but not cytoskeletal integrity, is required in poliovirus infection. *Arch Virol Suppl*, **9**, 159-72.

Doedens, J.R., Giddings, T.H., Jr. and Kirkegaard, K. (1997) Inhibition of endoplasmic reticulum-to-Golgi traffic by poliovirus protein 3A: genetic and ultrastructural analysis. *J Virol*, **71**, 9054-64.

Domingo, E., Holland, J.J. and Ahlquist, P. (1988) *RNA genetics*. CRC Press, Boca Raton, Fla.

Echeverri, A.C. and Dasgupta, A. (1995) Amino terminal regions of poliovirus 2C protein mediate membrane binding. *Virology*, **208**, 540-53.

Egger, D., Pasamontes, L., Bolten, R., Boyko, V. and Bienz, K. (1996) Reversible dissociation of the poliovirus replication complex: functions and interactions of its components in viral RNA synthesis. *J Virol*, **70**, 8675-8683.

Egger, D., Teterina, N., Ehrenfeld, E. and Bienz, K. (2000) Formation of the poliovirus replication complex requires coupled viral translation, vesicle production, and viral RNA synthesis. *J Virol*, **74**, 6570-80.

Finzi, D., Hermankova, M., Pierson, T., Carruth, L.M., Buck, C., Chaisson, R.E., Quinn, T.C., Chadwick, K., Margolick, J., Brookmeyer, R., Gallant, J., Markowitz, M., Ho, D.D., Richman, D.D. and Siliciano, R.F. (1997) Identification of a reservoir for HIV-1 in patients on highly active antiretroviral therapy [see comments]. *Science*, **278**, 1295-300.

Gohara, D.W., Crotty, S., Arnold, J.J., Yoder, J.D., Andino, R. and Cameron, C.E. (2000) Poliovirus RNA-dependent RNA Polymerase ($3D^{pol}$): Structural, biochemical, and biological analysis of conserved structural motifs A and B. *Journal of Biological Chemistry*, **275**, 25523-25532.

Gorbalenya, A.E., Koonin, E.V. and Wolf, Y.I. (1990) A new superfamily of putative NTP-binding domains encoded by genomes of small DNA and RNA viruses. *FEBS Lett*, **262**, 145-8.

Graff, J., Kasang, C., Normann, A., Pfisterer-Hunt, M., Feinstone, S.M. and Flehmig, B. (1994) Mutational events in consecutive passages of hepatitis A virus strain GBM during cell culture adaptation. *Virology*, **204**, 60-8.

Harrington, M. and Carpenter, C.C. (2000) Hit HIV-1 hard, but only when necessary [see comments]. *Lancet*, **355**, 2147-52.

Herold, J. and Andino, R. (2000) Poliovirus requires a precise 5' end for efficient positive-strand RNA synthesis. *J Virol*, **74**, 6394-400.

Irurzun, A., Perez, L. and Carrasco, L. (1992) Involvement of membrane traffic in the replication of poliovirus genomes: effects of brefeldin A. *Virology*, **191**, 166-75.

Klausner, R.D., Donaldson, J.G. and Lippincott-Schwartz, J. (1992) Brefeldin A: insights into the control of membrane traffic and organelle structure. *J Cell Biol*, **116**, 1071-80.

Lama, J., Sanz, M.A. and Carrasco, L. (1998) Genetic analysis of poliovirus protein 3A: characterization of a non- cytopathic mutant virus defective in killing Vero cells. *J Gen Virol*, **79**, 1911-21.

Maynell, L.A., Kirkegaard, K. and Klymkowsky, M.W. (1992) Inhibition of poliovirus RNA synthesis by brefeldin A. *J Virol*, **66**, 1985-94.

Meijer, L., Leclerc, S. and Leost, M. (1999) Properties and potential-applications of chemical inhibitors of cyclin- dependent kinases. *Pharmacol Ther*, **82**, 279-84.

Morace, G., Pisani, G., Beneduce, F., Divizia, M. and Pana, A. (1993) Mutations in the 3A genomic region of two cytopathic strains of hepatitis A virus isolated in Italy. *Virus Res*, **28**, 187-94.

Morse, S.S. (1994) *The Evolutionary biology of viruses*. Raven Press, New York.

Peyroche, A., Antonny, B., Robineau, S., Acker, J., Cherfils, J. and Jackson, C.L. (1999) Brefeldin A acts to stabilize an abortive ARF-GDP-Sec7 domain protein complex: involvement of specific residues of the Sec7 domain. *Mol Cell*, **3**, 275-85.

Pfister, T., Jones, K.W. and Wimmer, E. (2000) A cysteine-rich motif in poliovirus protein 2C(ATPase) is involved in RNA replication and binds zinc in vitro. *J Virol*, **74**, 334-43.

Pillay, D., Taylor, S. and Richman, D.D. (2000) Incidence and impact of resistance against approved antiretroviral drugs. *Rev Med Virol*, **10**, 231-53.

Racaniello, V.R. and Baltimore, D. (1981) Cloned poliovirus complementary DNA is infectious in mammalian cells. *Science*, **214**, 916-9.

Rodriguez, P.L. and Carrasco, L. (1995) Poliovirus protein 2C contains two regions involved in RNA binding activity. *J Biol Chem*, **270**, 10105-12.

Sandoval, I.V. and Carrasco, L. (1997) Poliovirus infection and expression of the poliovirus protein 2B provoke the disassembly of the Golgi complex, the organelle target for the antipoliovirus drug Ro-090179. *J Virol*, **71**, 4679-93.

Schang, L.M., Rosenberg, A. and Schaffer, P.A. (2000) Roscovitine, a specific inhibitor of cellular cyclin-dependent kinases, inhibits herpes simplex virus DNA synthesis in the presence of viral early proteins [In Process Citation]. *J Virol*, **74**, 2107-20.

Schlegel, A., Giddings, T.H., Jr., Ladinsky, M.S. and Kirkegaard, K. (1996) Cellular origin and ultrastructure of membranes induced during poliovirus infection. *J Virol*, **70**, 6576-88.

Schlegel, A. and Kirkegaard, K. (1995) Cell biology of enterovirus infection. In Rotbart, H. (ed.) *Human enterovirus infections*. ASM Press, Washington, D.C., pp. 135-154.

Suhy, D.A., Giddings, T.H., Jr. and Kirkegaard, K. (2000) Remodeling the Endoplasmic Reticulum by Poliovirus Infection and by Individual Viral Proteins: an Autophagy-Like Origin for Virus-Induced Vesicles. *J Virol*, **74**, 8953-8965.

Tang, S., van Rij, R., Silvera, D. and Andino, R. (1997) Toward a poliovirus-based simian immunodeficiency virus vaccine: correlation between genetic stability and immunogenicity. *Journal of Virology*, **71**, 7841-50.

Tershak, D.R. (1984) Association of poliovirus proteins with the endoplasmic reticulum. *J Virol*, **52**, 777-83.

Teterina, N.L., Gorbalenya, A.E., Egger, D., Bienz, K. and Ehrenfeld, E. (1997) Poliovirus 2C protein determinants of membrane binding and rearrangements in mammalian cells. *J Virol*, **71**, 8962-72.

Towner, J. and Semler, B.L. (1996) Determinants of membrane association on poliovirus protein 3AB. *J Biol Chem*, **271**, 26810-26818.

Vandamme, A.M., Van Laethem, K. and De Clercq, E. (1999) Managing resistance to anti-HIV drugs: an important consideration for effective disease management. *Drugs*, **57**, 337-61.

Figure legends

Figure 1. Brefeldin A specifically inhibits poliovirus replication.

(A) Poliovirus growth curve +/- brefeldin A. HeLa cells were infected with wildtype poliovirus at a multiplicity of infection (MOI) of 5 PFU/cell in the absence (■) or presence (●) of 2.0 ug/ml brefeldin A. Virus was harvested from parallel wells at the timepoints indicated. Titers below 1 x 10^5 PFU/ml are shown at 1 x 10^5 PFU/ml.

(B) Poliovirus replicon translation and replication +/- brefeldin A. Poliovirus replicon (PolioLuc) RNA has the capsid-coding sequence replaced by the luciferase gene. In the absence of replication, luciferase levels (RLU, relative light units) in HeLa cells transfected with replicon RNA are a measure of poliovirus translation. Translation alone was measured by transfecting cells with a mutant replicon, PolioLuc-3D^{pol}238A, possessing an inactive viral polymerase (▲). Normal poliovirus replication was measured by transfecting cells with wildtype PolioLuc (■). Luciferase levels in cells transfected with PolioLuc (●) or PolioLuc-3D^{pol}238A (◆) in the presence of 2.0 ug/ml are shown. Replicon luciferase levels in the presence brefeldin A are the same as the translation alone control, demonstrating a complete block of RNA replication.

(C) Titration of brefeldin A inhibition of poliovirus. HeLa cells were infected at an moi of 0.001 and incubated with the indicated concentration of brefeldin A. Virus was harvested and titered at 48 hrs post-infection.

Figure 2. Identification of brefeldin A resistant viruses

(A) Phenotype of brefeldin A resistant viruses. HeLa cells were infected at a low MOI (0.001 PFU/cell) and then incubated for two days in the absence or presence of 0.5 ug/ml brefeldin A. WT indicates wildtype poliovirus, (—) indicates control uninfected cells. Labels dr1, dr2, dr3, and dr4 indicate potential drug resistant mutants tested. All viruses replicated and spread throughout the plate in the absence of brefeldin A, causing 100% cytopathic effect (CPE). Wildtype poliovirus did not cause CPE in the presence of 0.5 ug/ml brefeldin A. Candidate mutant dr1 caused partial CPE in the presence of 0.5 ug/ml brefeldin A, as pinpoint plaques are visible. Candidate mutant dr1 was later confirmed to have a single point mutation in the 2C gene, at pos. 4361. Candidate mutants dr3 and dr4 caused 100% CPE in the presence of 0.5 ug/ml brefeldin A (also in 1.0 ug/ml and 2.0 ug/ml brefeldin A, data not shown). Candidate mutants dr3 and dr4 were later confirmed to both contain the double point mutations G4361A (in gene 2C) and C5190T (in gene 3A). Mutant dr2 was not identified in the original screen, but is instead the molecular clone-derived Mo5190T. Mutant dr2 exhibited significant drug resistance and caused > 90% CPE in the presence of 0.5 ug/ml brefeldin A.

(B) Location of brefeldin A resistance (BFA^r) mutations in the poliovirus genome. Poliovirus is a positive-strand RNA virus with a ~7500 nt genome. The full length poliovirus genome is diagrammed on the bottom, with expanded versions of the 2C and 3A genes shown above it. 2C is 329 a.a. long, and 3A is 87 a.a. long. One BFA^r mutation was found in replication protein 2C, a valine to isoleucine change at a.a. 80. A second BFA^r mutation was found in replication protein 3A, an alanine to valine change at a.a. 27.

Known domains of 2C and 3A are indicated. 2C contains an NTP^{ase} motif, and highly conserved motifs B and C (Gorbalenya et al., 1990), as well as a zinc finger (indicated by "Zn") (Pfister et al., 2000). 2C also contains at least one membrane binding domain ("mem") (Echeverri and Dasgupta, 1995) and an RNA binding domain (Bienz et al., 1990; Rodriguez and Carrasco, 1995). 3A contains a 22 a.a. hydrophobic stretch in its C-terminus ("hydro") that is thought to play a role in membrane binding (Towner and Semler, 1996).

Figure 3. Kinetic analysis of brefeldin A resistant viruses' growth. HeLa cells were infected at an MOI of 5 using the virus strains indicated below, in the absence (●) or presence (■) of 2.0 ug/ml brefeldin A. Virus was harvested at the indicated timepoints, and then titered by plaque assay. **(A)** wildtype (WT), **(B)** Mo4361A, **(C)** Mo5190T, **(D)** $MoBFA^r$. Titers off the bottom of the scale are indicated as 1 x 10^5 PFU.

Figure 4. Golgi phenotype of brefeldin A resistant virus. HeLa cells were infected at an MOI of 1 with either **(A)** wildtype (WT), or **(B)** $MoBFA^r$. Cells were fixed at 4 hrs post-infection and co-stained for poliovirus protein 2C (green) and a golgi marker (GM130, red). Several poliovirus infected cells are indicated by filled white arrows, and representative uninfected cells are indicated by empty arrows.

Figure 5. Subcellular localization of virus replication. HeLa cells were infected with wildtype (WT) or brefeldin A resistant poliovirus (MoBFA^r) for the time indicated and then fixed and stained for poliovirus protein 2C. The two lefthand columns were infections done in the absence of drug, and the righthand column shows MoBFA^r infections in the presence of 2.0 ug/ml brefeldin A. Note the unusual reticulated staining of MoBFA^r at late timepoints of infection (7-8 hours) in the presence of brefeldin A.

Figure 6. Subcellular localization of virus replication.

A) HeLa cells were infected with MoBFA^r for 5 hrs or 7 hrs in the presence of 2.0 ug/ml brefeldin A and then fixed and stained for poliovirus protein 2C (green) and ER resident protein calnexin (orange-red). Merged image are shown in the righthand column.

B) HeLa cells were infected with Mo4361A for 7 hrs or 9 hrs in the presence of 2.0 ug/ml brefeldin A and then fixed and stained for poliovirus protein 2C (green) and ER resident protein calnexin (orange-red). Merged image are shown in the righthand column.

C) HeLa cells were infected with Mo5190T for 7 hrs or 9 hrs in the presence of 2.0 ug/ml brefeldin A and then fixed and stained for poliovirus protein 2C (green) and ER resident protein calnexin (orange-red). Merged images are shown in the righthand column.

Figure 7. Additional examples of MoBFA^r replication in the presence of brefeldin A. HeLa cells were infected for 7-8 hrs in the presence of 2.0 ug/ml brefeldin A and then fixed and stained for poliovirus protein 2C.

Figure 1

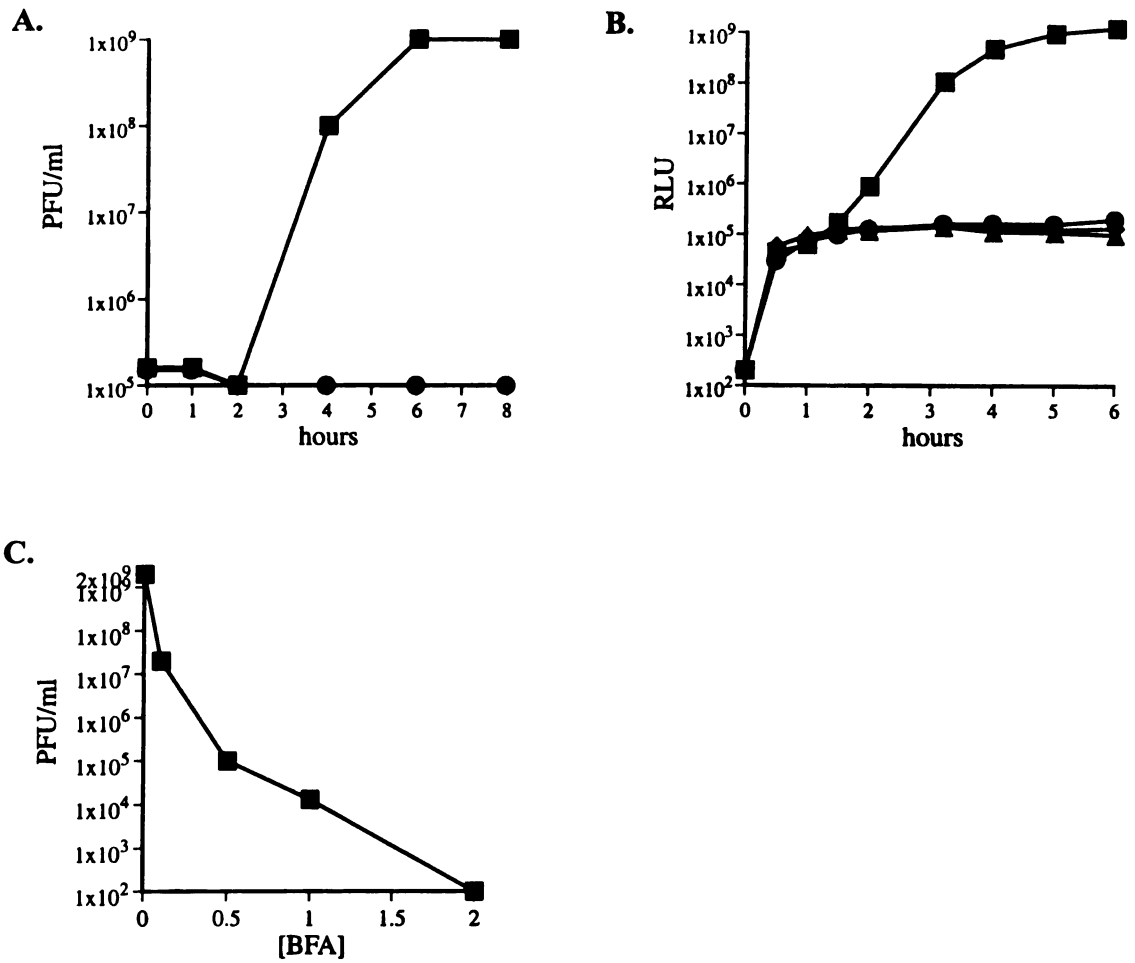
A.
PFU/ml
1x10^9
1x10^8
1x10^7
1x10^6
1x10^5
0 1 2 3 4 5 6 7 8
hours
B.
RLU
1x10^9
1x10^8
1x10^7
1x10^6
1x10^5
1x10^4
1x10^3
1x10^2
0 1 2 3 4 5 6
hours
C.
PFU/ml
2x10^8
1x10^8
1x10^7
1x10^6
1x10^5
1x10^4
1x10^3
1x10^2
0 0.5 1 1.5 2
[BFA]

Figure 2

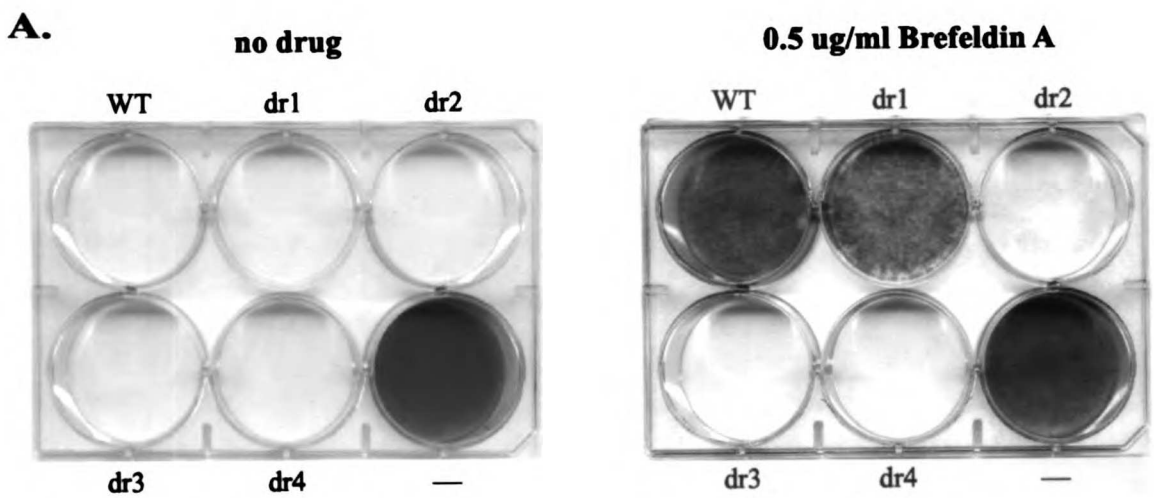
A.
no drug
0.5 ug/ml Brefeldin A
WT
dr1
dr2
dr3
dr4
—
WT
dr1
dr2
dr3
dr4
—

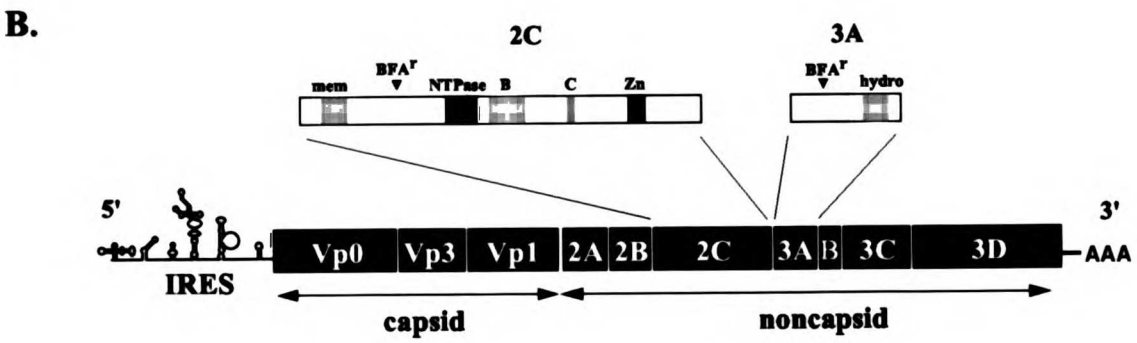
B.
2C
3A
mem
BFA^r
NTPase
B
C
Zn
BFA^r
hydro
5'
3'
Vp0
Vp3
Vp1
2A
2B
2C
3A
B
3C
3D
AAA
IRES
capsid
noncapsid

Figure 3

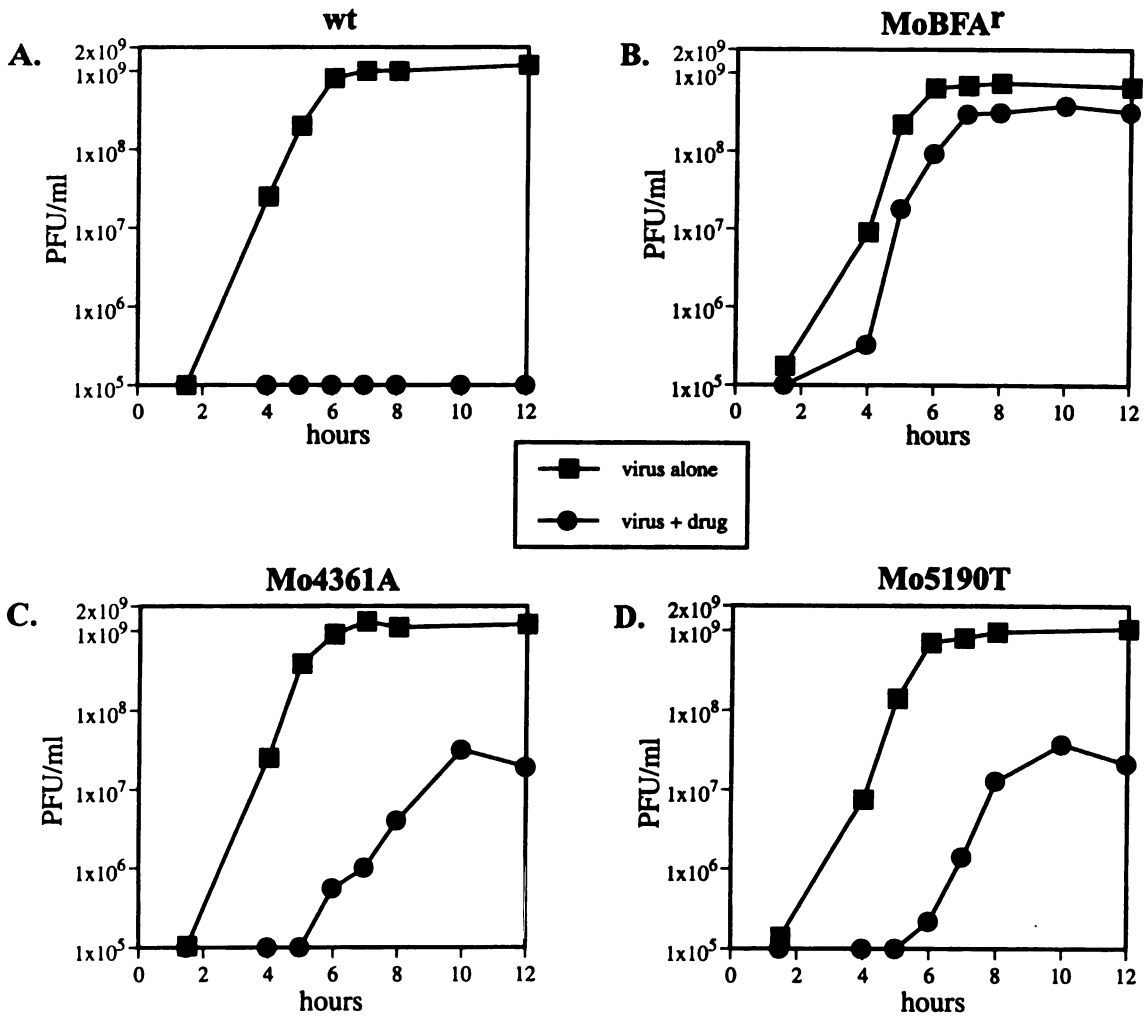
A.
wt
B.
MoBFA^r
C.
Mo4361A
D.
Mo5190T
PFU/ml
2x10^9
1x10^9
1x10^8
1x10^7
1x10^6
1x10^5
0
2
4
6
8
10
12
hours
virus alone
virus + drug

Figure 4

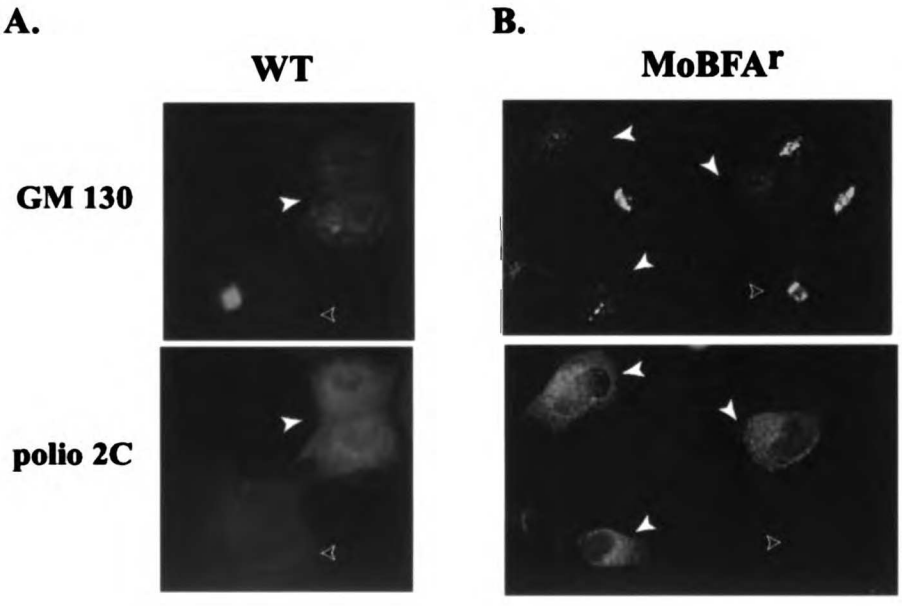

Figure 5

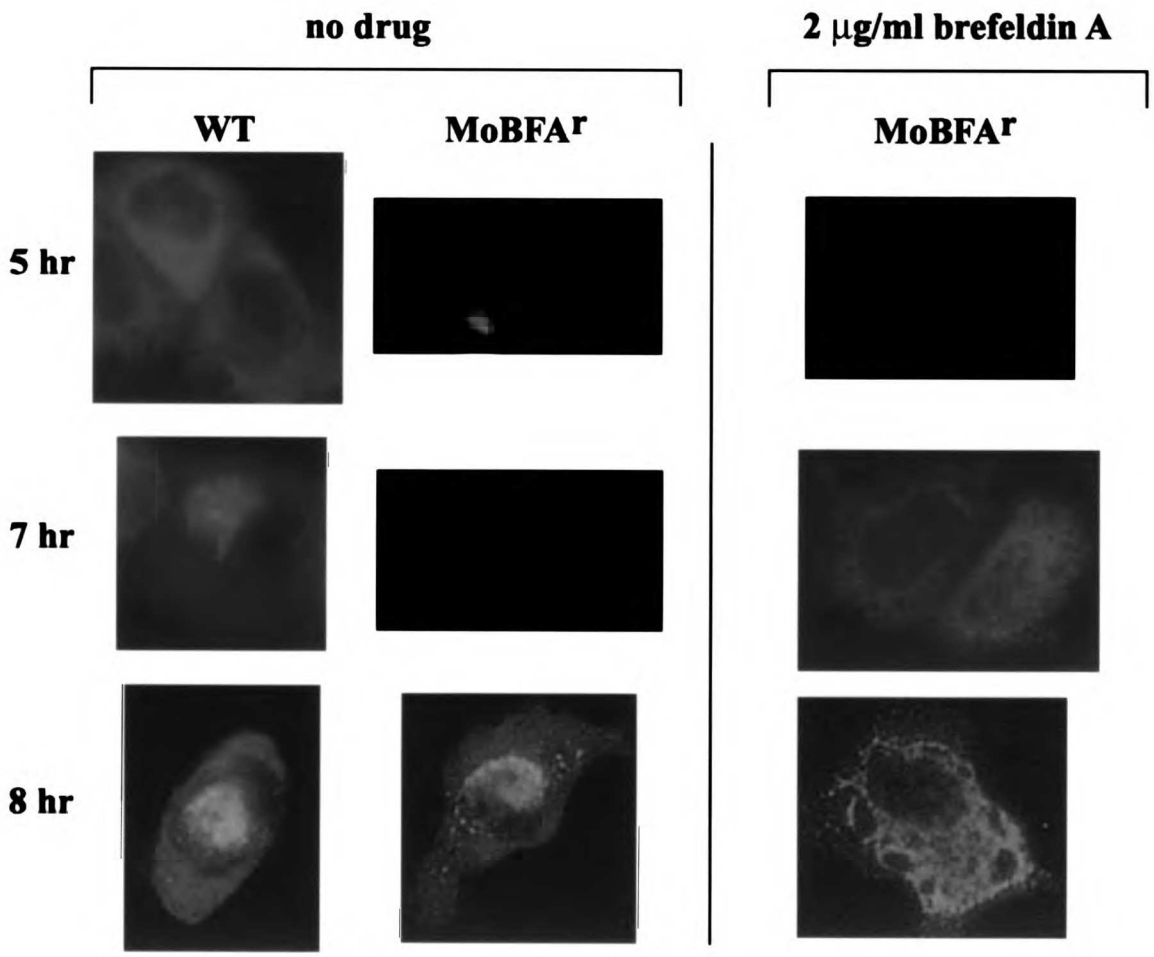

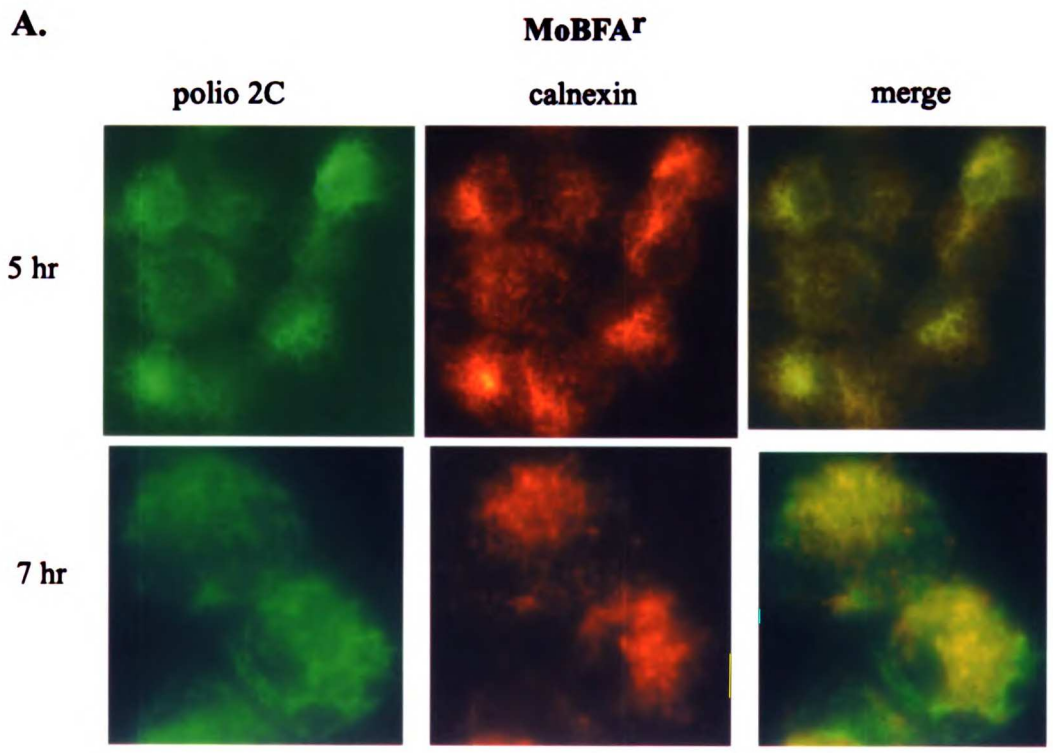
A.
MoBFA^r
polio 2C
calnexin
merge
5 hr
7 hr

Figure 6, cont.

B. **Mo4361A**

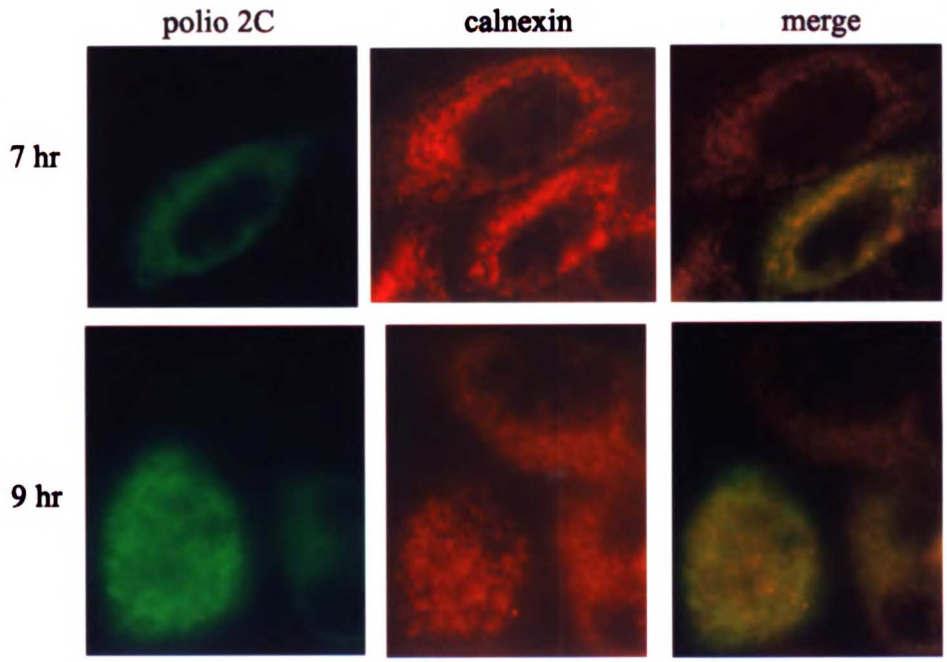

C. **Mo5190T**